

THESE DE DOCTORAT DE

L'UNIVERSITE DE NANTES
COMUE UNIVERSITE BRETAGNE LOIRE

ECOLE DOCTORALE N° 605
Biologie Santé
Spécialité : Médecine Régénératrice et Biomatériaux

Par

Luciano VIDAL

Large Bone Defects Reconstruction

by using vascularization and 3D Printing

Thèse présentée et soutenue à Nantes, le 20-12-2019
Unité de recherche : UMR 1238

Rapporteurs avant soutenance :

Nathalie, Chevallier Chargée de recherche, Unité d'Ingenierie et de Thérapie Cellulaire- EFS, Créteil.
Agnès, Dupret-Bories PH-HDR, IUCT Toulouse, Oncopole.

Composition du Jury :

Président :

Examineurs : Françoise, Rédini Directeur de Recherche, INSERM, UMR 1238 Phy-Os.
Philippe, Rosset PU-PH, CHU Tours.
Christophe, Marquette Directeur de Recherche, Université de Lyon 1, CNRS 5246 ICBMS.

Dir. de thèse : Pierre, Layrolle Directeur de Recherche , INSERM, UMR 1238 Phy-Os.
Co-dir. de thèse : Alain, Hoornaert MCU, Université de Nantes. UMR 1238 Phy-Os.
Co-encadrant : Meadhbh, Brennan Post-Doc, INSERM, UMR 1238 Phy-Os.

« A mi familia Clara, Taniel y Solal.

Gracias por acompañarme, sostenerme y siempre estar a mi lado.

Perdón por los momentos que les he robado este tiempo.

Son mi vida, LOS AMO !!! »

VALORIZATION OF THESIS WORK

Publications

1. Reconstruction of large skeletal defects: current clinical therapeutic strategies and future directions using 3D printing. (*Submitted to publication in Journal : Frontiers in Bioengineering and Biotechnology - Special Issue: 3D Printing for Implantable Medical Devices: From Surgical Reconstruction to Tissue/Organ Regeneration*);
Vidal L ; Kampleitner C ; Brennan MA ; Hoornaert A ; Layrolle P.
2. In situ production of a pre-vascularized synthetic bone graft for regeneration of critical size defects in rabbits. (*Submitted to publication in Journal : Biomaterials*).
Vidal L; Brennan MA ; Krissian S ; De Lima J ; Hoornaert A ; Rosset P ; Fellah BH ; Layrolle P.
3. Regeneration of segmental defects in metatarsus of sheep with vascularized and customized 3D-printed calcium phosphate scaffolds. (*Submitted to publication in Journal : Scientific Reports - Special Issue: 3D bioprinting of cells, tissues and organs*).
Vidal, L ; Kampleitner C ; Krissian S ; Hoffmann O ; Raymond S; Maazouz Y, Ginebra MP; Rosset P; Layrolle P.

Publications in collaboration

1. Bone regeneration strategies with bone marrow stromal cells in orthopaedic surgery.
Stanovici J, Le Nail LR, Brennan MA, **Vidal L**, Trichet V, Rosset P, Layrolle P.
Curr Res Transl Med. 2016 Apr-Jun;64(2):8390.doi:10.1016/j.retram.2016.04.006. Epub 2016 Jun 1. Review.

2. Bone microenvironment has an influence on the histological response of osteosarcoma to chemotherapy: retrospective analysis and preclinical modeling.
*Crenn V, Biteau K, Amiaud J, Dumars C, Guiho R, **Vidal L**, Nail LL, Heymann D, Moreau A, Gouin F, Redini F. Am J Cancer Res. 2017 Nov 1;7(11):2333-2349. eCollection 2017.*

3. Biocompatibility and osseointegration of nanostructured titanium dental implants in minipigs. *Clinical Oral Implants Research. (In Review).*
*Hoornaert A, **Vidal L**, Besnier R, Morlock JF, Louarn G, Layrolle P.*

4. Epinephrine infiltration of adipose tissue impacts MCF7 breast cancer cells and total lipid content. *International Journal of Molecular Science. (In Press).*
*Avril P, **Vidal L (co-first author)**, Barillé-Nion S, Le Nail LR, Rédini F, Layrolle P, Pinault M, Chevalier S, Perrot P, Trichet V.*

5. Osteogenic potential of human umbilical cord blood and bone marrow mesenchymal stromal cells after chondrogenic and BMP-4 priming. *Bone Research. (In Review).*
*Brennan MA, Barilani M, **Vidal L**, Lavazza L, Lazzari L, Giordano R, Layrolle P.*

Presentations in Congress

Oral Presentation

1. 29th Symposium and Annual Meeting of the International Society for Ceramics in Medicine. October 2017. **Best Oral Award.** *In situ production of a pre-vascularized synthetic bone graft for regeneration of critical size defects in rabbits.*
2. *Cancer and Biofabrication. 1st Workshop- 3D Bioprinting in Cancer Research.* Cancéropôle Grand Ouest. July 2017. *3D Printing of biomaterial scaffolds from CT Scan for bone regeneration after tumor resection.*

Poster Presentation

1. 2nd Workshop "BIOFABRICATION & CANCER". Cancéropôles Grand Sud-Ouest (GSO) et Grand Ouest (GO). June 2018. *3D Bioprinting of bone tumors for modeling the osteosarcoma microenvironment.*
2. EU - TERMIS Chapter (Tissue Engineering and Regenerative Medicine International Society). May 2019. *Reconstruction of Large bone defect in sheep with customized 3D printed calcium phosphate scaffolds.*
3. EU - TERMIS Chapter (Tissue Engineering and Regenerative Medicine International Society). May 2019. *An innovative bioink for 3D bioprinting of mesenchymal stem cells.*
4. EU -TERMIS Workshop: 3D Bioprinting in Cancer Research. August 2019. *Additive manufacture for in vitro modelling of human giant cell tumour of bone.*

TABLE OF CONTENTS

General Summary in French

Summary

List of Abbreviations

1. General Introduction	p 18
Bone Macroscopic Structure	p 18
Types of Bone	p 18
Bone Tissue	p 20
Bone Cells	p 20
Extracellular Bone Matrix	p 21
Bone Microscopic Structure	p 22
The Haversian System	p 24
Vasculature of Bone.....	p 24
Bone Healing	p 27
State of the Art in Bone Regeneration	p 29
Objectives of the Thesis	p 33
2. Chapter I	p 41

Reconstruction of large skeletal defects: current clinical therapeutic strategies and future directions using 3D printing. (Paper I)

3. Chapter IIp 78

In situ production of pre-vascularized synthetic bone grafts for regenerating critical-sized defects in rabbits. (Paper II)

4. Chapter IIIp 120

Regeneration of segmental defects in metatarsus of sheep with vascularized and customized 3D-printed calcium phosphate scaffolds. (Paper III)

5. General Discussionp 149

6. Conclusionp 153

7. Future Perspectivesp 155

8. Referencesp 156

9. Annexep 178

RÉSUMÉ

Suite à un traumatisme, l'os est capable de se réparer naturellement dans la plupart des situations. La consolidation osseuse, est un processus de régénération progressive et continue qui s'effectue en trois étapes principales. Dans un premier temps, les macrophages produisent des cytokines inflammatoires comme les interleukines-1 et -6 (IL-1, IL-6), le facteur de nécrose tumoral (TNF), la Chemokine C-C Ligand 2 (CCL2) qui favorisent la dégradation du caillot de fibrine et le recrutement de cellules stromales mésenchymateuses (CSM). Ensuite, les CSM produisent une matrice extracellulaire composée de glycoprotéines qui évolue d'un cal mou de tissu fibro-cartilagineux vers un tissu riche en fibres de collagène de type I dans lequel des cristaux d'hydroxyapatite précipitent. Ce processus de minéralisation s'accompagne d'une néo-vascularisation stimulée par la sécrétion de cytokines pro-angiogéniques comme le fibroblast growth factor (FGF) ou le vascular endothelial growth factor (VEGF). Les CSM se différencient progressivement en ostéoblastes et ostéocytes enchâssés dans la matrice extracellulaire minéralisée. Au cours de cette dernière étape, le cal osseux est remodelé sous l'action concertée des cellules multi-nucléées, les ostéoclastes, capables de résorber la matrice extracellulaire minéralisée, et des ostéoblastes qui la produisent. Ce processus de remodelage assure une consolidation mécanique et rend à l'os sa forme initiale, avec la réapparition du canal médullaire. La cicatrisation complète d'une fracture nécessite en général une immobilisation de 45 jours.

Cependant, certaines fractures ou pertes osseuses ne peuvent pas se régénérer spontanément. Ces défauts osseux de taille critique nécessitent une intervention

chirurgicale de reconstruction osseuse utilisant le plus souvent de l'os prélevé sur le patient. Chaque année, plus d'un million de patients bénéficient d'une reconstruction osseuse en Europe faisant de l'os le second tissu le plus transplanté après les transfusions sanguines.

Cette thèse aborde les traitements actuels et les options futures pour la reconstruction de grands défauts osseux, ce qui constitue aujourd'hui un défi pour les chirurgiens orthopédistes et les chirurgiens plasticiens qui souhaitent éviter l'amputation et améliorer la qualité de vie des patients. L'objectif de cette thèse est d'apporter de nouvelles solutions chirurgicales pour la régénération de grands défauts osseux en utilisant l'imagerie médicale, des biomatériaux anatomiques fabriqués par impression 3D et la vascularisation. Cette thèse est divisée en trois chapitres.

Le premier chapitre donne les différentes options chirurgicales actuelles et futures dans la reconstruction de grands défauts osseux. Ces défauts osseux peuvent résulter d'un traumatisme, d'une infection, d'une résection tumorale, des anomalies squelettiques ou lorsque le processus de remodelage osseux est compromis (par exemple, dans la nécrose avasculaire, la non-consolidation atrophique ou l'ostéoporose). La technique de référence en matière de reconstruction osseuse est la greffe autologue à lambeau libre qui contient les cellules du patient, ses facteurs de croissance et un apport vasculaire. Cependant, ses principaux inconvénients sont la morbidité au niveau du site de prélèvement, la microchirurgie laborieuse pour adapter le greffon à l'anatomie du défaut osseux et sa vascularisation. Une autre option possible est la technique de Masquelet qui consiste à placer dans le défaut osseux un ciment à base de polymère pour induire une membrane vascularisée et qui est remplacé après 6 semaines par des fragments d'os autologue. Cette technique de Masquelet a prouvé son efficacité pour la régénération des défauts segmentaires de

plusieurs centimètres dans les os longs, mais nécessite toujours un prélèvement de l'os iliaque autologue, ajoutant ainsi une morbidité avec deux interventions chirurgicales consécutives. Il est important de souligner que le stock osseux du patient est limité et que ces techniques de transplantation osseuse présentent de nombreuses complications post-chirurgicales. Ainsi, les chirurgiens utilisent en seconde intention les allogreffes osseuses massives provenant de banques de tissus pour la reconstruction de défauts complexes du squelette. Néanmoins, ces allogreffes présentent des risques de transfert de maladie et de rejet immunitaire. La méthode utilisant le patient comme bioréacteur a démontré qu'il est possible de préparer de manière exogène un substitut mandibulaire personnalisé dans le muscle et de le transplanter dans un défaut osseux existant. Cependant, cette méthode ne s'applique pas à l'urgence, nécessite deux sites chirurgicaux et au moins deux chirurgies affectant la qualité de vie des patients. Depuis plusieurs années, des substituts osseux synthétiques à base de phosphate de calcium ont été développés pour guider la régénération osseuse. Cependant, les propriétés de régénération de ces substituts osseux restent insuffisantes pour les défauts osseux importants en raison d'un manque de vascularisation initiale. Enfin, dans ce chapitre, les futures directions pour la reconstruction de grands défauts osseux sont proposées avec l'utilisation de nouvelles technologies telles que l'impression 3D et le bioprinting 3D. Ces méthodes de fabrication additive permettent de fabriquer des substituts osseux personnalisés correspondant à l'anatomie du patient à partir d'images médicales. La bioimpression 3D permettra également d'inclure des cellules vivantes et la vascularisation afin de produire ex vivo un organe osseux fonctionnel.

Le deuxième chapitre évalue une approche expérimentale consistant à produire *in situ* un greffon osseux synthétique pré-vascularisé et à le greffer par la suite dans un défaut

osseux de taille critique chez le lapin. Des chambres imprimées en 3D contenant des granules de phosphate de calcium biphasé (BCP), perfusées par un pédicule vasculaire local, avec ou sans addition de la fraction vasculaire stromale (FSV) du tissu adipeux ont été implantées dans un site sous-cutané chez des lapines de race blanche de Nouvelle-Zélande. Après huit semaines, ces substituts osseux 3D présentaient de nombreux vaisseaux sanguins provenant du pédicule vasculaire axial et une production abondante de collagène, mais pas d'os. Transplantés dans des défauts ulnaires segmentaires de taille critique de 15 mm, une régénération osseuse a été observée pour les substituts osseux vascularisés après huit semaines supplémentaires. Cependant, ces greffons n'ont pas été reconnectés au système vasculaire local du défaut osseux. Cette étude chez l'animal a démontré l'intérêt de la pré-vascularisation de greffes osseuses synthétiques pour la régénération de grands défauts osseux, mais nécessite toujours deux chirurgies.

Le troisième chapitre concerne la régénération de grands défauts osseux chez la brebis en une seule étape chirurgicale. Dans cette nouvelle approche, des biomatériaux de phosphate de calcium et des guides chirurgicaux personnalisés ont été imprimés en 3D à partir de scanners de tomodensitométrie préopératoires permettant de visualiser le métatarse et le système vasculaire local. L'impression 3D a permis la fabrication de biomatériaux 3D anatomiques comportant une porosité interconnectée et contrôlée. Des défauts segmentaires de taille critique (35 mm) ont été créés dans la région mesio-diaphysaire du métatarse. Ces défauts étaient soit laissés vides, soit comblés avec un biomatériau 3D, ou en combinaison avec un pédicule vasculaire axial translaté dans le défaut. La régénération osseuse évaluée à 1, 2 et 3 mois après l'implantation était significativement plus rapide et plus élevée pour les biomatériaux 3D comportant une vascularisation axiale que pour ceux sans,

et a fortiori pour le défaut laissé vide. Cette étude pré-clinique a démontré la faisabilité de la planification pour la reconstruction chirurgicale en une seule étape de grands défauts osseux en utilisant des biomatériaux personnalisés imprimés en 3D et une vascularisation axiale.

Cette thèse permet donc de proposer des alternatives chirurgicales prometteuses pour la régénération de grands défauts osseux qui restent encore aujourd'hui très difficiles à reconstruire. Néanmoins, nos études devront être confirmées par l'utilisation d'un plus grand nombre d'animaux, de sites anatomiques plus complexes que les os longs et de biomatériaux 3D plus résistants mécaniquement et possédant une dégradation concertée avec la régénération osseuse. Ce travail permet d'envisager des reconstructions du squelette complexes sans recours aux greffes grâce à l'apport de l'imagerie médicale, la planification pré chirurgicale, la fabrication additive de biomatériaux anatomiques et l'apport de la vascularisation.

SUMMARY

The present thesis addresses the actual treatments and future options for large bone defect reconstruction that constitutes a challenge for orthopedists and plastic surgeons. This thesis is divided into three chapters.

The first chapter consists of a review of the actual surgical options in large bone defects reconstruction. These bone defects can arise due to trauma, infection, tumor resection, skeletal abnormalities, or when the bone remodeling process is compromised (such as in avascular necrosis, atrophic non-union, or osteoporosis). The gold standard technique for bone reconstruction is autologous free flap transplantation that contains patient's own cells, growth factors and a vascularization bed. However, its main disadvantages are morbidity, laborious microsurgery and shaping to the anatomy of the bone defect. Another option is the Masquelet's technique that consists of placing a polymer cement to induce a vascularized membrane after 6 weeks before filling with autologous bone. It has proven efficacy for regenerating segmental defects in long bones but still requires to harvest autologous iliac bone, thus adding morbidity with two consecutive surgeries. It is important to emphasize that the patient's bone stock is limited. Massive bone allografts from tissue banks are alternatives for reconstruction of complex skeletal defects but present risks of disease transfer and immune rejection. In patient bioreactor has also been demonstrated to prepare exogenously a customized mandible replacement grown in muscle prior to transplantation to repair the existing defect but the method is not applicable to emergency and requires two surgical sites. Synthetic bone substitutes have insufficient regenerative properties for large bone defects due to a lack of initial vascularization. Finally, in this chapter, we described the future possible options for large bone defect reconstruction with the use

of new technology such as 3D printing and 3D Bioprinting. These additive manufacturing methods allow to fabricate customized bone substitutes fitting the anatomy of the patient from medical images. 3D bioprinting will also permit to include living cells and vascularization.

The second chapter evaluates an experimental approach consisting of the *in situ* production of a pre-vascularized synthetic bone graft and its subsequent transplantation to a critical-sized bone defect in rabbits. 3D printed chambers containing biphasic calcium phosphate (BCP) granules, perfused by a local vascular pedicle, with or without the addition of stromal vascular fraction (SVF) were subcutaneously implanted into New Zealand White female rabbits. After eight weeks, these 3D constructs exhibited many blood vessels sprouting from the axial vasculature and abundant collagen production, but no bone. When transplanted into 15 mm critical-sized segmental ulnar defects for a further eight weeks, these constructs enhanced bone regeneration although they were not reconnected to the local vasculature of the defect. This animal study demonstrated the benefit of pre-vascularization of synthetic bone grafts for regenerating large bone defects but required two surgeries.

The third chapter aimed to investigate the feasibility of regenerating large bone defects in one surgical step by using 3D-printed customized calcium phosphate scaffolds with or without vascularization. Pre-operative computed tomography scans were performed to visualize the metatarsus and vasculature and to fabricate customized scaffolds and surgical guides by 3D printing. Critical-sized segmental defects created in the mid-diaphyseal region of the metatarsus were either left empty or treated with the 3D scaffold alone or in combination with an axial vascular pedicle. Bone regeneration evaluated 1, 2, and 3 months post-implantation was significantly faster and higher for

3D scaffolds comprising an axial vasculature than without and a fortiori for the left empty defect. This pre clinical study demonstrated the feasibility of pre-surgical planning and reconstruction of large bone defects with 3D-printed personalized scaffolds and axial vascularization in a one step surgery.

LIST OF ABBREVIATIONS

BCP: Biphase calcium phosphate

BMP: Bone Morphogenetic Protein

β -TCP: Beta-tricalcium phosphate

CAD: computer-aided design (CAD)

CAO: Computer assisted ordering (CAO)

CCL2: Chemokine C-C Ligand 2

CD: Differentiation Cluster

CSM: Mesenchymal stromal stem cells

DMEM: Dulbecco's modified eagle medium

EDTA: Ethylene Diamine Tetra Acetic

FGF: Fibroblast growth factor

HA: Hydroxyapatite

IL-1 / IL-6: Interleukins 1 and 6

IV: Intravenous injection

MCAM: Melanoma Cell Adhesion Molecule

MEC: Extracellular Matrix (MEC)

MMPs: Matrix metalloproteinases

NZW: New-Zealand White

P / S: Penicillin / Streptomycin

PBS: Salted buffered phosphate

PCL: Polycaprolactone

PDGF: Platelet-derived growth factor

PLA: Polylactic acid

PLGA: Poly(lactic-co-glycolic acid)

PLLA: Poly-L-Lactic Acid

SD: Standard Deviation

SEM: Scanning Electron Microscopy

STL: Stereolithography

SVF: Vascular Stromal Fraction

CT: CT Scanner, Computed Tomography

MT: Masson's Trichrome Staining

TE: Tissue Engineering

TERMIS: Tissue Engineering and Regenerative Medicine International Society

TGF- β : Transforming growth factor- β

TNF: Tumor necrosis factor

VEGF: Vascular endothelial growth factor (VEGF)

GENERAL INTRODUCTION

The reconstruction of large de bone defects caused by trauma, infection, and tumor resection is a challenge for orthopedists and plastic surgeons. Bone is a vascularized connective tissue responsible for the support and protection of the organs of the body (Neto and Ferreira, 2018). Bone tissue is in a constant remodeling process to adapt itself to the mechanical demands of the body and to repair small lesions that may occur (Hadjidakis and Androulakis, 2006). However, large critical size bone defects, defined by Schmitz and Hollinger as a defect of a magnitude that the bone itself is unable to recover through its natural regeneration, require a medical reconstructive intervention (Schmitz and Hollinger, 1986). Chapter 1 of this manuscript is part of the introduction. In this chapter 1, we describe the current treatments for large bone defects reconstruction as well as future options for this type of reconstruction.

Bone Macroscopic Structure

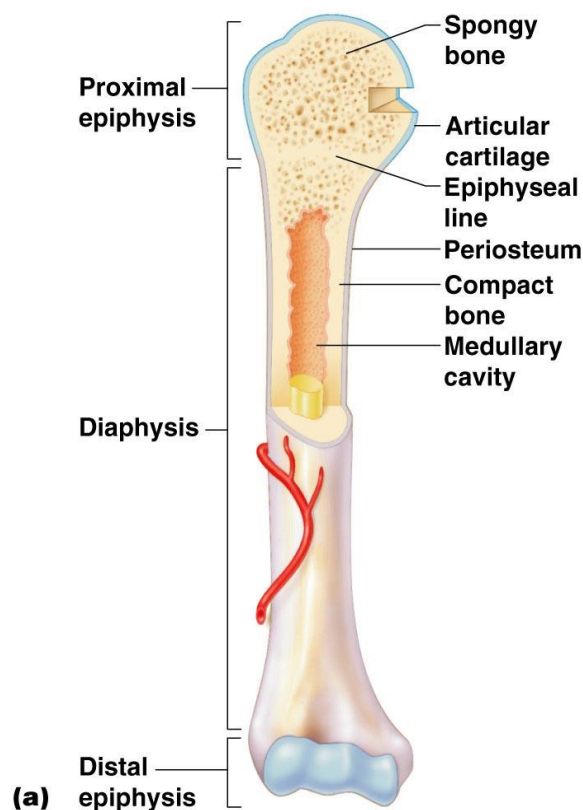
Types of Bone

There are two types of bones in the human skeleton, flat bones (ex: mandible, ilium, scapula) and long bones (ex: radius, tibia, femur). These types of bones not only differ by their anatomical structure but also by their primary development. Briefly, flat bones result from an intramembranous development while long bones undergo endochondral ossification, with cartilage as an intermediate stage.

In the case of long bones, different parts can be distinguished as in Figure 1. The shaft of the bone, called the diaphysis, consists of a hollow cylinder of dense, or compact, bone surrounding a marrow space. The compact bone in this location is the cortical bone. The methaphysis refers to the widened portion of bone situated in between the

diaphysis and the epiphysis. The metaphysis is occupied by cancellous, or trabecular bone, is organized into a three-dimensional latticework of inter-connecting struts of bone (trabeculae) that transmits forces between the joint and the shaft of the bone. This porous light bone composed of bone struts of 0.5mm of thickness, encloses spaces of 0.5mm to 1mm.

The epiphysis is the end of the long bone which supports the articular cartilage of the joint. The external surface of bone is called periosteum and the internal surface is the endosteum. Cortical bone fulfills a structural function and mechanical support, whereas trabecular bone serves to maintain mineral homeostasis as it contains the bone marrow.



Copyright © 2009 Pearson Education, Inc., publishing as Pearson Benjamin Cummings.

Figure 1: Long Bone Architecture.

Bone Tissue

Bone is a highly specialized connective tissue, formed by cells and of an extracellular bone matrix, that has different functions. It protects vital organs against trauma. It provides a rigid frame for organs and soft tissues performing the function of support, and it allows the locomotion (Mechanical Function). Bone participates in mineral storage and growth factors secretion (Metabolic Function). Moreover, bone tissue has also a hematopoietic function as it hosts bone marrow containing hematopoietic and mesenchymal stem cells (Forriol, 2009).

Bone Cells

There are five types of bone cells:

- Osteoprogenitor cells that derive from the bone marrow mesenchymal cells and will differentiate into osteoblasts.
- Osteoblasts are mononuclear cells that produce the bone extracellular matrix and are responsible for bone formation. They originate from mesenchymal stem cells. They secrete a wide variety of macromolecules such as collagen, alkaline phosphatase, osteonectin, fibronectin, vitronectin, osteopontin, and bone sialoprotein.
- Osteocytes are osteoblasts that have matured by being trapped inside the bone extracellular matrix. They make up 90% of mature bone cells. They have low synthesis activity, but it is believed that they are responsible for bone remodeling.
- Bone Lining cells correspond to osteoblasts that have concluded the synthesis of bone matrix and entered in a quiescent phase. These cells are localized in

the periosteum and the endosteum (Everts et al., 2002; Henriksen et al., 2009; Matsuo and Irie, 2008).

- Osteoclasts, are large and rounded multinucleated cells, specializing in bone resorption dissolving the proteinaceous bone matrix by the enzymatic activity of cathepsin K and matrix metalloproteinase 9. This activity is balanced with bone formation carried out by osteoblasts. They derive from the same hematopoietic precursors that give rise to monocytes and macrophages (Figure 2).

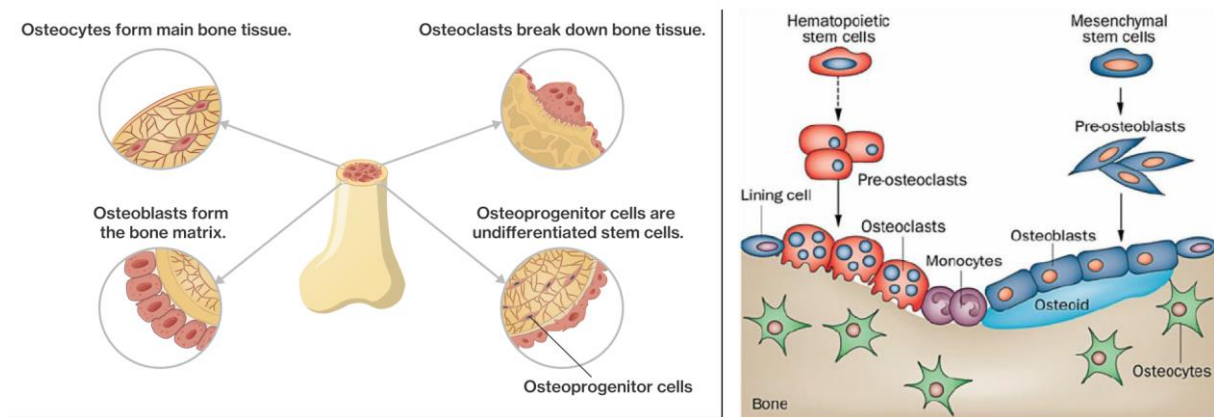


Figure 2 : Classification of bone cells based on source and function (Lian et al., 2012).

Extracellular Bone Matrix

The bone extracellular matrix is a complex connective tissue composed of an organic matrix (35% of total bone mass). This matrix presents mainly collagen fiber type I, approximately 90% of the extracellular matrix, and an inorganic matrix consisting of carbonated hydroxyapatite (HA) crystals. Only 20% of the bone is water. Non-collageneous bone proteins play an essential role in bone remodeling and osteogenesis. This group includes various growth factors, such as transforming growth

factor beta and bone morphogenetic proteins, cytokines, osteonectin, osteopontin, osteocalcin, bone sialoproteins, phosphoproteins thrombospondin, proteoglycans, Hyaluronic acid and phospholipids are also components of this extracellular matrix (Glimcher, 1989; Rho et al., 1998).

During life, bone tissue is continuously renewed by remodeling in order to repair the physiological micro-fractures but also to adapt to new mechanical constraints. Osteoclasts are responsible for the resorption of the bone tissues via acidification and enzymatic digestion processes. The formation of new bone is provided by osteoblasts, which can synthesize a matrix, which will imbibe carbonated hydroxyapatite to form bone tissue.

Bone Microscopic Structure

The principal mineral component in bone (45% of total bone mass), is calcium and phosphate in the form of hydroxyapatite. Osteoblasts secrete this mineral component in matrix vesicles. This crystalline precipitates of mineral permeate collagen type I protein substrate. At first, the bone is immature with its randomly oriented collagen fibers. This bone is named woven bone. Osteoclasts reabsorb this immature bone and replace it by new bone, the lamellar bone formed by osteoblasts in which collagen type I fibers are ordered and layered in alternating directions. This ordered extracellular matrix is a complex process. This procedure starts in the osteoblast and continues after secretion to form the triple-helical molecule, called tropocollagen. This alternating orientation of collagen fibers in different layers is essential to the mechanical strength and elasticity of the bone (Table 1). A capsule of collagen fibers covers the surface of the bone. These fibers are organized parallel to the surface of the bone. This capsule is called circumferential lamella. This proteinaceous matrix, known as osteoid, is the microenvironment where the mineral precipitates (Figure 3). Bone

morphogenetic platelet-derived growth factor, fibroblast growth factor, and other proteins as vitronectin control and regulate the hydroxyapatite crystals precipitation. This mineral precipitation impregnates the osteoid forming the composite material, the bone (Boskey and Robey, 2013; Combes and Rey, 2010; Ottani et al., 2001).

Compression tests	Resistance	167 – 213 MPa
	Young's modulus	14.7 – 34.3 GPa
Tracción test	Resistance	107 – 170 MPa
	Young's modulus	11.4 – 29.2 GPa
Bending tests	Resistance	103 – 238 MPa
	Young's modulus	9.8 – 15.7 GPa
Torsion test	Resistance	65 – 71 MPa
	Young's modulus	3.1 – 3.7 GPa

Table 1 : Values of maximum resistance and elastic modulus of human cortical bone for the different types of mechanical tests (Caeiro JR, 2013)

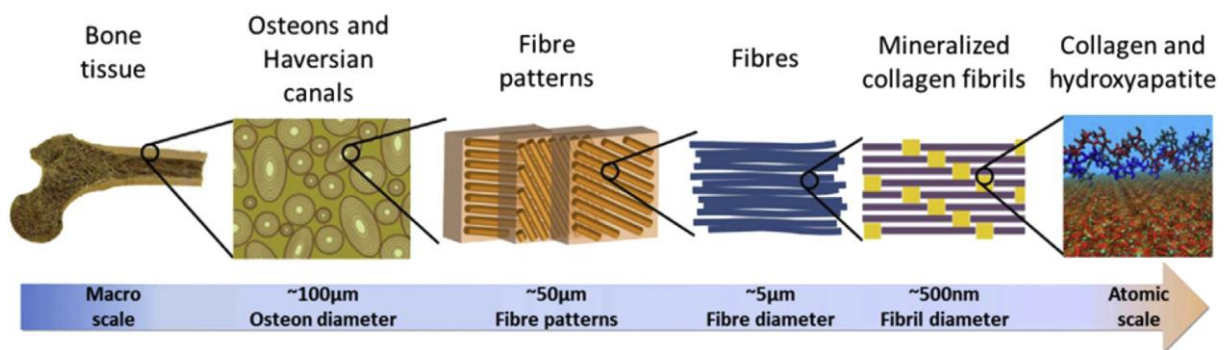


Figure 3 : Bone's microstructure. Macmillan Publishers Ltd:
Nature Communication.(Fielder and Nair, 2019)

The Haversian System

Cortical bone is too thick to allow the adequate nutrient of osteocytes. The Haversian system, composed of concentric cylinders of bone surrounding blood vessels and a nerve, ensure cortical bone vascularization (Figure 4). Blood vessels are located in a central Haversian canal oriented parallel to the long axis of the bone. One Haversian canal and its concentric lamella are called an osteon. The Haversian systems are interconnected by Volkmann's canal.

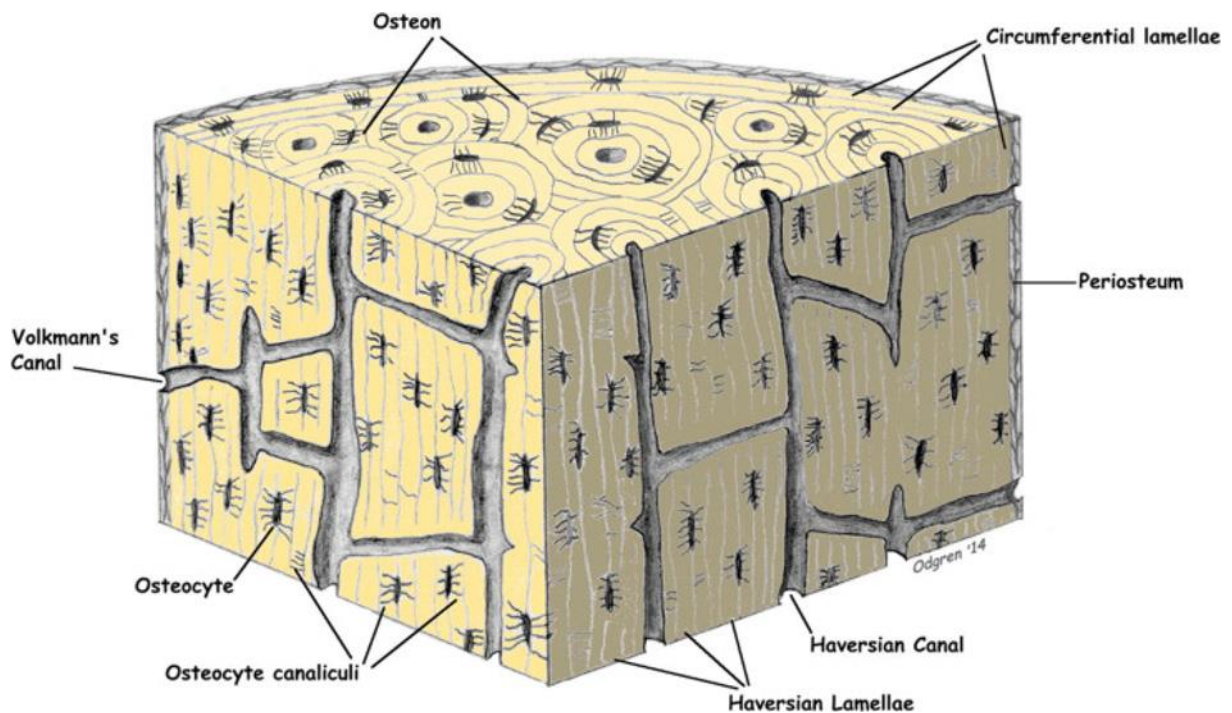


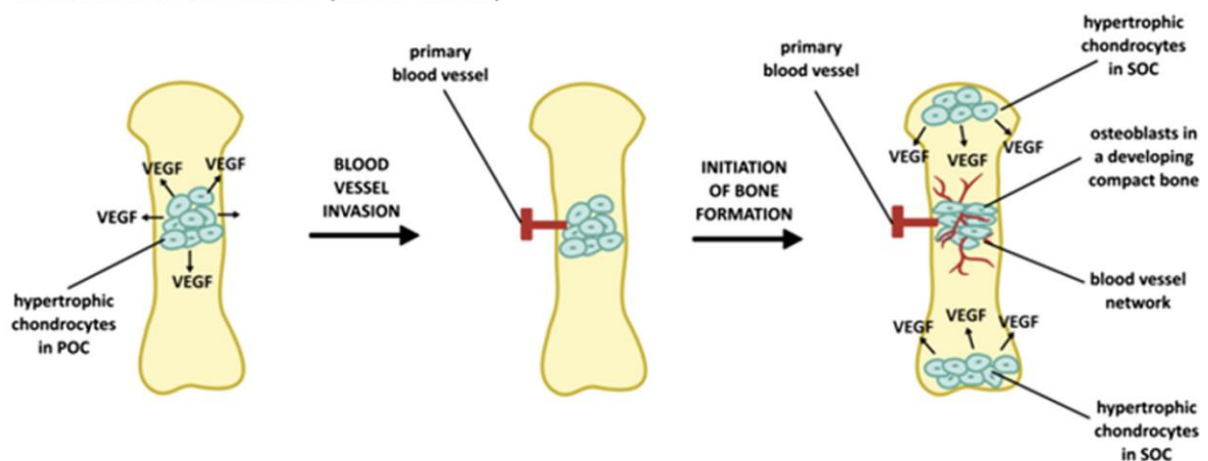
Figure 4 : *The Haversian System. (Johannesdottir et al. 2018)*

Vasculature of Bone

Bone is a highly vascularized tissue. This vascularization has a very important role in bone development, regeneration, and bone remodeling. The blood supply brings

oxygen, nutrients, and at the same time, growth factors that will stimulate bone cells activity. As described before, bone has two types of development, endochondral ossification, and intramembranous ossification (Figure 5). In both models, angiogenesis constitutes a crucial stage. This angiogenesis is dependent on the vascular endothelial growth factor (VEGF) produced by hypertrophic chondrocytes (endochondral ossification) or by the differentiation of the mesenchymal cells (intramembranous ossification) (Brandi and Collin-Osdoby, 2006; Dai and Rabie, 2007; Hankenson et al., 2011; Niedźwiedzki and Filipowska, 2015; Tomlinson and Silva, 2013)

A Endochondral ossification (LONG BONES)



B Intramembraneous ossification (FLAT BONES)

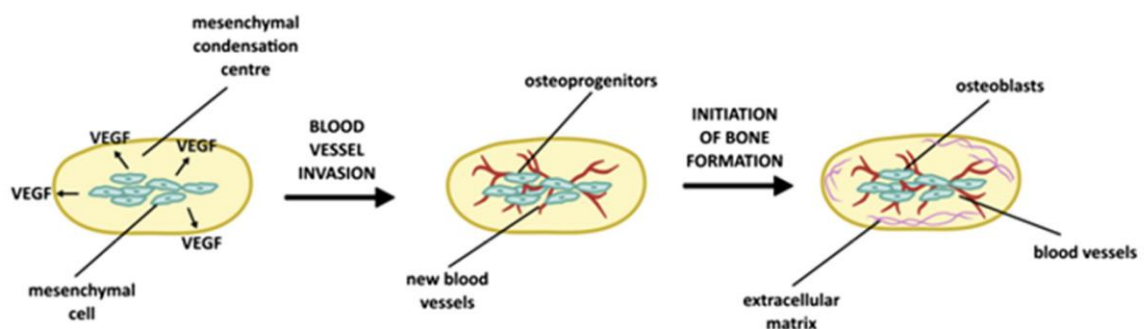


Figure 5 : Stages of blood vessel invasion during bone development.

(Liu Y et al. 2014)

During bone regeneration it was described that osteogenic precursor cells interact with endothelial cells type H enriched in the bone metaphysis at the endosteal surface. As shown in figure 6 Notch signaling activation and Noggin production regulates osteoprogenitor cells and osteogenesis (Kenswil et al., 2018; Kusumbe et al., 2014; Ramasamy et al., 2014)

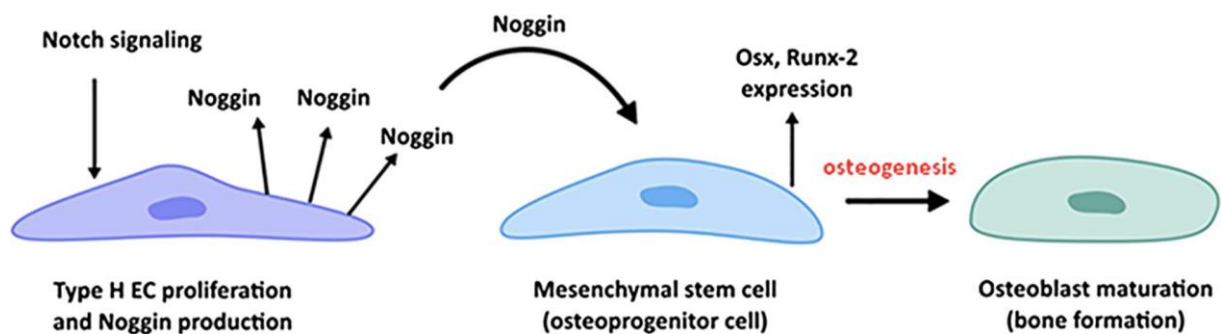


Figure 6 : Endothelial Notch signaling regulates osteogenesis (Filipowska et al. 2017).

The central nutrient artery, the epiphyseal metaphyseal vessels, and finally, the periosteal vessels are the three main systems for the long bone blood supply (Figure 7). The central nutrient artery supplies the entire medullar cavity and the 2/3 of the outer cortical bone. Periosteal arteries penetrate the outer cortical bone supplying the other 1/3. At the microscopic level, blood vessels of the long bones localize within the Haversian and Volkmann's canals in compact bone and further pass above the medullary cavity, penetrating the spongy bone. In flat bones periosteal arteries deliver the blood supply (Filipowska et al., 2017).

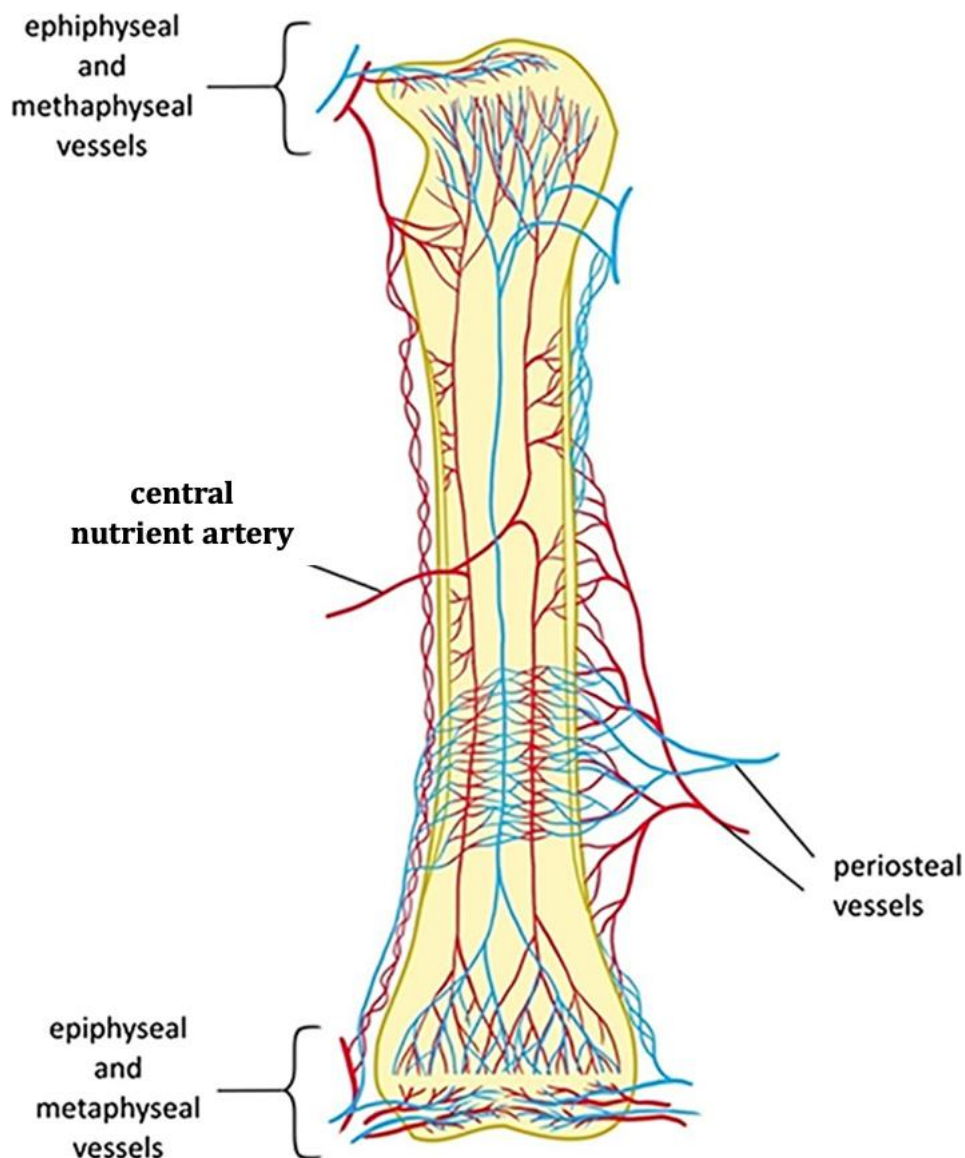


Figure 7 : Long bone vascular system. Arteries (red) Veins (blue) (Filipowska et al. 2017) (Brookes M, 1963)

Bone Healing

Following a trauma, a bone fracture is able to repair itself naturally in most cases. Bone healing is a progressive and continuous regeneration process that takes place in three main stages. In a first step, macrophages produce inflammatory cytokines such as interleukins-1 and -6 (IL-1, IL-6), tumor necrosis factor (TNF), Chemokine CC Ligand

2 (CCL2) that promote degradation. Fibrin clot and recruitment of mesenchymal stromal stem cells (MSCs). In a second step, MSCs differentiate into osteoblasts that produce an extracellular matrix composed of glycoproteins that evolve from a soft callus of fibro-cartilaginous tissue to a tissue rich in type I collagen fibers that progressively become impregnated with hydroxyapatite crystals. This latter process is accompanied by neovascularization stimulated by the secretion of pro-angiogenic cytokines such as fibroblast growth factor (FGF) or vascular endothelial growth factor (VEGF). MSCs progressively differentiate into osteoblasts and osteocytes embedded in the mineralized extracellular matrix. In this last step, a bone callus is remodeled under the concerted action of multinucleated cells, osteoclasts, capable of resorbing the mineralized extracellular matrix, and osteoblasts that produce it. This remodeling process provides mechanical consolidation and returns the bone to its original shape, with the recurrence of the medullary canal. Complete healing of a fracture usually requires 45 days (Matsuo and Irie, 2008). However, some fractures or bone loss, which may be due to trauma, bone resection related to infection or tumor, cannot regenerate spontaneously (Figure 8).

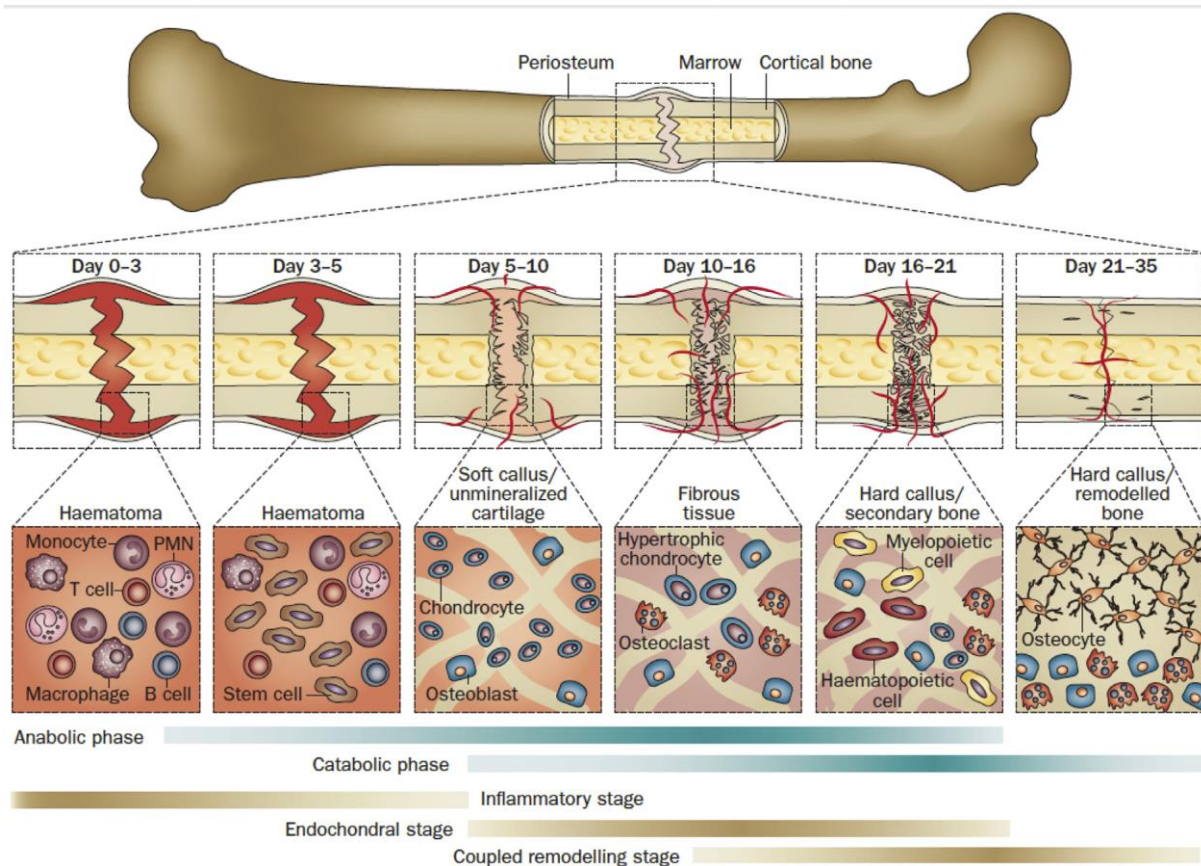
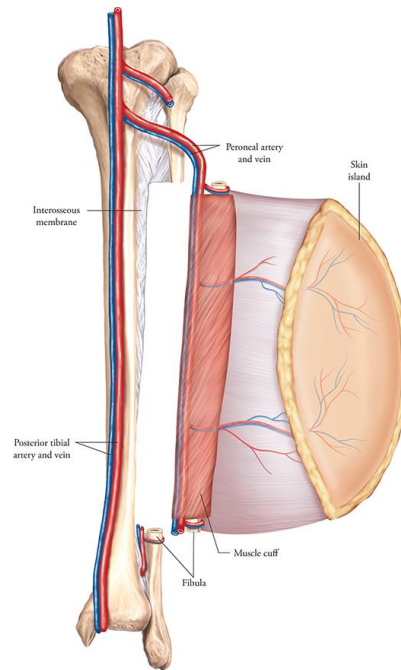


Figure 8 : Fracture healing process, biological events, and cellular activities at different phases. Macmillan Publishers Ltd: Nature Reviews Rheumatology. (Einhorn and Gerstenfeld, 2015)

State of the Art in Bone Regeneration

Large bone defects of critical size require a bone reconstruction surgery using most often bone taken from the patient, so called autologous bone grafting. Every year, more than one million patients benefit from bone reconstruction in Europe (Gómez-Barrena et al., 2011). The treatment of bone loss is based on autologous, allogeneic, or xenogeneic bone grafts and more recently to synthetic bone substitutes. The selection of the ideal bone graft is based on several factors such as the viability of the tissues, the shape, and volume of the defect. Autologous bone transplantation is still the gold standard for bone reconstruction because the autograft contains the patient's

cells and growth factors that promote tissue regeneration (Brydone et al., 2010; Dimitriou et al., 2011; Myeroff and Archdeacon, 2011; Oryan et al., 2014). Nevertheless, the reconstruction of large bone defects resulting from severe trauma or the resection of tumors and infections remains a challenge for orthopedic and plastic surgeons. In these severe cases, a bone flap with its vascular pedicle is taken from the patient's fibula and then transplanted into the site to be reconstructed, while vascularization is performed by microsurgery of the vessels (Figure 9) (Bakri et al., 2008; Campanacci et al., 2014; Garrigues et al., 2009; Innocenti et al., 2009). Although autologous bone graft transplantation remains the gold standard in bone regeneration, this technique has some disadvantages for the patient. The main problem is the need for a second operative site to harvest bone graft, which can lead to morbidity, severe pain, hematoma, infections, and wounds (Sawin et al., 1998). Besides, the amount and possibilities of taking bone from the patient are limited. Finally, complex surgical reconstructions require the shaping of the graft to adapt to the anatomical shape of the defect and microsurgical techniques to ensure its vascularization. Alternatively, allogeneic and xenogeneic bone grafts that do not require sampling from the patient are less osteogenic and may induce immunogenic rejection (Bucholz, 2002; De Long et al., 2007).



Source: Shane Y. Morita, Charles M. Balch, V. Suzanne Klimberg, Timothy M. Pawlik, Mitchell C. Posner, Kenneth K. Tanabe: *Textbook of Complex General Surgical Oncology*; www.accesssurgery.com
Copyright © McGraw-Hill Education. All rights reserved.

Figure 9 : Principle of transplantation of an autologous vascularized bone graft from the fibula (*Textbook of Complex General Surgical Oncology* -Shane Y. Morita, Charles M. Balch, V. Suzanne Klimberg, Timothy M. Pawlik, Mitchell C. Posner, Kenneth K. Tanabe).

Synthetic bone substitutes made of calcium phosphates have osteoconductive properties thus able to guide bone growth. However, these biomaterials have insufficient regenerative properties for large bone defect regeneration. Many groups have therefore added MSCs or BMPs to calcium phosphate biomaterials to regenerate bone and the field of tissue engineering has emerged.

Tissue engineering is potentially a promising alternative to autologous bone grafting (Rosset et al., 2014; Tang et al., 2016). Tissue engineering involves associating a biocompatible material with cells or biological factors in order to replace or repair tissues or organs and thus restore and regenerate their function within the body (Hutmacher et al., 2007; Kneser et al., 2006a; Langer and Vacanti, 1993). In bone

regeneration, a matrix (scaffold) serving as a support for cells and healing is needed. Among different biomaterials, calcium phosphate bioceramics that are chemically comparable to bone mineral are the most suitable because they have osteoconductive or guided bone regeneration properties (Albrektsson and Johansson, 2001; Fellah et al., 2006). The mesenchymal stromal stem cells present in human tissues in a very small proportion intervene in the healing of connective tissues, such as bone. These cells can be isolated from bone marrow or adipose tissue and amplified in culture. As shown in Figure 10, the vascular, stromal fraction of adipose tissue contains mesenchymal stromal stem cells and endothelial cells that can stimulate bone healing and angiogenesis.

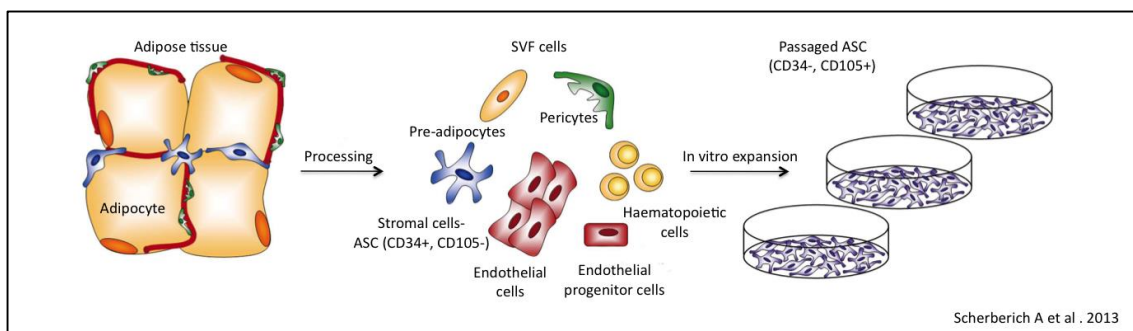


Figure 10 : Obtaining stromal vascular fraction (SVF) from adipose tissue and culturing mesenchymal stromal stem cells (MSCs) according to (Scherberich et al., 2013).

Numerous pre-clinical studies have demonstrated that the combination of MSCs with biphasic calcium phosphate (BCP) biomaterials can induce bone formation and facilitate the healing of critical-size defects (Brennan et al., 2014; Corre et al., 2015; Gamblin et al., 2014; Mankani et al., 2006). Some clinical trials have demonstrated the feasibility of amplifying autologous MSCs in culture from a bone marrow sample and associating them with a BCP biomaterial to regenerate unconsolidated fractures or bone loss in small volumes (Gómez-Barrena et al., 2011; Quarto et al., 2001).

However, these tissue engineering techniques do not yet allow the regeneration of large bone defects because of the absence of a sufficient vascular network to ensure cell survival and tissue healing (Kanczler and Oreffo, 2008; Lovett et al., 2009). In this context, several teams proposed the pre-vascularization of the bone filling material by implantation in an ectopic site before transplanting it into the defect to be reconstructed. Proof of concept has been demonstrated at the pre-clinical level by ectopic implantation in the ewe of a chamber containing the BCP biomaterial and an arteriovenous fistula (vascular loop). After 6 and 12 weeks of implantation, abundant microvasculature was observed in the chamber contents (Beier et al., 2010; Erol and Sira, 1980; Kaempfen et al., 2015; Kneser et al., 2006b; Kokemueller et al., 2010; Warnke et al., 2006). Large defects at the mandibular level have been successfully reconstructed in a few patients using this technique of transplanting a pre-vascularized biomaterial into an intramuscular site (Mesimäki et al., 2009; Warnke et al., 2004); In these studies, the pre-vascularization of the biomaterial appears to dominate for cell survival and bone regeneration.

Objectives of the Thesis

The aim of the present Philosophy Doctor (PhD) thesis was to develop new strategies for large bone defects regeneration by using vascularization and 3D printing.

Specific objectives of the thesis were:

- 1) To review the current surgical techniques and possible future methods for regeneration of large bone defects (Paper I)
- 2) To study the effect of pre-vascularization of a synthetic bone substitute contained in a 3D printed chamber prior to its transplantation into a segmental critical size defect in the ulna of rabbits (Paper II).

- 3) To develop and produce surgical guides and personalized 3D printed scaffolds for bone large defect reconstruction with local vascularization in a one-step surgery in segmental metatarsus of sheep. (Paper III).

REFERENCES

1. Albrektsson, T., and Johansson, C. (2001). Osteoinduction, osteoconduction and osseointegration. *Eur Spine J* 10, S96–S101.
2. Bakri, K., Stans, A., Mardini, S., and Moran, S. (2008). Combined Massive Allograft and Intramedullary Vascularized Fibula Transfer: The Capanna Technique for Lower-Limb Reconstruction. *Seminars in Plastic Surgery* 22, 234–241.
3. Beier, J.P., Horch, R.E., Hess, A., Arkudas, A., Heinrich, J., Loew, J., Gulle, H., Polykandriotis, E., Bleiziffer, O., and Kneser, U. (2010). Axial vascularization of a large volume calcium phosphate ceramic bone substitute in the sheep AV loop model. *J Tissue Eng Regen Med* 4, 216–223.
4. Boskey, A.L., and Robey, P.G. (2013). The Composition of Bone. In *Primer on the Metabolic Bone Diseases and Disorders of Mineral Metabolism*, (John Wiley & Sons, Ltd), pp. 49–58.
5. Brandi, M.L., and Collin-Osdoby, P. (2006). Vascular biology and the skeleton. *J. Bone Miner. Res.* 21, 183–192.
6. Brennan, M.Á., Renaud, A., Amiaud, J., Rojewski, M.T., Schrezenmeier, H., Heymann, D., Trichet, V., and Layrolle, P. (2014). Pre-clinical studies of bone regeneration with human bone marrow stromal cells and biphasic calcium phosphate. *Stem Cell Res Ther* 5.
7. Brydone, A.S., Meek, D., and Maclaine, S. (2010). Bone grafting, orthopaedic biomaterials, and the clinical need for bone engineering. *Proc Inst Mech Eng H* 224, 1329–1343.
8. Bucholz, R.W. (2002). Nonallograft osteoconductive bone graft substitutes. *Clin. Orthop. Relat. Res.* 44–52.
9. Caeiro JR (2013). Biomechanics and bone (& II) : Trials in different hierarchical levels of bone and alternative tools for the determination of bone strength. p.
10. Campanacci, D.A., Puccini, S., Caff, G., Beltrami, G., Piccioli, A., Innocenti, M., and Capanna, R. (2014). Vascularised fibular grafts as a salvage procedure in failed intercalary reconstructions after bone tumour resection of the femur. *Injury* 45, 399–404.
11. Combes, C., and Rey, C. (2010). Amorphous calcium phosphates: Synthesis, properties and uses in biomaterials. *Acta Biomaterialia* 6, 3362–3378.

12. Corre, P., Merceron, C., Longis, J., Khonsari, R.H., Pilet, P., Thi, T.N., Battaglia, S., Sourice, S., Masson, M., Sohier, J., et al. (2015). Direct comparison of current cell-based and cell-free approaches towards the repair of craniofacial bone defects - A preclinical study. *Acta Biomater* 26, 306–317.
13. Cruess, R.L., and Dumont, J. (1975). Fracture healing. *Can J Surg* 18, 403–413.
14. Dai, J., and Rabie, A.B.M. (2007). VEGF: an essential mediator of both angiogenesis and endochondral ossification. *J. Dent. Res.* 86, 937–950.
15. De Long, W.G., Einhorn, T.A., Koval, K., McKee, M., Smith, W., Sanders, R., and Watson, T. (2007). Bone grafts and bone graft substitutes in orthopaedic trauma surgery. A critical analysis. *J Bone Joint Surg Am* 89, 649–658.
16. Dimitriou, R., Jones, E., McGonagle, D., and Giannoudis, P.V. (2011). Bone regeneration: current concepts and future directions. *BMC Medicine* 9.
17. Einhorn, T.A., and Gerstenfeld, L.C. (2015). Fracture healing: mechanisms and interventions. *Nat Rev Rheumatol* 11, 45–54.
18. Erol, O.O., and Sira, M. (1980). New capillary bed formation with a surgically constructed arteriovenous fistula. *Plast. Reconstr. Surg.* 66, 109–115.
19. Everts, V., Delaissé, J.M., Korper, W., Jansen, D.C., Tigchelaar-Gutter, W., Saftig, P., and Beertsen, W. (2002). The bone lining cell: its role in cleaning Howship's lacunae and initiating bone formation. *J. Bone Miner. Res.* 17, 77–90.
20. Fellah, B.H., Weiss, P., Gauthier, O., Rouillon, T., Pilet, P., Daculsi, G., and Layrolle, P. (2006). Bone repair using a new injectable self-crosslinkable bone substitute. *J. Orthop. Res.* 24, 628–635.
21. Fielder, M., and Nair, A.K. (2019). Effects of hydration and mineralization on the deformation mechanisms of collagen fibrils in bone at the nanoscale. *Biomech Model Mechanobiol* 18, 57–68.
22. Filipowska, J., Tomaszewski, K.A., Niedźwiedzki, Ł., Walocha, J.A., and Niedźwiedzki, T. (2017). The role of vasculature in bone development, regeneration and proper systemic functioning. *Angiogenesis* 20, 291–302.
23. Forriol, F. (2009). Growth factors in cartilage and meniscus repair. *Injury* 40 *Suppl 3*, S12-16.
24. Gamblin, A.-L., Brennan, M.A., Renaud, A., Yagita, H., Lézot, F., Heymann, D., Trichet, V., and Layrolle, P. (2014). Bone tissue formation with human

- mesenchymal stem cells and biphasic calcium phosphate ceramics: The local implication of osteoclasts and macrophages. *Biomaterials* 35, 9660–9667.
25. Garrigues, G.E., Aldridge, J.M., Friend, J.K., and Urbaniak, J.R. (2009). Free Vascularized Fibular Grafting for treatment of osteonecrosis of the femoral head secondary to hip dislocation. *Microsurgery* 29, 342–345.
 26. Glimcher, M.J. (1989). Mechanism of calcification: role of collagen fibrils and collagen-phosphoprotein complexes in vitro and in vivo. *Anat. Rec.* 224, 139–153.
 27. Gómez-Barrena, E., Rosset, P., Müller, I., Giordano, R., Bunu, C., Layrolle, P., Konttinen, Y.T., and Luyten, F.P. (2011). Bone regeneration: stem cell therapies and clinical studies in orthopaedics and traumatology. *J Cell Mol Med* 15, 1266–1286.
 28. Hadjidakis, D.J., and Androulakis, I.I. (2006). Bone remodeling. *Ann. N. Y. Acad. Sci.* 1092, 385–396.
 29. Hankenson, K.D., Dishowitz, M., Gray, C., and Schenker, M. (2011). Angiogenesis in bone regeneration. *Injury* 42, 556–561.
 30. Henriksen, K., Neutzsky-Wulff, A.V., Bonewald, L.F., and Karsdal, M.A. (2009). Local communication on and within bone controls bone remodeling. *Bone* 44, 1026–1033.
 31. Hutmacher, D.W., Schantz, J.T., Lam, C.X.F., Tan, K.C., and Lim, T.C. (2007). State of the art and future directions of scaffold-based bone engineering from a biomaterials perspective. *J Tissue Eng Regen Med* 1, 245–260.
 32. Innocenti, M., Abed, Y.Y., Beltrami, G., Delcroix, L., Manfrini, M., and Capanna, R. (2009). Biological reconstruction after resection of bone tumors of the proximal tibia using allograft shell and intramedullary free vascularized fibular graft: long-term results. *Microsurgery* 29, 361–372.
 33. Kaempfen, A., Todorov, A., Güven, S., Largo, R.D., Jaquiéry, C., Scherberich, A., Martin, I., and Schaefer, D.J. (2015). Engraftment of Prevascularized, Tissue Engineered Constructs in a Novel Rabbit Segmental Bone Defect Model. *Int J Mol Sci* 16, 12616–12630.
 34. Kanczler, J.M., and Oreffo, R.O.C. (2008). Osteogenesis and angiogenesis: the potential for engineering bone. *Eur Cell Mater* 15, 100–114.
 35. Kenswil, K.J.G., Jaramillo, A.C., Ping, Z., Chen, S., Hoogenboezem, R.M., Mylona, M.A., Adisty, M.N., Bindels, E.M.J., Bos, P.K., Stoop, H., et al. (2018).

- Characterization of Endothelial Cells Associated with Hematopoietic Niche Formation in Humans Identifies IL-33 As an Anabolic Factor. *Cell Reports* 22, 666–678.
36. Kneser, U., Schaefer, D.J., Polykandriotis, E., and Horch, R.E. (2006a). Tissue engineering of bone: the reconstructive surgeon's point of view. *Journal of Cellular and Molecular Medicine* 10, 7–19.
37. Kneser, U., Polykandriotis, E., Ohnolz, J., Heidner, K., Grabinger, L., Euler, S., Amann, K.U., Hess, A., Brune, K., Greil, P., et al. (2006b). Engineering of vascularized transplantable bone tissues: induction of axial vascularization in an osteoconductive matrix using an arteriovenous loop. *Tissue Eng.* 12, 1721–1731.
38. Kokemueller, H., Spalthoff, S., Nolff, M., Tavassol, F., Essig, H., Stuehmer, C., Bormann, K.-H., Rücker, M., and Gellrich, N.-C. (2010). Prefabrication of vascularized bioartificial bone grafts in vivo for segmental mandibular reconstruction: experimental pilot study in sheep and first clinical application. *International Journal of Oral and Maxillofacial Surgery* 39, 379–387.
39. Kusumbe, A.P., Ramasamy, S.K., and Adams, R.H. (2014). Coupling of angiogenesis and osteogenesis by a specific vessel subtype in bone. *Nature* 507, 323–328.
40. Langer, R., and Vacanti, J.P. (1993). Tissue engineering. *Science* 260, 920–926.
41. Lian, J.B., Stein, G.S., van Wijnen, A.J., Stein, J.L., Hassan, M.Q., Gaur, T., and Zhang, Y. (2012). MicroRNA control of bone formation and homeostasis. *Nat Rev Endocrinol* 8, 212–227.
42. Lovett, M., Lee, K., Edwards, A., and Kaplan, D.L. (2009). Vascularization Strategies for Tissue Engineering. *Tissue Engineering Part B: Reviews* 15, 353–370.
43. Mankani, M.H., Kuznetsov, S.A., Wolfe, R.M., Marshall, G.W., and Robey, P.G. (2006). In vivo bone formation by human bone marrow stromal cells: reconstruction of the mouse calvarium and mandible. *Stem Cells* 24, 2140–2149.
44. Marsh, D. (1998). Concepts of fracture union, delayed union, and nonunion. *Clin. Orthop. Relat. Res.* S22-30.
45. Matsuo, K., and Irie, N. (2008). Osteoclast-osteoblast communication. *Arch.*

- Biochem. Biophys. 473, 201–209.
46. Mesimäki, K., Lindroos, B., Törnwall, J., Mauno, J., Lindqvist, C., Kontio, R., Miettinen, S., and Suuronen, R. (2009). Novel maxillary reconstruction with ectopic bone formation by GMP adipose stem cells. *Int J Oral Maxillofac Surg* 38, 201–209.
 47. Myeroff, C., and Archdeacon, M. (2011). Autogenous bone graft: donor sites and techniques. *J Bone Joint Surg Am* 93, 2227–2236.
 48. Neto, A.S., and Ferreira, J.M.F. (2018). Synthetic and Marine-Derived Porous Scaffolds for Bone Tissue Engineering. *Materials (Basel)* 11.
 49. Niedźwiedzki, T., and Filipowska, J. (2015). Bone remodeling in the context of cellular and systemic regulation: the role of osteocytes and the nervous system. *J. Mol. Endocrinol.* 55, R23-36.
 50. Oryan, A., Alidadi, S., Moshiri, A., and Maffulli, N. (2014). Bone regenerative medicine: classic options, novel strategies, and future directions. *J Orthop Surg Res* 9, 18.
 51. Ottani, V., Raspanti, M., and Ruggeri, A. (2001). Collagen structure and functional implications. *Micron* 32, 251–260.
 52. Quarto, R., Mastrogiacomo, M., Cancedda, R., Kutepov, S.M., Mukhachev, V., Lavroukov, A., Kon, E., and Marcacci, M. (2001). Repair of Large Bone Defects with the Use of Autologous Bone Marrow Stromal Cells. *New England Journal of Medicine* 344, 385–386.
 53. Ramasamy, S.K., Kusumbe, A.P., Wang, L., and Adams, R.H. (2014). Endothelial Notch activity promotes angiogenesis and osteogenesis in bone. *Nature* 507, 376–380.
 54. Rho, J.Y., Kuhn-Spearing, L., and Zioupos, P. (1998). Mechanical properties and the hierarchical structure of bone. *Med Eng Phys* 20, 92–102.
 55. Rosset, P., Deschaseaux, F., and Layrolle, P. (2014). Cell therapy for bone repair. *Orthop Traumatol Surg Res* 100, S107-112.
 56. Sawin, P.D., Traynelis, V.C., and Menezes, A.H. (1998). A comparative analysis of fusion rates and donor-site morbidity for autogeneic rib and iliac crest bone grafts in posterior cervical fusions. *J. Neurosurg.* 88, 255–265.
 57. Scherberich, A., Di Maggio, N.D., and McNagny, K.M. (2013). A familiar stranger: CD34 expression and putative functions in SVF cells of adipose tissue. *World J Stem Cells* 5, 1–8.

58. Schmitz, J.P., and Hollinger, J.O. (1986). The critical size defect as an experimental model for craniomandibulofacial nonunions. *Clin. Orthop. Relat. Res.* 299–308.
59. Tang, D., Tare, R.S., Yang, L.-Y., Williams, D.F., Ou, K.-L., and Oreffo, R.O.C. (2016). Biofabrication of bone tissue: approaches, challenges and translation for bone regeneration. *Biomaterials* 83, 363–382.
60. Tomlinson, R.E., and Silva, M.J. (2013). Skeletal Blood Flow in Bone Repair and Maintenance. *Bone Research* 1, 311–322.
61. Warnke, P.H., Springer, I.N.G., Wiltfang, J., Acil, Y., Eufinger, H., Wehmöller, M., Russo, P. a. J., Bolte, H., Sherry, E., Behrens, E., et al. (2004). Growth and transplantation of a custom vascularised bone graft in a man. *Lancet* 364, 766–770.
62. Warnke, P.H., Wiltfang, J., Springer, I., Acil, Y., Bolte, H., Kosmahl, M., Russo, P.A.J., Sherry, E., Lützen, U., Wolfart, S., et al. (2006). Man as living bioreactor: fate of an exogenously prepared customized tissue-engineered mandible. *Biomaterials* 27, 3163–3167.

CHAPTER I

Reconstruction of large skeletal defects : current clinical therapeutic strategies and future directions using 3D printing

Luciano Vidal^{1,§}, Carina Kampleitner^{2,§}, Meadhbh Á Brennan^{1,3}, Alain Hoornaert^{1,3},
Pierre Layrolle^{1*}

1 Inserm, UMR 1238, PHY-OS, Bone sarcomas and remodeling of calcified tissues,
Faculty of Medicine, University of Nantes, Nantes, France

2 Department of Pharmacology and Toxicology, University of Vienna, Vienna, Austria

3 Harvard School of Engineering and Applied Sciences, Harvard University,
Cambridge, Massachusetts 02138, USA

4 CHU Nantes, Department of Implantology, Faculty of Dental Surgery, University of
Nantes, Nantes, France

§ These authors contributed equally to this work.

* Correspondence:

Pierre Layrolle, PhD, Director of Research

pierre.layrolle@inserm.fr

**Keywords: large bone defects, bone regeneration, tissue engineering,
vascularization, three-dimensional printing**

Abstract

The healing of bone fractures is a well-orchestrated physiological process involving multiple cell types and signaling molecules interacting at the fracture site to replace and repair bone tissue without scar formation. However, when the lesion is too large, normal healing is compromised. These so-called non-union bone fractures, mostly arising due to trauma, tumor resection or disease, represent a major therapeutic challenge for orthopedic and reconstructive surgeons. In this review, we firstly present the current commonly employed surgical strategies comprising auto-, allo- and xenograft transplantations as well as synthetic biomaterials. Further to this, we discuss the multiple factors influencing the effectiveness of the reconstructive therapy. One essential parameter is adequate vascularization that ensures the vitality of the bone grafts and therefore supports the regeneration process, with deficient vascularization presenting as a serious problem frequently encountered in current management strategies. To address this challenge, vascularized bone grafts, including free or pedicled fibula flaps, or in situ approaches using the Masquelet induced membrane, or the patient's body as a bioreactor, comprise feasible alternatives. Finally, we highlight future challenges and novel strategies such as 3D printing and bioprinting which could overcome some of the current challenges in the field of bone defect reconstruction, with the benefit of fabricating personalized and vascularized scaffolds.

1. Introduction

The reconstruction of large bone defects caused by trauma, disease or tumor resection is a fundamental challenge for orthopedic and plastic surgeons. Their critical size exceeds the intrinsic capacity of self-regeneration and consequently bone repair is delayed and impaired. This type of lesion is termed a nonunion bone fracture and requires additional treatment with bone graft materials in order to restore pre-existing function (Dimitriou et al., 2011). Successful bone augmentation procedures should include an osteoconductive scaffold with sufficient mechanical stability, an osteoinductive stimulus to induce osteogenesis, and should enable osseointegration and vascularity (Albrektsson and Johansson, 2001; Giannoudis et al., 2008). The currently available treatment strategies of bone loss are based on autologous, allogeneic or xenogeneic bone transplantation, as well as synthetic biomaterials. Although autologous bone grafting still represents the gold standard technique for large bone reconstruction, several factors limit its application. A major restricting parameter is the volume of bone needed to treat this type of injury, as well as the associated pain and possible donor site complications due to the additional surgical intervention at the bone harvest site. Similar disadvantages are observed for allogenic bone grafts including morbidity, immunogenic reactions, transfer of diseases and limited osteogenic properties. Furthermore, many of these standard clinical grafting approaches fail due to the lack of adequate vascularization. Insufficient vascularity of the fracture site reduces the exchange of gas, nutrients and waste between the tissue and the blood system, as well as the delivery of cells to the site of injury, leading to inner graft necrosis (Mercado-Pagan et al., 2015; Fernandez de Grado et al., 2018). To circumvent this problem, vascularized bone transfers, either pedicled or free flaps, represent an excellent option that ensures bone vitality and avoids graft resorption.

Nevertheless, complex fractures and their reconstructions require modeling of the transferred bone to adapt to the anatomical shape and extensive microsurgical techniques to connect the graft to the blood system. Some patient bioreactor attempts have also been made whereby a customized bone graft is implanted ectopically in the patient for several weeks before transferring it into the bone defect. Innovative fabrication approaches in the field of bone tissue engineering include 3D printing and bioprinting to enable ex vivo personalized bone graft based on anatomical medical imaging. They are generally composed of calcium phosphate/polymer composites or porous titanium. To enhance the material healing properties, 3D printed scaffolds can potentially include cells, growth factors, and vasculature. In this review, we present the current techniques clinically available for the reconstruction of critical-sized bone defects and point out future challenges and possibilities of new treatment modalities using customized and vascularized bone grafts with a focus on 3D printing and bioprinting fabrication methods.

2. Present management strategies for large bone lesions

The current reconstructive options for large bone defects including autologous iliac grafting, autologous vascularized fibula transplantation, Masquelet's induced membrane, massive allografts and in vivo patient bioreactor strategies are presented in Figure 1 and discussed in this section.

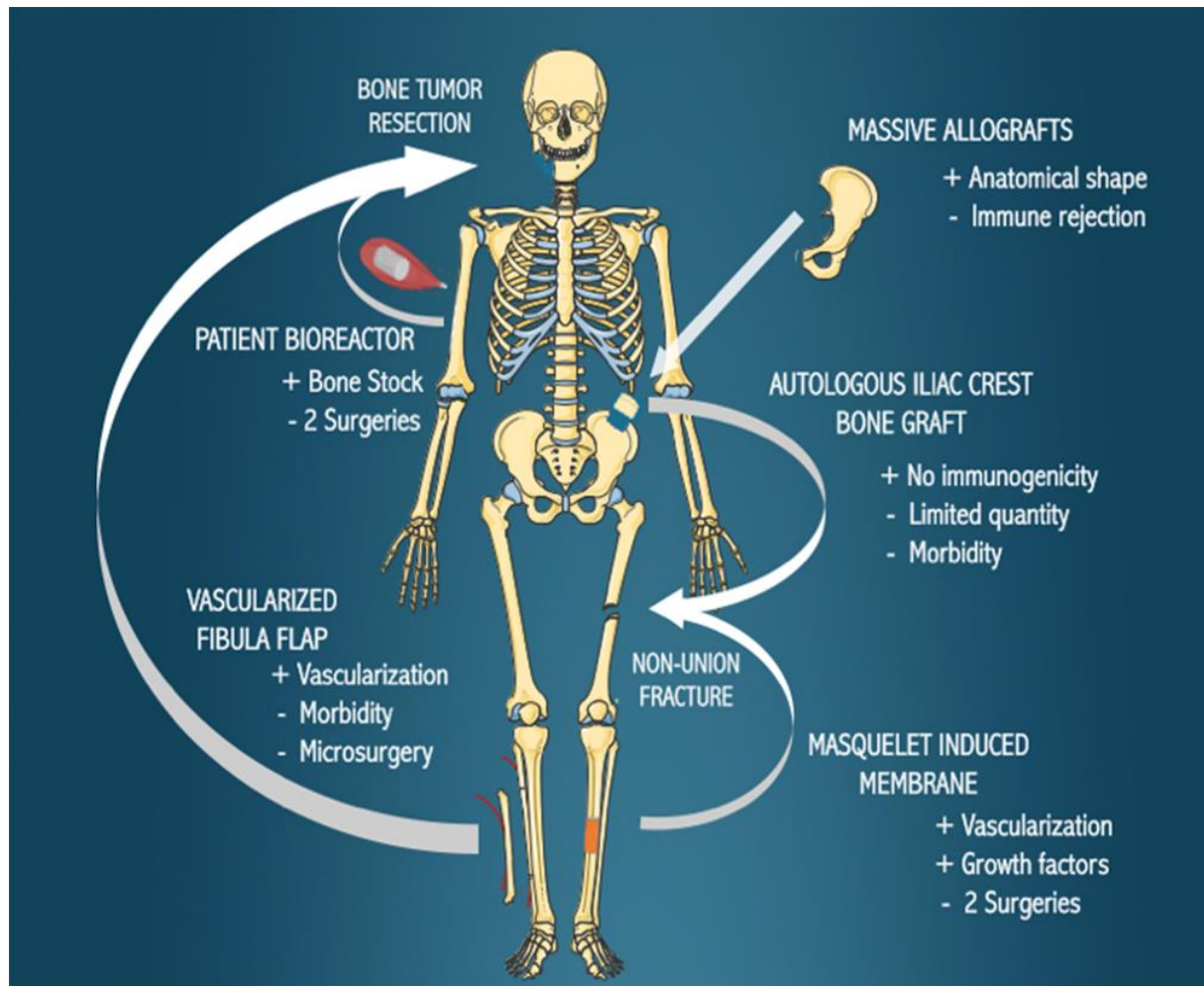


Figure 1 : Current biological bone reconstruction techniques. Bone defects arising due to the resection of tumors or non-union fractures can be treated with the various methods indicated, with the benefits (+) and disadvantages (-) of each technique outlined.

2.1. Bone grafts

The leading treatment for bone defect reconstruction remains bone grafting. The purpose of a bone graft is to support the repair process through osteoinduction, osteoconduction, and osteogenesis (Albrektsson and Johansson, 2001; Oryan et al., 2014). They can be categorized into different types based on the tissue source: autologous, allogeneic and xenogeneic bone grafts, as well as synthetic and biological biomaterials (Brydone et al., 2010). The selection of the ideal bone graft depends on

several factors including the geometry, size and tissue viability of the bone defect, the biological and biomechanically characteristics of the bone graft, and the known advantages and associated complications of each graft option (Laurencin et al., 2014).

2.1.1. Autografts

Autologous bone grafting, still the clinical standard reconstruction technique, entails harvesting bone tissue from an anatomical donor site and transplanting it to the recipient defect site (Sanan and Haines, 1997). The iliac crest is the preferred harvesting site for this type of transplant, whereby approximately 20 cm³ of cancellous bone is collected and used as a bone block or morselized into bone chips in order to fill a bone defect (Athanasίου et al., 2010). Autologous bone contains the patient's own osteogenic cells and osteoinductive proteins, such as BMP-2, BMP-7, and PDGF, providing an optimal osteogenic, osteoinductive, and osteoconductive properties without risk of viral transmissions, while pain, hematoma, and possible visceral injuries at the donor site and extended surgery time because of the two surgical sites are the main drawbacks (Albrektsson and Johansson, 2001; Parikh, 2002). Another disadvantage of cancellous bone grafting is that large amounts of bone graft cannot be obtained for critical-sized defect reconstruction (Oryan et al., 2013). Successful repair depends on osteogenic cell survival and tissue viability after transplantation to the recipient site, while neovascularization plays a determinant role. To overcome the disadvantage of limited vascularization, free vascularized bone flaps have been employed. Taylor et al reported the first successful large bone defect reconstruction using a free vascularized bone transfer (Taylor et al., 1975). Vascularized bone grafts, such as an autologous vascularized fibula flap, iliac crest flap, rib flap, and radius flap, allow the reconstruction of large bone defects and are often used as a last resort to avoid limb amputation for patients. Fibula and iliac crest free flaps have been used for

the pelvis, head of long bones, and neck reconstruction. Free flaps are particularly suitable for mandible reconstructions after ballistic trauma or tumor resections. An optimal option for bone large defect reconstruction using autografts is a vascularized cortical autografts (Rizzo and Moran, 2008). For a hemimandible, the iliac crest flap has an adequate bone height to ensure osseointegration (Taylor, 1982; 1983; 1985) and allows optimal shape reconstruction of the mandible ramus. However, for an angle to angle mandible reconstruction, fibula free flap is preferred. As shown in Figure 2, the fibula is dissected, harvested with a vascular pedicle, shaped and transplanted into the bone defect where it is reconnected to the local vasculature. This vascularized bone graft contains the patient's own cells, growth factors and a vascularization bed thereby reducing graft resorption, enhances healing and permitting better diffusion of antibiotics. Hidalgo et al. evaluated the fibula flap for mandible reconstruction and reported long-term outstanding functional and aesthetic results, without bone resorption in non-irradiated and irradiated patients (Hidalgo and Pusic, 2002). Free fibula flap transfers for mandibular and maxillary reconstruction achieved 98.7% graft survival in some studies (Peng et al., 2005; Taylor et al., 2016). Further to this, pelvic ring reconstruction employing a double-barreled free vascularized autologous patient fibula grafts after resection of malignant pelvic bone tumors was reported (Ogura et al., 2015). Additionally, lumbosacral spinal defects reconstruction was also achieved with the use of a fibula free flap (Moran et al., 2009). The major complications of free flaps are post-operative vascular thrombosis and associated tissue necrosis, laborious microsurgery to reconnect to the vasculature, and the need for sculpting of the graft to fit the anatomy of the bone defect. Furthermore, this technique requires extended anesthesia, specialized technical surgical skills and the sacrifice of blood vessels.

2.1.2. Allografts

Bone allografts are harvested from living donors during joint replacement (e.g., femoral heads) or from cadavers, and stored frozen and processed and transplanted into another patient (Keating and McQueen, 2001). Given the limitations of autografts, allografts became an alternative to large bone defect reconstruction. Allografts are used as powders, chips or complete bone structural forms, so called massive allografts and can be provided as a fresh graft, fresh-frozen, freeze-dried, demineralized, delipidized by solvents or supercritical carbon dioxide, and sterilized by irradiation (Bostrom and Seigerman, 2005; Zimmermann and Moghaddam, 2011). The primary advantage of allografts is their immediate availability in different sizes and shapes (Muscolo et al., 2004). They are composed of the extracellular bone matrix containing growth factors that stimulate regeneration, do not present complications associated with donor site harvesting, and present favorable mechanical strength (Mankin et al., 1996). For these reasons, allografts are particularly interesting for complex skeletal reconstruction after resection of bone tumors in pelvic bones of young patients. However, allografts present variable osteoinductive and osteoconductive properties and have lower osteogenic potential compared to autografts. Other disadvantages are the possibility of immune rejection, transmitting diseases and the lack of a pre-vascularized construct (Gomes et al., 2008). To overcome the latter disadvantage, Capanna et al. in 1993 described a technique for the reconstruction of large metadiaphyseal bone defects, combining a massive allograft to support a centrally located autologous fibula flap with the aim of improving allograft incorporation and decreasing the risk of mechanical instability (Capanna et al., 1993). This technique has proven efficacy for large bone defect reconstruction (Bakri et al., 2008). Other clinical studies described the use of allografts alone or associated with other therapies such

as autologous concentrated bone marrow-derived cell (Putzier et al., 2009; Faldini et al., 2011; Scaglione et al., 2014).

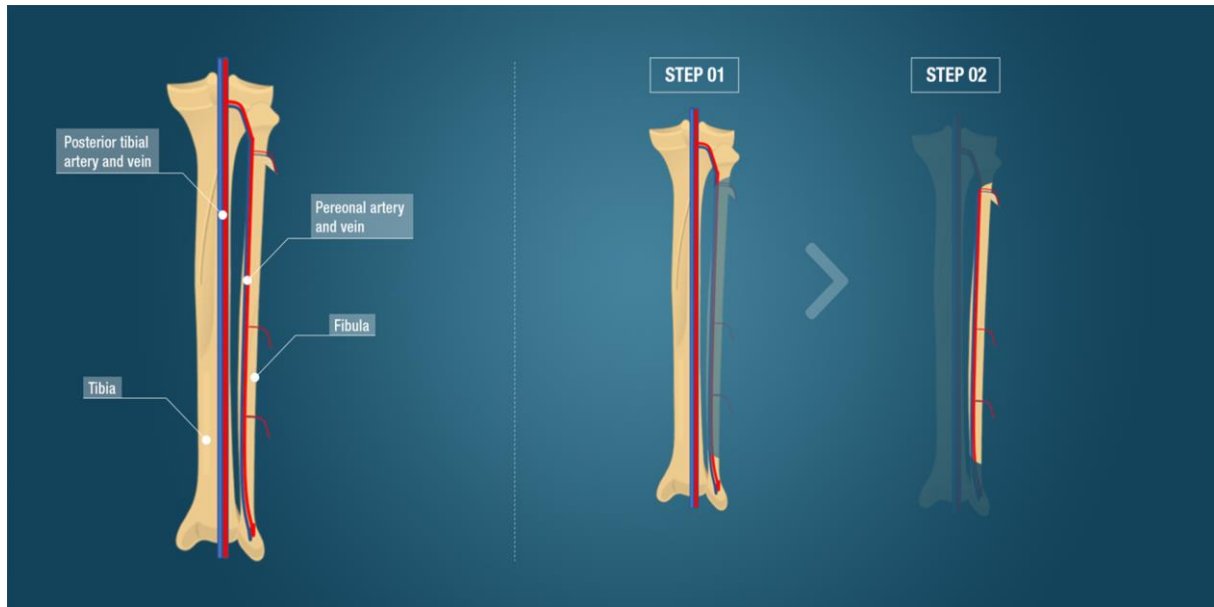


Figure 2: Fibula Free Flap. The anatomy including the tibia, fibula and major vessels is indicated. The surgical steps comprising the fibula free flap, the gold standard clinical technique for large bone defect reconstruction, is demonstrated.

2.1.3. Xenografts

Xenografts, are harvested from different species and transplanted for patient bone defect repair, with the most commonly used of bovine, porcine, or coral origin. The primary advantages are the high availability, favorable porosity for bone tissue ingrowth and comparable mechanical strength to native bone. However, similar to allografts, xenografts, when treated for clinical use, lose their osteoinductive and osteoconductive abilities (Dimitriou et al., 2011; Friesenbichler et al., 2014). Moreover, a significant disadvantage of xenografts is the possible transmission of zoonotic diseases and immune rejection. Finally, xenografts have ethical and religious concerns. Karalashvili et al. described the use of decellularized bovine bone graft in a

zygomatic large bone defect reconstruction and reported long-term retention of graft shape without resorption and bone integration (Karalashvili et al., 2017). Bovine cancellous xenografts have also been used in the treatment of tibial fractures in elderly patients and showed favorable healing outcomes (Bansal et al., 2009). However, the number of published studies using xenografts in large bone defect reconstruction is still limited and indeed clinical studies using bovine bone has showed poor results, describing graft rejection and failure in host tissue integration (Elliot and Richards, 2011; Patil et al., 2011; Shibuya et al., 2012; Ledford et al., 2013).

2.1.4. Synthetic biomaterials

Langer and Vacanti described tissue engineering by the use of biocompatible materials associated with cells and, or biological factors, in order to replace or repair tissues or organs. Various biomaterials have been employed in the treatment of bone defects. Calcium phosphate ceramics (CaP ceramics) are synthetic materials composed of calcium hydroxyapatites, therefore possessing a composition similar to the native bone matrix. Calcium phosphate ceramics are primarily produced by sintering at high temperatures and are available with variable porosity and in construct or granules format, with their main advantage being their osteoconductivity (Albrektsson and Johansson, 2001; Lee et al., 2006; Samavedi et al., 2013). Calcium phosphate ceramics most commonly employed in bone reconstruction are biphasic calcium phosphate (BCP), tricalcium phosphate (TCP), and hydroxyapatites (HA). Hydroxyapatites present excellent osteoconductive and osseointegration properties and their macroporosity and pore interconnectivity allow excellent cell adhesion and proliferation, leading to osteoconduction and osteoinduction after transplantation in vivo, as well as revascularization of the implant (Bucholz et al., 1987; Egli et al., 1988).

Tricalcium phosphate has higher pore interconnectivity than HA which is crucial for neovascularization and osteoconduction (Ogose et al., 2006), however, this higher interconnectivity gives TCP lower mechanical properties compared to HA and TCP is reabsorbed faster than HA after implantation (Torres et al., 2011). Biphasic calcium phosphate (BCP) is the combination of TCP and HA. BCP exploits the main advantages of both TCP and HA as they can be combined in various ratios (Daculsi et al., 1989). Calcium phosphate cement (CPC) differs from calcium phosphate ceramics because they are made at ambient temperatures from hydrolysis and are regarded as biomimetic. CPC can be used as filler by injection and for creating 3D printing constructs (Brown and Chow, 1983; Brown, 1987; Bertol et al., 2016), however their slow degradation may delay bone formation (Lodoso-Torrecilla et al., 2018). Bioactive glass or bioglass is a synthetic silicate-based ceramic. It is rapidly resorbed in the first two weeks after implantation allowing a rapid new bone and vascularized implant ingrowth (Gerhardt and Boccaccini, 2010; Kurien et al., 2013). Synthetic bone substitutes are an excellent alternative to biological grafts in small bone defect reconstruction. However, due to the insufficient strength to sustain the body load and insufficient neovascularization ingrowth, bone substitutes are not the best option for large bone defect reconstruction (Stanovici et al., 2016). Their association with recombinant human growth factors and/or stem cell therapies could be a solution for this main disadvantage (Gomez-Barrena et al., 2011; Gomez-Barrena et al., 2019). Orthounion is an ongoing clinical trial studying the use of bone marrow mesenchymal stem cells combined with a bone substitute to fill the non-union in a surgical procedure (Verboket et al., 2018). Another ongoing clinical trial, Maxibone, is studying the safety and efficacy of autologous cultured stem cells and calcium phosphate biomaterials in alveolar bone augmentation (Gjerde et al., 2018).

2.1.5. Megaprosthesis

After trauma or resection of a malignant or benign aggressive tumor, the reconstruction of large bone defects is necessary to prevent amputation. The use of metal megaprotheses began in the 70s, and in the 90s, it became popular. Megaprosthesis replace the affected bone tissue instead of regenerating bone tissue and there has been a significant evolution of their components since inception in order to ensure corrosion resistance, to avoid fractures of the material, for better fixation, and to guarantee osseointegration. Modular endoprosthesis today allow the association of different components to customize large bone defect reconstruction (Hattori et al., 2011). Prostheses may have a coating of hydroxyapatite and silver for osseointegration and to prevent infection and various studies have showed excellent limb survival after surgery with a follow up of up at 20 years (Mittermayer et al., 2001; Gosheger et al., 2006; Jeys and Grimer, 2009; Shehadeh et al., 2010). There are two significant complications after reconstruction with mega prosthesis, mechanical and non- mechanical complications. Implant design may cause inherent mechanical complications and those reported in the literature include aseptic loosening, failure of soft tissue attachments, and prosthesis stem fractures. These complication rates are between 5 and 48%, as described in the literature (Ahlmann et al., 2006; Gosheger et al., 2006; Holl et al., 2012) and robust modular mega prosthesis have helped to reduce this mechanical complication (Choong et al., 1996; Jawad and Brien, 2014). Non-mechanical complications include infection, tumor relapse, and wound healing disorders. Infection and wound necrosis are common complications in oncological cases due to malnutrition, immunosuppression, lack of local tissue vascularization, and extensive implant reconstruction (Jeys et al., 2005; Jeys and Grimer, 2009; Pala et al., 2015). Silver coated prosthesis, antibiotics therapy, and meticulous surgery techniques

may reduce these complications, however, non-mechanical complications are the primary threat in large bone defect reconstruction using mega prosthesis.

2.2. Masquelet induced membrane technique

The induced membrane method known as the Masquelet technique consists of a two-stage operative procedure. The first stage includes a debridement of the defect site, soft-tissue repair and the insertion of a cement spacer composed of polymethyl methacrylate (PMMA) that allows the maintenance of the bone height and stability, and the formation of a pseudosynovial membrane due to a foreign-body reaction. In the second step, performed 6 to 8 weeks later, the cement spacer is removed and the cavity is refilled with an autologous cancellous bone graft (e.g., from the iliac crests), while preserving the induced membrane. This membrane has various functions, in particular it prevents the resorption of the cancellous bone graft, supports vascularization and corticalization, and functions as a delivery system for osteomodulatory and angiogenic growth factors like transforming growth factor (TGF β), bone morphogenetic protein 2 (BMP2) and vascular endothelial derived growth factor (VEGF) (Masquelet, 2003; Pelissier et al., 2004; Masquelet and Begue, 2010). This innovative technique is indicated in acute and chronic infected or noninfected massive bone defects of any size (4-25 cm) and shape, at different anatomical sites in children and adults (Masquelet et al., 2000; Azi et al., 2019). Its consolidation rate varies from 82 to 100% with delays ranging from 4 months to one year. The main complications include infection, failure of a step in the surgical procedure (persisting infection or non-union), re-fracture and severe bone graft resorption (Morelli et al., 2016; Han et al., 2017). Different studies reported the Masquelet's approach as effective, for instance Sivakumar et al. and Mathieu et al.

described the use of the induced membrane technique in the management of large bone defect reconstruction in open fractures of the femur, tibia, and fibula bones (Sivakumar et al., 2016; Mathieu et al., 2019). A recently published review reported the application of the induced membrane technique in patients with osteomyelitis, suggesting this technique is an excellent alternative to solve long bone infected defects by controlling the local infection (Careri et al., 2019).

2.3. Ilizarov method

The Ilizarov method is a convenient tool for the treatment of patients suffering from poly-trauma conditions, with multiple fractures, osteomyelitis, and infected non-unions. The principle of the Ilizarov's technique is to stimulate bone growth by bone distraction that produces neovascularization, and stimulates new bone formation (Aronson et al., 1989; Ilizarov, 1990). The surgical procedure consists of the use of an external circular fixator and a corticotomy. The external fixator stabilizes the bone and allows early weight-bearing. A distraction of 0.25 mm, four times per day, commencing after a delay of 5 to 10 days post surgery is performed and an osteogenesis activity occurs in the bone gap (Spiegelberg et al., 2010). The length of bone that can be produced by this technique is up to 20 cm per limb segment. Barbarossa et al. conducted a study of 30 patients with osteomyelitis and infected non-union of the femur treated with the Ilizarov technique and reported efficacy in saving the limbs with osteomyelitis (Barbarossa et al., 2001). Large blood vessels expressing smooth muscle α -actin were shown to co-express BMP2 which was involved in enhancing osteogenesis activity at the site (Matsubara et al., 2012). The Ilizarov's bone distraction technique also offers the possibility of correcting a defect of axis, and allows a lengthening of the limb, however, it has associated drawbacks such as several weeks lag time required to heal large

segmental defects, with extended hospital recovery and discomfort for patients, as well as risks of osteomyelitis along the transcutaneous pins.

3. Future directions in large bone defect reconstruction

3.1. In-patient bioreactor

The principle of this approach is to use the patient as their own bioreactor, and entails the fabrication of a customized bone graft utilizing medical imaging and 3D printing, and the implantation of these osteoinductive materials in ectopic sites such as under the skin or in muscles. After several weeks, the pre-fabricated bone graft is used for large skeletal reconstruction. The possibility of producing substitute organs or body parts inside human bodies, therefore using the body as a living bioreactor was introduced (Cao et al., 1997; Vacanti and Langer, 1999) and Orringer et al. first treated an angle to angle mandible and total lower-lip reconstruction with a prefabricated osteocutaneous free flap. A dacron-polyurethane tray was packed with autologous cancellous bone graft and with BMP7. This tray was implanted in the fascia above the scapula for generating a composite pre-fabricated flap (Orringer et al., 1999). Warnke et al. developed the bone-muscle-flap prefabrication technique for maxillofacial reconstruction. They grew a subtotal mandible composed of a titanium mesh cage filled with bone bovine mineral blocks, bone mineral granules associated with BMP7, and autologous bone marrow concentrated cells inside the latissimus muscle and vascularization was provided by the thoracodorsal pedicle. Seven weeks postoperatively, the prefabricated bone muscle flap was microsurgically transplanted with its vascular pedicle in the mandible. Vascular supply of the free flap was successfully maintained. A favorable aesthetic and functional outcome was obtained. (Warnke et al., 2004). Mesimäki et al. then described a 3 step surgery method to

reconstruct a large bone maxillary defect by forming a prevascularized construct by filling a titanium mesh cage with autologous adipose-derived stem cells (ASCs), BMP2 and beta TCP granules and inserting it in the patient's left rectus abdominis muscle, with vascularization provided by the inferior epigastric artery, and subsequent transplantation for maxillary bone reconstruction (Mesimaki et al., 2009). Other studies described the use of the pectoralis major - hydroxyapatite blocks flap, pedicled using the thoracoacromial artery, for mandible reconstruction (Heliotis et al., 2006; Tatara et al., 2014). A further alternative comprised a polymethylmethacrylate chamber filled with autograft implanted against the periosteum of the iliac crest which after eight weeks was transplanted to the mandibular site, with the donor periosteum sutured with the local periosteum to reestablish the vascularization (Cheng et al., 2006). Kokemueller et al. reported hemimandible reconstruction by utilizing cylinders of beta-tricalcium phosphate loaded with cells and morcellized autologous bone graft that were implanted in the latissimus dorsi muscle with a central vascular bundle and transplanted after six months (Kokemueller et al., 2010). The main advantage of the patient bioreactor method compared to the alternative surgical treatments proposed for large bone defects reconstructions (e.g., autologous vascularized fibula, iliac crest) is that it avoids the process of harvesting native bone and creating further skeletal defects. However, this method does not apply to emergency cases and requires at least two surgical sites.

3.2. 3D printing techniques and production of personalized surgical guides and scaffolds

Three-dimensional (3D) printing is an emerging technology that permits the manufacture of complex-shaped structures with high precision using layer-by-layer

printing of different materials. The structures of the defects to be reconstructed in patients are identified based on digital images obtained from a computed tomography (CT) scan or magnetic resonance imaging (MRI) and by using computer-aided design (CAD) software, 3D printing technology and bioprinting can develop 3D medical models (Colin and Boire, 1997; Winder and Bibb, 2005). The 3D printing technologies used for polymer scaffold construction are: (1) fused deposition modeling (FDM), (2) selective laser sintering (SLS), and (3) stereolithography (SLA). The fused deposition method is the most popular technique developed in the 1980s and based on construction by melting deposition. The material commonly used is a thermoplastic polymer, in powder or filament format, which feeds an extruder tip that melts the plastic and at its exit is deposited on a surface at a much lower temperature so that it solidifies rapidly. The extruder tip moves in the x and y planes to print layer by layer the pattern of the scaffold (Xu et al., 2014). The resolution of the printed construct is defined by multiple factors: nozzle diameter, print speed, and number and height of the layers (Yang et al., 2018). This technique is simple, rapid, and cost-effective, however, there are limited choices of biocompatible, medical-grade thermoplastic polymers available. Selective laser sintering uses a CO₂ laser that sinters, layer by layer, the material in a powder state, forming the final piece. The final piece needs to be cleaned to withdraw the powder excess and to provide smoothness to the construct surface. SLS allows the fabrication of large and sophisticated structures (Deckard, 1989; Mazzoli, 2013). Stereolithography (SLA) produces 3D models by tracing a beam of UV light or a laser on a base of a photosensitive resin that polymerizes (Mondschein et al., 2017). The main benefit of this 3D printing technology is the high level of detail and the excellent surface resolution (Ji et al., 2018).

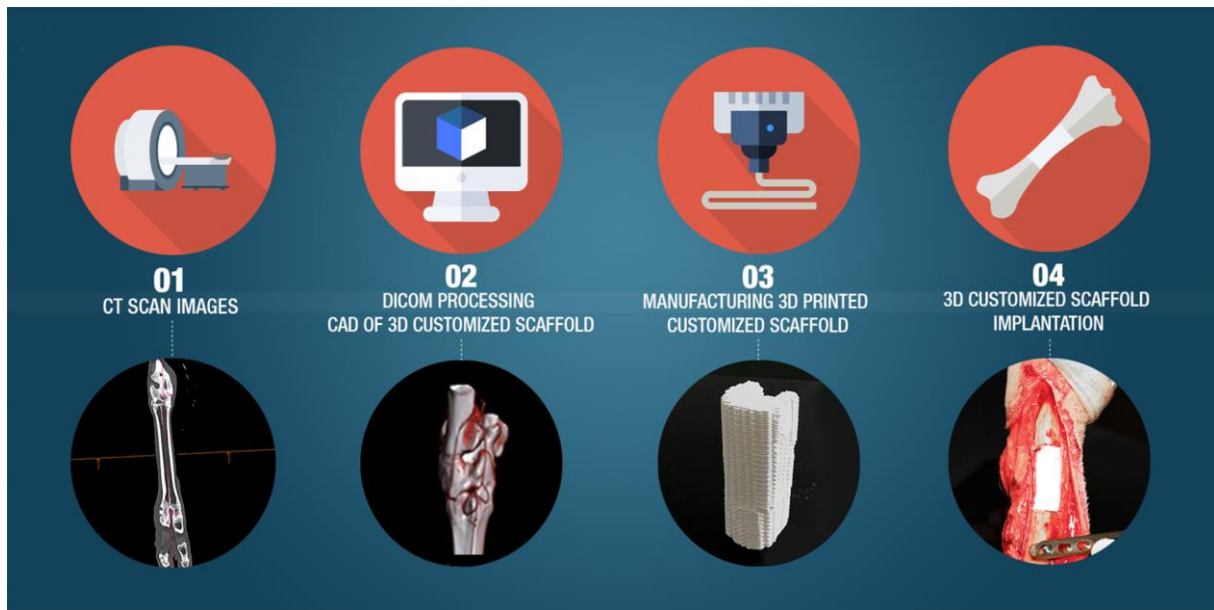


Figure 3: Workflow involved in customizable bone construct fabrication. 1) CT scans of the patient’s bone are acquired. 2) Computer aided software enables the processing of CT images in order to 3) 3D print personalized scaffolds for 4) bone defect reconstruction. The lower panel illustrates a real large bone defect reconstruction in a sheep metatarsal bone model.

3.3. 3D printing in bone tissue engineering applications

3D printing prototype models can significantly assist with pre-operative evaluation and intraoperative procedures, for example for the use of surgical guides in mandibular reconstruction with osteocutaneous free flaps (Bosc et al., 2017; Dupret-Bories et al., 2018). These studies showed the advantages of using 3D printed preoperative models and surgical guides including a reduction in operating time, flap ischemia, morbidity and associated complications such as infections. Many studies describe the use of 3D printing scaffolds for bone tissue engineering (Kao et al., 2015; Petrochenko et al., 2015; Saito et al., 2015; Wang et al., 2015). Various types of ceramics, like hydroxyapatite (HA), beta-tricalcium phosphate (β -TCP), alpha-tricalcium phosphate (α -TCP), biphasic calcium phosphates (BCP), bioactive glasses, and more, have been

used in recent years for the development of 3D printed scaffolds (Vorndran et al., 2008; Suwanprateeb et al., 2009; Klammert et al., 2010b), however these materials are often brittle and do not match the mechanical properties of bone. To obtain similar mechanical strength to bone, bioceramics can be blended with polymers, such as cellulose, poly(D,L-lactic acid-co-glycolic acid) or polycaprolactone (PCL), before being printed (Liao et al., 2011). PCL is a polymer, with FDA approval that is widely used in 3D printing. It has a low melting temperature (60°C) (Wang et al., 2015) favorable viscoelasticity, and is biodegradable. Its slow degradation and high stiffness make PCL one of the preferred polymers for the manufacture of a 3D printing scaffold for bone tissue engineering (Brunello et al., 2016). The use of computed tomography to create anatomically accurate scaffolds of calcium phosphate for cranial defects and alpha-tricalcium phosphate for maxillofacial deformities reconstruction have been described (Saijo et al., 2009; Klammert et al., 2010a). Direct ink writing (DIW), also called robocasting, has been one of the most studied and commonly used techniques for the development of 3D bioceramic scaffolds. DIW is an extrusion-based additive manufacturing method, in which a liquid-phase ink containing a high volume content of ceramic powder is dispensed through a nozzle, following a digitally defined pattern to create a 3D construct in a layer-by-layer manner (Lewis, 2006; Feilden et al., 2016). The chief advantages of DIW is that it applies to a wide range of bioceramics and it is possible to control pore size, pore orientation, and lattice design of the printed scaffold. Moreover, it is a high speed, simple and economic technique (Michna et al., 2005; Miranda et al., 2006) and has been used to create a hydroxyapatite scaffold for possible use in maxillofacial reconstruction (Cesarano Iii et al., 2005).

The main advantage of 3D printing is direct control over both the microarchitecture and macroarchitecture with complex anatomical structure. These 3D printed models allow

the manufacture of customized scaffolds that mimics the patient's anatomy (Wubneh et al., 2018). However, there are different challenges to the translation of 3D printing bioceramics to clinical application. Firstly, 3D printed bioceramics are brittle and not suitable for load-bearing clinical applications. Secondly, the fabrication of a large-size scaffold for large bone defect reconstruction is time-consuming and expensive. Moreover, for producing these 3D printed bioceramics, toxic solvents, and high-temperatures are used in the printing procedures which may compromise cell viability (Rodríguez-Lorenzo et al., 2001; Lewis et al., 2006; Trombetta et al., 2017; Wen et al., 2017; Chen et al., 2019). There have been multiple in vivo animal studies conducted with 3D printed customized scaffolds for bone regeneration (Park et al., 2018; Choi et al., 2019), however, these techniques are still in a developmental stage for clinical application and not capable of fabricating large-sized bioceramic scaffolds.

3.4. 3D bioprinting a custom living and vascularized bone graft

Bioprinting is another 3D printing technique that uses cell-laden hydrogels to print structures that after a period of maturation, will develop complex tissues, such as skin, cartilage, and bone. Vascularization can be aided by the incorporation of angiogenic growing factors or endothelial cells into bio-inks (Kolesky et al., 2014; Fahimipour et al., 2017; Benning et al., 2018). Three major procedures are the most used in bioprinting: inkjet, extrusion, and laser-assisted bioprinting. For tissue engineering applications, thermal and piezoelectric inkjet bioprinters are commonly used. In the piezoelectric inkjet bioprinter system, a piezoelectric crystal is used to create different potentials which generates pressure that allows the bioink ejection in the form of droplets. In thermal inkjet bioprinting, the printhead is heated up to 300°C that generates small air bubbles that produce pressure pulses to eject bioink droplets. The

size of droplets depends on multiple factors, such as ink viscosity, the frequency of the current pulse and the gradient of the temperature (Hock et al., 1996; Hudson et al., 2000; Cui et al., 2012), and the significant advantages of inkjet bioprinting is its rapid fabrication (Murphy and Atala, 2014). In extrusion bioprinting, a bioink is dispensed using pneumatic air pressure or mechanical systems composed of a screw or a piston. The flow of the bioink is more controlled in the mechanical system due to the action of the screw. With the pneumatic air, an interrupted filament is ejected, allowing high precision in the printed construct. Cells are exposed to high mechanical stress during this procedure, which may affect cell viability (Mandrycky et al., 2016). Extrusion bioprinting allows printing of different types of inks with different viscosities (Ozbolat and Hospodiuk, 2016; Paxton et al., 2017). The main disadvantage of this technique is that the high viscosity of the bioink or cell aggregation can clog the printer tip. Laser bioprinting consists of the interaction of a pulsed laser source with a ribbon. This ribbon contains an energy-absorbing layer, and below it, the bioink is located. A collector-slide receives the droplets of hydrogel created by the dynamic jet facilitated by the energy deposition that is created by the laser effect in the ribbon. In this procedure cells are not submitted to a mechanical stress (Gruene et al., 2011; Unger et al., 2011) and it is a nozzle-free cell printing technique with high resolution. Although 3D bioprinting brings the potential of producing a customized and vascularized living bone transplant, this biofabrication technique has not yet been tested in clinical cases. Numerous remaining challenges such as obtaining optimal cell numbers, adequate cell viability and spatial cell differentiation of the 3D construct, as well as reconnection to the local vasculature are yet to be resolved.

4. Conclusion

In this review, the current bone reconstructive options for large skeletal defects such as autologous, allogeneic, biological and synthetic bone grafts are presented, as well as the future directions in bone tissue engineering that take advantage of 3D printing. The current gold standard technique for large bone defect reconstruction is autologous free flap transplantation that contains the patient's cells, growth factors, and a vascularization bed. However, its main disadvantages are donor site morbidity, laborious microsurgery, and the need to sculpt the construct to the anatomy of the bone defect. Alternatively, allogeneic bone is also used to reconstruct large bone defects, but it is less osteogenic than autologous bone and may induce immunogenic rejection and transfer of disease. 3D printing technologies permit the fabrication of personalized bone grafts and the improvements in the incorporation of cells, growth factors, and vasculature may revolutionize bone tissue regeneration.

5. Conflict of Interest

The authors declare that the research was conducted in the absence of any commercial or financial relationships that could be construed as a potential conflict of interest.

6. Author Contributions

LV, CK, MAB, wrote the main manuscript text and prepared the figures; AH edited the manuscript; PL edited the manuscript and prepared the figures. All authors have read and approved the final version of the manuscript.

7. Funding

This work was supported by the European Commission through the H2020 projects ORTHOUNION “Orthopaedic randomized clinical trial with expanded bone marrow MSC and bioceramics versus autograft in long bone non-unions” under grant agreement #733288 and MAXIBONE “Personalised maxillofacial bone regeneration” under grant agreement #779322.

8. Acknowledgments

Luciano Vidal was financially supported for his PhD thesis by the patient’s charity ‘Ligue Française contre la neurofibromatose’ that is greatly acknowledged.

9. References

- 1) Ahlmann, E.R., Menendez, L.R., Kermani, C., and Gotha, H. (2006). Survivorship and clinical outcome of modular endoprosthetic reconstruction for neoplastic disease of the lower limb. *J Bone Joint Surg Br* 88(6), 790-795. doi: 10.1302/0301-620X.88B6.17519.
- 2) Albrektsson, T., and Johansson, C. (2001). Osteoinduction, osteoconduction and osseointegration. *Eur Spine J* 10 Suppl 2(Suppl 2), 96-101. doi: 10.1007/s005860100282.
- 3) Athanasiou, V.T., Papachristou, D.J., Panagopoulos, A., Saridis, A., Scopa, C.D., and Megas, P. (2010). Histological comparison of autograft, allograft-DBM, xenograft, and synthetic grafts in a trabecular bone defect: an experimental study in rabbits. *Med Sci Monit* 16(1), BR24-31.
- 4) Azi, M.L., Teixeira, A.A.A., Cotias, R.B., Joeris, A., and Kfuri, M. (2019). Induced-membrane technique in the management of posttraumatic bone defects. *JBJS Essent Surg Tech* 9(2), e22. doi: 10.2106/JBJS.ST.18.00099.
- 5) Bakri, K., Stans, A.A., Mardini, S., and Moran, S.L. (2008). Combined massive allograft and intramedullary vascularized fibula transfer: the capanna technique for lower-limb reconstruction. *Semin Plast Surg* 22(3), 234-241. doi: 10.1055/s-2008-1081406.
- 6) Bansal, M.R., Bhagat, S.B., and Shukla, D.D. (2009). Bovine cancellous xenograft in the treatment of tibial plateau fractures in elderly patients. *Int Orthop* 33(3), 779-784. doi: 10.1007/s00264-008-0526-y.
- 7) Benning, L., Gutzweiler, L., Trondle, K., Riba, J., Zengerle, R., Koltay, P., et al. (2018). Assessment of hydrogels for bioprinting of endothelial cells. *J Biomed Mater Res A* 106(4), 935-947. doi: 10.1002/jbm.a.36291.
- 8) Bertol, L.S., Schabbach, R., and dos Santos, L.A.L. (2016). Dimensional evaluation of patient-specific 3D printing using calcium phosphate cement for craniofacial bone reconstruction. *J Biomater Appl* 31(6), 799-806. doi: 10.1177/0885328216682672.
- 9) Bosc, R., Hersant, B., Carloni, R., Niddam, J., Bouhassira, J., De Kermadec, H., et al. (2017). Mandibular reconstruction after cancer: an in-house approach to manufacturing cutting guides. *Int J Oral Maxillofac Surg* 46(1), 24-31. doi: 10.1016/j.ijom.2016.10.004.

- 10) Bostrom, M.P.G., and Seigerman, D.A. (2005). The clinical use of allografts, demineralized bone matrices, synthetic bone graft substitutes and osteoinductive growth factors: a survey study. *HSS J* 1(1), 9-18. doi: 10.1007/s11420-005-0111-5.
- 11) Brown, W., and Chow, L. (1983). A new calcium-phosphate setting cement. *J Dent Res* 62, 672-672.
- 12) Brown, W.E. (1987). A new calcium phosphate, water-setting cement. *Cements research progress*, 351-279.
- 13) Brunello, G., Sivoletta, S., Meneghello, R., Ferroni, L., Gardin, C., Piattelli, A., et al. (2016). Powder-based 3D printing for bone tissue engineering. *Biotechnol Adv* 34(5), 740-753. doi: 10.1016/j.biotechadv.2016.03.009.
- 14) Brydone, A.S., Meek, D., and Maclaine, S. (2010). Bone grafting, orthopaedic biomaterials, and the clinical need for bone engineering. *Proc Inst Mech Eng H* 224(12), 1329-1343. doi: 10.1243/09544119JEIM770.
- 15) Bucholz, R.W., Carlton, A., and Holmes, R.E. (1987). Hydroxyapatite and tricalcium phosphate bone graft substitutes. *Orthop Clin North Am* 18(2), 323-334.
- 16) Cao, Y., Vacanti, J.P., Paige, K.T., Upton, J., and Vacanti, C.A. (1997). Transplantation of chondrocytes utilizing a polymer-cell construct to produce tissue-engineered cartilage in the shape of a human ear. *Plast Reconstr Surg* 100(2), 297-302; discussion 303-294. doi: 10.1097/00006534-199708000-00001.
- 17) Capanna, R., Bufalini, C., and Campanacci, M. (1993). A new technique for reconstructions of large metadiaphyseal bone defects. *Orthop Traumatol* 2(3), 159-177. doi: 10.1007/BF02620523.
- 18) Careri, S., Vitiello, R., Oliva, M.S., Ziranu, A., Maccauro, G., and Perisano, C. (2019). Masquelet technique and osteomyelitis: innovations and literature review. *Eur Rev Med Pharmacol Sci* 23(2 Suppl), 210-216. doi: 10.26355/eurrev_201904_17495.
- 19) Cesarano Iii, J., Dellinger, J.G., Saavedra, M.P., Gill, D.D., Jamison, R.D., Grosser, B.A., et al. (2005). Customization of load-bearing hydroxyapatite lattice scaffolds. *Int J Appl Ceram Technol* 2(3), 212-220. doi: 10.1111/j.1744-7402.2005.02026.x.

- 20)Chen, Z., Li, Z., Li, J., Liu, C., Lao, C., Fu, Y., et al. (2019). 3D printing of ceramics: A review. *J Eur Ceram Soc* 39(4), 661-687. doi: 10.1016/j.jeurceramsoc.2018.11.013.
- 21)Cheng, M.-H., Brey, E.M., Ulusal, B.G., and Wei, F.-C. (2006). Mandible augmentation for osseointegrated implants using tissue engineering strategies. *Plast Reconstr Surg* 118(1). doi: 10.1097/01.prs.0000221120.11128.1a.
- 22)Choi, S., Oh, Y.-I., Park, K.-H., Lee, J.-S., Shim, J.-H., and Kang, B.-J. (2019). New clinical application of three-dimensional-printed polycaprolactone/ β -tricalcium phosphate scaffold as an alternative to allograft bone for limb-sparing surgery in a dog with distal radial osteosarcoma. *J Vet Med Sci* 81(3), 434-439. doi: 10.1292/jvms.18-0158.
- 23)Choong, P.F., Sim, F.H., Pritchard, D.J., Rock, M.G., and Chao, E.Y. (1996). Megaprotheses after resection of distal femoral tumors. A rotating hinge design in 30 patients followed for 2-7 years. *Acta Orthop Scand* 67(4), 345-351. doi: 10.3109/17453679609002328.
- 24)Colin, A., and Boire, J.-Y. (1997). A novel tool for rapid prototyping and development of simple 3D medical image processing applications on PCs. *Comput Methods Programs Biomed* 53(2), 87-92. doi: 10.1016/S0169-2607(97)01807-5.
- 25)Cui, X., Boland, T., D'Lima, D.D., and Lotz, M.K. (2012). Thermal inkjet printing in tissue engineering and regenerative medicine. *Recent Pat Drug Deliv Formul* 6(2), 149-155. doi: 10.2174/187221112800672949.
- 26)Daculsi, G., LeGeros, R.Z., Nery, E., Lynch, K., and Kerebel, B. (1989). Transformation of biphasic calcium phosphate ceramics in vivo: ultrastructural and physicochemical characterization. *J Biomed Mater Res* 23(8), 883-894. doi: 10.1002/jbm.820230806.
- 27)Deckard, C.R. (1989). Method and apparatus for producing parts by selective sintering. Washington, DC: U.S. Patent and Trademark Office. patent application U.S. Patent No. 4,863,538.
- 28)Dimitriou, R., Jones, E., McGonagle, D., and Giannoudis, P.V. (2011). Bone regeneration: current concepts and future directions. *BMC Med* 9, 66. doi: 10.1186/1741-7015-9-66.
- 29)Dupret-Bories, A., Vergez, S., Meresse, T., Brouillet, F., and Bertrand, G. (2018). Contribution of 3D printing to mandibular reconstruction after cancer.

- Eur Ann Otorhinolaryngol Head Neck Dis 135(2), 133-136. doi: 10.1016/j.anorl.2017.09.007.
- 30) Eggli, P.S., Muller, W., and Schenk, R.K. (1988). Porous hydroxyapatite and tricalcium phosphate cylinders with two different pore size ranges implanted in the cancellous bone of rabbits. A comparative histomorphometric and histologic study of bony ingrowth and implant substitution. Clin Orthop Relat Res (232), 127-138.
- 31) Elliot, R.R., and Richards, R.H. (2011). Failed operative treatment in two cases of pseudarthrosis of the clavicle using internal fixation and bovine cancellous xenograft (Tutobone). J Pediatr Orthop 20(5). doi: 10.1097/BPB.0b013e328346c010.
- 32) Fahimipour, F., Rasouljanboroujeni, M., Dashtimoghadam, E., Khoshroo, K., Tahiri, M., Bastami, F., et al. (2017). 3D printed TCP-based scaffold incorporating VEGF-loaded PLGA microspheres for craniofacial tissue engineering. Dent Mater 33(11), 1205-1216. doi: 10.1016/j.dental.2017.06.016.
- 33) Faldini, C., Miscione, M.T., Acri, F., Chehrassan, M., Bonomo, M., and Giannini, S. (2011). Use of homologous bone graft in the treatment of aseptic forearm nonunion. Musculoskelet Surg 95(1), 31-35. doi: 10.1007/s12306-011-0117-8.
- 34) Feilden, E., Blanca, E.G.-T., Giuliani, F., Saiz, E., and Vandeperre, L. (2016). Robocasting of structural ceramic parts with hydrogel inks. J Eur Ceram Soc 36(10), 2525-2533. doi: 10.1016/j.jeurceramsoc.2016.03.001.
- 35) Fernandez de Grado, G., Keller, L., Idoux-Gillet, Y., Wagner, Q., Musset, A.-M., Benkirane-Jessel, N., et al. (2018). Bone substitutes: a review of their characteristics, clinical use, and perspectives for large bone defects management. J Tissue Eng 9, 1-18. doi: 10.1177/2041731418776819.
- 36) Friesenbichler, J., Maurer-Ertl, W., Sadoghi, P., Pirker-Fruehauf, U., Bodo, K., and Leithner, A. (2014). Adverse reactions of artificial bone graft substitutes: lessons learned from using tricalcium phosphate geneX®. Clin Orthop Relat Res 472(3), 976-982. doi: 10.1007/s11999-013-3305-z.
- 37) Gerhardt, L.C., and Boccaccini, A.R. (2010). Bioactive glass and glass-ceramic scaffolds for bone tissue engineering. Materials (Basel) 3(7), 3867-3910. doi: 10.3390/ma3073867.

- 38) Giannoudis, P.V., Einhorn, T.A., Schmidmaier, G., and Marsh, D. (2008). The diamond concept - open questions. *Injury* 39, S5-S8. doi: 10.1016/S0020-1383(08)70010-X.
- 39) Gjerde, C., Mustafa, K., Hellem, S., Rojewski, M., Gjengedal, H., Yassin, M.A., et al. (2018). Cell therapy induced regeneration of severely atrophied mandibular bone in a clinical trial. *Stem Cell Res Ther* 9. doi: 10.1186/s13287-018-0951-9.
- 40) Gomes, K.U., Carlini, J.L., Biron, C., Rapoport, A., and Dedivitis, R.A. (2008). Use of allogeneic bone graft in maxillary reconstruction for installation of dental implants. *J Oral Maxillofac Surg* 66(11), 2335-2338. doi: 10.1016/j.joms.2008.06.006.
- 41) Gomez-Barrena, E., Rosset, P., Gebhard, F., Hernigou, P., Baldini, N., Rouard, H., et al. (2019). Feasibility and safety of treating non-unions in tibia, femur and humerus with autologous, expanded, bone marrow-derived mesenchymal stromal cells associated with biphasic calcium phosphate biomaterials in a multicentric, non-comparative trial. *Biomaterials* 196, 100-108. doi: 10.1016/j.biomaterials.2018.03.033.
- 42) Gomez-Barrena, E., Rosset, P., Muller, I., Giordano, R., Bunu, C., Layrolle, P., et al. (2011). Bone regeneration: stem cell therapies and clinical studies in orthopaedics and traumatology. *J Cell Mol Med* 15(6), 1266-1286. doi: 10.1111/j.1582-4934.2011.01265.x.
- 43) Gosheger, G., Gebert, C., Ahrens, H., Streitbueger, A., Winkelmann, W., and Harges, J. (2006). Endoprosthetic reconstruction in 250 patients with sarcoma. *Clin Orthop Relat Res* 450, 164-171. doi: 10.1097/01.blo.0000223978.36831.39.
- 44) Gruene, M., Unger, C., Koch, L., Deiwick, A., and Chichkov, B. (2011). Dispensing pico to nanolitre of a natural hydrogel by laser-assisted bioprinting. *Biomed Eng Online* 10(1), 19. doi: 10.1186/1475-925X-10-19.
- 45) Han, W., Shen, J., Wu, H., Yu, S., Fu, J., and Xie, Z. (2017). Induced membrane technique: advances in the management of bone defects. *Int J Surg* 42, 110-116. doi: 10.1016/j.ijsu.2017.04.064.
- 46) Hattori, H., Mibe, J., and Yamamoto, K. (2011). Modular megaprosthesis in metastatic bone disease of the femur. *Orthopedics* 34(12), e871-876. doi: 10.3928/01477447-20111021-13.

- 47) Heliotis, M., Lavery, K.M., Ripamonti, U., Tsiridis, E., and di Silvio, L. (2006). Transformation of a prefabricated hydroxyapatite/osteogenic protein-1 implant into a vascularised pedicled bone flap in the human chest. *Int J Oral Maxillofac Surg* 35(3), 265-269. doi: 10.1016/j.ijom.2005.07.013.
- 48) Hidalgo, D.A., and Pusic, A.L. (2002). Free-flap mandibular reconstruction: a 10-year follow-up study. *Plast Reconstr Surg* 110(2), 438-451.
- 49) Hock, S.W., Johnson, D.A., and Van Veen, M.A. (1996). Print quality optimization for a color ink jet printer by using a larger nozzle for the black ink only.
- 50) Holl, S., Schlomberg, A., Gosheger, G., Dieckmann, R., Streitbueger, A., Schulz, D., et al. (2012). Distal femur and proximal tibia replacement with megaprosthesis in revision knee arthroplasty: a limb-saving procedure. *Knee Surg Sports Traumatol Arthrosc* 20(12), 2513-2518. doi: 10.1007/s00167-012-1945-2.
- 51) Hudson, K.R., Cowan, P.B., and Gondek, J.S. (2000). Ink drop volume variance compensation for inkjet printing.
- 52) Jawad, M.U., and Brien, E.W. (2014). Proximal femoral reconstruction with a constrained acetabulum in oncologic patients. *Orthopedics* 37(2), e187-193. doi: 10.3928/01477447-20140124-24.
- 53) Jeys, L., and Grimer, R. (2009). "The long-term risks of infection and amputation with limb salvage surgery using endoprostheses," in *Treatment of Bone and Soft Tissue Sarcomas*, ed. P.-U. Tunn. (Berlin, Heidelberg: Springer Berlin Heidelberg), 75-84.
- 54) Jeys, L.M., Grimer, R.J., Carter, S.R., and Tillman, R.M. (2005). Periprosthetic infection in patients treated for an orthopaedic oncological condition. *J Bone Joint Surg Am* 87(4), 842-849. doi: 10.2106/JBJS.C.01222.
- 55) Ji, K., Wang, Y., Wei, Q., Zhang, K., Jiang, A., Rao, Y., et al. (2018). Application of 3D printing technology in bone tissue engineering. *Bio-des Manuf* 1(3), 203-210. doi: 10.1007/s42242-018-0021-2.
- 56) Kao, C.T., Lin, C.C., Chen, Y.W., Yeh, C.H., Fang, H.Y., and Shie, M.Y. (2015). Poly(dopamine) coating of 3D printed poly(lactic acid) scaffolds for bone tissue engineering. *Mater Sci Eng C Mater Biol Appl* 56, 165-173. doi: 10.1016/j.msec.2015.06.028.

- 57) Karalashvili, L., Chichua, N., Menabde, G., Atskvereli, L., and Grdzeldze, T. (2017). Decellularized bovine bone graft for zygomatic bone reconstruction. *Med Case Rep* 4(1:52). doi: 10.21767/2471-8041.100087.
- 58) Keating, J.F., and McQueen, M.M. (2001). Substitutes for autologous bone graft in orthopaedic trauma. *J Bone Joint Surg Br* 83(1), 3-8. doi: 10.1302/0301-620x.83b1.11952.
- 59) Klammert, U., Gbureck, U., Vorndran, E., Rodiger, J., Meyer-Marcotty, P., and Kubler, A.C. (2010a). 3D powder printed calcium phosphate implants for reconstruction of cranial and maxillofacial defects. *J Craniomaxillofac Surg* 38(8), 565-570. doi: 10.1016/j.jcms.2010.01.009.
- 60) Klammert, U., Vorndran, E., Reuther, T., Muller, F.A., Zorn, K., and Gbureck, U. (2010b). Low temperature fabrication of magnesium phosphate cement scaffolds by 3D powder printing. *J Mater Sci Mater Med* 21(11), 2947-2953. doi: 10.1007/s10856-010-4148-8.
- 61) Kokemueller, H., Spalthoff, S., Nolff, M., Tavassol, F., Essig, H., Stuehmer, C., et al. (2010). Prefabrication of vascularized bioartificial bone grafts in vivo for segmental mandibular reconstruction: experimental pilot study in sheep and first clinical application. *Int J Oral Maxillofac Surg* 39(4), 379-387. doi: 10.1016/j.ijom.2010.01.010.
- 62) Kolesky, D.B., Truby, R.L., Gladman, A.S., Busbee, T.A., Homan, K.A., and Lewis, J.A. (2014). 3D bioprinting of vascularized, heterogeneous cell-laden tissue constructs. *Adv Mater* 26(19), 3124-3130. doi: 10.1002/adma.201305506.
- 63) Kurien, T., Pearson, R.G., and Scammell, B.E. (2013). Bone graft substitutes currently available in orthopaedic practice. *Bone Joint J* 95-B(5), 583-597. doi: 10.1302/0301-620X.95B5.30286.
- 64) Laurencin, C., Khan, Y., and Veronick, J. (2014). "Bone graft substitutes: past, present and future," in *Bone graft substitutes and bone regenerative engineering*. West Conshohocken, PA: ASTM International), 1-9.
- 65) Ledford, C.K., Nunley, J.A., 2nd, Viens, N.A., and Lark, R.K. (2013). Bovine xenograft failures in pediatric foot reconstructive surgery. *J Pediatr Orthop* 33(4), 458-463. doi: 10.1097/BPO.0b013e318287010d.

- 66) Lee, K.Y., Park, M., Kim, H.M., Lim, Y.J., Chun, H.J., Kim, H., et al. (2006). Ceramic bioactivity: progresses, challenges and perspectives. *Biomed Mater* 1(2), R31-R37. doi: 10.1088/1748-6041/1/2/r01.
- 67) Lewis, J.A. (2006). Direct ink writing of 3D functional materials. *Adv Funct Mater* 16(17), 2193-2204. doi: 10.1002/adfm.200600434.
- 68) Lewis, J.A., Smay, J.E., Stuecker, J., and Cesarano, J. (2006). Direct ink writing of three-dimensional ceramic structures. *J Am Ceram Soc* 89(12), 3599-3609. doi: 10.1111/j.1551-2916.2006.01382.x.
- 69) Liao, H.-T., Chang, K.-H., Jiang, Y., Chen, J.-P., and Lee, M.-Y. (2011). Fabrication of tissue engineered PCL scaffold by selective laser-sintered machine for osteogenesis of adipose-derived stem cells. *Virtual Phys Protoyp* 6(1), 57-60. doi: 10.1080/17452759.2011.559742.
- 70) Lodoso-Torrecilla, I., van Gestel, N.A.P., Diaz-Gomez, L., Grosfeld, E.C., Laperre, K., Wolke, J.G.C., et al. (2018). Multimodal pore formation in calcium phosphate cements. *J Biomed Mater Res A* 106(2), 500-509. doi: 10.1002/jbm.a.36245.
- 71) Mandrycky, C., Wang, Z., Kim, K., and Kim, D.-H. (2016). 3D bioprinting for engineering complex tissues. *Biotechnol Adv* 34(4), 422-434. doi: 10.1016/j.biotechadv.2015.12.011.
- 72) Mankin, H.J., Gebhardt, M.C., Jennings, L.C., Springfield, D.S., and Tomford, W.W. (1996). Long-term results of allograft replacement in the management of bone tumors. *Clin Orthop Relat Res* (324), 86-97. doi: 10.1097/00003086-199603000-00011.
- 73) Masquelet, A.C. (2003). Muscle reconstruction in reconstructive surgery: soft tissue repair and long bone reconstruction. *Langenbecks Arch Surg* 388(5), 344-346. doi: 10.1007/s00423-003-0379-1.
- 74) Masquelet, A.C., and Begue, T. (2010). The concept of induced membrane for reconstruction of long bone defects. *Orthop Clin North Am* 41(1), 27-37. doi: 10.1016/j.ocl.2009.07.011.
- 75) Masquelet, A.C., Fitoussi, F., Begue, T., and Muller, G.P. (2000). Reconstruction of the long bones by the induced membrane and spongy autograft. *Ann Chir Plast Esthet* 45(3), 346-353.

- 76) Mathieu, L., Bilichtin, E., Durand, M., de l'Escalopier, N., Murison, J.C., Collombet, J.M., et al. (2019). Masquelet technique for open tibia fractures in a military setting. *Eur J Trauma Emerg Surg*. doi: 10.1007/s00068-019-01217-y.
- 77) Mazzoli, A. (2013). Selective laser sintering in biomedical engineering. *Med Biol Eng Comput* 51(3), 245-256. doi: 10.1007/s11517-012-1001-x.
- 78) Mercado-Pagan, A.E., Stahl, A.M., Shanjani, Y., and Yang, Y. (2015). Vascularization in bone tissue engineering constructs. *Ann Biomed Eng* 43(3), 718-729. doi: 10.1007/s10439-015-1253-3.
- 79) Mesimaki, K., Lindroos, B., Tornwall, J., Mauno, J., Lindqvist, C., Kontio, R., et al. (2009). Novel maxillary reconstruction with ectopic bone formation by GMP adipose stem cells. *Int J Oral Maxillofac Surg* 38(3), 201-209. doi: 10.1016/j.ijom.2009.01.001.
- 80) Michna, S., Wu, W., and Lewis, J.A. (2005). Concentrated hydroxyapatite inks for direct-write assembly of 3D periodic scaffolds. *Biomaterials* 26(28), 5632-5639. doi: s10.1016/j.biomaterials.2005.02.040.
- 81) Miranda, P., Saiz, E., Gryn, K., and Tomsia, A.P. (2006). Sintering and robocasting of β -tricalcium phosphate scaffolds for orthopaedic applications. *Acta Biomater* 2(4), 457-466. doi: 10.1016/j.actbio.2006.02.004.
- 82) Mittermayer, F., Krepler, P., Dominkus, M., Schwameis, E., Sluga, M., Heinzl, H., et al. (2001). Long-term followup of uncemented tumor endoprostheses for the lower extremity. *Clin Orthop Relat Res* (388), 167-177. doi: 10.1097/00003086-200107000-00024.
- 83) Mondschein, R.J., Kanitkar, A., Williams, C.B., Verbridge, S.S., and Long, T.E. (2017). Polymer structure-property requirements for stereolithographic 3D printing of soft tissue engineering scaffolds. *Biomaterials* 140, 170-188. doi: 10.1016/j.biomaterials.2017.06.005.
- 84) Moran, S.L., Bakri, K., Mardini, S., Shin, A.Y., and Bishop, A.T. (2009). The use of vascularized fibular grafts for the reconstruction of spinal and sacral defects. *Microsurgery* 29(5), 393-400. doi: 10.1002/micr.20655.
- 85) Morelli, I., Drago, L., George, D.A., Gallazzi, E., Scarponi, S., and Romano, C.L. (2016). Masquelet technique: myth or reality? A systematic review and meta-analysis. *Injury* 47 Suppl 6, S68-S76. doi: 10.1016/S0020-1383(16)30842-7.
- 86) Murphy, S.V., and Atala, A. (2014). 3D bioprinting of tissues and organs. *Nat Biotechnol* 32, 773. doi: 10.1038/nbt.2958.

- 87) Muscolo, D.L., Ayerza, M.A., Aponte-Tinao, L., Ranalletta, M., and Abalo, E. (2004). Intercalary femur and tibia segmental allografts provide an acceptable alternative in reconstructing tumor resections. *Clin Orthop Relat Res* 426. doi: 10.1097/01.blo.0000141652.93178.10.
- 88) Ogose, A., Kondo, N., Umezu, H., Hotta, T., Kawashima, H., Tokunaga, K., et al. (2006). Histological assessment in grafts of highly purified beta-tricalcium phosphate (OSferion®) in human bones. *Biomaterials* 27(8), 1542-1549. doi: 10.1016/j.biomaterials.2005.08.034.
- 89) Ogura, K., Sakuraba, M., Miyamoto, S., Fujiwara, T., Chuman, H., and Kawai, A. (2015). Pelvic ring reconstruction with a double-barreled free vascularized fibula graft after resection of malignant pelvic bone tumor. *Arch Orthop Trauma Surg* 135(5), 619-625. doi: 10.1007/s00402-015-2197-7.
- 90) Orringer, J.S., Shaw, W.W., Borud, L.J., Freymiller, E.G., Wang, S.A., and Markowitz, B.L. (1999). Total mandibular and lower lip reconstruction with a prefabricated osteocutaneous free flap. *Plast Reconstr Surg* 104(3), 793-797. doi: 10.1097/00006534-199909030-00028.
- 91) Oryan, A., Alidadi, S., and Moshiri, A. (2013). Current concerns regarding healing of bone defects. *Hard Tissue* 2(2), 13.
- 92) Oryan, A., Alidadi, S., Moshiri, A., and Maffulli, N. (2014). Bone regenerative medicine: classic options, novel strategies, and future directions. *J Orthop Surg Res* 9(1), 18. doi: 10.1186/1749-799X-9-18.
- 93) Ozbolat, I.T., and Hospodiuk, M. (2016). Current advances and future perspectives in extrusion-based bioprinting. *Biomaterials* 76, 321-343. doi: 10.1016/j.biomaterials.2015.10.076.
- 94) Pala, E., Trovarelli, G., Calabro, T., Angelini, A., Abati, C.N., and Ruggieri, P. (2015). Survival of modern knee tumor megaprotheses: failures, functional results, and a comparative statistical analysis. *Clin Orthop Relat Res* 473(3), 891-899. doi: 10.1007/s11999-014-3699-2.
- 95) Parikh, S.N. (2002). Bone graft substitutes: past, present, future. *J Postgrad Med* 48(2), 142-148.
- 96) Park, S.A., Lee, H.J., Kim, K.S., Lee, S.J., Lee, J.T., Kim, S.Y., et al. (2018). In vivo evaluation of 3D-printed polycaprolactone scaffold implantation combined with beta-TCP powder for alveolar bone augmentation in a beagle defect model. *Materials (Basel)* 11(2). doi: 10.3390/ma11020238.

- 97) Patil, S., Auyeung, J., and Gower, A. (2011). Outcome of subtalar fusion using bovine cancellous bone graft: A retrospective case series. *J Foot Ankle Surg* 50(4), 388-390. doi: 10.1053/j.jfas.2011.04.019.
- 98) Paxton, N., Smolan, W., Böck, T., Melchels, F., Groll, J., and Jungst, T. (2017). Proposal to assess printability of bioinks for extrusion-based bioprinting and evaluation of rheological properties governing bioprintability. *Biofabrication* 9(4), 044107. doi: 10.1088/1758-5090/aa8dd8.
- 99) Pelissier, P.H., Masquelet, A.C., Bareille, R., Pelissier, S.M., and Amedee, J. (2004). Induced membranes secrete growth factors including vascular and osteoinductive factors and could stimulate bone regeneration. *J Orthop Res* 22(1), 73-79. doi: 10.1016/S0736-0266(03)00165-7.
- 100) Peng, X., Mao, C., Yu, G.Y., Guo, C.B., Huang, M.X., and Zhang, Y. (2005). Maxillary reconstruction with the free fibula flap. *Plast Reconstr Surg* 115(6), 1562-1569. doi: 10.1097/01.prs.0000160691.63029.74.
- 101) Petrochenko, P.E., Torgersen, J., Gruber, P., Hicks, L.A., Zheng, J., Kumar, G., et al. (2015). Laser 3D printing with sub-microscale resolution of porous elastomeric scaffolds for supporting human bone stem cells. *Adv Healthc Mater* 4(5), 739-747. doi: 10.1002/adhm.201400442.
- 102) Putzier, M., Strube, P., Funk, J.F., Gross, C., Monig, H.J., Perka, C., et al. (2009). Allogenic versus autologous cancellous bone in lumbar segmental spondylodesis: a randomized prospective study. *Eur Spine J* 18(5), 687-695. doi: 10.1007/s00586-008-0875-7.
- 103) Rizzo, M., and Moran, S.L. (2008). Vascularized bone grafts and their applications in the treatment of carpal pathology. *Semin Plast Surg* 22(3), 213-227. doi: 10.1055/s-2008-1081404.
- 104) Rodríguez-Lorenzo, L.M., Vallet-Regí, M., and Ferreira, J.M.F. (2001). Colloidal processing of hydroxyapatite. *Biomaterials* 22(13), 1847-1852. doi: 10.1016/S0142-9612(00)00366-5.
- 105) Saijo, H., Igawa, K., Kanno, Y., Mori, Y., Kondo, K., Shimizu, K., et al. (2009). Maxillofacial reconstruction using custom-made artificial bones fabricated by inkjet printing technology. *J Artif Organs* 12(3), 200-205. doi: 10.1007/s10047-009-0462-7.
- 106) Saito, E., Suarez-Gonzalez, D., Murphy, W.L., and Hollister, S.J. (2015). Biomineral coating increases bone formation by ex vivo BMP-7 gene therapy in

- rapid prototyped poly(L-lactic acid) (PLLA) and poly(epsilon-caprolactone) (PCL) porous scaffolds. *Adv Healthc Mater* 4(4), 621-632. doi: 10.1002/adhm.201400424.
- 107) Samavedi, S., Whittington, A.R., and Goldstein, A.S. (2013). Calcium phosphate ceramics in bone tissue engineering: A review of properties and their influence on cell behavior. *Acta Biomater* 9(9), 8037-8045. doi: 10.1016/j.actbio.2013.06.014.
- 108) Sanan, A., and Haines, S.J. (1997). Repairing holes in the head: a history of cranioplasty. *Neurosurgery* 40(3), 588-603. doi: 10.1097/00006123-199703000-00033.
- 109) Scaglione, M., Fabbri, L., Dell'Omo, D., Gambini, F., and Guido, G. (2014). Long bone nonunions treated with autologous concentrated bone marrow-derived cells combined with dried bone allograft. *Musculoskelet Surg* 98(2), 101-106. doi: 10.1007/s12306-013-0271-2.
- 110) Shehadeh, A., Noveau, J., Malawer, M., and Henshaw, R. (2010). Late complications and survival of endoprosthetic reconstruction after resection of bone tumors. *Clin Orthop Relat Res* 468(11), 2885-2895. doi: 10.1007/s11999-010-1454-x.
- 111) Shibuya, N., Jupiter, D.C., Clawson, L.D., and La Fontaine, J. (2012). Incorporation of bovine-based structural bone grafts used in reconstructive foot surgery. *J Foot Ankle Surg* 51(1), 30-33. doi: 10.1053/j.jfas.2011.09.008.
- 112) Sivakumar, R., Mohideen, M.G., Chidambaram, M., Vinoth, T., Singhi, P.K., and Somashekar, V. (2016). Management of large bone defects in diaphyseal fractures by induced membrane formation by Masquelet's technique. *J Orthop Case Rep* 6(3), 59-62. doi: 10.13107/jocr.2250-0685.508.
- 113) Stanovici, J., Le Nail, L.R., Brennan, M.A., Vidal, L., Trichet, V., Rosset, P., et al. (2016). Bone regeneration strategies with bone marrow stromal cells in orthopaedic surgery. *Curr Res Transl Med* 64(2), 83-90. doi: 10.1016/j.retram.2016.04.006.
- 114) Suwanprateeb, J., Sangam, R., Suvannapruk, W., and Panyathanmaporn, T. (2009). Mechanical and in vitro performance of apatite-wollastonite glass ceramic reinforced hydroxyapatite composite fabricated by 3D-printing. *J Mater Sci Mater Med* 20(6), 1281-1289. doi: 10.1007/s10856-009-3697-1.

- 115) Tataru, A.M., Wong, M.E., and Mikos, A.G. (2014). In vivo bioreactors for mandibular reconstruction. *J Dent Res* 93(12), 1196-1202. doi: 10.1177/0022034514547763.
- 116) Taylor, G.I. (1982). Reconstruction of the mandible with free composite iliac bone grafts. *Ann Plast Surg* 9(5), 361-376. doi: 10.1097/0000637-198211000-00003.
- 117) Taylor, G.I. (1983). The current status of free vascularized bone grafts. *Clin Plast Surg* 10(1), 185-209.
- 118) Taylor, G.I. (1985). Composite tissue transfer to the lower limb. *Recent Adv Plast Surg* 3, 83-109.
- 119) Taylor, G.I., Corlett, R.J., and Ashton, M.W. (2016). The evolution of free vascularized bone transfer: a 40-year experience. *Plast Reconstr Surg* 137(4), 1292-1305. doi: 10.1097/PRS.0000000000002040.
- 120) Taylor, G.I., Miller, G.D., and Ham, F.J. (1975). The free vascularized bone graft. A clinical extension of microvascular techniques. *Plast Reconstr Surg* 55(5), 533-544. doi: 10.1097/00006534-197505000-00002.
- 121) Torres, J., Tamimi, F., Alkhraisat, M., Prados-Frutos, J.C., and Lopez-Cabarcos, E. (2011). "Bone substitutes," in *Implant dentistry - the most promising discipline of dentistry*, ed. I. Turkyilmaz. Intech), 4-105.
- 122) Trombetta, R., Inzana, J.A., Schwarz, E.M., Kates, S.L., and Awad, H.A. (2017). 3D printing of calcium phosphate ceramics for bone tissue engineering and drug delivery. *Ann Biomed Eng* 45(1), 23-44. doi: 10.1007/s10439-016-1678-3.
- 123) Unger, C., Gruene, M., Koch, L., Koch, J., and Chichkov, B.N. (2011). Time-resolved imaging of hydrogel printing via laser-induced forward transfer. *Appl Phys A* 103(2), 271-277. doi: 10.1007/s00339-010-6030-4.
- 124) Vacanti, J.P., and Langer, R. (1999). Tissue engineering: the design and fabrication of living replacement devices for surgical reconstruction and transplantation. *Lancet* 354, S32-S34. doi: 10.1016/S0140-6736(99)90247-7.
- 125) Verboket, R., Leiblein, M., Seebach, C., Nau, C., Janko, M., Bellen, M., et al. (2018). Autologous cell-based therapy for treatment of large bone defects: from bench to bedside. *Eur J Trauma Emerg Surg* 44(5), 649-665. doi: 10.1007/s00068-018-0906-y.

- 126) Vorndran, E., Klarner, M., Klammert, U., Grover, L.M., Patel, S., Barralet, J.E., et al. (2008). 3D Powder printing of β -tricalcium phosphate ceramics using different strategies. *Adv Eng Mater* 10(12), B67-B71. doi: 10.1002/adem.200800179.
- 127) Wang, M.O., Vorwald, C.E., Dreher, M.L., Mott, E.J., Cheng, M.-H., Cinar, A., et al. (2015). Evaluating 3D-printed biomaterials as scaffolds for vascularized bone tissue engineering. *Adv Mater* 27(1), 138-144. doi: 10.1002/adma.201403943.
- 128) Warnke, P.H., Springer, I.N., Wiltfang, J., Acil, Y., Eufinger, H., Wehmoller, M., et al. (2004). Growth and transplantation of a custom vascularised bone graft in a man. *Lancet* 364(9436), 766-770. doi: 10.1016/S0140-6736(04)16935-3.
- 129) Wen, Y., Xun, S., Haoye, M., Baichuan, S., Peng, C., Xuejian, L., et al. (2017). 3D printed porous ceramic scaffolds for bone tissue engineering: a review. *Biomater Sci* 5(9), 1690-1698. doi: 10.1039/c7bm00315c.
- 130) Winder, J., and Bibb, R. (2005). Medical rapid prototyping technologies: state of the art and current limitations for application in oral and maxillofacial surgery. *J Oral Maxillofac Surg* 63(7), 1006-1015. doi: 10.1016/j.joms.2005.03.016.
- 131) Wubneh, A., Tsekoura, E.K., Ayranci, C., and Uludag, H. (2018). Current state of fabrication technologies and materials for bone tissue engineering. *Acta Biomater* 80, 1-30. doi: 10.1016/j.actbio.2018.09.031.
- 132) Xu, N., Ye, X., Wei, D., Zhong, J., Chen, Y., Xu, G., et al. (2014). 3D artificial bones for bone repair prepared by computed tomography-guided fused deposition modeling for bone repair. *ACS Appl Mater Interfaces* 6(17), 14952-14963. doi: 10.1021/am502716t.
- 133) Yang, X., Lu, Z., Wu, H., Li, W., Zheng, L., and Zhao, J. (2018). Collagen-alginate as bioink for three-dimensional (3D) cell printing based cartilage tissue engineering. *Mater Sci Eng C* 83, 195-201. doi: 10.1016/j.msec.2017.09.002.
- 134) Zimmermann, G., and Moghaddam, A. (2011). Allograft bone matrix versus synthetic bone graft substitutes. *Injury* 42 Suppl 2, S16-21. doi: 10.1016/j.injury.2011.06.199.

CHAPTER II

***In situ* production of pre-vascularized synthetic bone grafts for regenerating critical-sized defects in rabbits**

Luciano Vidal, MD, ^{1, §}; Meadhbh Á Brennan, PhD, ^{1,2, §}; Stéphanie Krissian, MD, ^{1,3};
Julien De Lima ¹; Alain Hoornaert, DDS, PhD, ^{1,4}; Philippe Rosset, MD, PhD, ^{1,3};
Borhane H Fellah, DVM, PhD, ⁵; Pierre Layrolle, PhD, ^{1*}

- 1) Inserm, UMR 1238, PHY-OS, Bone sarcomas and remodeling of calcified tissues, Faculty of Medicine, University of Nantes, 1 rue Gaston Veil, 44035 Nantes, France.
- 2) Harvard School of Engineering and Applied Sciences, Harvard University, Cambridge, MA, USA
- 3) CHRU Tours, Department of trauma and orthopedic surgery, Hospital Bretenneau, 2 Boulevard Tonnelé, 37000 Tours, France
- 4) CHU Nantes, Department of Implantology, Faculty of Dentistry, University of Nantes, 1 Place Alexis Ricordeau, 44042 Nantes, France
- 5) ONIRIS, CRIP, Veterinary School, 101 route de Gachet, 44307 Nantes, France

§ These authors contributed equally to this work

*** Corresponding author**

Prof. Pierre Layrolle, PhD, Director of Research, Inserm, UMR 1238, PHY-OS, Bone sarcomas and remodeling of calcified tissues, Faculty of Medicine, University of Nantes, 1 rue Gaston Veil, 44035 Nantes, France, email: pierre.layrolle@univ-nantes.fr

Abstract

Reconstructing large bone defects caused by severe trauma or resection of tumors remains a challenge for orthopedic and plastic surgeons. Free flaps comprised of a muscle flap with fibula bone and its vascularized bed can be transplanted to the reconstruction site to achieve healing. However, this transplantation technique adds morbidity, and requires extensive microsurgery and sculpting of the bone tissue to adapt the graft to both the vasculature and the anatomy of the bone defect. The aim of the current study is to evaluate an alternative approach consisting of the *in situ* production of a pre-vascularized synthetic bone graft and its subsequent transplantation to a critical-sized bone defect. 3D printed chambers containing biphasic calcium phosphate (BCP) granules, perfused by a local vascular pedicle, with or without the addition of stromal vascular fraction (SVF), were subcutaneously implanted into New Zealand White female rabbits. The SVF was prepared extemporaneously from autologous adipose tissue, while the vascular pedicle was isolated from the inguinal site. Chambers filled with BCP alone served as controls. After 8 weeks, the constructs containing a vascular pedicle exhibited abundant neovascularization, with significant numbers of blood vessels sprouting from the pedicle, which was further enhanced by the addition of SVF. These pre-vascularized synthetic bone grafts were then transplanted into 15 mm critical-sized segmental ulnar defects for a further 8 weeks. Micro-CT and decalcified histology revealed that pre-vascularization of synthetic bone grafts led to significantly enhanced bone regeneration. This pre-clinical study demonstrates the feasibility and efficacy of *in situ* production of pre-vascularized synthetic bone grafts for regenerating large bone defects, and will address an important clinical need.

Keywords:

Bone regeneration; vascularization; biphasic calcium phosphate; 3D printing; implantable chamber; bone graft transplantation.

Introduction

Although minor fractures and small bone defects can heal spontaneously, large and complex bone defects have limited capacity for regeneration. Reconstructing large bone defects that are the result of severe trauma or tumor ablation remains a critical challenge for orthopedic and plastic surgeons. Autologous bone grafting, whereby bone tissue is harvested from one site and transplanted into the defect site, is currently the gold standard procedure for regenerating large bone defects. Adequate vascularization is recognized as being a pivotal factor in ensuring the viability of a bone graft and the subsequent healing of the defect, indeed there is a statistically significant positive correlation between vascularization and bone formation [1]. Consequently, vascularized bone grafts are required for the regeneration of large bone defects. Free flaps, comprising harvested bone from sources such as the radius or fibula, together with a vascular supply and soft tissue, can be transplanted into the reconstruction site, where they are connected to the local vasculature [2]. Vascularized bone transfers have demonstrated faster healing, higher resistance to resorption and superior mechanical integrity than non-vascularized bone grafts [3]. However, this transplantation technique is associated with serious limitations. Firstly, the geometry of the graft rarely conforms to the shape and size of the bone defect, thereby requiring bone sculpting to attain an anatomically correct shape. Furthermore, connecting the vasculature of the graft to the vasculature of the defect site requires extensive microsurgery. Finally, the quantity of bone and soft tissue available to harvest from the donor site is limited, and most importantly, harvesting bone and surrounding tissue for grafting causes extreme pain and morbidity for the patient [4].

A major goal for orthopedic reconstructive surgery is therefore to avoid the need for the creation of a second surgical bone harvest site by using synthetic biomaterials as

an alternative to grafted autologous bone. Synthetic biomaterials alone do not have the adequate osteoinductive or angiogenic properties for healing large bone defects. However, osteoprogenitor/stem cells, in particular mesenchymal stem cells derived from bone marrow (BMSCs), combined with biomaterials, have been successful in regenerating bone tissue [5–8]. Nevertheless, it is well established that the lack of vascularization within a synthetic bone construct is the most critical obstacle to healing large bone defects [9]. Proximity to a vascular network is vital for cell viability, and sufficient delivery of nutrients and oxygen. Consequently, necrosis is often observed in the center of large synthetic implants as there is not enough extrinsic vascularization to produce vessel in-growth from the surrounding host tissue fast enough [10].

The aim of pre-vascularized synthetic constructs is to overcome the challenges of autologous bone grafting of free flaps and of synthetic biomaterial constructs. In the tissue engineering context, various efforts have been made to produce a network of blood vessels *in vitro* that has the capacity to anastomose after transplantation *in vivo* in order to deliver sufficient nutrients to the cells within the scaffold, thus enhancing their survival and functionality after implantation. The most sophisticated strategies target the delivery of MSCs together with endothelial cells, and *in vitro* these constructs have more advanced osteoblastic and endothelial differentiation compared to groups containing a single cell type [11]. However, when implanted into bone defects, these multicellular constructs did not enhance bone regeneration compared with the delivery of MSCs alone [12,13]. Recent work using 3D bio-printing has led to the creation of a perfusable vascular network using bio-inks and endothelial cells [14–16]. This approach seems promising although it is still a long way from clinical applications.

In situ-generated synthetic vascularized constructs have many advantages over the complex and labor-intensive culture required for *in vitro* generation of tissue-

engineered vascularized constructs. Several teams have suggested prefabricating synthetic bone substitutes by means of ectopic implantation, making pre-vascularization possible according to an '*in vivo* bioreactor' principle before transplanting it into the defect to be regenerated. To date, various strategies have been investigated to achieve pre-vascularization. Muscle tissue, which has a rich capillary network, has been wrapped around scaffolds in the form of an intramuscular pouch to encourage vessels to sprout from the muscle into the construct. Since this technique was first reported [17] its use has generated constructs with enhanced vascularization [18] however, its success was limited in pre-clinical and clinical studies by core necrosis [18,19]. This technique, along with adipose tissue stem cells and BMP-2, has nevertheless demonstrated success in large maxillofacial defect reconstruction. Arteriovenous (AV) loops have been used successfully to generate large vascularized synthetic constructs using fibrin matrix [20], coral scaffolds [21] and ceramics [22] in ectopic sites in animals. Recently, it was demonstrated that a ceramic construct, pre-vascularized using an AV loop in an ectopic site, showed superior bone healing following transplantation into a bone defect, compared to the construct without pre-vascularization [23]. However, in spite of these favorable outcomes, the applicability of the AV loop is restricted by the intricate microsurgical skills required for the construction of the arteriovenous shunt.

An alternative strategy to an AV loop is to provide vascularization by using a vascular pedicle. In this model, an artery and a vein are inserted centrally within an implantable chamber containing the biomaterial scaffold. The isolation of a vascular pedicle is relatively simple and does not require anastomosis of the blood vessels, thereby circumventing the complicated microsurgery required for an AV loop. An arteriovenous vascular bundle placed inside a construct with cadaver bovine bone [24] or autologous

ovine bone and bone marrow [25], achieved a fully-vascularized construct in ectopic sites in rats and sheep respectively. Further to this, chambers containing synthetic ceramic biomaterial with a vascular bundle, and growth factors [26] or BMSCs implanted ectopically demonstrated abundant microvasculature and tissue engineered bone [27,28]. Together, these studies demonstrate the utility of a pre-vascularized construct generated by using a vascular bundle. Appropriate evaluation of the performances of this type of construct following transplantation into a large bone defect has not yet been conducted, however.

The objective of this study was to produce a highly-vascularized graft *in situ* and to transplant it into a critical-sized defect in rabbits for bone reconstruction. In the current study, we used biphasic calcium phosphate (BCP) granules as the synthetic biomaterial, as this material has been shown in pre-clinical [5] and clinical studies [29,30] to be a suitable scaffold for bone healing. While ligated vascular pedicles can also achieve pre-vascularization constructs [28], we choose not to ligate the vascular pedicle due to increased risk of thrombosis. In line with our aim to prefabricate a graft with abundant microvasculature, we chose to deliver autologous stromal vascular fraction (SVF) isolated from adipose tissue, together with the vascular bundle, because SVF contains MSCs and endothelial cells [31] previously shown to stimulate angiogenesis [32,33]. The principal advantage of delivering SVF instead of expanded MSCs from adipose tissue is that the preparation the SVF could be performed extemporaneously in a single surgery, whereas the delivery of AT-MSCs requires *in vitro* culture and expansion, plus a second surgery. Chambers containing the BCP granules and a local vascular pedicle inserted centrally, with or without SVF supplementation, were implanted subcutaneously into New Zealand White female rabbits. After 8 weeks, the constructs were characterized by microtomography,

immunohistochemistry and histology for vascularization and bone tissue formation. In a second operative step, the bone construct was transplanted into a mid-diaphyseal segmental ulna defect. After a further 8 weeks, the animals were euthanized and samples were analyzed by micro-CT and decalcified histology for bone regeneration.

Materials and Methods

Biomaterials

Implantable chambers, to hold the synthetic biomaterials, SVF, and vascular pedicle, were designed using computer-aided design software (CAD, Space Claim Corporation, Concord, Massachusetts, USA). Chambers consisting of hollow cylinders measuring 15 mm in length and 10 mm in diameter, with a wall thickness of 1 mm, were designed to contain the BCP granules. A transversal window, measuring 3.5 mm in width and 15 mm in length, with two openings of 4.5 mm in diameter, was made to allow the vascular pedicle to pass through the implantable chamber. The drawing was exported in stereo lithography format (STL) and converted into a readable G-code file (Cura software). The implantable chambers were printed in 3D using polylactic acid (PLA) white filament, 3 mm in diameter (Ultimaker 2, Ultimaker B.V, Geldermalsen, The Netherlands). After 3D printing, the implantable chambers were deburred, cleaned with 70% ethanol, and air-dried. The sterilization of the chambers was ensured by immersion for 1 hour in a solution of glutaraldehyde followed by washing in a saline solution.

The synthetic bone substitute used in this study was macro- and micro-porous biphasic calcium phosphate (BCP, Biomatlante, Vigneux de Bretagne, France) in the form of irregular granules measuring 0.5-1 mm in size. These BCP granules were prepared by mixing calcium-deficient apatite with pore makers, compacting the material, sintering

at 1050 °C, crushing and sieving. The BCP granules were composed of 20 % hydroxyapatite (HA) and 80 % beta tricalcium phosphate (β -TCP) in weight as analyzed by X-ray diffraction. The BCP granules had an overall porosity of 70 %, consisting of macropores ($>100 \mu\text{m}$) and micropores ($10 < \mu\text{m}$). The BCP granules were sterilized by gamma irradiation at a dose $> 25 \text{ kGy}$.

In order to avoid bone regeneration of the ulna defect from the periosteum of the radius, a bi-layer membrane of polylactic glycolic acid (PLGA, Tisseos®, Biomedical Tissues, Nantes, France) was placed between the radius and ulna. This synthetic resorbable bi-layered membrane was manufactured from medical grade PLGA copolymer (Purasorb PLG 8531, Corbion Purac BV, Gorinchem, The Netherlands) using a proprietary process in a clean room [34]. The PLGA membrane, $10 \times 20 \text{ mm}$ in size, was packaged in double-sealed pouches and sterilized with gamma irradiation at 25 kGy (Ionisos SA, Dagneux, France).

Study design and ethical approval

The study was carried out on a total of 32 New Zealand White (NZW) rabbits in two surgical phases, as shown in Figure 1. The experiments were conducted in accordance with European Directive 2010/60/EU. Ethical approval for this study was obtained from the local ethics committee (CEEA, Pays de Loire, France) under the authorization project numbers CEEA.2012.119 and Apafis # 1917. The experiments were carried out at the Preclinical Investigation Research Center (CRIP) of the National Veterinary School of Nantes (ONIRIS, Nantes, France) under the supervision of a doctor in veterinary medicine. NZW adult female rabbits with a body weight of 4.5 kg were purchased from a professional breeder (Hypharm, Roussay, France). The animals were housed in individual cages with unlimited water and food. The room was

ventilated and air-conditioned to a temperature of 20 ± 1 °C. An artificial day / night cycle of 12 h was applied. The rabbits were acclimated for at least 10 days prior to surgery.

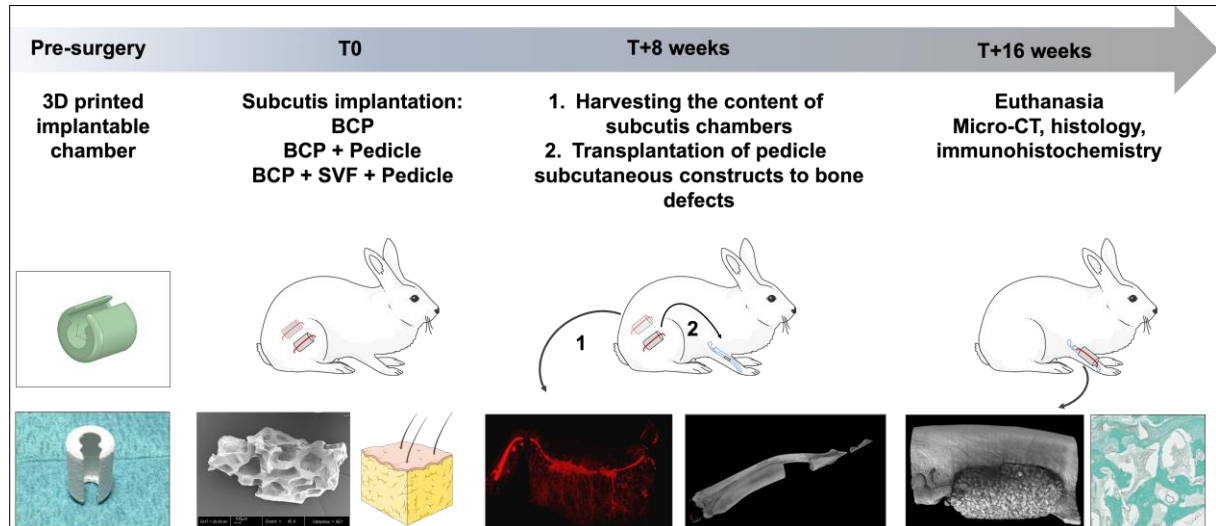


Figure 1 : Design of the study. Flow chart of the surgery steps and euthanasia; Design of the chamber and photograph of the implantable PLA chamber manufactured with 3D printing; Subcutis implantation of the PLA chambers loaded with BCP granules and autologous SVF with or without a vascular pedicle passing through; At 8 weeks, harvesting of the content of the subcutis chambers and transplantation in mid-diaphyseal segmental defects of 15 mm in the ulna of rabbits. At 16 weeks, euthanasia and micro CT and histology analysis.

In the first surgery, 25 rabbits were operated on. Two chambers containing the BCP granules and a central vascular pedicle, with or without supplementation with autologous stromal vascular fraction (SVF), were implanted into inguinal sites. Adipose tissue was collected and processed for preparation of the SVF during the first surgery. Chambers containing BCP alone served as controls. Each rabbit received two identical implants, with groups defined according to the content of the implanted chambers: synthetic bone filler alone (BCP), BCP with a vascular pedicle (BCP + Pedicle), or BCP

supplemented with autologous SVF and a vascular pedicle (BCP + SVF + Pedicle). A group of 9 rabbits (3/group) was sacrificed after 8 weeks in order to evaluate the vascularization inside the chambers by injection of a vascular contrast agent.

The second surgery was performed on 19 rabbits. 12 rabbits that had received 2 subcutis chambers containing BCP + Pedicle (n=6) and BCP + SVF + Pedicle (n=6) for 8 weeks were re-operated on for transplantation of the content of the chambers into ulnar defects. The rabbits were placed under general anesthesia and the chambers were explanted from the inguinal subcutis sites. The outer 3D-printed PLA chamber was removed and the content was transplanted into the ulna defect. The second chamber was collected and fixed in buffered formaldehyde for histological evaluation. A further seven rabbits of the same age and body weight were used for creation of ulnar defects that were left empty (n=3) or filled with BCP granules (n=4). Eight weeks after the second surgery, the animals were euthanized. The ulnas were dissected and immediately fixed in buffered formaldehyde for micro-CT and histology.

Subcutis implantation of chambers in rabbits

The rabbits were placed under general anesthesia by means of an intramuscular injection of a mixture of xylazine (Rompun® 2%, 0.2 mg / kg, Bayer Pharma, Puteaux, France) and ketamine (Imalgène 1000®, 20 mg / kg, Merial, Lyon, France). The inguinal sites were shaved and disinfected with povidone and sterile gauzes, and sterile fields were set up to delimit the surgical area. The general anesthesia was maintained by the intravenous injection of the same mixture through a catheter placed in the marginal vein of the ear. The rabbit was monitored for body temperature and heart pulse during the surgery.

The primary surgical steps for inguinal subcutis implantation are shown in Figure 2. A

medial cutaneous incision measuring 3-4 cm was made in the inguinal region. Two identical chambers were implanted into the subcutaneous inguinal sites of each rabbit. In control samples, BCP was added directly to the chambers (BCP). In the case of pre-vascularized implants, two pedicles were isolated from the left and right femoral artery branches respectively. The dissection of the femoral artery was performed in deep planes in the inguinal site. Once the branch of the femoral artery was identified, delicate dissection of the pedicle was conducted with careful hemostasis by using an electrical bistoury. Some BCP particles were put into the chamber, then the vascular pedicle was placed in the transverse position and the chamber was then completely filled with BCP granules, taking care not to compress the blood vessel. Hemostasis and the patency of the vessels upstream and downstream of the chamber were verified. After smooth dissection of the subcutaneous connective tissue, 5 g of adipose tissue adjacent to the mammary tissue was harvested and processed for isolation of the SVF. While harvesting the adipose tissue, hemostasis was ensured by using an electric scalpel. Preparation of the SVF required less than 1 hour while the rabbit was maintained under general anesthesia, with the open wound moistened with saline gauzes. Chambers with a vascular pedicle were filled with BCP granules alone (BCP + Pedicle) or BCP granules mixed with SVF (BCP + SVF + Pedicle). All chambers were fixed to the abdominal muscle with non-absorbable sutures (Prolene®, 2/0, Ethicon). The surgical site was closed in layers using subcutaneous and cutaneous sutures with resorbable braided sutures (Polysorb Dec.2®, 2/0 and 3/0, Tyco Healthcare). Post-operative analgesia was provided by a transdermal patch of Fentanyl (Durogesic®, 15 µg/kg/h) placed on the ear, ensuring continuous release of the active substance for 3 to 5 days. Post-operative s.c. injection of non-steroidal anti-inflammatory drugs (Meloxicam, Metacam®, Boehringer-Ingelheim, Reims, at a dose of 0.1 to 0.2

mg/kg/day) was administered for 5 days. An antibiotic treatment of marbofloxacin (3 mg/kg, s.c. injection, Marbocyl, Vetoquinol, Paris, France) was started the day of surgery and repeated for 5 days. After surgery, the animals were monitored for signs of suffering, and the surgical wounds were inspected daily to check for skin healing and the absence of infections.

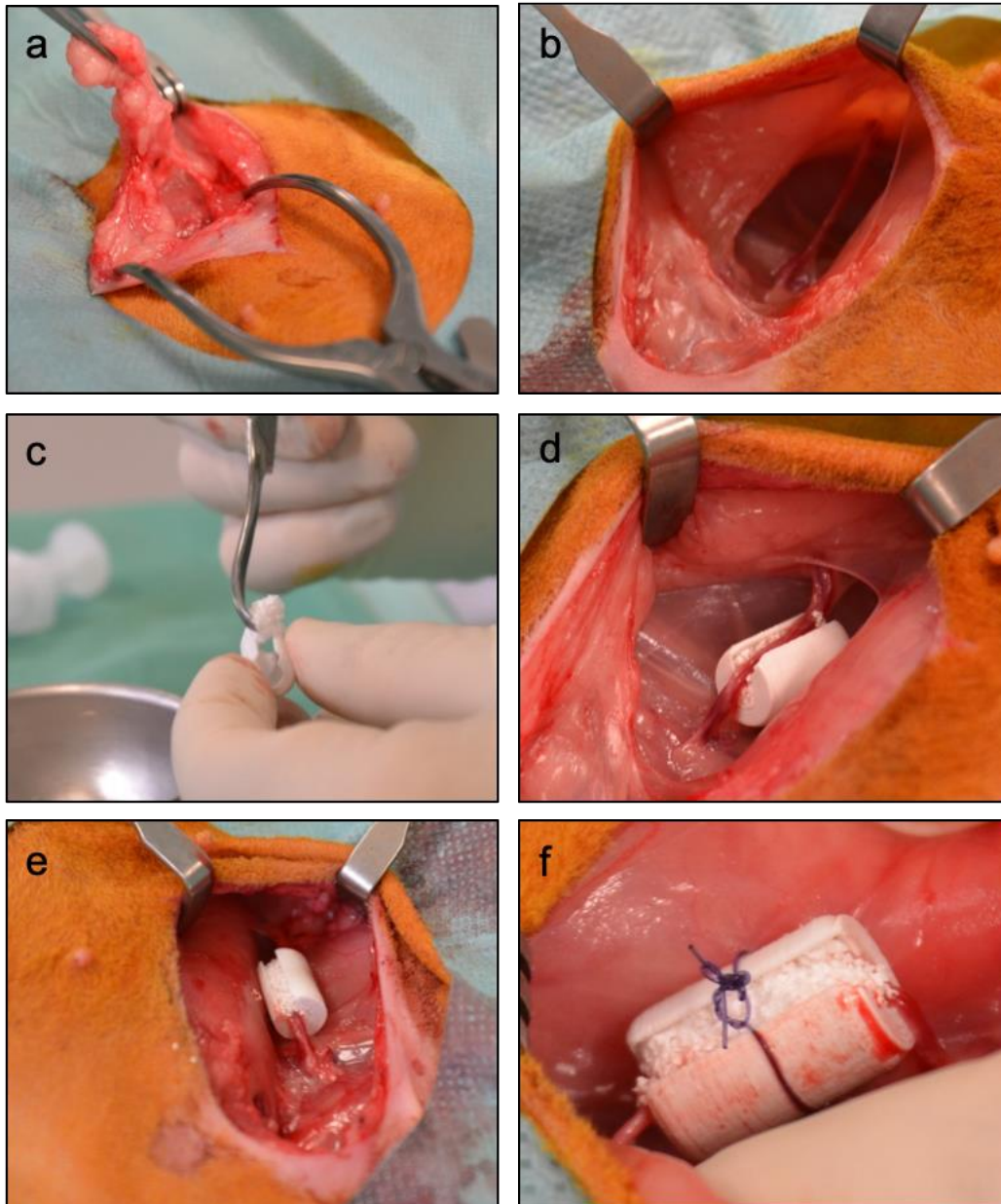


Figure 2 : Photographs showing (a) the harvesting of adipose tissue; (b) isolation of the vascular pedicle from a femoral artery branch; (c) pre-filling of the chamber with BCP granules; (d) insertion of the vascular pedicle; (e, f) filling and fixation of the implantable chamber in an inguinal subcutaneous site in rabbits.

Extemporaneous preparation and characterization of the stromal vascular fraction of adipose tissue from rabbits

Autologous adipose tissue (AT), 5 g per rabbit, was harvested in the inguinal-abdominal region of rabbits during the first surgery. The AT was placed in a sterile 50 ml tube (Falcon, BD). The stromal vascular fraction (SVF) was prepared in aseptic conditions under a laminar flow cabinet. The AT was washed three times with phosphate buffered saline (PBS, Gibco) to eliminate red blood cells. Mechanical digestion was performed to roughly dissociate the AT with scissors and vortexing for 1 to 2 minutes. Enzymatic digestion was performed with 0.075% collagenase A (Roche) at 37 °C for 45 min with 3 vortex agitations for 1 to 2 min. After digestion, the yellow viscous solution was filtered through 70 µm (Becton-Dickinson), to remove tissue debris, and centrifuged at 1600 rpm for 5 min. After removal of the oily supernatant, the cell pellet corresponding to the SVF was suspended in 1.5 ml of PBS to allow it to associate with the BCP granules. The SVF was implanted subcutaneously into the same rabbit as the harvested AT sample to avoid an immune response against allogeneic cells. Cell counting of the SVF preparation was performed using an automated cell counter (Nucleocounter® NC-100, Denmark).

In order to demonstrate their multi potency, 1.5×10^5 nucleated cells from the SVF of rabbits were cultured in a 75 cm² flask in Dulbecco's modified Eagle-based culture medium (Gibco® DMEM, Life Technologies, Inc. Saint Aubin, France) supplemented with 10% fetal calf serum (FCS, GE Healthcare, Vélizy-Villacoublay, France) and 1% penicillin / streptomycin (Gibco) at 37 °C in a humidified atmosphere (5% CO₂ / 95 % of air). The culture medium was refreshed every 2-3 days. After 7 days of culture, the adherent cells (adipose tissue-derived stromal cells – ATSCs) were approximately 80 % confluent and were detached from the plastic by trypsin/EDTA (Lonza, Belgium) and

centrifuged at 1600 rpm for 5 min (Passage 0). After cell counting, the cells were amplified in a 500 cm² triple flask at a cell density of 5×10^3 cells/cm² for 7 days (passage 1). After detachment and counting, the cells were cultured in 24-well plates at an initial cell density of 2×10^4 and 5×10^3 cells/cm² under adipogenic and osteogenic conditions respectively, with 500 μ L of differentiation media (StemPro® Differentiation kits, Life Technologies, Saint Aubin, France). For chondrocyte differentiation, 1×10^6 ATSCs were pelleted at 1600 rpm for 5 min and pellets were cultured under standard chondrogenic conditions (StemPro kits ®Differentiation). The culture medium was refreshed every 2-3 days. After 21 days of culture, cells were fixed in 4% paraformaldehyde. Staining with oil red O (M312512, Fisher), Alizarin red (Sigma) and Alcian blue (Sigma) was performed to highlight, respectively, the presence of adipocytes, the mineralized matrix produced by osteoblasts, and glycosaminoglycans produced by chondrocytes.

Transplantation of the pre-vascularized bone grafts into the ulnar defects

Eight weeks after implanting the chambers into the inguinal site, a second surgery was performed. The rabbits were placed under general anesthesia and prepared for surgery as previously described. The chambers containing the pre-fabricated synthetic bone grafts were exposed by smooth dissection. The chambers were removed after verifying that the permeability of the pedicles was being maintained, and placement of the vascular ligatures. The vascular permeability was assessed by clamping and sectioning the distal end of the pedicle, and after unclamping by observation of the bleeding of the pedicle. As shown in Figure 3, the vascularized synthetic grafts were gently removed from the PLA breakable chambers and stored in a sterile gauze moistened with physiological saline for transplantation into the ulna defect. The second

construct resected from each rabbit was put in 10% formalin fixative for further analysis by micro CT and histology.

In the second surgery, the osseous site was prepared to create a critical size segmental defect at the mid-diaphysis level of the left ulna. One critical-sized defect site per rabbit was created. The surgical approach was performed caudo-laterally with respect to the ulna in its middle third, so as to retain the stabilizing function of the interosseous ligament, thus avoiding the use of a fixation device. As illustrated in Figure 3, a bone defect measuring 15 mm length was created by medio-diaphyseal osteotomy using a wireless battery oscillating saw (Acculan 3Ti, Aesculap, Germany). A physiological saline rinse was performed to remove bone debris. To avoid bone regeneration of the defect created from the periosteum of the radius, a bi-layer membrane of polylactic glycolic acid (PLGA, Tisseos®, Biomedical Tissues, Nantes, France) [34] was interposed between the radius and the BCP granules or the pre-vascularized synthetic graft. The segmental bone defect was either left empty, filled with BCP granules moistened with saline, or a vascularized synthetic graft produced in a subcutaneous site of the same rabbit (BCP + Pedicle or BCP + SVF + pedicle). The surgical wound was closed in layers using resorbable sutures. As before, the operated animals were monitored daily to check their locomotion and proper cutaneous healing of the surgical site. After 8 weeks of implantation, the animals were euthanized as previously described. The ulna was dissected and immediately fixed in buffered 10% formalin solution and stored at 4°C for micro CT and histology analysis.

Injection of the radio-opaque vascular compound into rabbits

After 8 weeks of subcutaneous implantation, 9 rabbits were sacrificed in order to study vascularization inside the chambers containing either the BCP, BCP + Pedicle or BCP

+ SVF + Pedicle. The animals were placed under general anesthesia as previously described and received a dose of heparin (50 IU/kg, Heparin Choay® 25000 IU/5 mL, Sanofi-Aventis) to reduce blood coagulation. The animals were immediately euthanized by intravenous injection of pentobarbital (1 ml / kg, Dolethal, Vetoquinol). After euthanasia, a medial skin incision in the abdominal region was performed. The dissection was performed to expose the abdominal aorta, which was clamped and ligated proximally with a resorbable suture (Vycril® 3-0 coil, Ethicon, Johnson & Johnson, France). The aorta was catheterized with a silicone tube of similar diameter to inject a polymerizable silicone-based vascular contrast product containing lead (Microfil®, MV-122, Flow Tech Inc., Carver, MA, USA). The silicon tube was pre-filled with heparinized saline in order to avoid air bubbles, using a peristaltic pump (Masterflex™, France). The radio-opaque solution (containing a yellow dye) was prepared according to the manufacturer's instructions. It consisted of 45% vol. MV-122, 50% vol. of the diluent solution and 5% vol. of the curing agent. The vascular contrast agent was perfused into the carotid artery using a peristaltic pump at a flow rate of 20 ml/min, corresponding to a physiological pressure of 100–120 mm Hg. Complete filling of the arteries and capillaries was assessed when the blood vessels appeared yellow. The vascular contrast agent was left to polymerize at room temperature for 30 min. The chambers were then dissected and immediately fixed in buffered 10% formalin solution and stored at 4°C for micro CT and histology analysis.

Micro-computed tomography

Samples which were perfused with the contrast agent to demonstrate vasculature were characterized by high-resolution X-ray micro-tomography (Skyscan uCT 1076, Kontich, Belgium) before and after decalcification. The acquisition was carried out at

50 kV over 180 ° with axial sections measuring 0.7 mm, giving a resolution of 18 µm / pixel. 3D reconstruction of the images was carried out using NRecon, Dataviewer, CTvox and CTan (Bruker, Skyscan) software. Given this spatial resolution, large vessel diameters as well as fine vasculature down to 50 µm can be observed and measured. The filling of the chambers with BCP was measured and expressed as material volume. The vascular volume was determined using the bone volume / total volume parameter (BV/TV) after decalcification of the samples.

Histology and immunohistochemistry

After fixation, the samples were decalcified in 4.13% ethylenediamine tetra acetic acid (EDTA)/0.2% paraformaldehyde in phosphate-buffered saline, pH 7.4 for 96 hours at 50°C using automated microwave decalcifying apparatus (KOS Histostation; Milestone Medical, Kalamazoo, Michigan, USA). The samples were then dehydrated in ascending series of ethanol baths (80, 95 and 100%) and finally in butanol for 30 minutes in an automated dehydration station (Microm Microtech, Lyon, France). The samples were then impregnated with liquid paraffin at 56°C (Histowax; Histolab, Gottenburg, Sweden) and embedded at -16°C. Blocks were cut using a standard microtome (Leica RM2255; Leica Biosystems, Nanterre, France). Thin histology sections (3 to 5 µm thick) were made radially for subcutis implants and longitudinally for ulnar defects. Sections were stained using the Masson trichrome technique in an automated coloration station (Microm Microtech). This staining combines hematoxylin for cell nuclei (blue/black), fuchsine for cytoplasm, muscle and erythrocytes (red), and a light green solution for collagen (green). The stained slices were scanned (NanoZoomer; Hamamatsu, Photonics, Hamamatsu City, Shizuoka Prefecture, Japan) and observed with the virtual microscope (NDP view; Hamamatsu). The number of

blood vessels per field (objective x10) was determined on histological sections stained with Masson Trichrome. The number of blood vessels was counted using image analysis software (ImageJ, National Institute of Health, USA).

Vascularization in the subcutis chambers was also identified with the anti-CD31 antibody which labels endothelial cells. Briefly, heat-mediated antigen retrieval was performed for 20 hours with Tris-EDTA (pH 9) at 60°C on deparaffinized sections. Quenching of endogenous peroxidase activity was mediated by 3% hydrogen peroxide incubation. Nonspecific binding sites were blocked with 5% goat serum, 1% bovine serum albumin (BSA) in Tris Buffered Saline 1X pH=7.4 Tween 0.05% (T.B.S., ScyTek Laboratories, Utah, USA). All washing steps were conducted using T.B.S. 1X pH=7.4 Tween 0.05%. Mouse monoclonal antibody to CD31/PECAM-1 (SPM122, M01513, Bosterbio) at a dilution of 1:25 was used, followed by incubation with a secondary goat anti-mouse antibody at a dilution of 1:100 (E0433, Dako, Denmark). The target antigen signal was amplified using streptavidin peroxidase (P0397, Dako, Denmark), revealed by diaminobenzidine (DAB). All sections were dehydrated and counterstained using Gill's hematoxylin and mounted using Pertex mounting medium. Sections were scanned (NanoZoomer; Hamamatsu, Photonics, Hamamatsu City, Shizuoka, Japan) and observed using a virtual microscope (NDP view; Hamamatsu). Blood vessels were counted using ImageJ and presented as the number of blood vessel/mm².

Statistics

The data were expressed as an average \pm standard error of the mean. Analysis of the results of *in vivo* experiments was performed using the GraphPad Prism 6.0 software with a one-way ANOVA test. Tukey's multiple comparisons tests was conducted to

assess statistical differences between the distinct groups. The significance threshold was set at $p \leq 0.05$.

Results

Preparation of SVF and multipotency of ATSCs

Approximately 5 g (mean=5.8 \pm 1.4 g ; n=6) of adipose tissue was harvested and the stromal vascular fraction (SVF) was prepared extemporaneously within 1 hour by mechanical disruption, enzyme digestion and centrifugation. The average number of nucleated cells in the prepared SVF was 3.57 $10^5 \pm 1.24 10^5$ cells/ml ; n=6) after re-suspension in PBS and 1.5ml cell suspension was mixed with BCP granules. The cellular constituents of SVF from rabbits has been previously well characterized [35]. SVF was cultured *in vitro* and the constituent plastic adherent cells exhibited the tri-lineage characteristics of MSCs (supplementary Figure 1). Briefly, in adipogenic differentiation conditions, lipid droplets were observed after staining with Red Oil. After osteogenic induction, the cells produced a mineralized collagen matrix, highlighted by Alizarin red staining. Cell pellets, cultured in the presence of chondrogenic differentiation factors, showed the production of an extracellular matrix rich in glycosaminoglycans, as demonstrated by Alcian blue staining.

Characterizing the content of the subcutis implanted chambers

All rabbits survived the surgery without complications. After 8 weeks of subcutaneous implantation, all implants appeared well-integrated into the surrounding subcutis tissue, with no evidence of either rejection or necrosis. Vascular patency of the artery and vein passing through the chamber was observed for all pedicle implants (Figure 3a). The contents of the vascularized pedicle chambers exhibited a cylindrical shape with a good cohesion between the BCP granules due to abundant fibrosis (Figure 3b).

In contrast, the BCP granules implanted without a pedicle appeared loose after opening the chambers (Supplementary Figure 2).

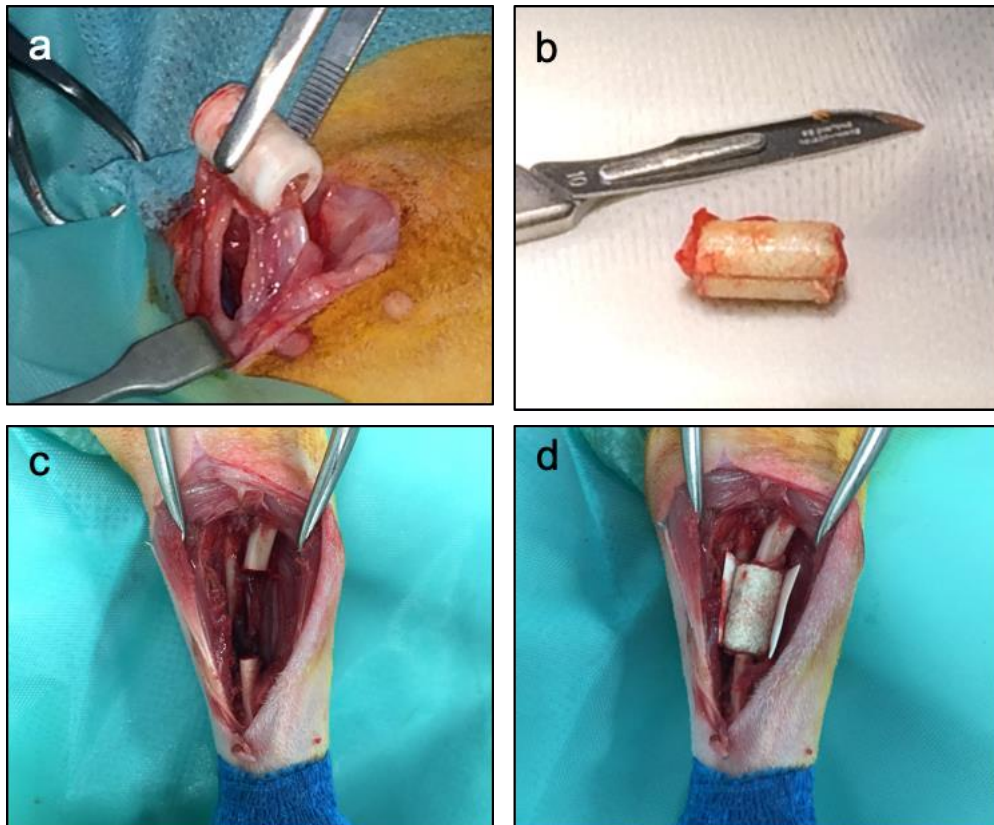


Figure 3 : Photographs of the surgery steps showing (a) the harvesting of the implantable chamber with the vascular pedicle passing through after subcutis implantation for 8 weeks; (b) the content of the chamber; note the cohesion of the BCP granules due to abundant collagen matrix; (c) the creation of a mid-diaphyseal segmental defect measuring 15 mm in the ulna; (d) the transplantation of the content of the chamber into the ulnar defect with a surrounding PLGA membrane to isolate the radius.

Micro-tomography showed that the BCP biomaterial granules had a cylindrical shape formed by the 3D printed PLGA chamber (Figure 4a-c). As shown in Figure 4g, the three groups had very comparable dimensions and biomaterial filling percentages. After injecting the contrast agent and decalcifying the explants, it was possible to observe the vascular pedicle and new vasculature following 3D reconstruction of the μ CT images. As shown in Figure 4d, the vascularization was negligible inside the chambers containing the BCP granules without a pedicle and was mainly located in the surrounding fibrous tissue capsule that had formed around the implantable chambers. Conversely, abundant vasculature with many small blood vessels was observed inside chambers containing BCP granules with a vascular pedicle (Figure 4e-f). Both the BCP + Pedicle and BCP + SVF + Pedicle groups exhibited abundant blood vessel branches that had grown from the main artery (see supplementary video). Quantification of the micro-CT vascular volume data demonstrated significantly higher vascular volume in the BCP + Pedicle group (2.33 ± 0.67 , n=5) compared to the control BCP group without a pedicle (0.45 ± 0.19 , n=3) (Figure 4h).

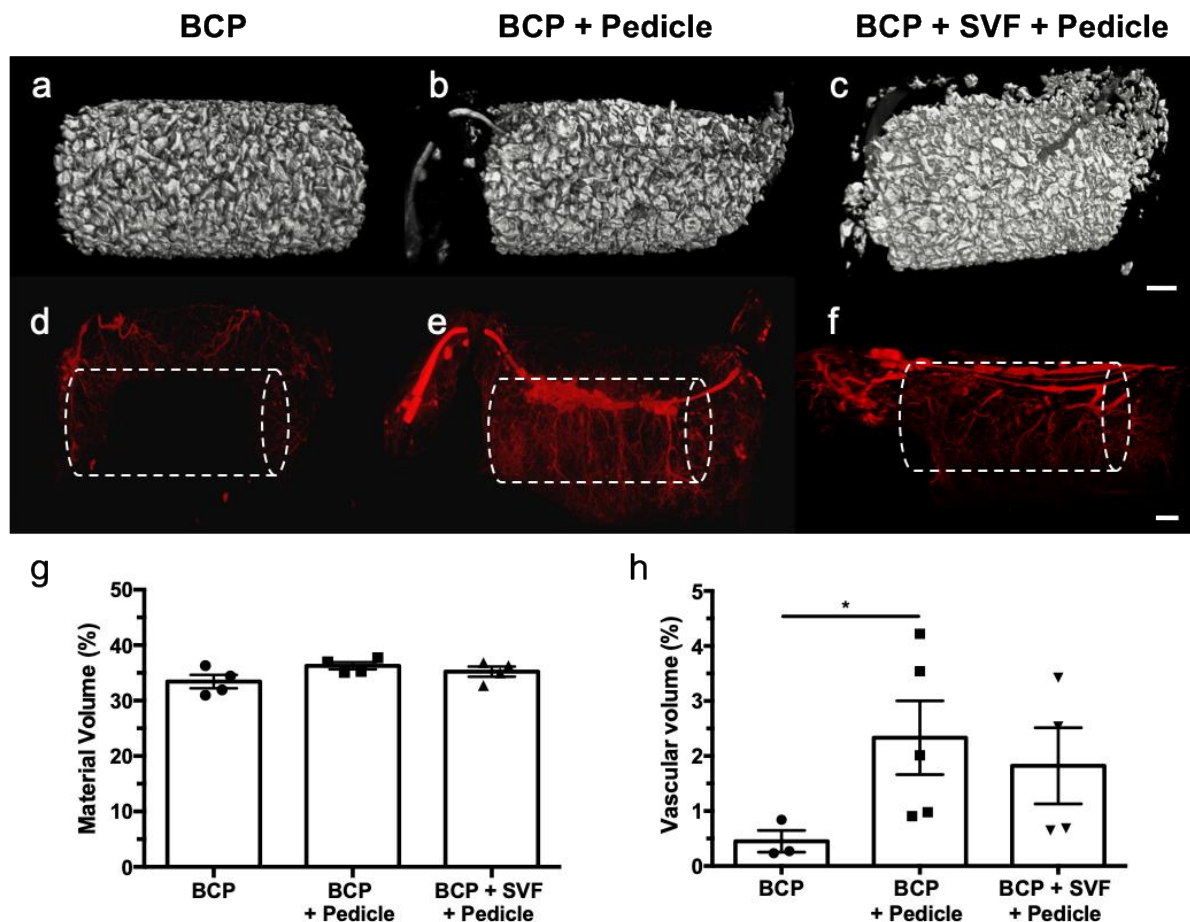


Figure 4 : 3D micro-CT reconstructions of the contents of 3D-printed PLGA chambers after subcutis implantation into inguinal sites in rabbits for 8 weeks. (a, b,c) before decalcification; (d,e,f) after injection of the vascular contrast agent and decalcification; (a,d) BCP granules; (b,e) BCP + vascular pedicle passing through the chamber; (c,f) BCP + SVF + Pedicle (scale bar: 1 mm; see supplementary figures with video showing the vascularization); (g) percentage of material volume in the chambers; (h) percentage of vascular volume in the chambers after decalcification (mean \pm SEM, * indicates significant difference between groups).

Histological Masson Trichrome images showed that the BCP granules were encapsulated in a dense collagen matrix for all three implant groups (Figure 5a). The pediculated implants appeared to be richer in collagen, with stronger fiber condensation, compared with the control BCP without a pedicle, however, bone tissue was not observed in any of the three implant groups. At higher magnification, giant

nucleated cells were present in contact with the BCP biomaterial, and were more prevalent in the BCP group without a pedicle. The vascular pedicles were clearly visible on the histological sections of the BCP + Pedicle and BCP + SVF + Pedicle groups. In the latter, higher neovascularization with many blood vessels sprouting from the main vasculature was observed in comparison to the other groups. This observation was confirmed by the quantification of blood vessels in each group (Figure 5b), whereby significantly higher vascularization was found in the BCP + SVF + Pedicle group (122.5 ± 20.07 , n=4) compared to the control BCP group (16.75 ± 9.29 , n=4) without a pedicle. While the number of blood vessels was also higher in the BCP + Pedicle group (55.00 ± 10.95 , n=5) compared to the control BCP group, this did not reach statistical significance.

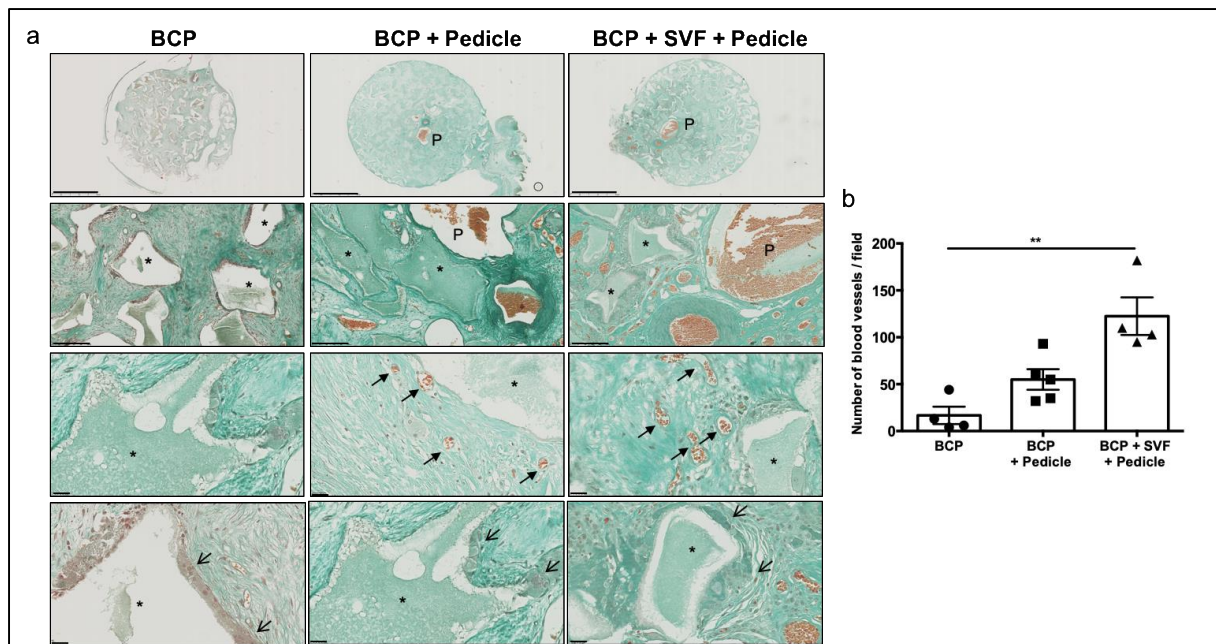


Figure 5 : (a) Histology of the content of chambers after subcutis implantation into inguinal sites in rabbits for 8 weeks (Masson's Trichrome staining; low magnification images top row, scale bars: 2.5 mm; scale bars of second row: 250 μm; high magnification images in rows 3 and 4 scale bars: 25 μm; P: vascular pedicle, *: BCP granules; black arrows: blood vessels; open arrows: multinucleated giant cells). (b) Number of blood vessels per field as a function of groups (mean ± SEM; * indicates statistical differences).

The above results were corroborated by CD31 immunohistochemistry staining of endothelial cells shown in Figure 6. It is clear that the central vasculature helped to develop new vascularization, with sprouting of many capillaries visible, while a limited number of blood vessels were observed in the control BCP group without a pedicle. As shown in Figure 6b, the number of blood vessels was greater for pedicle groups (24.20 ± 3.63 , $n=6$, and 26.9 ± 3.44 , $n=5$, for the BCP + Pedicle and BCP + SVF + Pedicle respectively), compared to the BPC alone group (20.06 ± 3.94 , $n=3$) although the differences did not reach statistical significance. Taken together, these results revealed the creation of a vascularized construct through inclusion of a pedicle and, furthermore, that adding autologous SVF, stimulated angiogenesis.

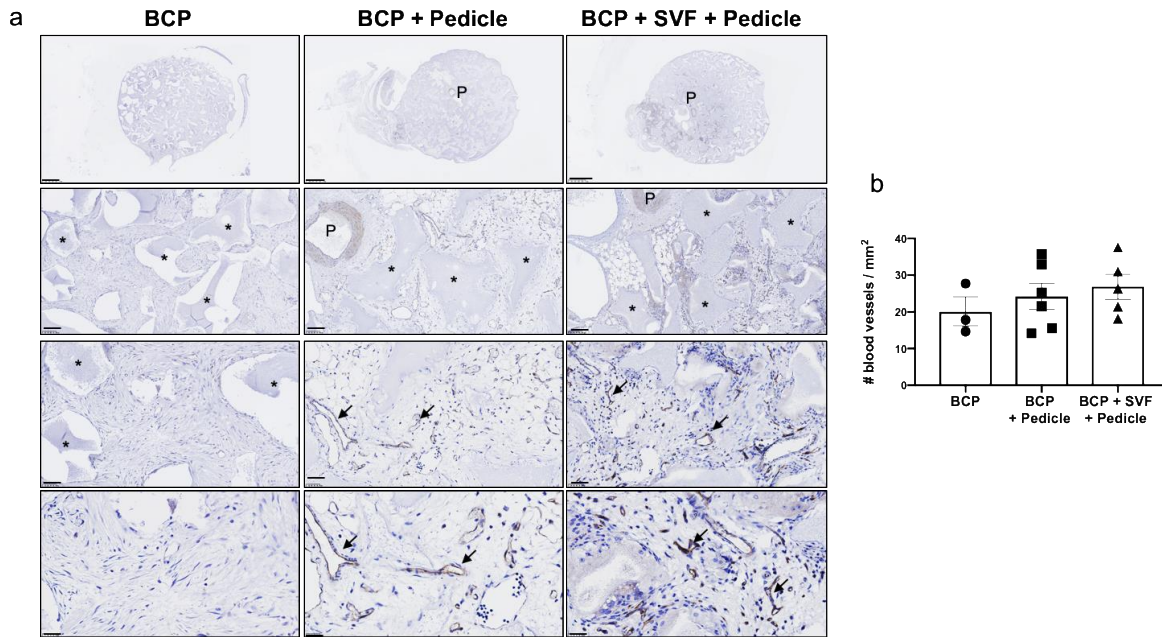


Figure 6 : (a) Immunohistochemistry of CD31 endothelial cells showing vascularization in the chambers after subcutis implantation into inguinal sites in rabbits for 8 weeks (CD31 immunohistochemistry hematoxylin staining; low magnification images top row, scale bars: 1 mm; scale bars of second row: 100 μ m; scale bars of third row: 50 μ m; scale bars of fourth row: 25 μ m; P: vascular pedicle, *: BCP granules; black arrows: blood vessels). (b) Number of blood vessels per mm^2 as a function of groups (mean \pm SEM; * indicates statistical differences).

Transplantation of pre-vascularized synthetic grafts enhanced bone healing in ulna defects in rabbits

As shown in Figure 3, a segmental critical-sized defect was created at the mid-diaphyseal level of the ulna. After 8 weeks in subcutis sites, the pre-vascularized constructs were transplanted into this defect and isolated from the radius using a PLGA membrane. Eight weeks after transplantation, the ulnas were characterized by micro-computed tomography and histology. As shown in Figure 7, the ulna defect that was left empty exhibited limited bone healing, proving that a critical-sized defect was created. The ulna defects filled with BCP granules had lower radio-opacity than those filled with the pre-vascularized grafts. BV/TV measurements revealed higher bone

content in the pre-vascularized grafts, BCP + Pedicle (34.53 ± 4.00 , $n=6$) and BCP + SVF + Pedicle grafts (37.65 ± 1.72 , $n=6$) compared with the BCP group (23.73 ± 3.59 , $n=4$) and empty defects (4.82 ± 1.49 , $n=3$).

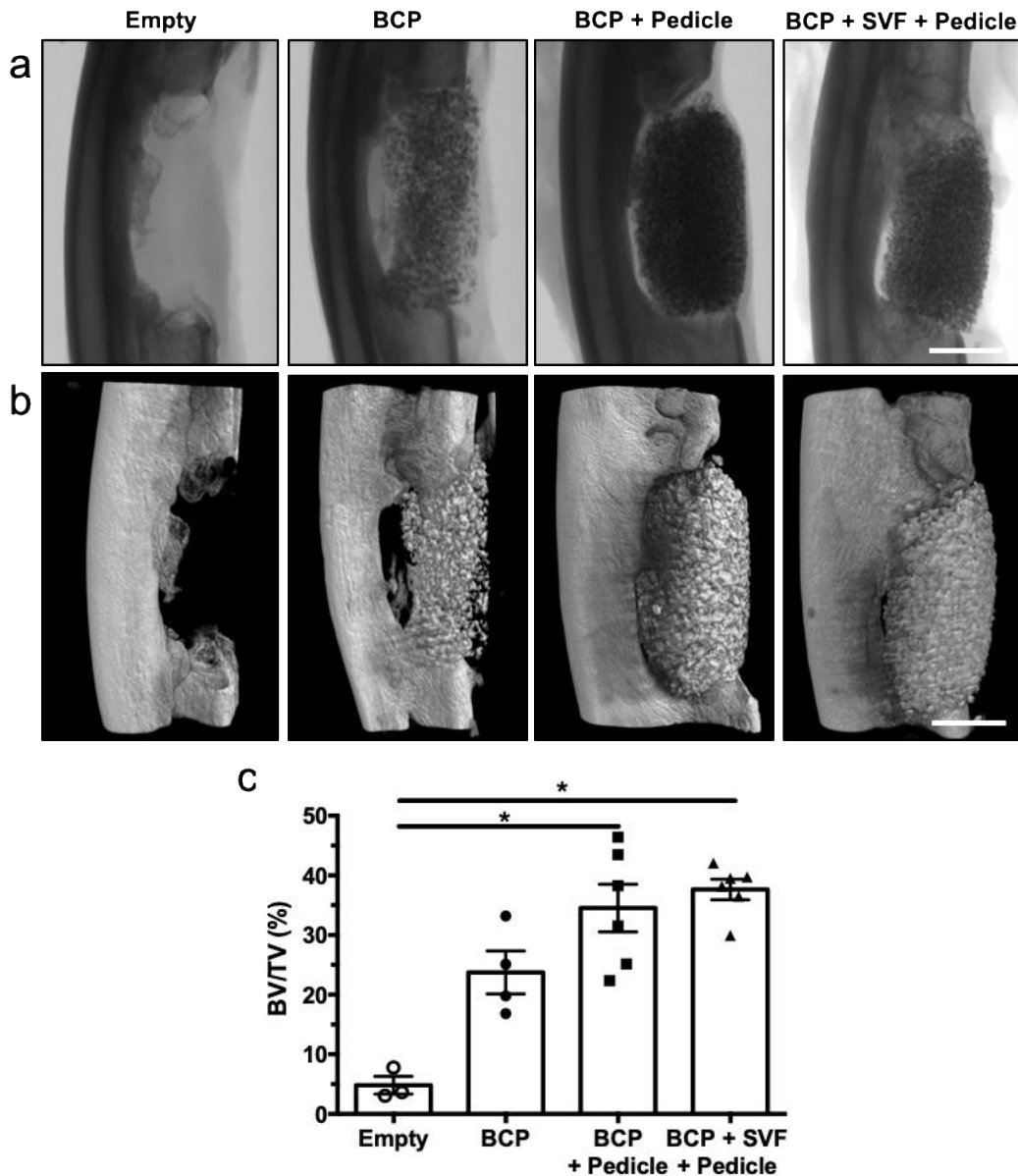


Figure 7 : (a) Micro-CT radiographs and (b) 3D reconstructions of ulnar defects in rabbits after 8 weeks of healing for the empty defect, defect filled with BCP granules, defect filled with the transplanted content of the chamber containing the BCP granules with vascular pedicle or BCP supplemented with SVF and vascular pedicle (scale bars: 10 mm); (c) Percentage of bone volume / total volume in the different groups (mean \pm SEM, * indicates significant difference).

As illustrated in Figure 8, histological examination corroborated the micro-computed tomography results. The empty defects were filled with fibrous vascularized tissue. Ulna defects filled with BCP granules showed limited bone healing from the edges. Bone formation was observed within the defects that received the transplanted pre-vascularized synthetic constructs, however some tissue necrosis was also observed. In both pre-vascularized constructs, new bone tissue was found in contact with the BCP biomaterials as evidenced in Figure 8.

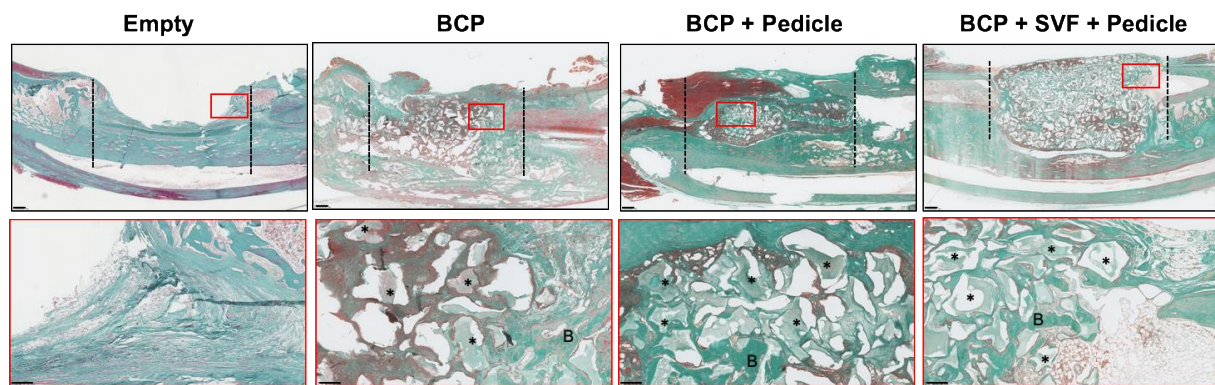


Figure 8 : Histology of the ulnar defects in rabbits after 8 weeks of healing for the empty defect, defect filled with BCP granules, defect filled with the transplanted content of the chamber containing the BCP granules with vascular pedicle or BCP supplemented with SVF and vascular pedicle (Masson's Trichrome staining; low magnification images scale bars, upper: 1 mm, dashed lines show margins of the mid-diaphyseal defect of 15 mm; high magnification images scale bars: 250 μ m; B: bone, *: BCP granules).

Discussion

Bone is a highly vascularized tissue with bone cells residing within a 100-200 μm proximity to a blood vessel or capillary in order to ensure adequate supply of vital oxygen and nutrients. For this reason, when a biomaterial construct is not vascularized at the time of implantation, ischemia occurs and high cell mortality is observed at the site. In the current study, implants were constructed by filling 3D-printed implantable chambers with BCP granules, a ceramic with proven bone-forming capabilities in pre-clinical and clinical trials [6,30]. The chamber held the granules in place, giving the construct a compact shape, while also making it easy to position the vascular pedicle. This pre-clinical study in rabbits demonstrates the feasibility of producing vascularized synthetic grafts in inguinal subcutaneous sites, and their capacity for bone healing after transplantation into a critical-sized bone defect.

There have been considerable advances in regenerative approaches aimed at overcoming the limitations of autologous bone grafting, however lack of adequate vascularization of synthetic grafts remains a major obstacle for reconstructing large bone defects. In the current study, we created a vascularized construct *in situ* by using an isolated pedicle composed of a peripheral artery and an adjacent vein, which were easily isolated from the surrounding tissues and passed through the implantable chamber. This achieved extensive neo vascularization with blood vessels sprouting from the central vasculature following subcutaneous implantation compared to the BCP group without a pedicle, as observed by both micro-CT and histology. This finding is in agreement with previous studies demonstrating the enhancement of neovascularization by using a vascular pedicle in unison with synthetic biomaterials [36]. Furthermore, this technique has advantages over previous *in situ* vascularized biomaterial constructs made using AV loops as it overcame the laborious stage of

microsurgical anastomosis [37]. The delivery of SVF to the pedicle construct, increased the number of blood vessels as demonstrated by histology, while showing no increased vascular volume as evaluated by the micro-CT. This could be explained by the different resolutions of the two measuring techniques: while micro-CT measures vessels as small as 50 μm , histology can detect vessels as small as 3 μm in diameter. High resolution CT, such as nano-CT and synchrotron CT equipment, could improve this resolution but still require the infusion of a vascular contrast agent. Increased number of new blood vessels by delivery of SVF is in agreement with previous studies [38].

While pre-vascularized constructs were successfully achieved by using our approach, there was an absence of bone formation in the subcutis constructs following implantation for 8 weeks. This is in contrast to a recent study which observed bone formation using SVF in a similar vascular pedicle approach [1], with differences possibly caused by the much lower cell number used in the current study. However, the bone induction observed by Epple et al was likely due to another aspect of their construct since the SVF showed no increase in bone formation compared to other groups without SVF, or could be due to the longer implantation time of 12 weeks in contrast to the 8 week period employed here. We have previously observed that cultured expanded MSCs derived from adipose tissue significantly enhanced neovascularization *in vivo* but failed to induce *de novo* bone in subcutis sites [39], in agreement with our present results. A comparable study encompassing a vascular pedicle, albeit just the vein, passing centrally through a 3D printed calcium phosphate scaffold has recently been reported [40]. Autologous bone marrow was placed in unison with the biomaterial around the femoral vein of rats in subcutaneous site for 8 weeks. Contrary to our study, newly formed bone tissue was observed in the explants loaded with bone marrow aspirates [40]. Together, this suggests the superiority of

employing bone marrow rather than SVF, whilst still permitting delivery in a single surgery. While promising, these studies have not assessed the potential of bone regeneration of critical size bone defects by transplantation of the pre-vascularized constructs. The current study represents the first evaluation of this type of *in situ* vascularized construct in a bone defect. Autologous transplantation of this vascularized synthetic graft into a rabbit ulna bone defect was possible without tissue morbidity and furthermore, after 8 weeks, micro-tomographic and histological examination showed good bone integration of the synthetic pre-vascularized graft and bone defect healing. Some limitations of the current study include firstly, that since the granules of the BCP group fell apart upon opening of the chambers, in contrast to the pedicle groups where firm constructs in the shape of the chambers were formed, this dictated that fresh BCP granules were used for the BCP control group in the bone defect surgery rather than those that had been implanted subcutaneously 8 weeks prior, as was the case for the two pedicle groups. It must also be noted that while our prevascularized construct approach circumvents issues of autologous bone graft harvesting and tissue availability, it required two surgeries and an 8 week preparation time for prevascularization, which is incompatible with severe and urgent trauma. Furthermore, the creation of the ulna defects was not standardized, which may have contributed to some non-unions at the extremity of the defects (Figure 7a) which may be overcome by the use of surgical guides customized to the skeletal anatomy. In addition, the prevascularized construct was transplanted into the ulna defect without anastomosis to the local vasculature. The limited size of the rabbit model and the availability of a suitable local vasculature to connect the transplant prevented us from performing anastomoses. This may be responsible for the small quantity of necrosis observed within these constructs after transplantation into the bone defects, nevertheless, new

bone tissue was formed and significant defect healing was observed. Finally, we did not conduct mechanical testing of the bone constructs which would have evaluated the functional strength of the implants and given a more precise view of the integrity of the bone tissue that was formed. While calcium phosphate biomaterials, such as the BCP used in the current study, have proven osteoconductive properties, they have very low mechanical properties in comparison with those of native bone tissue and it will thus undoubtedly be necessary to provide them with mechanical reinforcement through the addition of polymers or by adequate bone formation of high quality subcutaneously prior to transplantation. An anatomically shaped, mechanically suitable, vascularized construct has the potential to ensure effective bone healing of large bone defects.

Conclusion

This study has demonstrated the feasibility of *in situ* fabrication of vascularized synthetic grafts in an ectopic site using a vascular pedicle passing through the biomaterial. After inguinal subcutaneous implantation, all the pedicle implants exhibited excellent vascular permeability, and sprouting of a vascular network. The addition of SVF further stimulated angiogenesis. The transplantation of the pre-vascularized synthetic bone grafts into critical-sized ulnar defects led to significantly higher bone regeneration compared to the transplantation of the BCP biomaterial without a pedicle. This surgical technique was simple, fast and reproducible, and offers the possibility to preserve bone stock and overcome the limitations of autologous grafting.

Acknowledgments

This work was financially supported by a grant from the European Commission: ORTHOUNION (#773288). The patients' association 'Ligue Française contre les neurofibromatoses' is greatly acknowledged for supporting the PhD thesis of Luciano Vidal. Meadhbh Brennan is supported by the Marie Skłodowska Curie Individual Fellowship PARAGEN H2020-MSCA-IF-2015-708711. We appreciate the technical assistance of Clémence, Thébaud, and Jérôme Amiaud for preparation of the SVF and for histology, respectively. We also acknowledge the staff of the CRIP platform at the Veterinary school for the care, anesthesia and post-operative treatment of the animals.

Data availability

The raw/processed data required to reproduce these findings can be accessed by contacting the authors directly.

References

- [1] C. Epple, A. Haumer, T. Ismail, A. Lunger, A. Scherberich, D.J. Schaefer, I. Martin, Prefabrication of a large pedicled bone graft by engineering the germ for de novo vascularization and osteoinduction, *Biomaterials*. 192 (2019) 118–127. doi:10.1016/j.biomaterials.2018.11.008.
- [2] G. Merlino, M. Borsetti, M. Boltri, Reverse radial artery bone flap reconstruction of segmental metacarpal losses, *J Hand Surg Eur Vol.* 32 (2007) 98–101. doi:10.1016/j.jhsb.2006.08.015.
- [3] J.B. Moore, J.M. Mazur, D. Zehr, P.K. Davis, E.G. Zook, A biomechanical comparison of vascularized and conventional autogenous bone grafts, *Plast. Reconstr. Surg.* 73 (1984) 382–386.
- [4] J.E. Lipa, C.B. Novak, P.A. Binhammer, Patient-reported donor-site morbidity following anterolateral thigh free flaps, *J Reconstr Microsurg.* 21 (2005) 365–370. doi:10.1055/s-2005-915203.
- [5] M.Á. Brennan, A. Renaud, J. Amiaud, M.T. Rojewski, H. Schrezenmeier, D. Heymann, V. Trichet, P. Layrolle, Pre-clinical studies of bone regeneration with human bone marrow stromal cells and biphasic calcium phosphate, *Stem Cell Res Ther.* 5 (2014). doi:10.1186/scrt504.
- [6] A.-L. Gamblin, M.A. Brennan, A. Renaud, H. Yagita, F. Lézot, D. Heymann, V. Trichet, P. Layrolle, Bone tissue formation with human mesenchymal stem cells and biphasic calcium phosphate ceramics: the local implication of osteoclasts and macrophages, *Biomaterials*. 35 (2014) 9660–9667. doi:10.1016/j.biomaterials.2014.08.018.

- [7] M.H. Mankani, S.A. Kuznetsov, P.G. Robey, Formation of hematopoietic territories and bone by transplanted human bone marrow stromal cells requires a critical cell density, *Exp. Hematol.* 35 (2007) 995–1004.
- [8] M.H. Mankani, S.A. Kuznetsov, R.M. Wolfe, G.W. Marshall, P.G. Robey, In vivo bone formation by human bone marrow stromal cells: reconstruction of the mouse calvarium and mandible, *Stem Cells.* 24 (2006) 2140–2149. doi:10.1634/stemcells.2005-0567.
- [9] M.A. Brennan, J.-M. Davaine, P. Layrolle, Pre-vascularization of bone tissue-engineered constructs, *Stem Cell Res Ther.* 4 (2013) 96. doi:10.1186/scrt307.
- [10] J. Marler, J. Upton, R. Langer, J. Vacanti, Transplantation of cells in matrices for tissue regeneration, *Adv. Drug Deliv. Rev.* 33 (1998) 165–182.
- [11] N.B. Thébaud, R. Siadous, R. Bareille, M. Remy, R. Daculsi, J. Amédée, L. Bordenave, Whatever their differentiation status, human progenitor derived - or mature - endothelial cells induce osteoblastic differentiation of bone marrow stromal cells, *J Tissue Eng Regen Med.* 6 (2012) e51-60. doi:10.1002/term.1539.
- [12] M. Maisani, D. Pezzoli, O. Chassande, D. Mantovani, Cellularizing hydrogel-based scaffolds to repair bone tissue: How to create a physiologically relevant micro-environment?, *J Tissue Eng.* 8 (2017). doi:10.1177/2041731417712073.
- [13] X. Liu, W. Chen, C. Zhang, W. Thein-Han, K. Hu, M.A. Reynolds, C. Bao, P. Wang, L. Zhao, H.H.K. Xu, Co-Seeding Human Endothelial Cells with Human-Induced Pluripotent Stem Cell-Derived Mesenchymal Stem Cells on Calcium Phosphate Scaffold Enhances Osteogenesis and Vascularization in Rats, *Tissue Eng Part A.* 23 (2017) 546–555. doi:10.1089/ten.tea.2016.0485.

- [14] S.V. Murphy, A. Atala, 3D bioprinting of tissues and organs, *Nat. Biotechnol.* 32 (2014) 773–785. doi:10.1038/nbt.2958.
- [15] D.B. Kolesky, K.A. Homan, M.A. Skylar-Scott, J.A. Lewis, Three-dimensional bioprinting of thick vascularized tissues, *Proc Natl Acad Sci U S A.* 113 (2016) 3179–3184. doi:10.1073/pnas.1521342113.
- [16] H.-W. Kang, S.J. Lee, I.K. Ko, C. Kengla, J.J. Yoo, A. Atala, A 3D bioprinting system to produce human-scale tissue constructs with structural integrity, *Nat. Biotechnol.* 34 (2016) 312–319. doi:10.1038/nbt.3413.
- [17] R.K. Khouri, B. Koudsi, H. Reddi, Tissue transformation into bone in vivo. A potential practical application, *JAMA.* 266 (1991) 1953–1955.
- [18] A. Kaempfen, A. Todorov, S. Güven, R.D. Largo, C. Jaquiéry, A. Scherberich, I. Martin, D.J. Schaefer, Engraftment of Prevascularized, Tissue Engineered Constructs in a Novel Rabbit Segmental Bone Defect Model, *Int J Mol Sci.* 16 (2015) 12616–12630. doi:10.3390/ijms160612616.
- [19] P.H. Warnke, J. Wiltfang, I. Springer, Y. Acil, H. Bolte, M. Kosmahl, P.A.J. Russo, E. Sherry, U. Lützen, S. Wolfart, H. Terheyden, Man as living bioreactor: fate of an exogenously prepared customized tissue-engineered mandible, *Biomaterials.* 27 (2006) 3163–3167. doi:10.1016/j.biomaterials.2006.01.050.
- [20] J.P. Beier, R.E. Horch, A. Arkudas, E. Polykandriotis, O. Bleiziffer, E. Adamek, A. Hess, U. Kneser, De novo generation of axially vascularized tissue in a large animal model, *Microsurgery.* 29 (2009) 42–51. doi:10.1002/micr.20564.

- [21] Q. Dong, C. Lin, H. Shang, W. Wu, F. Chen, X. Ji, Y. Liu, J. Zhang, T. Mao, Modified approach to construct a vascularized coral bone in rabbit using an arteriovenous loop, *J Reconstr Microsurg.* 26 (2010) 95–102. doi:10.1055/s-0029-1243293.
- [22] A.M. Boos, J.S. Loew, A. Weigand, G. Deschler, D. Klumpp, A. Arkudas, O. Bleiziffer, H. Gulle, U. Kneser, R.E. Horch, J.P. Beier, Engineering axially vascularized bone in the sheep arteriovenous-loop model, *Journal of Tissue Engineering and Regenerative Medicine.* 7 (2013) 654–664. doi:10.1002/term.1457.
- [23] A. Arkudas, A. Lipp, G. Buehrer, I. Arnold, D. Dafinova, A. Brandl, J.P. Beier, C. Körner, S. Lyer, C. Alexiou, U. Kneser, R.E. Horch, Pedicled Transplantation of Axially Vascularized Bone Constructs in a Critical Size Femoral Defect, *Tissue Eng Part A.* 24 (2018) 479–492. doi:10.1089/ten.TEA.2017.0110.
- [24] E. Polykandriotis, A. Arkudas, R.E. Horch, M. Stürzl, U. Kneser, Autonomously vascularized cellular constructs in tissue engineering: opening a new perspective for biomedical science, *Journal of Cellular and Molecular Medicine.* 11 (2007) 6–20. doi:10.1111/j.1582-4934.2007.00012.x.
- [25] H. Kokemueller, S. Spalthoff, M. Nolff, F. Tavassol, H. Essig, C. Stuehmer, K.-H. Bormann, M. Rücker, N.-C. Gellrich, Prefabrication of vascularized bioartificial bone grafts in vivo for segmental mandibular reconstruction: experimental pilot study in sheep and first clinical application, *International Journal of Oral and Maxillofacial Surgery.* 39 (2010) 379–387. doi:10.1016/j.ijom.2010.01.010.

- [26] G.E. Holt, J.L. Halpern, C.C. Lynch, C.J. Devin, H.S. Schwartz, Imaging Analysis of the In vivo Bioreactor: A Preliminary Study, *Clin Orthop Relat Res.* 466 (2008) 1890–1896. doi:10.1007/s11999-008-0295-3.
- [27] D. Han, X. Guan, J. Wang, J. Wei, Q. Li, Rabbit Tibial Periosteum and Saphenous Arteriovenous Vascular Bundle as an In Vivo Bioreactor to Construct Vascularized Tissue-Engineered Bone: A Feasibility Study, *Artificial Organs.* 38 (2014) 167–174. doi:10.1111/aor.12124.
- [28] X. Wu, Q. Wang, N. Kang, J. Wu, C. Gu, J. Bi, T. Lv, F. Xie, J. Hu, X. Liu, Y. Cao, R. Xiao, The effects of different vascular carrier patterns on the angiogenesis and osteogenesis of BMSC-TCP-based tissue-engineered bone in beagle dogs, *J Tissue Eng Regen Med.* 11 (2017) 542–552. doi:10.1002/term.2076.
- [29] C. Gjerde, K. Mustafa, S. Hellem, M. Rojewski, H. Gjengedal, M.A. Yassin, X. Feng, S. Skaale, T. Berge, A. Rosen, X.-Q. Shi, A.B. Ahmed, B.T. Gjertsen, H. Schrezenmeier, P. Layrolle, Cell therapy induced regeneration of severely atrophied mandibular bone in a clinical trial, *Stem Cell Res Ther.* 9 (2018). doi:10.1186/s13287-018-0951-9.
- [30] E. Gómez-Barrena, P. Rosset, F. Gebhard, P. Hernigou, N. Baldini, H. Rouard, L. Sensebé, R.M. Gonzalo-Daganzo, R. Giordano, N. Padilla-Eguiluz, E. García-Rey, J. Cordero-Ampuero, J.C. Rubio-Suárez, J. Stanovici, C. Ehrnthaller, M. Huber-Lang, C.H. Flouzat-Lachaniette, N. Chevallier, D.M. Donati, G. Ciapetti, S. Fleury, M.-N. Fernandez, J.-R. Cabrera, C. Avendaño-Solá, T. Montemurro, C. Panaitescu, E. Veronesi, M.T. Rojewski, R. Lotfi, M. Dominici, H. Schrezenmeier, P. Layrolle, Feasibility and safety of treating non-unions in tibia, femur and humerus with autologous, expanded, bone marrow-derived mesenchymal stromal cells associated

with biphasic calcium phosphate biomaterials in a multicentric, non-comparative trial, *Biomaterials*. 196 (2019) 100–108. doi:10.1016/j.biomaterials.2018.03.033.

[31] P.A. Zuk, M. Zhu, H. Mizuno, J. Huang, J.W. Futrell, A.J. Katz, P. Benhaim, H.P. Lorenz, M.H. Hedrick, Multilineage cells from human adipose tissue: implications for cell-based therapies, *Tissue Eng.* 7 (2001) 211–228. doi:10.1089/107632701300062859.

[32] M. Mazo, S. Hernández, J.J. Gavira, G. Abizanda, M. Araña, T. López-Martínez, C. Moreno, J. Merino, A. Martino-Rodríguez, A. Uixeira, J.A. García de Jalón, J. Pastrana, D. Martínez-Caro, F. Prósper, Treatment of reperfused ischemia with adipose-derived stem cells in a preclinical Swine model of myocardial infarction, *Cell Transplant.* 21 (2012) 2723–2733. doi:10.3727/096368912X638847.

[33] L. Casteilla, V. Planat-Bénard, B. Cousin, P. Laharrague, P. Bourin, Vascular and endothelial regeneration, *Curr Stem Cell Res Ther.* 5 (2010) 141–144.

[34] A. Hoornaert, C. d'Arros, M.-F. Heymann, P. Layrolle, Biocompatibility, resorption and biofunctionality of a new synthetic biodegradable membrane for guided bone regeneration, *Biomed Mater.* 11 (2016) 045012. doi:10.1088/1748-6041/11/4/045012.

[35] G. Desando, I. Bartolotti, L. Martini, G. Giavaresi, N. Nicoli Aldini, M. Fini, A. Roffi, F. Perdisa, G. Filardo, E. Kon, B. Grigolo, Regenerative Features of Adipose Tissue for Osteoarthritis Treatment in a Rabbit Model: Enzymatic Digestion Versus Mechanical Disruption, *Int J Mol Sci.* 20 (2019). doi:10.3390/ijms20112636.

[36] P. Yang, X. Huang, J. Shen, C. Wang, X. Dang, H. Mankin, Z. Duan, K. Wang, Development of a new pre-vascularized tissue-engineered construct using pre-

differentiated rADSCs, arteriovenous vascular bundle and porous nano-hydroxyapatite-polyamide 66 scaffold, *BMC Musculoskelet Disord.* 14 (2013) 318. doi:10.1186/1471-2474-14-318.

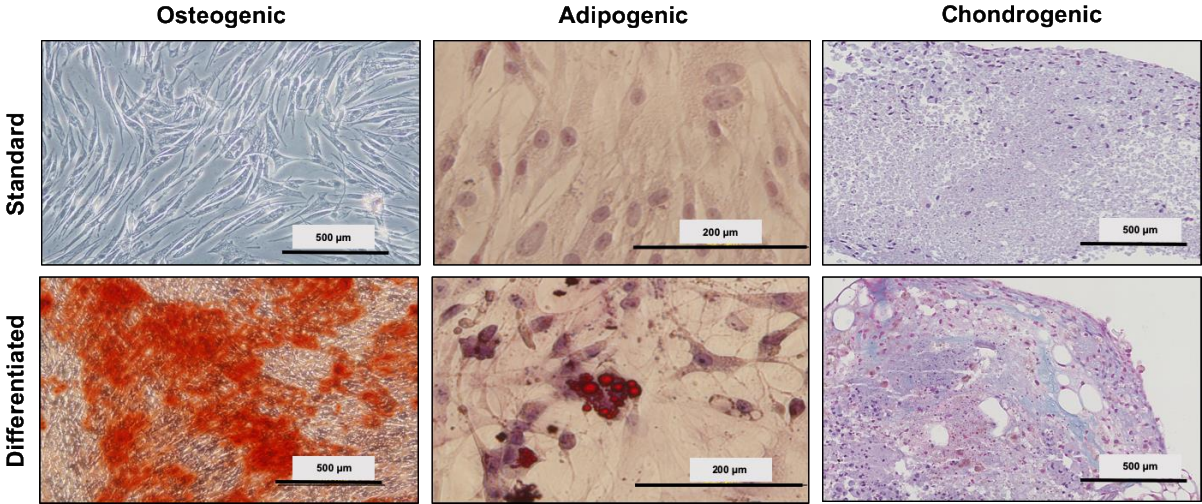
[37] J.P. Beier, R.E. Horch, A. Hess, A. Arkudas, J. Heinrich, J. Loew, H. Gulle, E. Polykandriotis, O. Bleiziffer, U. Kneser, Axial vascularization of a large volume calcium phosphate ceramic bone substitute in the sheep AV loop model, *J Tissue Eng Regen Med.* 4 (2010) 216–223. doi:10.1002/term.229.

[38] E. Farré-Guasch, N. Bravenboer, M.N. Helder, E.A.J.M. Schulten, C.M. Ten Bruggenkate, J. Klein-Nulend, Blood Vessel Formation and Bone Regeneration Potential of the Stromal Vascular Fraction Seeded on a Calcium Phosphate Scaffold in the Human Maxillary Sinus Floor Elevation Model, *Materials (Basel).* 11 (2018). doi:10.3390/ma11010161.

[39] M.A. Brennan, A. Renaud, F. Guilloton, M. Mebarki, V. Trichet, L. Sensebé, F. Deschaseaux, N. Chevallier, P. Layrolle, Inferior In Vivo Osteogenesis and Superior Angiogenesis of Human Adipose Tissue: A Comparison with Bone Marrow-Derived Stromal Stem Cells Cultured in Xeno-Free Conditions, *Stem Cells Transl Med.* 6 (2017) 2160–2172. doi:10.1002/sctm.17-0133.

[40] B. Charbonnier, A. Baradaran, D. Sato, O. Alghamdi, Z. Zhang, Y.-L. Zhang, U. Gbureck, M. Gilardino, E. Harvey, N. Makhoul, J. Barralet, Material-Induced Venosome-Supported Bone Tubes, *Advanced Science.* 0 (n.d.) 1900844. doi:10.1002/advs.201900844.

Supplementary Figures



Supplementary Figure 1 : Characterization of MSC from SVF of rabbits. Tri-lineage differentiation capacity of MSC without induction of differentiation and with osteogenic (alizarin red staining), adipogenic (Red Oil staining), and chondrogenic (Alcian blue staining) differentiation.



Supplementary Figure 2 : Photographs of the content of the chamber after subcutis implantation for 8 weeks ; a) with the vascular pedicle passing through; note the cohesion of the BCP granules due to abundant collagen matrix ; and b) without the pedicle ; note the loose BCP granules.

CHAPTER III

Regeneration of segmental defects in metatarsus of sheep with vascularized and customized 3D-printed calcium phosphate scaffolds

Luciano Vidal ¹, Carina Kampleitner ^{2,§}, Stéphanie Krissian ^{3,§}, Oskar Hoffmann ², Santiago Raymond ^{4,5,6}, Yassine Maazouz ^{4,5,6}, Maria-Pau Ginebra ^{4,5,7}, Philippe Rosset ^{1,3,8}, Pierre Layrolle ^{1,*}

¹ Inserm, UMR 1238, PHY-OS, Bone sarcomas and remodelling of calcified tissues, Faculty of Medicine, University of Nantes, Nantes, 44035, France

² University of Vienna, Department of Pharmacology and Toxicology, Vienna, 1090, Austria

³ Department of Trauma and Orthopaedic Surgery, University Hospital of Tours, University of Tours, Tours, 37000, France

⁴ Universitat Politècnica de Catalunya, Department of Materials Science and Metallurgical Engineering, Group of Biomaterials, Biomechanics and Tissue Engineering, Barcelona, 08019, Spain

⁵ Universitat Politècnica de Catalunya, Barcelona Research Centre for Multiscale Science and Engineering, Barcelona, 08019, Spain

⁶ Mimetis Biomaterials, Cerdanyola del Vallès, Barcelona, 08290, Spain

⁷ Institute for Bioengineering of Catalonia, Barcelona Institute of Science and Technology, Barcelona, 08036, Spain

⁸ Platform CIRE, Surgery and Imaging for Research and Education, INRA, Nouzilly, 37380 France

§ These authors contributed equally to this work.

* Corresponding author: pierre.layrolle@inserm.fr

ABSTRACT

Although autografts are considered to be the gold standard for reconstruction of large bone defects resulting from trauma or diseases, donor site morbidity and limited availability restrict their use. Successful bone repair also depends on sufficient vascularization. To address this challenge, novel strategies are being drafted to develop vascularized biomaterial scaffolds. This pilot study aimed to investigate the feasibility of regenerating large bone defects in sheep using 3D-printed customized calcium phosphate scaffolds with or without surgical vascularization. Pre-operative computed tomography scans were performed to visualize the metatarsus and vasculature and to fabricate customized scaffolds and surgical guides by 3D printing. Critical-sized segmental defects created in the mid-diaphyseal region of the metatarsus were either left empty or treated with the 3D scaffold alone or in combination with an axial vascular pedicle. Bone regeneration was evaluated 1, 2 and 3 months post-implantation. After 3 months, the untreated defect remained non-bridged while the 3D scaffold guided bone regeneration. The presence of the vascular pedicle further enhanced bone formation. Histology confirmed bone growth inside the porous 3D scaffolds with or without vascular pedicle inclusion. Taken together, this study demonstrated the feasibility of pre-surgical planning and reconstruction of large bone defects with 3D-printed personalized scaffolds.

KEYWORDS

Bone regeneration, vascularization, 3D printing, customized scaffolds, calcium-deficient hydroxyapatite, *in vivo* segmental defect, direct ink writing

INTRODUCTION

Bone is a dynamic tissue that possesses the intrinsic capacity to heal within 6-8 weeks after immobilization of a fracture. However, there are some conditions in which bone regeneration is delayed, compromised or beyond the physiological healing potential^{1,2}. Notably, the successful repair of large bone defects caused by trauma, tumor resection or disease remains a clinical challenge for orthopedic and plastic surgeons and often requires additional treatments.

Autologous bone grafting is still considered as the gold standard due to its osteoconductive, osteoinductive and osteogenic properties. This procedure demands to harvest the patient's own bone and subsequently transplant it into the defect site. Bone can be taken from several areas e.g., iliac crest, fibula or ribs, depending on the severity and amount needed for reconstruction of the defect. Nevertheless, the amount of bone is limited and the procedure adds morbidity at the harvesting site. Therefore, this surgical procedure is often associated with complications such as infection, hematoma, postoperative pain, muscular and neural damage. Transplantation of vascularized bone also requires extensive microsurgery to adapt to both the local vasculature and skeleton^{3,4}. Other procedures for large bone regeneration are the Masquelet's induced membrane, the Ilizarov's distraction or advanced therapies with bone morphogenetic proteins or cultured expanded bone marrow mesenchymal stem cells. These alternatives have however inherent disadvantages adding morbidity, surgical procedures, costs and safety concerns⁵⁻¹⁰.

For several decades, researchers and clinicians have attempted to develop a safe and potent alternative to autologous bone grafting for the regeneration of large bone

defects. Among them, synthetic calcium phosphate biomaterials that resemble the inorganic phase of bone have proven to be biocompatible and osteoconductive. Most commercially available calcium phosphate-based bone substitutes are composed of either hydroxyapatite (HA), β -tricalcium phosphate (β -TCP), or a mixture of both, termed as biphasic calcium phosphate (BCP). They are made at high sintering temperatures and are generally used as granules or porous blocks. Although these bioceramics share some compositional similarities with bone minerals, the conventional processes employed to manufacture them limit the possibilities to tune their pore architecture, often lacking interconnections and hindering their osteogenic potential to support healing of large bone defects¹¹⁻¹⁴.

One fabrication technique that allows controlling the external shape and internal porosity is three-dimensional (3D) printing. Customized scaffolds and surgical guides can be produced based on the patient's anatomy from computed tomography (CT) scans that are essential for surgical planning, precise resection and accurate bone reconstruction. Recently, biomimetic calcium phosphate inks have been developed to manufacture 3D scaffolds consisting of calcium-deficient hydroxyapatite (CDHA) using a layer-by-layer deposition, also known as 3D-microextrusion. The advantages of this 3D printed biomaterial are the structural and compositional features that closely resemble the mineral phase of bones as compared to conventional bioceramics, and the ambient temperatures manufacturing process that offers the possibility to reinforce the structure with polymers or incorporate drugs. Furthermore, 3D printing allows accurate control of their interconnected porosity favoring body fluids permeability, cells invasion, vascularization and bone ingrowth, making these 3D scaffolds promising therapeutic alternatives to treat large bone defects¹⁵⁻¹⁸.

Another essential aspect of bone transplantation is vascularization. The development of a vascular network is crucial for the exchange of nutrients, minerals and soluble molecules which are important during the repair process and ensure the viability of the bone graft. Lack of vascularization causes inner tissue necrosis and results in graft failure, particularly in large bone defects. In this respect, the interconnected porosity of the 3D scaffold facilitates the formation of new blood vessels throughout the entire material. Recent studies have attempted to enhance vascularization by either pre-vascularizing the construct before implantation or by adding angiogenic growth factors like vascular endothelial growth factor (VEGF) or platelet-derived growth factor (PDGF) during the grafting procedure. Although these approaches showed promising results, novel strategies are required to further enable vascularization, in particular for large bone defects¹⁹⁻²².

This work aims to investigate the feasibility of a one-step surgical skeletal reconstruction and regeneration of large bone defects in a relevant pre-clinical animal model. We hypothesize that the application of a 3D-printed CDHA scaffold with pre-defined shape and interconnected porosity combined with a local and axial vascular pedicle will result in bone regeneration and improvement of vascularization.

RESULTS

Pre-operative computed tomography (CT) for designing customized surgical guides and 3D scaffolds

One month before surgery, a CT angioscan of the metatarsus of sheep was performed to visualize the local vasculature and bone (Figure 1a). This 3D reconstruction shows that 3 main blood vessels were present along the metatarsal bone while the lateral plantar artery was selected for axial vasculature of the 3D scaffolds. As shown in Figure 1b, a customized surgical guide was designed to assist for the creation of a critical-sized segmental diaphyseal defect (length: 35 mm) in the metatarsus of sheep, and for drilling the holes for the osteosynthesis screws to fix the plate that stabilizes the fracture. This pre-operative CT scan was also used for manufacturing a customized 3D scaffold with interconnected porosity that fitted the defect and a groove to incorporate the axial vascular pedicle.

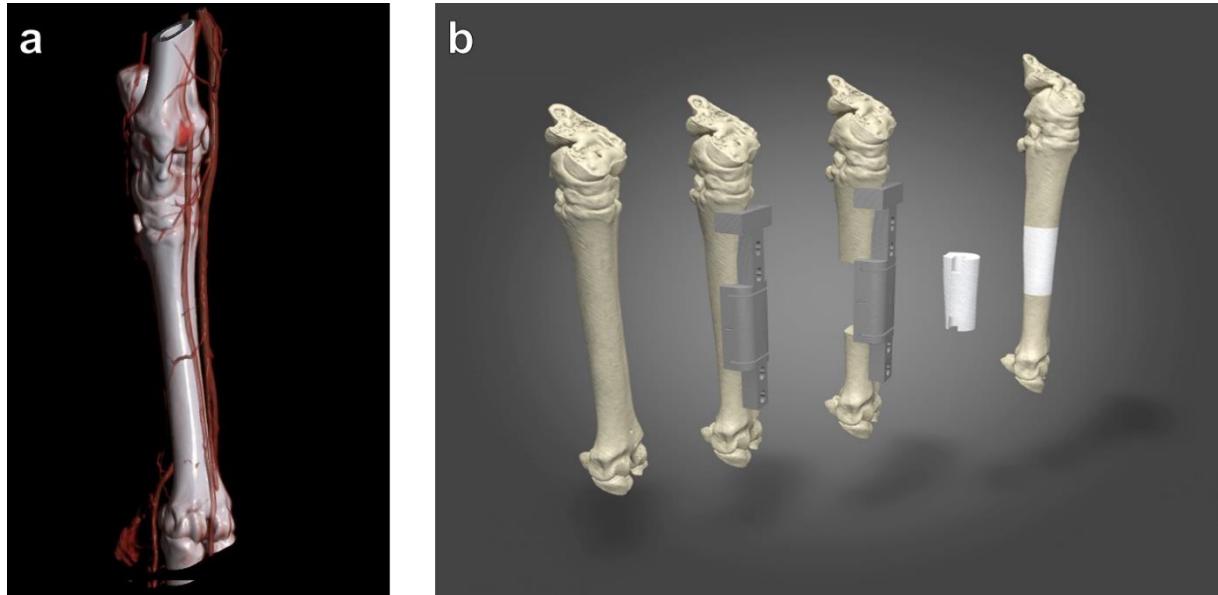


Figure 1 : Design of the surgical cutting guide for the creation of a segmental mid-diaphyseal defect with 35 mm length and the customized 3D scaffold for filling this defect. (a) Preoperative CT scans were taken one month before surgery and three-dimensionally reconstructed. The image visualizes the metatarsal bone and the local vasculature. (b) Schematic diagram demonstrating the operating principle of the surgical guide and the filling of defect with a customized 3D scaffold with a groove for axial vascularization.

Physicochemical characterization of the 3D-printed calcium phosphate scaffolds

As shown in Figure 2, the 3D scaffolds were designed with interconnected porosity and a groove to accommodate the axial vascular pedicle. The 3D scaffolds were then printed by using a robocasting device with a syringe containing the calcium phosphate paste coupled to a nozzle. A vascular plug with rounded edges was used for retaining the axial vascular pedicle inside the 3D scaffold. The porosity had an orthogonal rectilinear pattern with alternate crisscrossed layers rotated 90° relative to the previous layer creating an interconnected pore network mesh. The microstructure of the 3D

scaffolds, as observed by SEM, consisted of an entangled network of nanosized needle-like hydroxyapatite crystals.

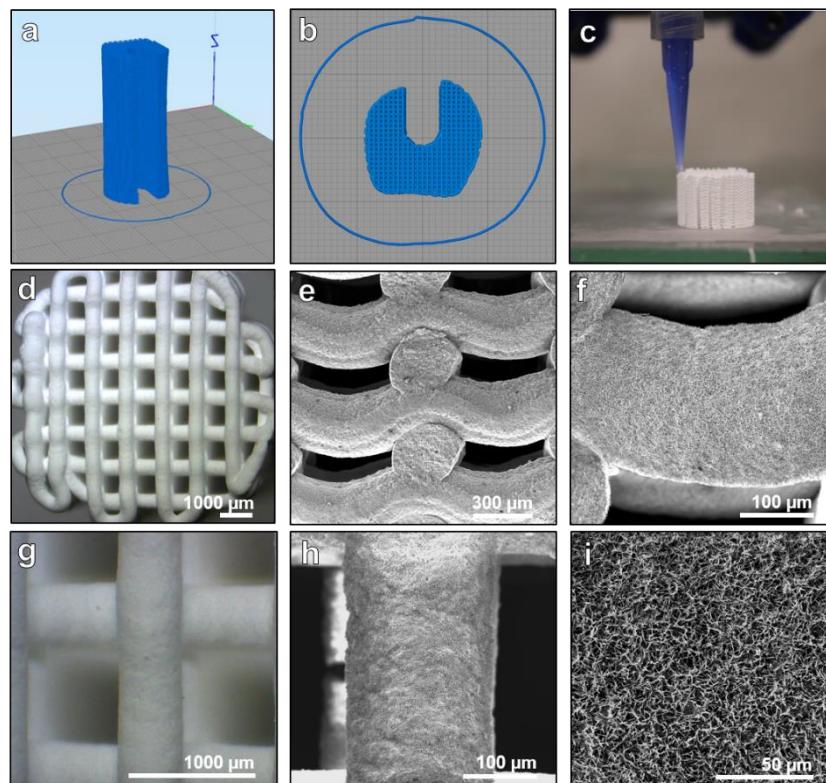


Figure 2 : Photographs of the fabrication and structure of the 3D-printed customized calcium phosphate scaffolds. (a-c) Design and printing of a calcium phosphate scaffold by 3D-microextrusion. (d-i) Optical and scanning electron microscopy (SEM) images of the 3D-printed scaffolds. Images were taken at different levels of magnification to visualize the structure and surface of the material.

The physicochemical characteristics of the 3D scaffolds are reported in Table 1. After setting, the 3D scaffolds were composed of 80.3% of CDHA, 18.7% of β -TCP and no presence of its alpha polymorph (α -TCP). The main body presented an inter-strand gap of $703.2 \pm 23.9 \mu\text{m}$ and a filament width of $489.7 \pm 9.7 \mu\text{m}$ in line with the 410 μm -nozzle used for 3D printing, whereas the scaffolds printed with the 311 μm -nozzle-setup presented an inter-filament separation of $529.4 \pm 25.3 \mu\text{m}$ and a filament width of $364.2 \pm 11.9 \mu\text{m}$. According to the mercury intrusion porosimetry (MIP) analysis, the

scaffold presented 81.03% of open porosity of which 59.52% correspond to pores with entrance sizes larger than 10 μm (macro-pores) and the remaining 21.52% corresponding to pores with entrance sizes smaller than 10 μm (micro/nano-pores). The specific surface area of the 3D scaffolds was 22.1 m^2/g in agreement with their microstructure. The uniaxial compression testing assays resulted in similar values for both conditions: the scaffolds printed with the 410 μm -nozzle-setup and 311 μm -nozzle-setup had an ultimate compressive strength of 2.10 ± 0.30 and 2.45 ± 0.53 MPa respectively.

3D Scaffolds	Shape size (mm)	Crystal phase composition	Filament width (μm)	Pore size (μm)	Porosity (%)	Specific surface area (m^2/g)	Ultimate compressive strength (MPa)
Main body printed with 410 μm -nozzle	Cylinder (H x \varnothing): 35 x 15 Groove (D x W): 7 x 5	80.3% CDHA 18.7% β -TCP 0% α -TCP	489.7 \pm 9.7	703.2 \pm 23.9	Total: 81.03 Macro (>10 μm): 59.52 Micro (<10 μm): 21.52	22.1	2.10 \pm 0.30
Vascular plug printed with 311 μm -nozzle	Trapezoid (L x H): 30 x 8		364.2 \pm 11.9	529.4 \pm 25.3			2.45 \pm 0.53

Table 1 : Physicochemical properties of the 3D scaffolds.

Animal welfare and surgical procedure

All sheep survived the operative intervention without any early or long-term post-operative complications. Figure 3 demonstrates the surgical procedure using the pre-designed customized surgical guide and the 3D printed scaffold. The application of the guides supported the creation of a segmental critical-sized defect of 35 mm at the mid-diaphyseal level of the metatarsal bone and directed the drilling for the osteosynthesis plate. This controlled drilling allowed an accurate positioning during the perforation and avoided damage to the surrounding soft tissues. Besides, they helped to maintain the reproducibility in all the procedures. The lateral plantar artery (Arteria plantaris

lateralis) that was isolated and passed through the 3D-printed scaffold to improve vascularization (3D scaffold + pedicle group) is shown Figure 3d. Figure 3e indicates identical anatomical shapes of the customized 3D-printed calcium phosphate scaffolds made by reverse engineering from CT scans compared to the bone resected at the day of surgery. The final reconstruction with the axial vascular pedicle passing through the anatomical 3D scaffold held by the fixation plate and screws is illustrated in Figure 3f.

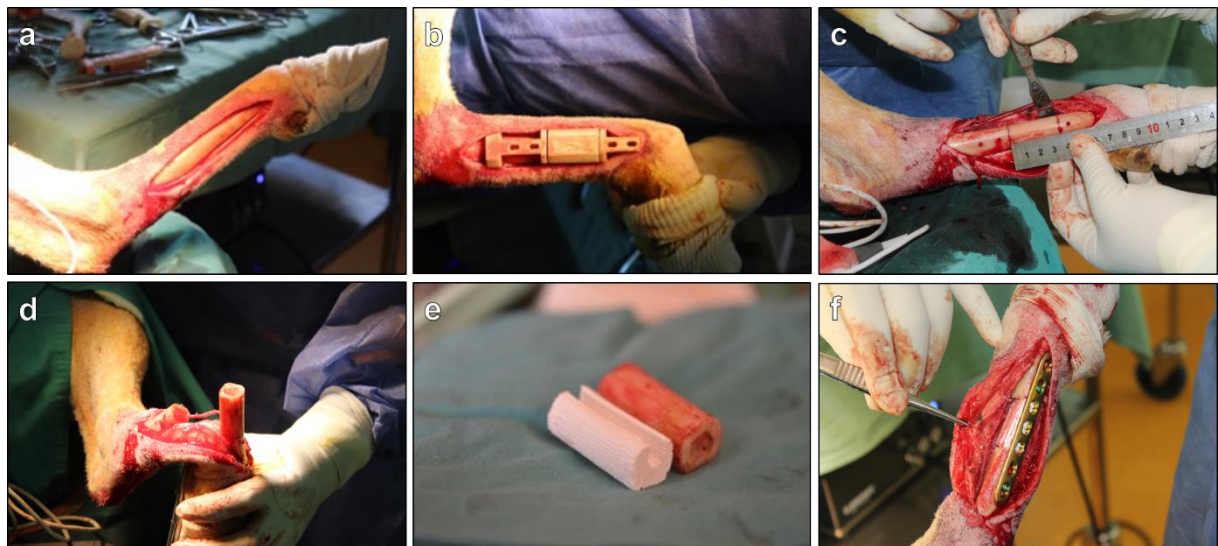


Figure 3 : Photographs of the surgery steps showing (a) the metatarsal bone, (b) the surgical guides used to create the bone defect, (c) the creation of a mid-diaphyseal segmental defect measuring 35 mm in the metatarsal bone, (d) the vascular pedicle used for the axial vascularization to the 3D-printed scaffold, (e) the customized shape of the 3D-printed scaffold and (f) the final result with the osteosynthesis plate fixation.

***In vivo* evaluation of 3D-printed calcium phosphate scaffolds**

To study the ability of the scaffold to regenerate a large bone defect, the bone repair was examined by *in vivo* CT scans over a healing period of 3 months (day 0, 30, 60 and 90). As shown in Figure 4, some bone regeneration occurred from the edges of the left empty defect on the side opposite to the osteosynthesis plate as early as D30. It indicated the endogenous healing potential of the mid-diaphyseal defect created in the metatarsus of sheep. In contrast, the defect filled with the 3D-printed scaffold and the 3D-printed scaffold combined with the vascular pedicle showed enhanced bone formation over the 3 months healing period. The scaffolds appeared well-integrated into the defect and surrounded by newly formed bone tissue. The origin of the bone regrowth was similar to that of the empty defect group and predominantly started from the external lateral side, opposite to the osteosynthesis plate. To monitor and control the durability of the vascular pedicle and vascular patency, angioscans were conducted by injecting an iodine contrast agent during the CT scan at day 30, 60 and 90. The vascular patency of the vascularized 3D-printed scaffold group was maintained during the 3 months of the study.

MicroCT scans calculations corroborated that the 3D scaffold before implantation had a rectangular interconnected porosity with a material volume / total volume (MV/TV) of 34.4 % (n=1) giving a macroporosity of 65.6 % in good agreement with the macroporosity of 59.5 % measured by MIP (Figure 5 and Table 1). Additionally, *ex vivo* high-resolution micro-computed CT (microCT) was performed at the endpoint of the study (day 90) (Figure 5). The left empty metatarsal defect had limited bone regeneration with a BV/TV value of 8.7 % (n=1). On the opposite, the metatarsal

defects filled with the customized 3D scaffolds and *a fortiori* in combination with the vascular pedicle showed a higher bone content with BV+MV/TV value of 48.2 % (n=1) and 61.7 % (n=1), respectively.

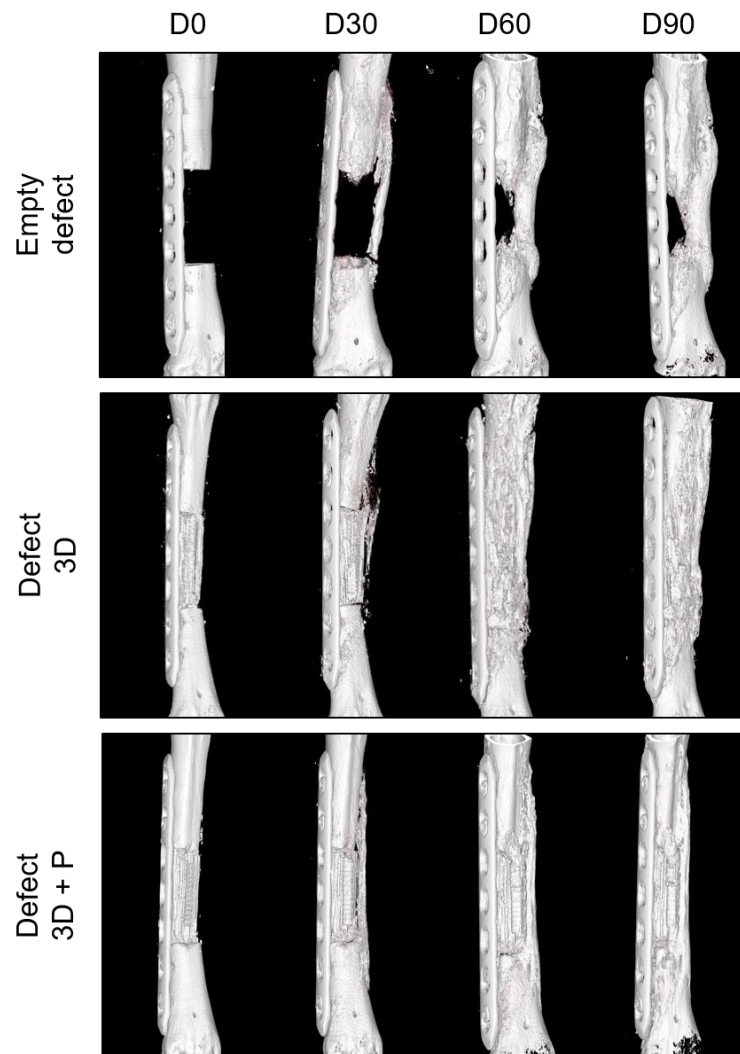


Figure 4 : 3D bone reconstructions of metatarsal defects in sheep. CT scans are shown post-surgery (D0) and at 30, 60 and 90 days (D30, D60, D90) of healing. Treatment groups included the empty defect (control), defect filled with the 3D-printed scaffold (Defect 3D) and defect treated with the 3D-printed scaffold and the axial vascular pedicle (Defect 3D + P).

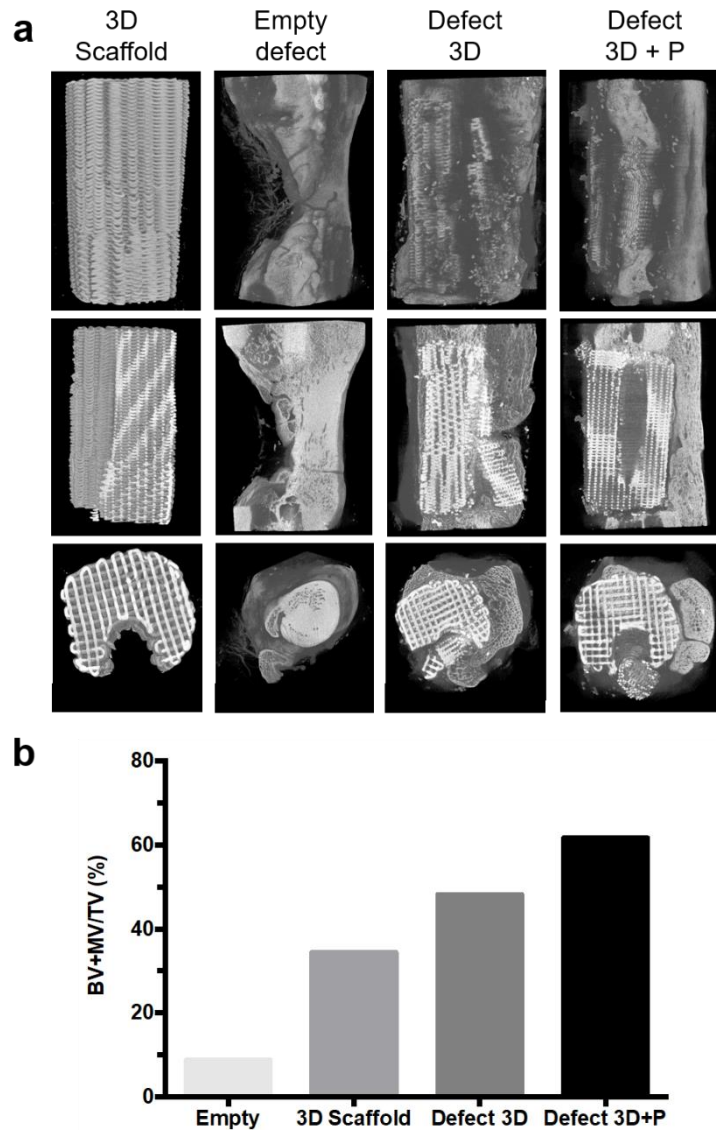


Figure 5 : (a) MicroCT 3D reconstructions of metatarsal defects in sheep 90 days post-operation. Images are presented for the scaffold before implantation (3D Scaffold), empty defect, defect filled with the 3D-printed scaffold (Defect 3D) and the defect filled with the 3D-printed scaffold associated with a vascular pedicle (Defect 3D + P). (b) Percentage of bone volume + material volume / total volume (BV+MV/TV) for the different treatment groups. The percentage of BV+MV/TV was calculated in the area of interest and compared to the microCT of the 3D scaffold taken before implantation.

As illustrated in Figure 6, the histological evaluation corroborated the CT and microCT findings. The empty defect was mainly filled with fibrous tissue and demonstrated limited bone tissue formation from the defect edges, whereas metatarsal bone defects filled with a customized 3D-printed scaffold or the 3D-printed scaffold combined with the axial vascular pedicle demonstrated bone ingrowth into the 3D structure of the biomaterial. At higher magnification, bone tissue containing osteocytes was present in contact with the 3D scaffold material. Osteocytes were more prevalent in the 3D-printed scaffold in combination with a vascular pedicle indicating the formation of mature bone tissue on this latter group.

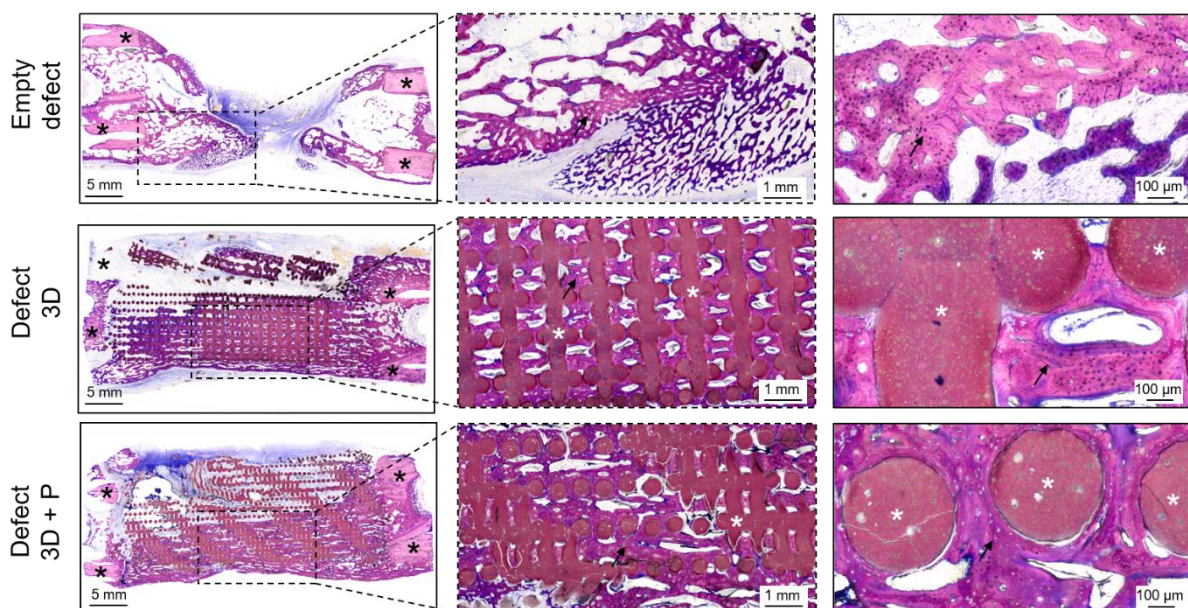


Figure 6 : Representative undecalcified histological thin ground sections of critical-sized metatarsal defects in sheep were prepared in longitudinal plane and stained with Levai-Laczko dye 90 days post-surgery. Photomicrographs are presented at three different magnifications. The black asterisk denotes the host bone (old bone) stained in light purple, whereas the black arrow demonstrates newly formed bone tissue visible in dark purple. The white asterisk highlights the 3D scaffold.

DISCUSSION

Bone is the second most transplanted tissue after blood transfusion. State of the art in the reconstruction of large bone defect has shown that vascularization of the transplanted bone graft is predominant for favorable clinical outcomes. Indeed, bone cells are located near blood vessels to ensure access to oxygen and to receive the necessary nutrients to regenerate tissues. It has been shown that with a sufficient amount of vascularization these bone cells, can differentiate into osteocytes and thus regenerate bone tissue²³⁻²⁵. However, the current transplantation of vascularized bone requires extensive microsurgery to reconnect vasculature and to fit the anatomy of a defect as well as adding morbidity at the harvesting site. Tissue engineering and in particular customized 3D scaffolds is potentially a promising alternative to autologous vascularized bone grafting for reconstruction of large skeletal defects²⁶⁻²⁹. Nevertheless, vascularization of the tissue-engineered constructs has been reported as a major limitation in bone regeneration³⁰.

In our work, we present a solution to supply vascularization to the biomaterial scaffold and to enhance bone regeneration in a clinically relevant animal model. Other published works proposed different options for improving vascularization. One of the strategies for improving the vascularization of tissue-engineered bone is the pre-vascularization of the constructs. Numerous pre-clinical studies have demonstrated that the combination of mesenchymal stem cells (MSCs) with biphasic calcium phosphates biomaterials (BCP) can induce bone formation and facilitate the healing of critical size defects³¹⁻³⁴. Some clinical trials have demonstrated the feasibility of amplifying autologous MSCs in culture from a bone marrow sample and associating

them with a BCP biomaterial to regenerate unconsolidated fractures or bone loss in small defect volumes. However, these tissue engineering techniques do not allow the regeneration of large bone defects yet because of the absence of a sufficient vascular network to ensure cell survival and tissue healing^{35,36}. In this context, several teams have proposed the pre-vascularization of the bone filling material by implantation in an ectopic site before transplanting it into the defect to be reconstructed. Proof of concept has been demonstrated at the pre-clinical level by ectopic implantation in the ewe of a chamber containing the BCP biomaterial and an arteriovenous fistula (vascular loop). After 6 and 12 weeks of implantation, abundant microvasculature was observed in the chamber contents³⁷⁻⁴². Large defects at the mandibular level have been successfully reconstructed in a few patients using this technique of transplanting a pre-vascularized biomaterial from an intramuscular site^{43,44}. In these studies, the pre-vascularization of the biomaterial appears to dominate for cell survival and bone regeneration. Recently, *Charbonnier et al.* published a new arteriovenous bundle technique study enclosing a vascular pedicle, just the vein, passing centrally through a 3D printed calcium phosphate scaffold⁴⁵.

To our knowledge, our contribution is the first work in which, a pre-surgical angioscan allowed to create a truly personalized biomaterial scaffold that has the same anatomical shape as the defect to be reconstructed. Moreover with this pre-surgical angioscan, we were able to study the vasculature in the defect area to be reconstructed, allowing us to evaluate the possibility to isolate a pedicle composed of a peripheral artery and an adjacent vein. This pedicle was dissected from the surrounding tissues and passed through the implantable 3D printed scaffold to provide with vascularization without adding laborious microsurgery.

This pre-clinical study in sheep demonstrates the feasibility of fabricating customized 3D scaffolds and surgical guides based on the patient`s CT scans that are essential for surgical planning, precise resection and accurate reconstruction. It is important to emphasize that in our work we proposed and we succeed to do a personalized large bone defect reconstruction with a 3D printed scaffold associated with a local vascular pedicle in a one-step surgery. Furthermore, 3D printing did not only allow to control the shape of the 3D scaffolds for fitting the anatomy of defects but also permitted to design and produce an interconnected porosity favorable for body fluid permeability, vasculature and bone ingrowth.

Some limitations of the current study include firstly a little bone tissue regeneration in the empty defect that has been previously described as a critical size bone defect³⁸. We consider that this regenerated bone tissue was developed from the vascularized membrane that is constituted around the metatarsal bone and in the subcutaneous tissue. This membrane was not resected in this first study. In a following study, we have resected this membrane and our empty defect did not regenerate any bone tissue during the first 3 months (Supplementary figure). Secondly, the 3D scaffolds, even though they supported bone ingrowth, had insufficient mechanical properties in comparison with those of native bone tissue. It will be necessary to provide them a better mechanical reinforcement through for example, the addition of polymers.

Further study in a larger population of animals is needed to assess the clinical efficacy of this innovative approach.

To conclude, our approach that uses pre-operative medical imaging, 3D printing of customized surgical guides and 3D scaffolds with a local and axial vascularization

constitutes a new and promising synthetic bone substitute option that mimics the today's most used autologous technique in the reconstruction of large bone defects, the fibula flap.

METHODS

Ethical approval

Ethical approval for animal experimentation was obtained from the local ethics committee (ref. number 9235; CEEA19, Val de Loire, France) and the French Ministry of Superior Education, Research and Innovation on February 28, 2018, by following the European Guidelines for Animal Care Directive 2010/63/EU.

Animals

The animal study was performed at the CIRE platform (agreement number: A371754; INRA, Nouzilly, France) that is fully equipped with an operating theatre, housing and medical imaging. The Ile de France sheep were supplied from the INRA breeder and were housed in boxes at the experimental facility. The animals were fed with straw and received water ad libitum. The animals were acclimated for a minimum of 2 weeks prior to the first intervention.

Pre-operative computed tomography (CT)

One month before surgery, the sheep were placed under general anaesthesia by intravenous injection of ketamine (20 mg/kg, Kétamidor[®], Axience, France) and xylazine (0.05 mg/kg, Rompun[®] 2%, Bayer, France). Animals were intubated and put under gaseous relay with 3% isoflurane (Isoflurin[®], Axience, France) carried by 100% oxygen. The sheep was then placed in the right lateral decubitus position on the CT scanner table (Dual-source 64-slice spiral Somatom[®], Siemens, France) with the left limb immobilized. Acquisition of the bone metatarsus on the left leg was performed at 300 mAs and 140 kV with a section of 0.6 mm generating 748 DICOM images in approximately 15 s. To visualize the vasculature, 80 ml of iodine contrast agent (350 mg I/ml; Omnipaque[™], GE Healthcare, France) was injected in the jugular vein via a catheter (5 ml/s). Acquisitions were performed at 80, 120, 140 and 160 s post-injection of the contrast agent. CT scans were reconstructed and analyzed by using the imaging software syngo.via, (Siemens, France).

Design and fabrication of customized surgical guides using 3D printing

The customized surgical guide was designed to assist for the creation of a critical-sized segmental diaphyseal defect (length: 35 mm) in the metatarsus of sheep, and for drilling the holes for the osteosynthesis screws to fix the plate that stabilizes the fracture. Its main objective was to hold precisely the surgical oscillating blade and the drilling bur. To fabricate the surgical guide, DICOM images from the pre-operative CT scans of the metatarsi and the titanium osteosynthesis plates (LCP 3.5, 7 holes, L98 mm, Johnson & Johnson Medical) were converted to 3D stereolithography (STL) files

using an open-source software (3D Slicer). Thereafter, the surgical guide was planned in the CAD program (Cinema 4D, Maxon, Germany). A phantom of the 3D scaffold and the metatarsus were produced in the same manner to examine the anatomical shape and size of the design (Figure 1). The STL files of the different components (customized surgical guide, 3D scaffold and metatarsus) were translated into a printable g-code (3D printing software, Ultimaker Cura 3.0, Ultimaker, The Netherlands). The customized surgical guide was printed with nylon filament (2.85 ± 0.05 mm, Ultimaker) that sustained autoclave sterilization using a commercial 3D printer (Ultimaker 3 extended, Ultimaker). The metatarsus and 3D scaffold were printed with thermoplastic poly-lactic acid (PLA, 2.85 ± 0.10 mm, Ultimaker) in order to control their precise fitting to anatomy prior to surgery.

3D printing of the customized calcium phosphate scaffolds

The customized 3D calcium phosphate scaffolds (MimetikOss 3D, Mimetis Biomaterials S.L., Spain) were designed by reverse engineering from CT scans of the metatarsus of sheep and fabricated by robot casting as previously published¹⁵. Briefly, a calcium-deficient hydroxyapatite self-setting ink was prepared by mixing 35 wt% aqueous solution of poloxamer 407 (P2443 – Pluronic, F-127, Sigma-Aldrich, Missouri, USA) and α -tricalcium phosphate (α -TCP, Innotere GmbH, Radebeul, Germany) powder at a ratio of 0.5 g/g. 3D scaffolds were printed by using a robocasting device (Heavy Duty Paste Extruder, BCN3D Technologies, Barcelona, Spain) with a syringe (Optimum[®] Syringe, Nordson EFD, U.S.A) containing the paste coupled to a tapered dispensing tip (SmoothFlow Tapered Tips, Nordson EFD) mounted on the machine. The 3D scaffold consisted of a two-part assembly as displayed in Figure 1. The main

body was a cylinder (length: 35 mm, diameter: 15-17 mm) with a central groove of 5 mm in width and 7 mm in depth for passing through the axial vascular pedicle. A vascular plug (length: 30 mm, height: 8 mm) with rounded edges was used for retaining the vascular pedicle inside the 3D scaffold. The geometry of the pores had an orthogonal rectilinear pattern with alternate crisscrossed layers rotated 90° relative to the previous layer creating an interconnected pore network mesh. Two different printing setups were defined for the two parts of the assembly: For the main body, we used a nozzle diameter of 410 µm (410 µm-nozzle-setup, 22 gauge) and for the vascular plug, a nozzle diameter of 311 µm (311 µm-nozzle-setup, 24 gauge). The filament width was set to 370 µm and 490 µm respectively. The printing process was followed by a hydrothermal treatment for hardening as described elsewhere⁴⁶. Subsequently, the samples were packaged in a double sterilization pouch and sterilized by autoclaving. The physicochemical properties of the customized 3D scaffolds were characterized using different techniques and are reported in the supplementary methods.

Critical-sized defects in sheep metatarsus

In this pilot-study, three 3-year old female Ile de France sheep with an average weight of 65 kg were supplied from the INRA breeder and deprived of food 24 hours before anaesthesia. The technique used for creating a segmental defect in the metatarsus was according to a validated and previously described experimental model⁴⁷. Briefly, the animals were anaesthetized and treated with morphine hydrochloride (0.3 mg/kg, CDM Lavoisier, France) and oxytetracycline (20 mg/kg, Tenaline[®] LA, Ceva, France) for analgesia and antibiotic prophylaxis. During the surgical procedure, general

anaesthesia was maintained by orotracheal intubation and inhalation of 3% isoflurane in oxygen. The heart and breathing rates were continuously monitored. After shaving and disinfecting the surgical site, a longitudinal incision was made to expose the medial surface of the left metatarsus. The customized, sterile surgical guide was positioned on the medial surface of the long bone and a surgical saw was inserted. A segmental critical-sized defect of 35 mm in length was created under constant saline irrigation to remove bone debris and prevent overheating. The defect was either left empty, treated with a customized 3D-printed scaffold alone or in combination with a vascular pedicle passing through. The metatarsus was stabilized by using a seven-hole dynamic compression plate (LCP 3.5 L98, Depuy Synthes, Johnson & Johnson Medical, France) and four head-locking screws (diameter: 3.5 mm, length: 20 mm). The holes for the osteosynthesis screws were made by drilling them at appropriate positions with the surgical guide. To close the wound, subcutaneous tissues and skin were sutured in separate layers with resorbable sutures (Optime[®] 4/0, Péters Medical, France). The limb was immobilized using a resin plaster and splint. Post-operative pain was managed by administration of flunixin (1.5 mg/kg, Finadyne[®], MSD Santé Animale, France).

Imaging and histological analyses

To follow bone regeneration and vascularization, CT scans were taken at day 0 (post-operative), 30, 60 and 90 using the same parameters as described for the pre-operative phase. After completing the CT scans at day 90, metatarsi were harvested and fixed in 4% formalin (Roti[®]-Histofix 4%, Carl Roth, France).

To receive high-resolution images of the metatarsus at the endpoint of the study, explants were scanned using an *in vivo* cone-beam micro-computed tomography (microCT) scanner (Skyscan 1076, Bruker, Kontich, Belgium) during the fixation period. Therefore, the X-ray tube was operated at 50 kV and 200 μ A. Scans were recorded with 1° rotation step over 180° and exposure of 400 ms giving a resolution of 18 μ m per pixel. The 3D reconstruction was performed using the accompanying software NRecon (Bruker, Kontich, Belgium). The percentage of bone volume + material volume over total volume (BV+MV/TV) was calculated in the selected region of interest corresponding to the diaphyseal defect and compared to the microCT of the 3D scaffold taken before implantation by the Skysan CT Analyzer (CTAn) software. For histological examination, fixed samples were dehydrated in ascending grades of ethanol, immersed in xylol (Carl Roth) as intermedium and embedded in methyl methacrylate (Sigma Aldrich). Undecalcified thin ground sections were prepared in longitudinal plane using the EXAKT cutting and grinding equipment (EXAKT Advanced Technologies, Norderstedt, Germany) according to the method established by Donath⁴⁸. The sections were reduced to a thickness of 60 μ m and stained with Leiva-Laczko dye to differentiate between new bone, old bone and the 3D-printed scaffold⁴⁹. For descriptive histological evaluation, the slides were scanned using an Olympus VS120 virtual slide microscope (Olympus, Tokyo, Japan) with a 20x objective.

Data analysis

All results were expressed as average \pm standard deviation and graphed with GraphPad Prism software (GraphPad Software Inc., La Jolla, CA).

REFERENCES

- 1 Dimitriou, R., Jones, E., McGonagle, D. & Giannoudis, P. V. Bone regeneration: current concepts and future directions. *BMC Med* 9, 66, doi:10.1186/1741-7015-9-66 (2011).
- 2 Kalfas, I. H. Principles of bone healing. *Neurosurg Focus* 10, E1, doi:10.3171/foc.2001.10.4.2 (2001).
- 3 Jakoi, A. M., Iorio, J. A. & Cahill, P. J. Autologous bone graft harvesting: a review of grafts and surgical techniques. *Musculoskelet Surg* 99, 171-178, doi:10.1007/s12306-015-0351-6 (2015).
- 4 Dimitriou, R., Mataliotakis, G. I., Angoules, A. G., Kanakaris, N. K. & Giannoudis, P. V. Complications following autologous bone graft harvesting from the iliac crest and using the RIA: A systematic review. *Injury* 42, S3-S15, doi:10.1016/j.injury.2011.06.015 (2011).
- 5 Cecchi, S., Bennet, S. J. & Arora, M. Bone morphogenetic protein-7: Review of signalling and efficacy in fracture healing. *J Orthop Transl* 4, 28-34, doi:10.1016/j.jot.2015.08.001 (2016).
- 6 Friedlaender, G. E. *et al.* Osteogenic protein-1 (bone morphogenetic protein-7) in the treatment of tibial nonunions. *J Bone Joint Surg Am* 83-A Suppl 1, S151-158 (2001).
- 7 Giannoudis, P. V., Harwood, P. J., Tosounidis, T. & Kanakaris, N. K. Restoration of long bone defects treated with the induced membrane technique: protocol and outcomes. *Injury* 47 Suppl 6, S53-S61, doi:10.1016/S0020-1383(16)30840-3 (2016).
- 8 Gomez-Barrena, E. *et al.* Feasibility and safety of treating non-unions in tibia, femur and humerus with autologous, expanded, bone marrow-derived mesenchymal

stromal cells associated with biphasic calcium phosphate biomaterials in a multicentric, non-comparative trial. *Biomaterials* 196, 100-108, doi:10.1016/j.biomaterials.2018.03.033 (2019).

9 Gubin, A., Borzunov, D. & Malkova, T. Ilizarov method for bone lengthening and defect management review of contemporary literature. *Bull Hosp Jt Dis* (2013) 74, 145-154 (2016).

10 Verboket, R. *et al.* Autologous cell-based therapy for treatment of large bone defects: from bench to bedside. *Eur J Trauma Emerg Surg* 44, 649-665, doi:10.1007/s00068-018-0906-y (2018).

11 Albrektsson, T. & Johansson, C. Osteoinduction, osteoconduction and osseointegration. *Eur Spine J* 10 Suppl 2, S96-101, doi:10.1007/s005860100282 (2001).

12 de Grado, G. F. *et al.* Bone substitutes: a review of their characteristics, clinical use, and perspectives for large bone defects management. *J Tissue Eng* 9, doi:10.1177/2041731418776819 (2018).

13 Neto, A. S. & Ferreira, J. M. F. Synthetic and marine-derived porous scaffolds for bone tissue engineering. *Materials* 11, doi:10.3390/ma11091702 (2018).

14 Wang, W. & Yeung, K. W. K. Bone grafts and biomaterials substitutes for bone defect repair: A review. *Bioact Mater* 2, 224-247, doi:10.1016/j.bioactmat.2017.05.007 (2017).

15 Barba, A. *et al.* Osteogenesis by foamed and 3D-printed nanostructured calcium phosphate scaffolds: Effect of pore architecture. *Acta Biomater* 79, 135-147, doi:10.1016/j.actbio.2018.09.003 (2018).

- 16 Barba, A. *et al.* Osteoinduction by foamed and 3D-printed calcium phosphate scaffolds: effect of nanostructure and pore architecture. *ACS Appl Mater Interfaces* 9, 41722-41736, doi:10.1021/acsami.7b14175 (2017).
- 17 Lin, K., Sheikh, R., Romanazzo, S. & Roohani, I. 3D Printing of bioceramic scaffolds-barriers to the clinical translation: from promise to reality, and future perspectives. *Materials (Basel)* 12, doi:10.3390/ma12172660 (2019).
- 18 Papastavrou, E., Breedon, P. & Fairhurst, D. Low-temperature deposition modeling of beta-TCP scaffolds with controlled bimodal porosity. *Methods Mol Biol* 1758, 41-54, doi:10.1007/978-1-4939-7741-3_4 (2018).
- 19 Fernandez de Grado, G. *et al.* Bone substitutes: a review of their characteristics, clinical use, and perspectives for large bone defects management. *J Tissue Eng* 9, 1-18, doi:10.1177/2041731418776819 (2018).
- 20 Griffin, K. S. *et al.* Evolution of bone grafting: bone grafts and tissue engineering strategies for vascularized bone regeneration. *Clinic Rev Bone Miner Metab* 13, 232-244, doi:10.1007/s12018-015-9194-9 (2015).
- 21 Mercado-Pagan, A. E., Stahl, A. M., Shanjani, Y. & Yang, Y. Vascularization in bone tissue engineering constructs. *Ann Biomed Eng* 43, 718-729, doi:10.1007/s10439-015-1253-3 (2015).
- 22 Filipowska, J., Tomaszewski, K. A., Niedzwiedzki, L., Walocha, J. A. & Niedzwiedzki, T. The role of vasculature in bone development, regeneration and proper systemic functioning. *Angiogenesis* 20, 291-302, doi:10.1007/s10456-017-9541-1 (2017).
- 23 Bose, S., Roy, M. & Bandyopadhyay, A. Recent advances in bone tissue engineering scaffolds. *Trends Biotechnol* 30, 546-554, doi:10.1016/j.tibtech.2012.07.005 (2012).

- 24 Liu, Y., Lim, J. & Teoh, S. H. Review: development of clinically relevant scaffolds for vascularised bone tissue engineering. *Biotechnol Adv* 31, 688-705, doi:10.1016/j.biotechadv.2012.10.003 (2013).
- 25 O'Keefe, R. J. & Mao, J. Bone tissue engineering and regeneration: from discovery to the clinic--an overview. *Tissue Eng Part B Rev* 17, 389-392, doi:10.1089/ten.TEB.2011.0475 (2011).
- 26 Hutmacher, D. W., Schantz, J. T., Lam, C. X., Tan, K. C. & Lim, T. C. State of the art and future directions of scaffold-based bone engineering from a biomaterials perspective. *J Tissue Eng Regen Med* 1, 245-260, doi:10.1002/term.24 (2007).
- 27 Kneser, U., Schaefer, D. J., Polykandriotis, E. & Horch, R. E. Tissue engineering of bone: the reconstructive surgeon's point of view. *J Cell Mol Med* 10, 7-19, doi:10.1111/j.1582-4934.2006.tb00287.x (2006).
- 28 Rosset, P., Deschaseaux, F. & Layrolle, P. Cell therapy for bone repair. *Orthop Traumatol Surg Res* 100, S107-112, doi:10.1016/j.otsr.2013.11.010 (2014).
- 29 Tang, D. *et al.* Biofabrication of bone tissue: approaches, challenges and translation for bone regeneration. *Biomaterials* 83, 363-382, doi:10.1016/j.biomaterials.2016.01.024 (2016).
- 30 Hutmacher, D. W. Scaffolds in tissue engineering bone and cartilage. *Biomaterials* 21, 2529-2543, doi:10.1016/s0142-9612(00)00121-6 (2000).
- 31 Brennan, M. A. *et al.* Pre-clinical studies of bone regeneration with human bone marrow stromal cells and biphasic calcium phosphate. *Stem Cell Res Ther* 5, 114, doi:10.1186/scrt504 (2014).
- 32 Corre, P. *et al.* Direct comparison of current cell-based and cell-free approaches towards the repair of craniofacial bone defects - A preclinical study. *Acta Biomater* 26, 306-317, doi:10.1016/j.actbio.2015.08.013 (2015).

- 33 Gamblin, A. L. *et al.* Bone tissue formation with human mesenchymal stem cells and biphasic calcium phosphate ceramics: the local implication of osteoclasts and macrophages. *Biomaterials* 35, 9660-9667, doi:10.1016/j.biomaterials.2014.08.018 (2014).
- 34 Mankani, M. H., Kuznetsov, S. A., Wolfe, R. M., Marshall, G. W. & Robey, P. G. In vivo bone formation by human bone marrow stromal cells: reconstruction of the mouse calvarium and mandible. *Stem Cells* 24, 2140-2149, doi:10.1634/stemcells.2005-0567 (2006).
- 35 Kanczler, J. M. & Oreffo, R. O. Osteogenesis and angiogenesis: the potential for engineering bone. *Eur Cell Mater* 15, 100-114 (2008).
- 36 Lovett, M., Lee, K., Edwards, A. & Kaplan, D. L. Vascularization strategies for tissue engineering. *Tissue Eng Part B Rev* 15, 353-370, doi:10.1089/ten.TEB.2009.0085 (2009).
- 37 Beier, J. P. *et al.* Axial vascularization of a large volume calcium phosphate ceramic bone substitute in the sheep AV loop model. *J Tissue Eng Regen Med* 4, 216-223, doi:10.1002/term.229 (2010).
- 38 Erol, O. O. & Sira, M. New capillary bed formation with a surgically constructed arteriovenous fistula. *Plast Reconstr Surg* 66, 109-115, doi:10.1097/00006534-198007000-00021 (1980).
- 39 Kaempfen, A. *et al.* Engraftment of prevascularized, tissue engineered constructs in a novel rabbit segmental bone defect model. *Int J Mol Sci* 16, 12616-12630, doi:10.3390/ijms160612616 (2015).
- 40 Kneser, U. *et al.* Engineering of vascularized transplantable bone tissues: Induction of axial vascularization in an osteoconductive matrix using an arteriovenous loop. *Tissue Eng* 12, 1721-1731, doi:10.1089/ten.2006.12.1721 (2006).

- 41 Kokemueller, H. *et al.* Prefabrication of vascularized bioartificial bone grafts in vivo for segmental mandibular reconstruction: experimental pilot study in sheep and first clinical application. *Int J Oral Maxillofac Surg* 39, 379-387, doi:10.1016/j.ijom.2010.01.010 (2010).
- 42 Warnke, P. H. *et al.* Man as living bioreactor: Fate of an exogenously prepared customized tissue-engineered mandible. *Biomaterials* 27, 3163-3167, doi:10.1016/j.biomaterials.2006.01.050 (2006).
- 43 Mesimaki, K. *et al.* Novel maxillary reconstruction with ectopic bone formation by GMP adipose stem cells. *Int J Oral Maxillofac Surg* 38, 201-209, doi:10.1016/j.ijom.2009.01.001 (2009).
- 44 Warnke, P. H. *et al.* Growth and transplantation of a custom vascularised bone graft in a man. *Lancet* 364, 766-770, doi:10.1016/S0140-6736(04)16935-3 (2004).
- 45 Charbonnier, B. *et al.* Material-induced venosome-supported bone tubes. *Adv Sci (Weinh)* 6, 1900844, doi:10.1002/advs.201900844 (2019).
- 46 Raymond, S. *et al.* Accelerated hardening of nanotextured 3D-plotted self-setting calcium phosphate inks. *Acta Biomater* 75, 451-462, doi:10.1016/j.actbio.2018.05.042 (2018).
- 47 Petite, H. *et al.* Tissue-engineered bone regeneration. *Nat Biotechnol* 18, 959-963, doi:10.1038/79449 (2000).
- 48 Donath, K. & Breuner, G. A method for the study of undecalcified bones and teeth with attached soft tissues. The Sage-Schliff (sawing and grinding) technique. *J Oral Pathol* 11, 318-326 (1982).
- 12of ossifying cartilage and bone tissues embedded in epoxy resin. *Mikroskopie* 31, 1-4 (1975).

General Discussion

The studies presented in this thesis were motivated by the objective to propose surgical alternatives to the current autologous bone grafting for the reconstruction of large bone defects.

Chapter I presents the state of the art of the current options for the reconstruction of large bone defects. One of the conclusions we could get from this chapter is that there are two significant limitations in the current large bone defects reconstructions. Firstly, a considerable amount of bone tissue needs to be harvested from the donor area inducing morbidity, post-surgical complications, extensive and repetitive surgeries and thus, hampering the quality of life of patients. Secondly, given the critical amount of bone tissue required, vascularization of the bone graft is a condition sine qua non for a functional reconstruction. We confirm that although bone autografts have osteoconductive, osteoinductive and osteogenic properties, they cannot be used as an isolated surgical technique for this type of reconstruction. The amount of bone is limited for this type of procedure, and it is a non-vascularized tissue. To circumvent this difficulty, the Masquelet's technique has proven that pre-vascularization before bone grafting could regenerate large bone defects, but still requires two surgeries. Thanks to the neovascularization and the secretion of various growth factors, and the presence of mesenchymal stem cells in the induced membrane, that contribute to the bone regeneration of long bone defects. At the same time, instead of using a bone autograft, one could use synthetic bone substitutes or a combination of autograft and bone substitutes associated with an induced membrane of Masquelet.

Massive bone allografts solve the problem of morbidity and two surgeries but present significant disadvantages such as safety with possible disease transfer and immune rejection as well as the lack of vascularization. The Capanna's technique solves this problem by associating a vascularized bone graft with the allograft. Again, vascularization of the bone graft appears to be the best surgical option for the reconstruction of large bone defects. Indeed, the vascularized bone graft has an adequate amount of bone tissue serving as scaffold and has a vascular pedicle that allows its vitality to be maintained after reconstruction. However, the significant disadvantages of this solution are the possible surgical complications and the associated morbidities. At the same time, although being the best option, it is a surgical technique that does not allow a personalized reconstruction in the bone defect to be reconstructed. The surgeon must adapt the bone graft to the shape of the bone defect. Based on this problematic of the not possible customization, the problem of vascularization, and with the limited amount of bone tissue, we developed the study presented as Chapter II in this thesis.

In chapter II, the study aimed to produce a highly-vascularized graft *in situ* and to transplant it into a critical-sized defect in rabbits for bone reconstruction. We used biphasic calcium phosphate (BCP) granules as the synthetic biomaterial. To give the granules an anatomical shape similar to the bone defect, we developed a 3D printed PLA chamber, which was filled with the BCP granules. In this study, we observed that BCP groups without vascularization fell apart upon the opening of the chambers, in contrast to the pedicle groups where firm constructs in the shape of the chambers were formed. Moreover, the vascular bundle pedicle generates vascular sprouting regenerating the vascularization of the synthetic graft. The use of the stroma vascular fraction of the adipose tissue helped to create vascular capillaries. When constructions

were transplanted into the ulna defect, there was a new bone formation, but it was not complete. Maybe it was due to the limitations that we had in this study. Firstly, the creation of the ulna defect was not standardized., giving; as a result, some no bone union with the BCP construct. Secondly, it is a two-step surgery. At the same time, we did not keep the vascularization after the reconstruction, so our graft can finally behave like a non-vascularized autograft. Taking into account these limitations, we decided to develop a customized 3D printed synthetic similar fibula flap (Chapter III). In this study, to standardize the large bone defects created in the sheep metatarsus, we have developed the use of surgical guides. The 3D printed scaffolds were designed based on the CT scan images to give the exact anatomical shape of the bone defect when doing the reconstruction. To mimic the fibula vascularization, a local pedicle was dissected and passing it through the 3D printed scaffold. Using these different steps, we were able to create a customized vascular synthetic bone large defect reconstruction supplying vascularization to the biomaterial. The limitation of this study was that 3D scaffolds, even though they supported bone ingrowth, had insufficient mechanical properties in comparison with those of native bone tissue. This limitation is a critical clinical requirement which must be resolved. In chapters I and III, we presented 3D printed constructs as a promise option in clinical application for large bone defect reconstruction. The most important clinical use of tissue engineering is the reconstruction of large and critically defects. In these cases, body self-repair is limited. The main reason why 3D printing complex tissue-engineering constructs have not done a meaningful translation to clinical use is due to challenges faced when scaling up to treat the large bone defects. In tissue engineering, 3D printing and 3D bioprinting have comparable potential and could replace current treatments in the future. This technology is in a starting period. Multidisciplinary investment in research and

development will find the solutions for translation to clinical application to treat large bone defects.

Conclusion

This doctoral thesis gives the current options in large bone defect reconstruction. At the same time, based on this study, we proposed new possible solutions for treating large bone defects.

Concerning the current options for large bone defects reconstruction, we can conclude that given the large amount of bone tissue for this reconstruction:

- a) Current techniques generate donor site morbidity, are complex and have their own limitations.
- b) At least two surgical steps are usually needed.
- c) Vascularization of the transferred tissue is essential for bone regeneration.

Concerning the study to produce a highly-vascularized graft *in situ* and to transplant it into a critical-sized defect in rabbits for bone reconstruction, we conclude that:

- a) The use of a 3D printed chamber allowed us to create a BCP anatomical shaped firm construct.
- b) The vascular bundle pedicle generates vascular sprouting regenerating the vascularization of the synthetic graft.
- c) The use of the stroma vascular fraction of the adipose tissue helped to create vascular capillaries.

Regarding the development of a customized 3D printed synthetic scaffold with a axial vascular pedicle in segmental defects in sheep, we conclude that:

- a) Preoperative CT scan allowed us to create a patient-specific 3D scaffold for the large bone defect reconstruction.
- b) The use of surgical guides allowed us to standardize the large bone defect in the study and may be useful for surgical resection of tumors.

- c) We showed the utility of using a local pedicle inserted axially in the 3D scaffold for producing a one-step surgery reconstruction.
- d) 3D scaffolds had insufficient mechanical properties in comparison with those of native bone tissue and should be improved.

Futures Perspectives

Another way in which we could improve the mechanical properties thanks to the development of 3D printing is developing 3D composite constructs, association titanium, and bone substitutes.

Different option models could be considered. Customized titanium hollowed prosthesis filled with biomaterials, as described in Chapter II.

We could propose a 3D printed customized titanium coated with hydroxyapatite. Thanks to the evolution of 3D printing, nowadays, we can design a scaffolding lattice similar to the cortical and trabecular bone using little quantity of material. With this approach, we could propose a light 3D printed structure with excellent mechanical properties. In all the options mentioned before, we will associate a vascular pedicle, as proposed in all the studies presented in this work.

The work presented in this thesis and the future perspectives will help clinicians and patients to solve and profit of this new technology which could solve this challenge.

REFERENCES

1. Ahlmann, E.R., Menendez, L.R., Kermani, C., and Gotha, H. (2006). Survivorship and clinical outcome of modular endoprosthetic reconstruction for neoplastic disease of the lower limb. *J Bone Joint Surg Br* 88(6), 790-795. doi: 10.1302/0301-620X.88B6.17519.
2. Albrektsson T, Johansson C. Osteoinduction, osteoconduction and osseointegration. *Eur Spine J.* 2001 Oct;10(Suppl 2):S96–101.
3. Albrektsson, T. & Johansson, C. Osteoinduction, osteoconduction and osseointegration. *Eur Spine J* 10 Suppl 2, S96-101, doi:10.1007/s005860100282 (2001).
4. Arkudas A, Lipp A, Buehrer G, Arnold I, Dafinova D, Brandl A, et al. Pedicled Transplantation of Axially Vascularized Bone Constructs in a Critical Size Femoral Defect. *Tissue Eng Part A.* 2018 Mar;24(5–6):479–92.
5. Athanasiou, V.T., Papachristou, D.J., Panagopoulos, A., Saridis, A., Scopa, C.D., and Megas, P. (2010). Histological comparison of autograft, allograft-DBM, xenograft, and synthetic grafts in a trabecular bone defect: an experimental study in rabbits. *Med Sci Monit* 16(1), BR24-31.
6. Azi, M.L., Teixeira, A.A.A., Cotias, R.B., Joeris, A., and Kfuri, M. (2019). Induced-membrane technique in the management of posttraumatic bone defects. *JBJS Essent Surg Tech* 9(2), e22. doi: 10.2106/JBJS.ST.18.00099.
7. Bakri K, Stans A, Mardini S, Moran S. Combined Massive Allograft and Intramedullary Vascularized Fibula Transfer: The Capanna Technique for Lower-Limb Reconstruction. *Seminars in Plastic Surgery.* 2008 Aug;22(03):234–41.
8. Bansal, M.R., Bhagat, S.B., and Shukla, D.D. (2009). Bovine cancellous xenograft in the treatment of tibial plateau fractures in elderly patients. *Int Orthop* 33(3), 779-784. doi: 10.1007/s00264-008-0526-y.
9. Barba, A. et al. Osteogenesis by foamed and 3D-printed nanostructured calcium phosphate scaffolds: Effect of pore architecture. *Acta Biomater* 79, 135-147, doi:10.1016/j.actbio.2018.09.003 (2018).
10. Barba, A. et al. Osteoinduction by foamed and 3D-printed calcium phosphate scaffolds: effect of nanostructure and pore architecture. *ACS Appl Mater Interfaces* 9, 41722-41736, doi:10.1021/acsami.7b14175 (2017).
11. Beier JP, Horch RE, Arkudas A, Polykandriotis E, Bleiziffer O, Adamek E, et al. De novo generation of axially vascularized tissue in a large animal model. *Microsurgery.* 2009 Jan 1;29(1):42–51.

12. Beier JP, Horch RE, Hess A, Arkudas A, Heinrich J, Loew J, et al. Axial vascularization of a large volume calcium phosphate ceramic bone substitute in the sheep AV loop model. *J Tissue Eng Regen Med*. 2010 Mar;4(3):216–23.
13. Beier, J. P. et al. Axial vascularization of a large volume calcium phosphate ceramic bone substitute in the sheep AV loop model. *J Tissue Eng Regen Med* 4, 216-223, doi:10.1002/term.229 (2010).
14. Bertol, L.S., Schabbach, R., and dos Santos, L.A.L. (2016). Dimensional evaluation of patient-specific 3D printing using calcium phosphate cement for craniofacial bone reconstruction. *Journal of Biomaterials Applications* 31(6), 799-806. doi: 10.1177/0885328216682672.
15. Boos AM, Loew JS, Weigand A, Deschler G, Klumpp D, Arkudas A, et al. Engineering axially vascularized bone in the sheep arteriovenous-loop model. *Journal of Tissue Engineering and Regenerative Medicine*. 2013 Aug 1;7(8):654–64.
16. Bosc, R., Hersant, B., Carloni, R., Niddam, J., Bouhassira, J., De Kermadec, H., et al. (2017). Mandibular reconstruction after cancer: an in-house approach to manufacturing cutting guides. *Int J Oral Maxillofac Surg* 46(1), 24-31. doi: 10.1016/j.ijom.2016.10.004.
17. Bose, S., Roy, M. & Bandyopadhyay, A. Recent advances in bone tissue engineering scaffolds. *Trends Biotechnol* 30, 546-554, doi:10.1016/j.tibtech.2012.07.005 (2012).
18. Boskey AL, & Robey PG. (2013). The Composition of Bone. *Primer on the Metabolic Bone Diseases and Disorders of Mineral Metabolism*, 49–58.
19. Bostrom, M.P.G., and Seigerman, D.A. (2005). The clinical use of allografts, demineralized bone matrices, synthetic bone graft substitutes and osteoinductive growth factors: a survey study. *HSS journal : the musculoskeletal journal of Hospital for Special Surgery* 1(1), 9-18. doi: 10.1007/s11420-005-0111-5.
20. Brandi ML, Collin-Osdoby P (2006) Vascular biology and the skeleton. *J Bone Miner Res* 21(2):183–192
21. Brennan MA, Davaine J-M, Layrolle P. Pre-vascularization of bone tissue-engineered constructs. *Stem Cell Res Ther*. 2013 Aug 14;4(4):96.
22. Brennan MÁ, Renaud A, Amiaud J, Rojewski MT, Schrezenmeier H, Heymann D, et al. Pre-clinical studies of bone regeneration with human bone marrow stromal cells and biphasic calcium phosphate. *Stem Cell Res Ther* [Internet]. 2014 Oct 13 [cited 2019 Feb 25];5(5). Available from: <https://www.ncbi.nlm.nih.gov/pmc/articles/PMC4445278/>
23. Brennan MA, Renaud A, Guilloton F, Mebarki M, Trichet V, Sensebé L, et al. Inferior In Vivo Osteogenesis and Superior Angiogenesis of Human Adipose

- Tissue: A Comparison with Bone Marrow-Derived Stromal Stem Cells Cultured in Xeno-Free Conditions. *Stem Cells Transl Med.* 2017 Oct 19;6(12):2160–72.
24. Brennan, M. A. et al. Pre-clinical studies of bone regeneration with human bone marrow stromal cells and biphasic calcium phosphate. *Stem Cell Res Ther* 5, 114, doi:10.1186/scrt504 (2014).
 25. Brookes M (1963) Cortical vascularization and growth in foetal tubular bones. *J Anat* 97:597–609
 26. Brown, W., and Chow, L. (1983). A new calcium-phosphate setting cement. *J Dent Res* 62, 672-672.
 27. Brown, W.E. (1987). A new calcium phosphate, water-setting cement. *Cements research progress*, 351-279.
 28. Brunello, G., Sivoletta, S., Meneghello, R., Ferroni, L., Gardin, C., Piattelli, A., et al. (2016). Powder-based 3D printing for bone tissue engineering. *Biotechnology Advances* 34(5), 740-753. doi: <https://doi.org/10.1016/j.biotechadv.2016.03.009>.
 29. Brydone AS, Meek D, Maclaine S. Bone grafting, orthopaedic biomaterials, and the clinical need for bone engineering. *Proc Inst Mech Eng H.* 2010 Dec;224(12):1329–43.
 30. Brydone, A.S., Meek, D., and Maclaine, S. (2010). Bone grafting, orthopaedic biomaterials, and the clinical need for bone engineering. *Proc Inst Mech Eng H* 224(12), 1329-1343. doi: 10.1243/09544119JEIM770.
 31. Bucholz RW. Nonallograft osteoconductive bone graft substitutes. *Clin Orthop Relat Res.* 2002 Feb;(395):44–52.
 32. Bucholz, R.W., Carlton, A., and Holmes, R.E. (1987). Hydroxyapatite and tricalcium phosphate bone graft substitutes. *Orthop Clin North Am* 18(2), 323-334.
 33. Campanacci DA, Puccini S, Caff G, Beltrami G, Piccioli A, Innocenti M, et al. Vascularised fibular grafts as a salvage procedure in failed intercalary reconstructions after bone tumour resection of the femur. *Injury.* 2014 Feb;45(2):399–404.
 34. Cao, Y., Vacanti, J.P., Paige, K.T., Upton, J., and Vacanti, C.A. (1997). Transplantation of chondrocytes utilizing a polymer-cell construct to produce tissue-engineered cartilage in the shape of a human ear. *Plast Reconstr Surg* 100(2), 297-302; discussion 303-294. doi: 10.1097/00006534-199708000-00001.
 35. Capanna, R., Bufalini, C., and Campanacci, M. (1993). A new technique for reconstructions of large metadiaphyseal bone defects. *Orthopedics and Traumatology* 2(3), 159-177. doi: 10.1007/BF02620523.

36. Careri, S., Vitiello, R., Oliva, M.S., Ziranu, A., Maccauro, G., and Perisano, C. (2019). Masquelet technique and osteomyelitis: innovations and literature review. *Eur Rev Med Pharmacol Sci* 23(2 Suppl), 210-216. doi: 10.26355/eurrev_201904_17495.
37. Casteilla L, Planat-Bénard V, Cousin B, Laharrague P, Bourin P. Vascular and endothelial regeneration. *Curr Stem Cell Res Ther*. 2010 Jun;5(2):141–4.
38. Cecchi, S., Bennet, S. J. & Arora, M. Bone morphogenetic protein-7: Review of signalling and efficacy in fracture healing. *J Orthop Transl* 4, 28-34, doi:10.1016/j.jot.2015.08.001 (2016).
39. Cesarano Iii, J., Dellinger, J.G., Saavedra, M.P., Gill, D.D., Jamison, R.D., Grosser, B.A., et al. (2005). Customization of load-bearing hydroxyapatite lattice scaffolds. *International Journal of Applied Ceramic Technology* 2(3), 212-220. doi: 10.1111/j.1744-7402.2005.02026.x.
40. Charbonnier B, Baradaran A, Sato D, Alghamdi O, Zhang Z, Zhang Y-L, et al. Material-Induced Venosome-Supported Bone Tubes. *Advanced Science*. 0(0):1900844.
41. Charbonnier, B. et al. Material-induced venosome-supported bone tubes. *Adv Sci (Weinh)* 6, 1900844, doi:10.1002/advs.201900844 (2019).
42. Chen, Z., Li, Z., Li, J., Liu, C., Lao, C., Fu, Y., et al. (2019). 3D printing of ceramics: A review. *Journal of the European Ceramic Society* 39(4), 661-687. doi: <https://doi.org/10.1016/j.jeurceramsoc.2018.11.013>.
43. Cheng, M.-H., Brey, E.M., Ulusal, B.G., and Wei, F.-C. (2006). Mandible augmentation for osseointegrated implants using tissue engineering strategies. *Plastic and Reconstructive Surgery* 118(1).
44. Choi, S., Oh, Y.-I., Park, K.-H., Lee, J.-S., Shim, J.-H., and Kang, B.-J. (2019). New clinical application of three-dimensional-printed polycaprolactone/ β -tricalcium phosphate scaffold as an alternative to allograft bone for limb-sparing surgery in a dog with distal radial osteosarcoma. *The Journal of veterinary medical science* 81(3), 434-439. doi: 10.1292/jvms.18-0158.
45. Colin, A., and Boire, J.-Y. (1997). A novel tool for rapid prototyping and development of simple 3D medical image processing applications on PCs. *Computer Methods and Programs in Biomedicine* 53(2), 87-92. doi: [https://doi.org/10.1016/S0169-2607\(97\)01807-5](https://doi.org/10.1016/S0169-2607(97)01807-5).
46. Combes C, Rey C. Amorphous calcium phosphates: Synthesis, properties and uses in biomaterials. *Acta Biomaterialia*. 2010 Sep 1;6(9):3362–78.
47. Corre P, Merceron C, Longis J, Khonsari RH, Pilet P, Thi TN, et al. Direct comparison of current cell-based and cell-free approaches towards the repair of craniofacial bone defects - A preclinical study. *Acta Biomater*. 2015 Oct;26:306–17.

48. Corre, P. et al. Direct comparison of current cell-based and cell-free approaches towards the repair of craniofacial bone defects - A preclinical study. *Acta Biomater* 26, 306-317, doi:10.1016/j.actbio.2015.08.013 (2015).
49. Cruess RL, Dumont J. Fracture healing. *Can J Surg.* 1975 Sep;18(5):403–13.
50. Cui, X., Boland, T., D'Lima, D.D., and Lotz, M.K. (2012). Thermal inkjet printing in tissue engineering and regenerative medicine. *Recent Pat Drug Deliv Formul* 6(2), 149-155.
51. Daculsi, G., LeGeros, R.Z., Nery, E., Lynch, K., and Kerebel, B. (1989). Transformation of biphasic calcium phosphate ceramics in vivo: ultrastructural and physicochemical characterization. *J Biomed Mater Res* 23(8), 883-894. doi: 10.1002/jbm.820230806.
52. Dai J, Rabie BM (2007) VEGF: an essential mediator of both angiogenesis and endochondral ossification. *J Dent Res* 86(10):937–950
53. de Grado, G. F. et al. Bone substitutes: a review of their characteristics, clinical use, and perspectives for large bone defects management. *J Tissue Eng* 9, doi:10.1177/2041731418776819 (2018).
54. De Long WG, Einhorn TA, Koval K, McKee M, Smith W, Sanders R, et al. Bone grafts and bone graft substitutes in orthopaedic trauma surgery. A critical analysis. *J Bone Joint Surg Am.* 2007 Mar;89(3):649–58.
55. Deckard, C.R. (1989). Method and apparatus for producing parts by selective sintering. Washington, DC: U.S. Patent and Trademark Office. patent application U.S. Patent No. 4,863,538.
56. Desando G, Bartolotti I, Martini L, Giavaresi G, Nicoli Aldini N, Fini M, et al. Regenerative Features of Adipose Tissue for Osteoarthritis Treatment in a Rabbit Model: Enzymatic Digestion Versus Mechanical Disruption. *Int J Mol Sci.* 2019 May 29;20(11).
57. Dimitriou, R., Jones, E., McGonagle, D., and Giannoudis, P.V. (2011). Bone regeneration: current concepts and future directions. *BMC Med* 9, 66. doi: 10.1186/1741-7015-9-66.
58. Dimitriou, R., Mataliotakis, G. I., Angoules, A. G., Kanakaris, N. K. & Giannoudis, P. V. Complications following autologous bone graft harvesting from the iliac crest and using the RIA: A systematic review. *Injury* 42, S3-S15, doi:10.1016/j.injury.2011.06.015 (2011).
59. Donath, K. & Breuner, G. A method for the study of undecalcified bones and teeth with attached soft tissues. The Sage-Schliff (sawing and grinding) technique. *J Oral Pathol* 11, 318-326 (1982).
60. Dong Q, Lin C, Shang H, Wu W, Chen F, Ji X, et al. Modified approach to construct a vascularized coral bone in rabbit using an arteriovenous loop. *J Reconstr Microsurg.* 2010 Feb;26(2):95–102.

61. Dupret-Bories, A., Vergez, S., Meresse, T., Brouillet, F., and Bertrand, G. (2018). Contribution of 3D printing to mandibular reconstruction after cancer. *Eur Ann Otorhinolaryngol Head Neck Dis* 135(2), 133-136. doi: 10.1016/j.anorl.2017.09.007.
62. Eggli, P.S., Muller, W., and Schenk, R.K. (1988). Porous hydroxyapatite and tricalcium phosphate cylinders with two different pore size ranges implanted in the cancellous bone of rabbits. A comparative histomorphometric and histologic study of bony ingrowth and implant substitution. *Clin Orthop Relat Res* (232), 127-138.
63. Elliot, R.R., and Richards, R.H. (2011). Failed operative treatment in two cases of pseudarthrosis of the clavicle using internal fixation and bovine cancellous xenograft (Tutobone). *Journal of Pediatric Orthopaedics B* 20(5).
64. Epple C, Haumer A, Ismail T, Lunger A, Scherberich A, Schaefer DJ, et al. Prefabrication of a large pedicled bone graft by engineering the germ for de novo vascularization and osteoinduction. *Biomaterials*. 2019 Feb;192:118–27.
65. Erol, O. O. & Sira, M. New capillary bed formation with a surgically constructed arteriovenous fistula. *Plast Reconstr Surg* 66, 109-115, doi:10.1097/00006534-198007000-00021 (1980).
66. Everts V, Delaissé JM, Korper W, Jansen DC, Tigchelaar-Gutter W, Saftig P, et al. The bone lining cell: its role in cleaning Howship's lacunae and initiating bone formation. *J Bone Miner Res*. 2002 Jan;17(1):77–90.
67. Faldini, C., Miscione, M.T., Acri, F., Chehrassan, M., Bonomo, M., and Giannini, S. (2011). Use of homologous bone graft in the treatment of aseptic forearm nonunion. *MUSCULOSKELETAL SURGERY* 95(1), 31-35. doi: 10.1007/s12306-011-0117-8.
68. Farré-Guasch E, Bravenboer N, Helder MN, Schulten EAJM, Ten Bruggenkate CM, Klein-Nulend J. Blood Vessel Formation and Bone Regeneration Potential of the Stromal Vascular Fraction Seeded on a Calcium Phosphate Scaffold in the Human Maxillary Sinus Floor Elevation Model. *Materials (Basel)*. 2018 Jan 20;11(1).
69. Feilden, E., Blanca, E.G.-T., Giuliani, F., Saiz, E., and Vandeperre, L. (2016). Robocasting of structural ceramic parts with hydrogel inks. *Journal of the European Ceramic Society* 36(10), 2525-2533. doi: <https://doi.org/10.1016/j.jeurceramsoc.2016.03.001>.
70. Fella BH, Weiss P, Gauthier O, Rouillon T, Pilet P, Daculsi G, et al. Bone repair using a new injectable self-crosslinkable bone substitute. *J Orthop Res*. 2006 Apr;24(4):628–35.
71. Fernandez de Grado, G. et al. Bone substitutes: a review of their characteristics, clinical use, and perspectives for large bone defects management. *J Tissue Eng* 9, 1-18, doi:10.1177/2041731418776819 (2018).

72. Fernandez de Grado, G., Keller, L., Idoux-Gillet, Y., Wagner, Q., Musset, A.-M., Benkirane-Jessel, N., et al. (2018). Bone substitutes: a review of their characteristics, clinical use, and perspectives for large bone defects management. *J Tissue Eng* 9, 1-18. doi: 10.1177/2041731418776819.
73. Filipowska J, Tomaszewski KA, Niedźwiedzki Ł, Walocha JA, Niedźwiedzki T. The role of vasculature in bone development, regeneration and proper systemic functioning. *Angiogenesis*. 2017 Aug;20(3):291–302.
74. Forriol F. Growth factors in cartilage and meniscus repair. *Injury*. 2009 Dec;40 Suppl 3:S12-16.
75. Friedlaender, G. E. et al. Osteogenic protein-1 (bone morphogenetic protein-7) in the treatment of tibial nonunions. *J Bone Joint Surg Am* 83-A Suppl 1, S151-158 (2001).
76. Friesenbichler, J., Maurer-Ertl, W., Sadoghi, P., Pirker-Fruehauf, U., Bodo, K., and Leithner, A. (2014). Adverse reactions of artificial bone graft substitutes: lessons learned from using tricalcium phosphate geneX®. *Clinical orthopaedics and related research* 472(3), 976-982. doi: 10.1007/s11999-013-3305-z.
77. Gamblin A-L, Brennan MA, Renaud A, Yagita H, Lézot F, Heymann D, et al. Bone tissue formation with human mesenchymal stem cells and biphasic calcium phosphate ceramics: The local implication of osteoclasts and macrophages. *Biomaterials*. 2014 Dec 1;35(36):9660–7.
78. Gamblin, A. L. et al. Bone tissue formation with human mesenchymal stem cells and biphasic calcium phosphate ceramics: the local implication of osteoclasts and macrophages. *Biomaterials* 35, 9660-9667, doi:10.1016/j.biomaterials.2014.08.018 (2014).
79. Garrigues GE, Aldridge JM, Friend JK, Urbaniak JR. Free Vascularized Fibular Grafting for treatment of osteonecrosis of the femoral head secondary to hip dislocation. *Microsurgery*. 2009;29(5):342–5.
80. Gerhardt, L.C., and Boccaccini, A.R. (2010). Bioactive glass and glass-ceramic scaffolds for bone tissue engineering. *Materials (Basel)* 3(7), 3867-3910. doi: 10.3390/ma3073867.
81. Giannoudis, P. V., Harwood, P. J., Tosounidis, T. & Kanakaris, N. K. Restoration of long bone defects treated with the induced membrane technique: protocol and outcomes. *Injury* 47 Suppl 6, S53-S61, doi:10.1016/S0020-1383(16)30840-3 (2016).
82. Giannoudis, P.V., Einhorn, T.A., Schmidmaier, G., and Marsh, D. (2008). The diamond concept – open questions. *Injury* 39, S5-S8. doi: 10.1016/S0020-1383(08)70010-X.
83. Gjerde C, Mustafa K, Hellem S, Rojewski M, Gjengedal H, Yassin MA, et al. Cell therapy induced regeneration of severely atrophied mandibular bone in a

clinical trial. *Stem Cell Res Ther* [Internet]. 2018 Aug 9 [cited 2019 Feb 25];9. Available from: <https://www.ncbi.nlm.nih.gov/pmc/articles/PMC6085689/>

84. Gomes, K.U., Carlini, J.L., Biron, C., Rapoport, A., and Dedivitis, R.A. (2008). Use of allogeneic bone graft in maxillary reconstruction for installation of dental implants. *Journal of Oral and Maxillofacial Surgery* 66(11), 2335-2338. doi: 10.1016/j.joms.2008.06.006.
85. Gómez-Barrena E, Rosset P, Gebhard F, Hernigou P, Baldini N, Rouard H, et al. Feasibility and safety of treating non-unions in tibia, femur and humerus with autologous, expanded, bone marrow-derived mesenchymal stromal cells associated with biphasic calcium phosphate biomaterials in a multicentric, non-comparative trial. *Biomaterials*. 2019 Mar 1;196:100–8.
86. Gómez-Barrena E, Rosset P, Müller I, Giordano R, Bunu C, Layrolle P, et al. Bone regeneration: stem cell therapies and clinical studies in orthopaedics and traumatology. *J Cell Mol Med*. 2011 Jun;15(6):1266–86.
87. Gomez-Barrena, E. et al. Feasibility and safety of treating non-unions in tibia, femur and humerus with autologous, expanded, bone marrow-derived mesenchymal stromal cells associated with biphasic calcium phosphate biomaterials in a multicentric, non-comparative trial. *Biomaterials* 196, 100-108, doi:10.1016/j.biomaterials.2018.03.033 (2019).
88. Gosheger, G., Gebert, C., Ahrens, H., Streitbueger, A., Winkelmann, W., and Harges, J. (2006). Endoprosthetic reconstruction in 250 patients with sarcoma. *Clin Orthop Relat Res* 450, 164-171. doi: 10.1097/01.blo.0000223978.36831.39.
89. Griffin, K. S. et al. Evolution of bone grafting: bone grafts and tissue engineering strategies for vascularized bone regeneration. *Clinic Rev Bone Miner Metab* 13, 232-244, doi:10.1007/s12018-015-9194-9 (2015).
90. Gruene, M., Unger, C., Koch, L., Deiwick, A., and Chichkov, B. (2011). Dispensing pico to nanolitre of a natural hydrogel by laser-assisted bioprinting. *BioMedical Engineering OnLine* 10(1), 19. doi: 10.1186/1475-925X-10-19.
91. Gubin, A., Borzunov, D. & Malkova, T. Ilizarov method for bone lengthening and defect management review of contemporary literature. *Bull Hosp Jt Dis* (2013) 74, 145-154 (2016).
92. Hadjidakis DJ, Androulakis II. Bone remodeling. *Ann N Y Acad Sci*. 2006 Dec;1092:385–96.
93. Han D, Guan X, Wang J, Wei J, Li Q. Rabbit Tibial Periosteum and Saphenous Arteriovenous Vascular Bundle as an In Vivo Bioreactor to Construct Vascularized Tissue-Engineered Bone: A Feasibility Study. *Artificial Organs*. 2014;38(2):167–74.

94. Han, W., Shen, J., Wu, H., Yu, S., Fu, J., and Xie, Z. (2017). Induced membrane technique: advances in the management of bone defects. *Int J Surg* 42, 110-116. doi: 10.1016/j.ijsu.2017.04.064.
95. Hankenson KD, Dishowitz M, Gray C, Schenker M (2011). Angiogenesis in bone regeneration. *Injury* 42(6):556–561
96. Hattori, H., Mibe, J., and Yamamoto, K. (2011). Modular megaprosthesis in metastatic bone disease of the femur. *Orthopedics* 34(12), e871-876. doi: 10.3928/01477447-20111021-13.
97. Heliotis, M., Lavery, K.M., Ripamonti, U., Tsiridis, E., and di Silvio, L. (2006). Transformation of a prefabricated hydroxyapatite/osteogenic protein-1 implant into a vascularised pedicled bone flap in the human chest. *International Journal of Oral and Maxillofacial Surgery* 35(3), 265-269. doi: 10.1016/j.ijom.2005.07.013.
98. Henriksen K, Neutzsky-Wulff AV, Bonewald LF, Karsdal MA. Local communication on and within bone controls bone remodeling. *Bone*. 2009 Jun;44(6):1026–33.
99. Hidalgo, D.A., and Pusic, A.L. (2002). Free-flap mandibular reconstruction: a 10-year follow-up study. *Plast Reconstr Surg* 110(2), 438-451.
100. Hock, S.W., Johnson, D.A., and Van Veen, M.A. (1996). Print quality optimization for a color ink jet printer by using a larger nozzle for the black ink only.
101. Holl, S., Schlomberg, A., Gosheger, G., Dieckmann, R., Streitbuerger, A., Schulz, D., et al. (2012). Distal femur and proximal tibia replacement with megaprosthesis in revision knee arthroplasty: a limb-saving procedure. *Knee Surg Sports Traumatol Arthrosc* 20(12), 2513-2518. doi: 10.1007/s00167-012-1945-2.
102. Holt GE, Halpern JL, Lynch CC, Devin CJ, Schwartz HS. Imaging Analysis of the In vivo Bioreactor: A Preliminary Study. *Clin Orthop Relat Res*. 2008 Aug;466(8):1890–6.
103. Hoornaert A, d'Arros C, Heymann M-F, Layrolle P. Biocompatibility, resorption and biofunctionality of a new synthetic biodegradable membrane for guided bone regeneration. *Biomed Mater*. 2016 10;11(4):045012.
104. Hudson, K.R., Cowan, P.B., and Gondek, J.S. (2000). Ink drop volume variance compensation for inkjet printing.
105. Hutmacher DW, Schantz JT, Lam CXF, Tan KC, Lim TC. State of the art and future directions of scaffold-based bone engineering from a biomaterials perspective. *J Tissue Eng Regen Med*. 2007 Jul 1;1(4):245–60.
106. Hutmacher, D. W. Scaffolds in tissue engineering bone and cartilage. *Biomaterials* 21, 2529-2543, doi:10.1016/s0142-9612(00)00121-6 (2000).

107. Hutmacher, D. W., Schantz, J. T., Lam, C. X., Tan, K. C. & Lim, T. C. State of the art and future directions of scaffold-based bone engineering from a biomaterials perspective. *J Tissue Eng Regen Med* 1, 245-260, doi:10.1002/term.24 (2007).
108. Innocenti M, Abed YY, Beltrami G, Delcroix L, Manfrini M, Capanna R. Biological reconstruction after resection of bone tumors of the proximal tibia using allograft shell and intramedullary free vascularized fibular graft: long-term results. *Microsurgery*. 2009;29(5):361–72.
109. Jakoi, A. M., Iorio, J. A. & Cahill, P. J. Autologous bone graft harvesting: a review of grafts and surgical techniques. *Musculoskelet Surg* 99, 171-178, doi:10.1007/s12306-015-0351-6 (2015).
110. Jenó, L. & Geza, L. A simple differential staining method for semi-thin sections of ossifying cartilage and bone tissues embedded in epoxy resin. *Mikroskopie* 31, 1-4 (1975).
111. Jeys, L., and Grimer, R. (2009). "The long-term risks of infection and amputation with limb salvage surgery using endoprostheses," in *Treatment of Bone and Soft Tissue Sarcomas*, ed. P.-U. Tunn. (Berlin, Heidelberg: Springer Berlin Heidelberg), 75-84.
112. Jeys, L.M., Grimer, R.J., Carter, S.R., and Tillman, R.M. (2005). Periprosthetic infection in patients treated for an orthopaedic oncological condition. *J Bone Joint Surg Am* 87(4), 842-849. doi: 10.2106/JBJS.C.01222.
113. Ji, K., Wang, Y., Wei, Q., Zhang, K., Jiang, A., Rao, Y., et al. (2018). Application of 3D printing technology in bone tissue engineering. *Bio-Design and Manufacturing* 1(3), 203-210. doi: 10.1007/s42242-018-0021-2.
114. Kaempfen A, Todorov A, Güven S, Largo RD, Jaquíery C, Scherberich A, et al. Engraftment of Prevascularized, Tissue Engineered Constructs in a Novel Rabbit Segmental Bone Defect Model. *Int J Mol Sci*. 2015 Jun 4;16(6):12616–30.
115. Kalfas, I. H. Principles of bone healing. *Neurosurg Focus* 10, E1, doi:10.3171/foc.2001.10.4.2 (2001).
116. Kanczler JM, Oreffo ROC. Osteogenesis and angiogenesis: the potential for engineering bone. *Eur Cell Mater*. 2008;15:100–14.
117. Kang H-W, Lee SJ, Ko IK, Kengla C, Yoo JJ, Atala A. A 3D bioprinting system to produce human-scale tissue constructs with structural integrity. *Nat Biotechnol*. 2016 Mar;34(3):312–9.
118. Kao, C.T., Lin, C.C., Chen, Y.W., Yeh, C.H., Fang, H.Y., and Shie, M.Y. (2015). Poly(dopamine) coating of 3D printed poly(lactic acid) scaffolds for bone tissue engineering. *Mater Sci Eng C Mater Biol Appl* 56, 165-173. doi: 10.1016/j.msec.2015.06.028.

119. Karalashvili, L., Chichua, N., Menabde, G., Atskvereli, L., and Grdzeldze, T. (2017). Decellularized bovine bone graft for zygomatic bone reconstruction. *Med Case Rep* 4(1:52). doi: 10.21767/2471-8041.100087.
120. Keating, J.F., and McQueen, M.M. (2001). Substitutes for autologous bone graft in orthopaedic trauma. *J Bone Joint Surg Br* 83(1), 3-8. doi: 10.1302/0301-620x.83b1.11952.
121. Khouri RK, Koudsi B, Reddi H. Tissue transformation into bone in vivo. A potential practical application. *JAMA*. 1991 Oct 9;266(14):1953–5.
122. Klammert, U., Gbureck, U., Vorndran, E., Rodiger, J., Meyer-Marcotty, P., and Kubler, A.C. (2010a). 3D powder printed calcium phosphate implants for reconstruction of cranial and maxillofacial defects. *J Craniomaxillofac Surg* 38(8), 565-570. doi: 10.1016/j.jcms.2010.01.009.
123. Klammert, U., Vorndran, E., Reuther, T., Muller, F.A., Zorn, K., and Gbureck, U. (2010b). Low temperature fabrication of magnesium phosphate cement scaffolds by 3D powder printing. *J Mater Sci Mater Med* 21(11), 2947-2953. doi: 10.1007/s10856-010-4148-8.
124. Kneser U, Polykandriotis E, Ohnolz J, Heidner K, Grabinger L, Euler S, et al. Engineering of vascularized transplantable bone tissues: induction of axial vascularization in an osteoconductive matrix using an arteriovenous loop. *Tissue Eng*. 2006 Jul;12(7):1721–31.
125. Kneser U, Schaefer DJ, Polykandriotis E, Horch RE. Tissue engineering of bone: the reconstructive surgeon's point of view. *Journal of Cellular and Molecular Medicine*. 2006 Enero;10(1):7–19.
126. Kneser, U. et al. Engineering of vascularized transplantable bone tissues: Induction of axial vascularization in an osteoconductive matrix using an arteriovenous loop. *Tissue Eng* 12, 1721-1731, doi:10.1089/ten.2006.12.1721 (2006).
127. Kneser, U., Schaefer, D. J., Polykandriotis, E. & Horch, R. E. Tissue engineering of bone: the reconstructive surgeon's point of view. *J Cell Mol Med* 10, 7-19, doi:10.1111/j.1582-4934.2006.tb00287.x (2006).
128. Kokemueller H, Spalthoff S, Nolff M, Tavassol F, Essig H, Stuehmer C, et al. Prefabrication of vascularized bioartificial bone grafts in vivo for segmental mandibular reconstruction: experimental pilot study in sheep and first clinical application. *International Journal of Oral and Maxillofacial Surgery*. 2010 Apr;39(4):379–87.
129. Kokemueller, H. et al. Prefabrication of vascularized bioartificial bone grafts in vivo for segmental mandibular reconstruction: experimental pilot study in sheep and first clinical application. *Int J Oral Maxillofac Surg* 39, 379-387, doi:10.1016/j.ijom.2010.01.010 (2010).

130. Kokemueller, H., Spalthoff, S., Nolff, M., Tavassol, F., Essig, H., Stuehmer, C., et al. (2010). Prefabrication of vascularized bioartificial bone grafts in vivo for segmental mandibular reconstruction: experimental pilot study in sheep and first clinical application. *Int J Oral Maxillofac Surg* 39(4), 379-387. doi: 10.1016/j.ijom.2010.01.010.
131. Kolesky DB, Homan KA, Skylar-Scott MA, Lewis JA. Three-dimensional bioprinting of thick vascularized tissues. *Proc Natl Acad Sci U S A*. 2016 Mar 22;113(12):3179–84.
132. Kurien, T., Pearson, R.G., and Scammell, B.E. (2013). Bone graft substitutes currently available in orthopaedic practice. *The Bone & Joint Journal* 95-B(5), 583-597. doi: 10.1302/0301-620X.95B5.30286.
133. Langer R, Vacanti JP. Tissue engineering. *Science*. 1993 May 14;260(5110):920–6.
134. Laurencin, C., Khan, Y., and Veronick, J. (2014). "Bone graft substitutes: past, present and future," in *Bone graft substitutes and bone regenerative engineering*. West Conshohocken, PA: ASTM International), 1-9.
135. Ledford, C.K., Nunley, J.A., 2nd, Viens, N.A., and Lark, R.K. (2013). Bovine xenograft failures in pediatric foot reconstructive surgery. *J Pediatr Orthop* 33(4), 458-463. doi: 10.1097/BPO.0b013e318287010d.
136. Lee, K.Y., Park, M., Kim, H.M., Lim, Y.J., Chun, H.J., Kim, H., et al. (2006). Ceramic bioactivity: progresses, challenges and perspectives. *Biomedical Materials* 1(2), R31-R37. doi: 10.1088/1748-6041/1/2/r01.
137. Lewis, J.A. (2006). Direct ink writing of 3D functional materials. *Advanced Functional Materials* 16(17), 2193-2204. doi: 10.1002/adfm.200600434.
138. Lewis, J.A., Smay, J.E., Stuecker, J., and Cesarano, J. (2006). Direct ink writing of three-dimensional ceramic structures. *Journal of the American Ceramic Society* 89(12), 3599-3609. doi: 10.1111/j.1551-2916.2006.01382.x.
139. Liao, H.-T., Chang, K.-H., Jiang, Y., Chen, J.-P., and Lee, M.-Y. (2011). Fabrication of tissue engineered PCL scaffold by selective laser-sintered machine for osteogenesis of adipose-derived stem cells. *Virtual and Physical Prototyping* 6(1), 57-60. doi: 10.1080/17452759.2011.559742.
140. Lin, K., Sheikh, R., Romanazzo, S. & Roohani, I. 3D Printing of bioceramic scaffolds-barriers to the clinical translation: from promise to reality, and future perspectives. *Materials (Basel)* 12, doi:10.3390/ma12172660 (2019).
141. Lipa JE, Novak CB, Binhammer PA. Patient-reported donor-site morbidity following anterolateral thigh free flaps. *J Reconstr Microsurg*. 2005 Aug;21(6):365–70.
142. Liu X, Chen W, Zhang C, Thein-Han W, Hu K, Reynolds MA, et al. Co-Seeding Human Endothelial Cells with Human-Induced Pluripotent Stem Cell-

Derived Mesenchymal Stem Cells on Calcium Phosphate Scaffold Enhances Osteogenesis and Vascularization in Rats. *Tissue Eng Part A*. 2017 Jun 1;23(11–12):546–55.

143. Liu, Y., Lim, J. & Teoh, S. H. Review: development of clinically relevant scaffolds for vascularised bone tissue engineering. *Biotechnol Adv* 31, 688-705, doi:10.1016/j.biotechadv.2012.10.003 (2013).
144. Lodoso-Torrecilla, I., van Gestel, N.A.P., Diaz-Gomez, L., Grosfeld, E.C., Laperre, K., Wolke, J.G.C., et al. (2018). Multimodal pore formation in calcium phosphate cements. *J Biomed Mater Res A* 106(2), 500-509. doi: 10.1002/jbm.a.36245.
145. Lovett M, Lee K, Edwards A, Kaplan DL. Vascularization Strategies for Tissue Engineering. *Tissue Engineering Part B: Reviews*. 2009 Sep;15(3):353–70.
146. Maisani M, Pezzoli D, Chassande O, Mantovani D. Cellularizing hydrogel-based scaffolds to repair bone tissue: How to create a physiologically relevant micro-environment? *J Tissue Eng [Internet]*. 2017 Jun 8 [cited 2019 Feb 26];8. Available from: <https://www.ncbi.nlm.nih.gov/pmc/articles/PMC5467968/>
147. Mandrycky, C., Wang, Z., Kim, K., and Kim, D.-H. (2016). 3D bioprinting for engineering complex tissues. *Biotechnology Advances* 34(4), 422-434. doi: <https://doi.org/10.1016/j.biotechadv.2015.12.011>.
148. Mankani MH, Kuznetsov SA, Robey PG. Formation of hematopoietic territories and bone by transplanted human bone marrow stromal cells requires a critical cell density. *Exp Hematol*. 2007 Jun;35(6):995–1004.
149. Mankani MH, Kuznetsov SA, Wolfe RM, Marshall GW, Robey PG. In vivo bone formation by human bone marrow stromal cells: reconstruction of the mouse calvarium and mandible. *Stem Cells*. 2006 Sep;24(9):2140–9.
150. Mankin, H.J., Gebhardt, M.C., Jennings, L.C., Springfield, D.S., and Tomford, W.W. (1996). Long-term results of allograft replacement in the management of bone tumors. *Clin Orthop Relat Res* (324), 86-97. doi: 10.1097/00003086-199603000-00011.
151. Marler J, Upton J, Langer R, Vacanti J. Transplantation of cells in matrices for tissue regeneration. *Adv Drug Deliv Rev*. 1998 03;33(1–2):165–82.
152. Marsh D. Concepts of fracture union, delayed union, and nonunion. *Clin Orthop Relat Res*. 1998 Oct;(355 Suppl):S22-30.
153. Masquelet, A.C. (2003). Muscle reconstruction in reconstructive surgery: soft tissue repair and long bone reconstruction. *Langenbecks Arch Surg* 388(5), 344-346. doi: 10.1007/s00423-003-0379-1.

154. Masquelet, A.C., and Begue, T. (2010). The concept of induced membrane for reconstruction of long bone defects. *Orthopedic Clinics of North America* 41(1), 27-37. doi: <https://doi.org/10.1016/j.ocl.2009.07.011>.
155. Masquelet, A.C., Fitoussi, F., Begue, T., and Muller, G.P. (2000). Reconstruction of the long bones by the induced membrane and spongy autograft. *Ann Chir Plast Esthet* 45(3), 346-353.
156. Mathieu, L., Bilichtin, E., Durand, M., de l'Escalopier, N., Murison, J.C., Collombet, J.M., et al. (2019). Masquelet technique for open tibia fractures in a military setting. *Eur J Trauma Emerg Surg*. doi: 10.1007/s00068-019-01217-y.
157. Matsuo K, Irie N. Osteoclast-osteoblast communication. *Arch Biochem Biophys*. 2008 May 15;473(2):201–9.
158. Mazo M, Hernández S, Gavira JJ, Abizanda G, Araña M, López-Martínez T, et al. Treatment of reperfused ischemia with adipose-derived stem cells in a preclinical Swine model of myocardial infarction. *Cell Transplant*. 2012;21(12):2723–33.
159. Mazzoli, A. (2013). Selective laser sintering in biomedical engineering. *Med Biol Eng Comput* 51(3), 245-256. doi: 10.1007/s11517-012-1001-x.
160. Mercado-Pagan, A. E., Stahl, A. M., Shanjani, Y. & Yang, Y. Vascularization in bone tissue engineering constructs. *Ann Biomed Eng* 43, 718-729, doi:10.1007/s10439-015-1253-3 (2015).
161. Mercado-Pagan, A.E., Stahl, A.M., Shanjani, Y., and Yang, Y. (2015). Vascularization in bone tissue engineering constructs. *Ann Biomed Eng* 43(3), 718-729. doi: 10.1007/s10439-015-1253-3.
162. Merlino G, Borsetti M, Boltri M. Reverse radial artery bone flap reconstruction of segmental metacarpal losses. *J Hand Surg Eur Vol*. 2007 Feb;32(1):98–101.
163. Mesimäki K, Lindroos B, Törnwall J, Mauno J, Lindqvist C, Kontio R, et al. Novel maxillary reconstruction with ectopic bone formation by GMP adipose stem cells. *Int J Oral Maxillofac Surg*. 2009 Mar;38(3):201–9.
164. Mesimaki, K. et al. Novel maxillary reconstruction with ectopic bone formation by GMP adipose stem cells. *Int J Oral Maxillofac Surg* 38, 201-209, doi:10.1016/j.ijom.2009.01.001 (2009).
165. Michna, S., Wu, W., and Lewis, J.A. (2005). Concentrated hydroxyapatite inks for direct-write assembly of 3D periodic scaffolds. *Biomaterials* 26(28), 5632-5639. doi: <https://doi.org/10.1016/j.biomaterials.2005.02.040>.
166. Miranda, P., Saiz, E., Gryn, K., and Tomsia, A.P. (2006). Sintering and robocasting of β -tricalcium phosphate scaffolds for orthopaedic applications. *Acta Biomaterialia* 2(4), 457-466. doi: <https://doi.org/10.1016/j.actbio.2006.02.004>.

167. Mittermayer, F., Krepler, P., Dominkus, M., Schwameis, E., Sluga, M., Heinzl, H., et al. (2001). Long-term followup of uncemented tumor endoprostheses for the lower extremity. *Clin Orthop Relat Res* (388), 167-177. doi: 10.1097/00003086-200107000-00024.
168. Mondschein, R.J., Kanitkar, A., Williams, C.B., Verbridge, S.S., and Long, T.E. (2017). Polymer structure-property requirements for stereolithographic 3D printing of soft tissue engineering scaffolds. *Biomaterials* 140, 170-188. doi: <https://doi.org/10.1016/j.biomaterials.2017.06.005>.
169. Moore JB, Mazur JM, Zehr D, Davis PK, Zook EG. A biomechanical comparison of vascularized and conventional autogenous bone grafts. *Plast Reconstr Surg*. 1984 Mar;73(3):382–6.
170. Moran, S.L., Bakri, K., Mardini, S., Shin, A.Y., and Bishop, A.T. (2009). The use of vascularized fibular grafts for the reconstruction of spinal and sacral defects. *Microsurgery* 29(5), 393-400. doi: 10.1002/micr.20655.
171. Morelli, I., Drago, L., George, D.A., Gallazzi, E., Scarponi, S., and Romano, C.L. (2016). Masquelet technique: myth or reality? A systematic review and meta-analysis. *Injury* 47 Suppl 6, S68-S76. doi: 10.1016/S0020-1383(16)30842-7.
172. Murphy, S.V., and Atala, A. (2014). 3D bioprinting of tissues and organs. *Nature Biotechnology* 32, 773. doi: 10.1038/nbt.2958.
173. Muscolo, D.L., Ayerza, M.A., Aponte-Tinao, L., Ranalletta, M., and Abalo, E. (2004). Intercalary femur and tibia segmental allografts provide an acceptable alternative in reconstructing tumor resections. *Clinical Orthopaedics and Related Research*® 426.
174. Myeroff C, Archdeacon M. Autogenous bone graft: donor sites and techniques. *J Bone Joint Surg Am*. 2011 Dec 7;93(23):2227–36.
175. Neto AS, Ferreira JMF. Synthetic and Marine-Derived Porous Scaffolds for Bone Tissue Engineering. *Materials (Basel)*. 2018 Sep 13;11(9).
176. Niedz´wiedzki T, Filipowska J (2015) Bone remodeling in the context of cellular and systemic regulation: the role of osteocytes and the nervous system. *J Mol Endocrinol* 55(2):R23–R36
177. Ogose, A., Kondo, N., Umezū, H., Hotta, T., Kawashima, H., Tokunaga, K., et al. (2006). Histological assessment in grafts of highly purified beta-tricalcium phosphate (OSferion®) in human bones. *Biomaterials* 27(8), 1542-1549. doi: <https://doi.org/10.1016/j.biomaterials.2005.08.034>.
178. Ogura, K., Sakuraba, M., Miyamoto, S., Fujiwara, T., Chuman, H., and Kawai, A. (2015). Pelvic ring reconstruction with a double-barreled free vascularized fibula graft after resection of malignant pelvic bone tumor. *Arch Orthop Trauma Surg* 135(5), 619-625. doi: 10.1007/s00402-015-2197-7.

179. O'Keefe, R. J. & Mao, J. Bone tissue engineering and regeneration: from discovery to the clinic--an overview. *Tissue Eng Part B Rev* 17, 389-392, doi:10.1089/ten.TEB.2011.0475 (2011).
180. Orringer, J.S., Shaw, W.W., Borud, L.J., Freymiller, E.G., Wang, S.A., and Markowitz, B.L. (1999). Total mandibular and lower lip reconstruction with a prefabricated osteocutaneous free flap. *Plast Reconstr Surg* 104(3), 793-797. doi: 10.1097/00006534-199909030-00028.
181. Oryan A, Alidadi S, Moshiri A, Maffulli N. Bone regenerative medicine: classic options, novel strategies, and future directions. *J Orthop Surg Res*. 2014;9(1):18.
182. Oryan, A., Alidadi, S., and Moshiri, A. (2013). Current concerns regarding healing of bone defects. *Hard Tissue* 2(2), 13.
183. Oryan, A., Alidadi, S., Moshiri, A., and Maffulli, N. (2014). Bone regenerative medicine: classic options, novel strategies, and future directions. *J Orthop Surg Res* 9(1), 18. doi: 10.1186/1749-799X-9-18.
184. Ottani V, Raspanti M, Ruggeri A. Collagen structure and functional implications. *Micron*. 2001 Apr 1;32(3):251–60.
185. Ozbolat, I.T., and Hospodiuk, M. (2016). Current advances and future perspectives in extrusion-based bioprinting. *Biomaterials* 76, 321-343. doi: <https://doi.org/10.1016/j.biomaterials.2015.10.076>.
186. Pala, E., Trovarelli, G., Calabro, T., Angelini, A., Abati, C.N., and Ruggieri, P. (2015). Survival of modern knee tumor megaprotheses: failures, functional results, and a comparative statistical analysis. *Clin Orthop Relat Res* 473(3), 891-899. doi: 10.1007/s11999-014-3699-2.
187. Papastavrou, E., Breedon, P. & Fairhurst, D. Low-temperature deposition modeling of beta-TCP scaffolds with controlled bimodal porosity. *Methods Mol Biol* 1758, 41-54, doi:10.1007/978-1-4939-7741-3_4 (2018).
188. Parikh, S.N. (2002). Bone graft substitutes: past, present, future. *J Postgrad Med* 48(2), 142-148.
189. Park, S.A., Lee, H.J., Kim, K.S., Lee, S.J., Lee, J.T., Kim, S.Y., et al. (2018). In Vivo Evaluation of 3D-Printed Polycaprolactone Scaffold Implantation Combined with beta-TCP Powder for Alveolar Bone Augmentation in a Beagle Defect Model. *Materials (Basel)* 11(2). doi: 10.3390/ma11020238.
190. Patil, S., Auyeung, J., and Gower, A. (2011). Outcome of Subtalar Fusion Using Bovine Cancellous Bone Graft: A Retrospective Case Series. *The Journal of Foot and Ankle Surgery* 50(4), 388-390. doi: 10.1053/j.jfas.2011.04.019.
191. Paxton, N., Smolan, W., Böck, T., Melchels, F., Groll, J., and Jungst, T. (2017). Proposal to assess printability of bioinks for extrusion-based bioprinting

and evaluation of rheological properties governing bioprintability. *Biofabrication* 9(4), 044107. doi: 10.1088/1758-5090/aa8dd8.

192. Pelissier, P.H., Masquelet, A.C., Bareille, R., Pelissier, S.M., and Amedee, J. (2004). Induced membranes secrete growth factors including vascular and osteoinductive factors and could stimulate bone regeneration. *Journal of Orthopaedic Research* 22(1), 73-79. doi: 10.1016/S0736-0266(03)00165-7.
193. Peng, X., Mao, C., Yu, G.Y., Guo, C.B., Huang, M.X., and Zhang, Y. (2005). Maxillary reconstruction with the free fibula flap. *Plast Reconstr Surg* 115(6), 1562-1569. doi: 10.1097/01.prs.0000160691.63029.74.
194. Petite, H. et al. Tissue-engineered bone regeneration. *Nat Biotechnol* 18, 959-963, doi:10.1038/79449 (2000).
195. Petrochenko, P.E., Torgersen, J., Gruber, P., Hicks, L.A., Zheng, J., Kumar, G., et al. (2015). Laser 3D printing with sub-microscale resolution of porous elastomeric scaffolds for supporting human bone stem cells. *Adv Healthc Mater* 4(5), 739-747. doi: 10.1002/adhm.201400442.
196. Polykandriotis E, Arkudas A, Horch RE, Stürzl M, Kneser U. Autonomously vascularized cellular constructs in tissue engineering: opening a new perspective for biomedical science. *Journal of Cellular and Molecular Medicine*. 2007 Jan;11(1):6–20.
197. Putzier, M., Strube, P., Funk, J.F., Gross, C., Monig, H.J., Perka, C., et al. (2009). Allogenic versus autologous cancellous bone in lumbar segmental spondylodesis: a randomized prospective study. *Eur Spine J* 18(5), 687-695. doi: 10.1007/s00586-008-0875-7.
198. Quarto R, Mastrogiacomo M, Cancedda R, Kutepov SM, Mukhachev V, Lavroukov A, et al. Repair of Large Bone Defects with the Use of Autologous Bone Marrow Stromal Cells. *New England Journal of Medicine*. 2001 Feb 1;344(5):385–6.
199. Raymond, S. et al. Accelerated hardening of nanotextured 3D-plotted self-setting calcium phosphate inks. *Acta Biomater* 75, 451-462, doi:10.1016/j.actbio.2018.05.042 (2018).
200. Rizzo, M., and Moran, S.L. (2008). Vascularized bone grafts and their applications in the treatment of carpal pathology. *Seminars in plastic surgery* 22(3), 213-227. doi: 10.1055/s-2008-1081404.
201. Rodríguez-Lorenzo, L.M., Vallet-Regí, M., and Ferreira, J.M.F. (2001). Colloidal processing of hydroxyapatite. *Biomaterials* 22(13), 1847-1852. doi: [https://doi.org/10.1016/S0142-9612\(00\)00366-5](https://doi.org/10.1016/S0142-9612(00)00366-5).
202. Rosset, P., Deschaseaux, F. & Layrolle, P. Cell therapy for bone repair. *Orthop Traumatol Surg Res* 100, S107-112, doi:10.1016/j.otsr.2013.11.010 (2014).

203. Saijo, H., Igawa, K., Kanno, Y., Mori, Y., Kondo, K., Shimizu, K., et al. (2009). Maxillofacial reconstruction using custom-made artificial bones fabricated by inkjet printing technology. *Journal of Artificial Organs* 12(3), 200-205. doi: 10.1007/s10047-009-0462-7.
204. Saito, E., Suarez-Gonzalez, D., Murphy, W.L., and Hollister, S.J. (2015). Biomineral coating increases bone formation by ex vivo BMP-7 gene therapy in rapid prototyped poly(L-lactic acid) (PLLA) and poly(epsilon-caprolactone) (PCL) porous scaffolds. *Adv Healthc Mater* 4(4), 621-632. doi: 10.1002/adhm.201400424.
205. Samavedi, S., Whittington, A.R., and Goldstein, A.S. (2013). Calcium phosphate ceramics in bone tissue engineering: A review of properties and their influence on cell behavior. *Acta Biomaterialia* 9(9), 8037-8045. doi: <https://doi.org/10.1016/j.actbio.2013.06.014>.
206. Sanan, A., and Haines, S.J. (1997). Repairing holes in the head: a history of cranioplasty. *Neurosurgery* 40(3), 588-603. doi: 10.1097/00006123-199703000-00033.
207. Sawin PD, Traynelis VC, Menezes AH. A comparative analysis of fusion rates and donor-site morbidity for autogeneic rib and iliac crest bone grafts in posterior cervical fusions. *J Neurosurg*. 1998 Feb;88(2):255–65.
208. Scaglione, M., Fabbri, L., Dell’Omo, D., Gambini, F., and Guido, G. (2014). Long bone nonunions treated with autologous concentrated bone marrow-derived cells combined with dried bone allograft. *MUSCULOSKELETAL SURGERY* 98(2), 101-106. doi: 10.1007/s12306-013-0271-2.
209. Scherberich A, Di Maggio ND, McNagny KM. A familiar stranger: CD34 expression and putative functions in SVF cells of adipose tissue. *World J Stem Cells*. 2013 Jan 26;5(1):1–8.
210. Schmitz JP, Hollinger JO. The critical size defect as an experimental model for craniomandibulofacial nonunions. *Clin Orthop Relat Res*. 1986 Apr;(205):299–308.
211. Shehadeh, A., Noveau, J., Malawer, M., and Henshaw, R. (2010). Late complications and survival of endoprosthetic reconstruction after resection of bone tumors. *Clin Orthop Relat Res* 468(11), 2885-2895. doi: 10.1007/s11999-010-1454-x.
212. Shibuya, N., Jupiter, D.C., Clawson, L.D., and La Fontaine, J. (2012). Incorporation of bovine-based structural bone grafts used in reconstructive foot surgery. *The Journal of Foot and Ankle Surgery* 51(1), 30-33. doi: 10.1053/j.jfas.2011.09.008.
213. Sivakumar, R., Mohideen, M.G., Chidambaram, M., Vinoth, T., Singhi, P.K., and Somashekar, V. (2016). Management of large bone defects in

- diaphyseal fractures by induced membrane formation by Masquelet's technique. *J Orthop Case Rep* 6(3), 59-62. doi: 10.13107/jocr.2250-0685.508.
214. Stanovici, J., Le Nail, L.R., Brennan, M.A., Vidal, L., Trichet, V., Rosset, P., et al. (2016). Bone regeneration strategies with bone marrow stromal cells in orthopaedic surgery. *Curr Res Transl Med* 64(2), 83-90. doi: 10.1016/j.retram.2016.04.006.
215. Suwanprateeb, J., Sangam, R., Suvannapruk, W., and Panyathanmaporn, T. (2009). Mechanical and in vitro performance of apatite-wollastonite glass ceramic reinforced hydroxyapatite composite fabricated by 3D-printing. *J Mater Sci Mater Med* 20(6), 1281-1289. doi: 10.1007/s10856-009-3697-1.
216. Tang D, Tare RS, Yang L-Y, Williams DF, Ou K-L, Oreffo ROC. Biofabrication of bone tissue: approaches, challenges and translation for bone regeneration. *Biomaterials*. 2016 Mar;83:363–82.
217. Tang, D. et al. Biofabrication of bone tissue: approaches, challenges and translation for bone regeneration. *Biomaterials* 83, 363-382, doi:10.1016/j.biomaterials.2016.01.024 (2016).
218. Tatara, A.M., Wong, M.E., and Mikos, A.G. (2014). In vivo bioreactors for mandibular reconstruction. *Journal of dental research* 93(12), 1196-1202. doi: 10.1177/0022034514547763.
219. Taylor, G.I. (1982). Reconstruction of the mandible with free composite iliac bone grafts. *Ann Plast Surg* 9(5), 361-376. doi: 10.1097/0000637-198211000-00003.
220. Taylor, G.I. (1983). The current status of free vascularized bone grafts. *Clin Plast Surg* 10(1), 185-209.
221. Taylor, G.I. (1985). Composite tissue transfer to the lower limb. *Recent Adv Plast Surg* 3, 83-109.
222. Taylor, G.I., Corlett, R.J., and Ashton, M.W. (2016). The evolution of free vascularized bone transfer: a 40-year experience. *Plast Reconstr Surg* 137(4), 1292-1305. doi: 10.1097/PRS.0000000000002040.
223. Taylor, G.I., Miller, G.D., and Ham, F.J. (1975). The free vascularized bone graft. A clinical extension of microvascular techniques. *Plast Reconstr Surg* 55(5), 533-544. doi: 10.1097/00006534-197505000-00002.
224. Thébaud NB, Siadous R, Bareille R, Remy M, Daculsi R, Amédée J, et al. Whatever their differentiation status, human progenitor derived - or mature - endothelial cells induce osteoblastic differentiation of bone marrow stromal cells. *J Tissue Eng Regen Med*. 2012 Nov;6(10):e51-60.
225. Thompson TJ, Owens PD, Wilson DJ (1989) Intramembranous osteogenesis and angiogenesis in the chick embryo. *J Anat* 166:55–65

226. Tomlinson RE, Silva MJ (2013) Skeletal blood flow in bonerepair and maintenance. *Bone Res* 1(4):311–322
227. Torres, J., Tamimi, F., Alkhraisat, M., Prados-Frutos, J.C., and Lopez-Cabarcos, E. (2011). "Bone substitutes," in *Implant dentistry - the most promising discipline of dentistry*, ed. I. Turkyilmaz. Intech), 4-105.
228. Trombetta, R., Inzana, J.A., Schwarz, E.M., Kates, S.L., and Awad, H.A. (2017). 3D printing of calcium phosphate ceramics for bone tissue engineering and drug delivery. *Ann Biomed Eng* 45(1), 23-44. doi: 10.1007/s10439-016-1678-3.
229. Unger, C., Gruene, M., Koch, L., Koch, J., and Chichkov, B.N. (2011). Time-resolved imaging of hydrogel printing via laser-induced forward transfer. *Applied Physics A* 103(2), 271-277. doi: 10.1007/s00339-010-6030-4.
230. Vacanti, J.P., and Langer, R. (1999). Tissue engineering: the design and fabrication of living replacement devices for surgical reconstruction and transplantation. *The Lancet* 354, S32-S34. doi: 10.1016/S0140-6736(99)90247-7.
231. Verboket, R. et al. Autologous cell-based therapy for treatment of large bone defects: from bench to bedside. *Eur J Trauma Emerg Surg* 44, 649-665, doi:10.1007/s00068-018-0906-y (2018).
232. Verboket, R., Leiblein, M., Seebach, C., Nau, C., Janko, M., Bellen, M., et al. (2018). Autologous cell-based therapy for treatment of large bone defects: from bench to bedside. *Eur J Trauma Emerg Surg* 44(5), 649-665. doi: 10.1007/s00068-018-0906-y.
233. Vorndran, E., Klarner, M., Klammert, U., Grover, L.M., Patel, S., Barralet, J.E., et al. (2008). 3D Powder printing of β -tricalcium phosphate ceramics using different strategies. *Advanced Engineering Materials* 10(12), B67-B71. doi: 10.1002/adem.200800179.
234. Wang, M.O., Vorwald, C.E., Dreher, M.L., Mott, E.J., Cheng, M.-H., Cinar, A., et al. (2015). Evaluating 3D-printed biomaterials as scaffolds for vascularized bone tissue engineering. *Advanced Materials* 27(1), 138-144. doi: 10.1002/adma.201403943.
235. Wang, W. & Yeung, K. W. K. Bone grafts and biomaterials substitutes for bone defect repair: A review. *Bioact Mater* 2, 224-247, doi:10.1016/j.bioactmat.2017.05.007 (2017).
236. Warnke PH, Springer ING, Wiltfang J, Acil Y, Eufinger H, Wehmöller M, et al. Growth and transplantation of a custom vascularised bone graft in a man. *Lancet*. 2004 Sep 28;364(9436):766–70.
237. Warnke PH, Wiltfang J, Springer I, Acil Y, Bolte H, Kosmahl M, et al. Man as living bioreactor: fate of an exogenously prepared customized tissue-engineered mandible. *Biomaterials*. 2006 Jun;27(17):3163–7.

238. Warnke, P. H. et al. Growth and transplantation of a custom vascularised bone graft in a man. *Lancet* 364, 766-770, doi:10.1016/S0140-6736(04)16935-3 (2004).
239. Warnke, P. H. et al. Man as living bioreactor: Fate of an exogenously prepared customized tissue-engineered mandible. *Biomaterials* 27, 3163-3167, doi:10.1016/j.biomaterials.2006.01.050 (2006).
240. Warnke, P.H., Springer, I.N., Wiltfang, J., Acil, Y., Eufinger, H., Wehmoller, M., et al. (2004). Growth and transplantation of a custom vascularised bone graft in a man. *Lancet* 364(9436), 766-770. doi: 10.1016/S0140-6736(04)16935-3.
241. Wen, Y., Xun, S., Haoye, M., Baichuan, S., Peng, C., Xuejian, L., et al. (2017). 3D printed porous ceramic scaffolds for bone tissue engineering: a review. *Biomater Sci* 5(9), 1690-1698. doi: 10.1039/c7bm00315c.
242. Winder, J., and Bibb, R. (2005). Medical rapid prototyping technologies: state of the art and current limitations for application in oral and maxillofacial surgery. *J Oral Maxillofac Surg* 63(7), 1006-1015. doi: 10.1016/j.joms.2005.03.016.
243. Wu X, Wang Q, Kang N, Wu J, Gu C, Bi J, et al. The effects of different vascular carrier patterns on the angiogenesis and osteogenesis of BMSC-TCP-based tissue-engineered bone in beagle dogs. *J Tissue Eng Regen Med*. 2017;11(2):542–52.
244. Wubneh, A., Tsekoura, E.K., Ayranci, C., and Uludag, H. (2018). Current state of fabrication technologies and materials for bone tissue engineering. *Acta Biomater* 80, 1-30. doi: 10.1016/j.actbio.2018.09.031.
245. Xu, N., Ye, X., Wei, D., Zhong, J., Chen, Y., Xu, G., et al. (2014). 3D artificial bones for bone repair prepared by computed tomography-guided fused deposition modeling for bone repair. *ACS Applied Materials & Interfaces* 6(17), 14952-14963. doi: 10.1021/am502716t.
246. Yang P, Huang X, Shen J, Wang C, Dang X, Mankin H, et al. Development of a new pre-vascularized tissue-engineered construct using pre-differentiated rADSCs, arteriovenous vascular bundle and porous nano-hydroxyapatite-polyamide 66 scaffold. *BMC Musculoskelet Disord*. 2013 Nov 8;14:318.
247. Yang, X., Lu, Z., Wu, H., Li, W., Zheng, L., and Zhao, J. (2018). Collagen-alginate as bioink for three-dimensional (3D) cell printing based cartilage tissue engineering. *Materials Science and Engineering: C* 83, 195-201. doi: <https://doi.org/10.1016/j.msec.2017.09.002>.
248. Zimmermann, G., and Moghaddam, A. (2011). Allograft bone matrix versus synthetic bone graft substitutes. *Injury* 42 Suppl 2, S16-21. doi: 10.1016/j.injury.2011.06.199.

249. Zuk PA, Zhu M, Mizuno H, Huang J, Futrell JW, Katz AJ, et al. Multilineage cells from human adipose tissue: implications for cell-based therapies. *Tissue Eng.* 2001 Apr;7(2):211–28.

ANNEXE



Article

Epinephrine Infiltration of Adipose Tissue Impacts MCF7 Breast Cancer Cells and Total Lipid Content

Pierre Avril ^{1,†}, Luciano Vidal ^{1,†}, Sophie Barille-Nion ² , Louis-Romée Le Nail ¹,
Françoise Redini ¹, Pierre Layrolle ¹ , Michelle Pinault ³, Stéphane Chevalier ³, Pierre Perrot ^{1,4,*}
and Valérie Trichet ¹

¹ INSERM, Université de Nantes, UMR1238, Phy-Os, Sarcomes osseux et remodelage des tissus calcifiés, F-44035 Nantes, France; pierre.avril.44@gmail.com (P.A.); luciano.vidal@univ-nantes.fr (L.V.); lrlnail@hotmail.com (L.-R.L.N.); francoise.redini@univ-nantes.fr (F.R.); pierre.layrolle@univ-nantes.fr (P.L.); valerie.trichet@univ-nantes.fr (V.T.)

² CRCINA, INSERM, Université d'Angers, Université de Nantes, F-44035 Nantes, France; sophie.barille@univ-nantes.fr

³ INSERM Université de Tours, UMR1069, Nutrition, Croissance et Cancer, F-37032 Tours, France; michelle.pinault@univ-tours.fr (M.P.); stephane.chevalier@univ-tours.fr (S.C.)

⁴ CHU de Nantes, Service de Chirurgie Plastique et des Brûlés, F-44035 Nantes, France

* Correspondence: pierre.perrot@chu-nantes.fr; Tel.: +33-2-40-08-73-02

† These authors contributed equally to this work.

Received: 6 October 2019; Accepted: 4 November 2019; Published: 11 November 2019



Abstract: Background: Considering the positive or negative potential effects of adipocytes, depending on their lipid composition, on breast tumor progression, it is important to evaluate whether adipose tissue (AT) harvesting procedures, including epinephrine infiltration, may influence breast cancer progression. Methods: Culture medium conditioned with epinephrine-infiltrated adipose tissue was tested on human Michigan Cancer Foundation-7 (MCF7) breast cancer cells, cultured in monolayer or in oncospheres. Lipid composition was evaluated depending on epinephrine-infiltration for five patients. Epinephrine-infiltrated adipose tissue (EI-AT) or corresponding conditioned medium (EI-CM) were injected into orthotopic breast carcinoma induced in athymic mouse. Results: EI-CM significantly increased the proliferation rate of MCF7 cells. Moreover EI-CM induced an output of the quiescent state of MCF7 cells, but it could be either an activator or inhibitor of the epithelial mesenchymal transition as indicated by gene expression changes. EI-CM presented a significantly higher lipid total weight compared with the conditioned medium obtained from non-infiltrated-AT of paired-patients. In vivo, neither the EI-CM or EI-AT injection significantly promoted MCF7-induced tumor growth. Conclusions: Even though conditioned media are widely used to mimic the secretome of cells or tissues, they may produce different effects on tumor progression, which may explain some of the discrepancy observed between in vitro, preclinical and clinical data using AT samples.

Keywords: adipose tissue; breast cancer; epinephrine; breast reconstruction

1. Introduction

Adipose tissue (AT) is a biologically active tissue, which releases soluble growth factors (vascular endothelium growth factor, insulin growth factor) inducing tissue revascularization, but also produces hormones (leptin, adiponectin), cytokines (interleukin 6) and insoluble fatty acids, which all interact through complex networks within a tumor microenvironment. Different in vitro and pre-clinical studies have demonstrated that AT including mature adipocytes and stem cells, promotes the proliferation, invasion and survival of breast cancer cells through different secreted factors [1–5].

In contrast specific lipids content in peritumoral AT of breast cancer patients were correlated with therapeutic benefits. Decreased levels of two polyunsaturated n-3 fatty acids (n-3 PUFA), docosahexaenoic and eicosapentaenoic acids (DHA 22:6n-3 and EPA 20:5n-3), in peritumoral AT of women were associated with aggressive multifocal tumors compared to unifocal ones. Moreover it was shown that DHA and EPA decreased resistance of experimental mammary tumors to taxanes, anthracyclines or radio-therapy. These preclinical results are supported by the improved outcome of chemotherapy on metastatic breast cancer that was observed in a phase II clinical study including dietary supplementation with n-3 PUFA [6–11].

In addition, AT transfer does not increase the risk of recurrence of breast cancer as recently suggested by large retrospective clinical studies [12–14]. However one retrospective study observed that patients presenting either ductal or lobular intraepithelial neoplasia, had an increased risk of local events in the group who had undergone lipofilling [15]. The method to harvest AT is one of the most important steps governing the success of AT transplantation. Different methods have been described in the literature studying the variables (fat harvesting technique, infiltration solution, donor site, fat processing, etc.) that influence adipocyte survival and the AT engraftment [16–19]. However, the breast cancer recurrence risk related to the AT harvesting method has not yet been investigated. To harvest fat tissue, some surgical teams use for fat harvesting, an infiltration solution that contains epinephrine, to induce vasoconstriction [20], but it is worth noting that epinephrine may enhance lipolysis in AT [21].

In our study, the epinephrine-lactated Ringer's infiltrated solution adipose tissue conditioned medium (EI-CM) was tested on proliferative and quiescent human Michigan Cancer Foundation-7 (MCF7) breast cancer cells. The lipid composition of conditioned media of non-infiltrated or epinephrine infiltrated-AT from five donors was investigated. EI-CM and epinephrine-infiltrated adipose tissue (EI-AT) were injected into orthotopic induced breast carcinoma in athymic mouse.

2. Results

2.1. MCF7 Cell Proliferation was Enhanced by Epinephrine-Infiltrated Adipose Tissue Conditioned Medium

Proliferation of MCF7 breast carcinoma cells was analyzed in adherent culture conditions by measuring mitochondrial activity (WST-1 assay) and cell viability was controlled by cell counting with trypan blue staining. As cancer cells lost their adherence to plastic when whole epinephrine-infiltrated adipose tissue (EI-AT) was used, EI-AT was replaced by EI-CM to complement cell culture medium in order to mimic secreted factors by EI-AT. Before being treated, cells were cultured overnight (16 h) in a standard medium without fetal bovine serum (FBS) in order to observe a synchronized response to growth factor stimulation. FBS supplementation (10%) enhanced MCF7 mitochondrial activity up to 240% compared to that without FBS (Figure 1a). Similarly supplementation with 50% epinephrine-infiltrated adipose tissue conditioned medium (EI-CM) and 50% MEM α medium (0% FBS) from three different donors enhanced MCF7 mitochondrial activity from 150 to 200% (Figure 1a). The increases of mitochondrial activity were correlated with an increase in cell number by trypan blue counting. Moreover, independent experiments performed with 50% or 25% of EI-CM of patients n°1 to 3 showed similar increases of MCF7 cell proliferation. The inhibition of the ERK1/2 signaling pathway using 5 μ M UO126 induced a 30% decrease of the MCF7 proliferation with EI-CM, whereas it did not change the MCF7 proliferation with 10% FBS (Figure 1b). These results indicate that EI-CM increases MCF7 cell proliferation at least partially through the ERK1/2 signaling pathway.

Cell distribution in each cell-cycle phases was observed by flow cytometry after DNA staining with propidium iodide. During culture without FBS, at least half of the MCF7 cells were in G₀/G₁ phase (54% in Figure 1c, top panel). FBS treatment decreased the proportion of cells in G₀/G₁ phase by half and increased the proportion of cells preparing their mitosis and those replicating their DNA (Figure 1c, middle panel). When MCF7 cells were treated with 25% EI-CM (Figure 1c, low panel), the proportion of cells in G₀/G₁ phase was also reduced by half compared to 0% FBS culture condition. With 25% EI-CM, a higher increase in cells in G₂/M phase was observed compared to 10% FBS (plus

20% versus plus 11%) whereas the increase of cell proportion in S phase was weaker than with 10% FBS (plus 4% versus plus 15%). These results indicate that EI-CM complementation induced cell-cycle activation in MCF7 cells allowing cells to reach the G₂/M phase faster than FBS complementation.

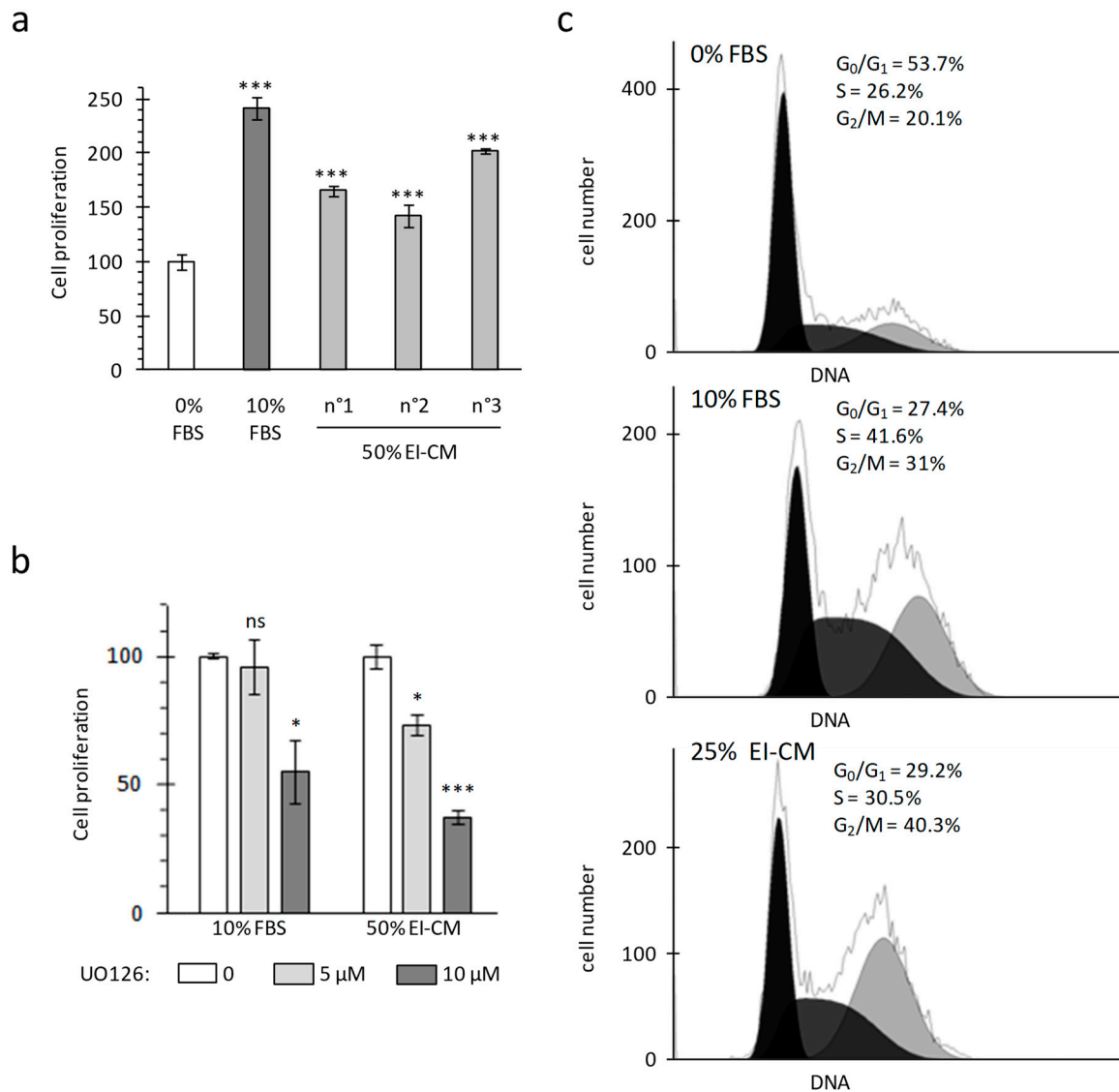


Figure 1. Michigan Cancer Foundation-7 (MCF7) cell growth with ELR solution-infiltrated adipose tissue conditioned medium (EI-CM). MCF7 cells were cultured during 24 h in a medium without any growth factor (0% FBS) or supplemented with fetal bovine serum (10% FBS) or EI-CM (25 to 50%) and MEM with 0%FBS. (a) Histogram shows the mitochondrial activity of MCF7 cells, measured by WST-1 assay. EI-CM were derived from 3 different donors (n^o1 to n^o3). Results are the means of 3 wells and are presented as a percentage of 0% FBS value with standard deviations. Statistically significant differences are indicated in comparison with 0% FBS (***: $p < 0.0001$). Each patient EI-CM was tested in 3 independent experiments. (b) Mitochondrial activity of MCF7 cells measured by WST-1 assay. Cells were cultured for 24 h with or without 5 or 10 μM of ERK inhibitor UO126. Results are the means of 3 wells and are presented as a percentage of condition without UO126 with standard deviations. Statistically significant differences are indicated in comparison with 0 UO126 (*: $p < 0.05$; ***: $p < 0.0001$). Two independent experiments were performed. (c) Histograms show the distribution of MCF7 cells in cell-cycle phases following DNA detection by flow cytometry. Because only 2–3% of cells were identified in the subG₀ phase, only the proportion of cells in the G₀/G₁, S and G₂/M phases are indicated.

2.2. MCF7 Cell Quiescence was Increased by Spheroid Culture and Reduced by Epinephrine-Infiltrated Adipose Tissue Conditioned Medium

Cell culture under anchorage-independent conditions induces carcinoma cells to form spheres and to undergo epithelial mesenchymal transition (EMT) which may correlate with a more invading phenotype such as carcinoma stem cells [22,23]. From MCF7 spheres, messenger ribonucleic acids (mRNAs) were isolated for relative gene expression analysis after three days in culture. Five genes *MYC*, *CD44*, *TWIST1*, *TWIST2* and *SNAI1* (official symbols and full gene names presented in Table 1) which are activated in breast carcinoma stem cells and during EMT exhibited a higher expression in MCF7 cells cultured as spheroids (3-D) compared to that in MCF7 cells cultured in monolayer (2-D) (Figure 2a). In accordance with EMT, E-cadherin gene (*CDH1*) expression was lower in MCF7 spheroids than in monolayers. EI-CM treatment of 3-D cultured MCF7 cells increased expression of *MYC* and *TWIST2* while it decreased that of *CD44* and *SNAI1*, suggesting that the effect of EI-CM on EMT in MCF7 cells could be either as an activator or inhibitor of the EMT.

Tumor recurrence can be explained by the persistence of cancer cells in a quiescent/non-dividing stage that enables them to escape to chemotherapy agents during treatment, whereas microenvironment changes may later activate a cellular switch towards cell division. Quiescent cells corresponding to cells in G₀ phase do not express the Ki-67 protein which is strictly associated with dividing cells in the G₁, S, G₂ or M phases [24]. Under anchorage-independent conditions (3-D), 26.9% of MCF7 cells were in G₀ phase (Figure 2b, left panel). In 3-D culture conditions, 10% FBS complementation did not change cell distribution (Figure 2b, middle panel). In contrast, EI-CM complementation of 3-D cultured MCF7 cells induced a decrease of cell proportion in G₀ phase (13.9%; Figure 2b, right panel).

Immunohistochemistry (IHC) targeting the Ki-67 protein was performed on spheroids formed by MCF7 cells cultured under anchorage-independent conditions (Figure 2c). Consistent with flow cytometry, 25% EI-CM treatment induced an increase of the Ki-67 positive cell proportion (+25%; Figure 2d left panel). Despite cell cycle activation by EI-CM, sphere number and volume (Figure 2d, right panel) were not significantly different between 1% FBS and 25% EI-CM complementation. Altogether, this indicates that EI-CM enabled G₀ to G₁ phase transition of MCF7 cells.

Table 1. List of genes analyzed by real time RT-PCR: Genes are presented with official gene symbols and corresponding full name. Forward and reverse primer sequences used to perform the analyses are indicated.

Official Symbol	Official Full Name	Reverse Primer
<i>HPTR1</i>	Hypoxanthine PhosphoRibosyl Transferase 1	CGAGCAAGACGTTTCAGTCCT
<i>CD44</i>	Cluster of Differentiation 44	CGGCAGGTTATATTCAAATCG
<i>TWIST1</i>	Twist-related protein 1	TGCAGAGGTGTGAGGATGGTGC
<i>TWIST2</i>	Twist-related protein 2	AGAAGGTCTGGCAATGGCAGCA
<i>SNAI1</i>	Snail family transcriptional repressor 1	CAGCAGGTGGGCCTGGTCGTA
<i>CDH1</i>	Cadherin 1	CCAGCGGCCCTTCACAGTC
<i>MYC</i>	Myelocytomatosis viral oncogene homolog	GATCCAGACTCTGACCTTTTGC

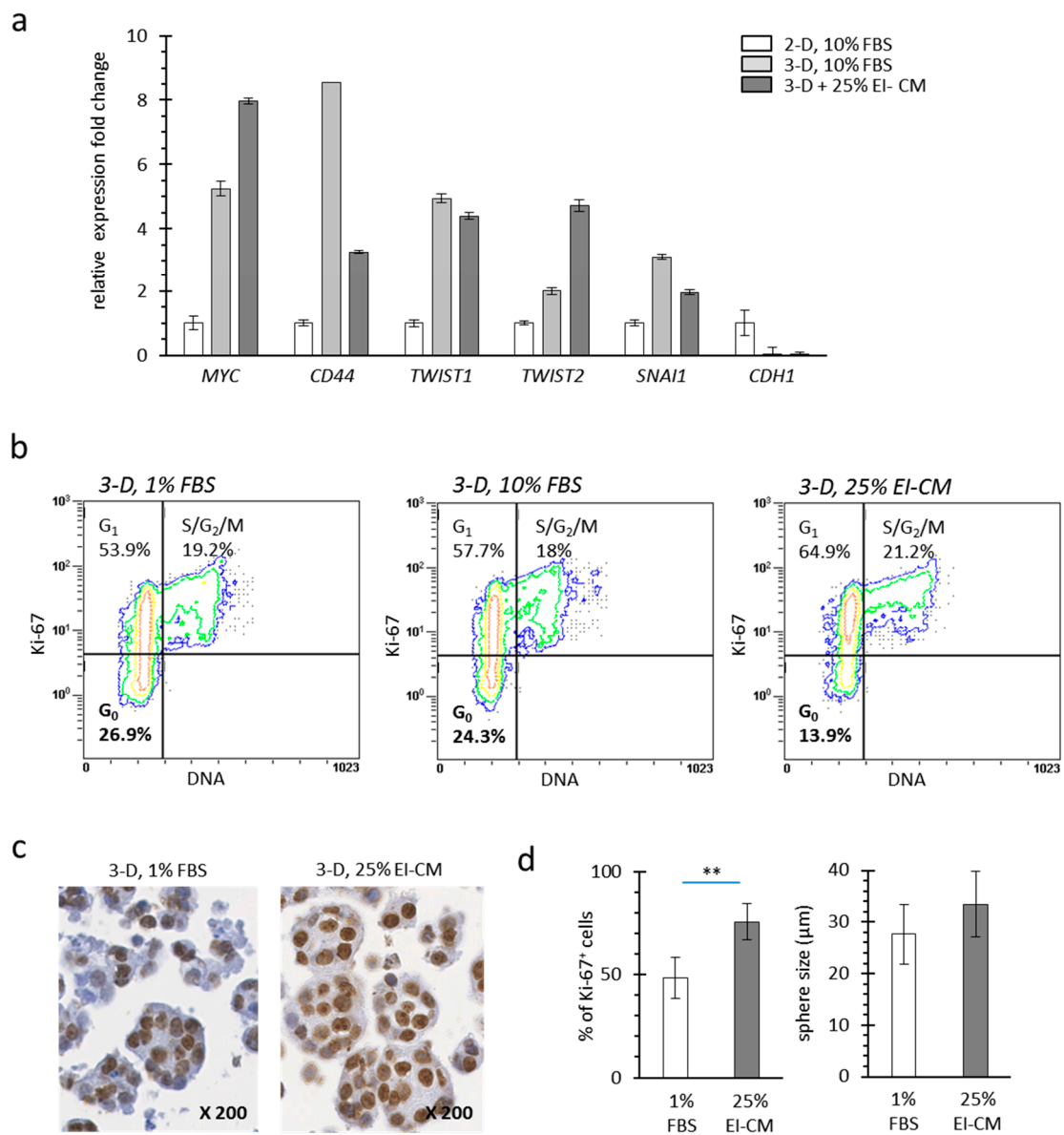


Figure 2. Quiescence of MCF7 cells with ELR solution-infiltrated adipose tissue conditioned medium (EI-CM). **(a)** Relative expression fold changes are presented for mRNA of MCF7 cells cultured either in monolayer (2-D) or in sphere (non-anchorage conditions, 3-D) during 3 days and treated 48 h in a medium supplemented with 1 or 10% FBS or with 25% EI-CM. Expression change of those 5 genes has been correlated to epithelial mesenchymal transition leading to invading phenotype of carcinoma cells. Full gene names and symbols are indicated in Table 1. Means of 3 samples are presented with standard deviations. Significant differences are not indicated as this experiment was not repeated. **(b)** Dot plots show the distribution in cell cycle phases (G₀, G₁ and S/G₂/M) following DNA and Ki-67 detection in MCF7 cells cultured in spheres (3-D). Because only 2–3% of cells were identified in subG₀ phase, only the proportion of cells in G₀, G₁, and S/G₂/M phases are indicated. **(c)** Representative images of IHC detection of Ki-67 on MCF7 spheres (3-D). Magnification is indicated. **(d)** Histograms show the Ki-67 index (left panel) and the mean diameter (right panel) of MCF7 spheres. In the left panel, percentages were counted on 6 representative regions for each treatment after Ki-67 detection by IHC. In the right panel, mean diameter was calculated on 90 different spheres for each condition. Statistically significant differences are indicated in comparison with 1% FBS (**: $p < 0.001$). Three independent experiments were performed.

2.3. Epinephrine Infiltration Changed Lipid Content and Proliferative Effect of Adipose Tissue Conditioned Medium

For patients n°4 to 10, two AT samples were successively collected: a first one without epinephrine infiltration and a second one following infiltration with the epinephrine-lactated Ringer's solution (ELR) and were used to obtain, respectively, NI-CM and EI-CM. As previously observed with EI-CM from patients n°1 to 3, the CM obtained from EI-AT samples had an increased proliferative effect on MCF7 cells, whereas their counterpart CM obtained with non-infiltrated AT did not (Figure 3a, left panel). As shown in Figure 3a (right panel), the ELR by itself had no effect on MCF7 cell proliferation. Because epinephrine infiltration may modify the metabolite composition of the AT samples through lipolysis enhanced by beta-adrenergic receptor activation, the comparison of lipid contents between NI-CM and EI-CM was performed to identify potential molecular mediators leading to EI-CM pro-proliferative effects. We compared the fatty acid content of AT-CM samples that were obtained from 5 donor sites either non-injected (NI) or epinephrine-lactated Ringer's infiltrated (EI). EI-CM showed a higher total lipid content compared to NI-CM of the corresponding donors (Figure 3b). This result suggested that EI-CM and NI-CM may present a different lipid content; however, the percentages of saturated, mono-unsaturated or polyunsaturated fatty acids (PUFAs n-3 and n-6) were similar (Figure 3c) and there were no statistically significant differences in individual fatty acid between EI-CM and NI-CM samples which were derived from 5 donor sites either infiltrated or non-infiltrated with ELR.

2.4. Injection of Epinephrine-Infiltrated Adipose Tissue or Corresponding Conditioned Medium into MCF7 Tumor in Mice

We were able to compare EI-AT and EI-CM injection in a preclinical model of breast carcinoma. Orthotopic breast carcinoma were induced in athymic mice by intraductal injection of MCF7 cells and a single injection of either PBS, EI-CM or EI-AT was performed at the tumor site after 90 days when tumors were detectable ($>70 \text{ mm}^3$).

PBS-treated group (Figure 4b, top panel) showed a slow tumor development, reaching a mean volume of 200 mm^3 at day 160. Human Ki-67 protein detection confirmed the presence of tumor cells in mammary ducts (Figure 4a, top panel) as well as in surrounding adipose and connective structures (Figure 4a, middle panel). These observations may indicate that the tumor first grew within mammary ducts before invading the rest of mammary fat pad, as a ductal carcinoma in situ that would have turned invasive.

Two of six tumors in the EI-CM-injected group showed faster development compared to tumors of the PBS-injected group (Figure 4b, top and middle panels, respectively); however differences between the tumor volume means of these two groups were not significant at day 160. Tumor growth was more similar between PBS- and EI-AT-injected groups (Figure 4b, top and low panels, respectively) than between PBS- and EI-CM-injected groups. However the percentages of Ki-67 positive cells ranging from 18 to 26% were not significantly different between EI-AT-, EI-CM- and PBS-treated groups as determined after human Ki-67 protein immunohistochemical staining on tumor samples (Figure 4a). These results indicate that EI-CM may have slightly (but not significantly) promoted MCF7 tumor growth while corresponding whole EI-AT may not have modified breast tumor growth.

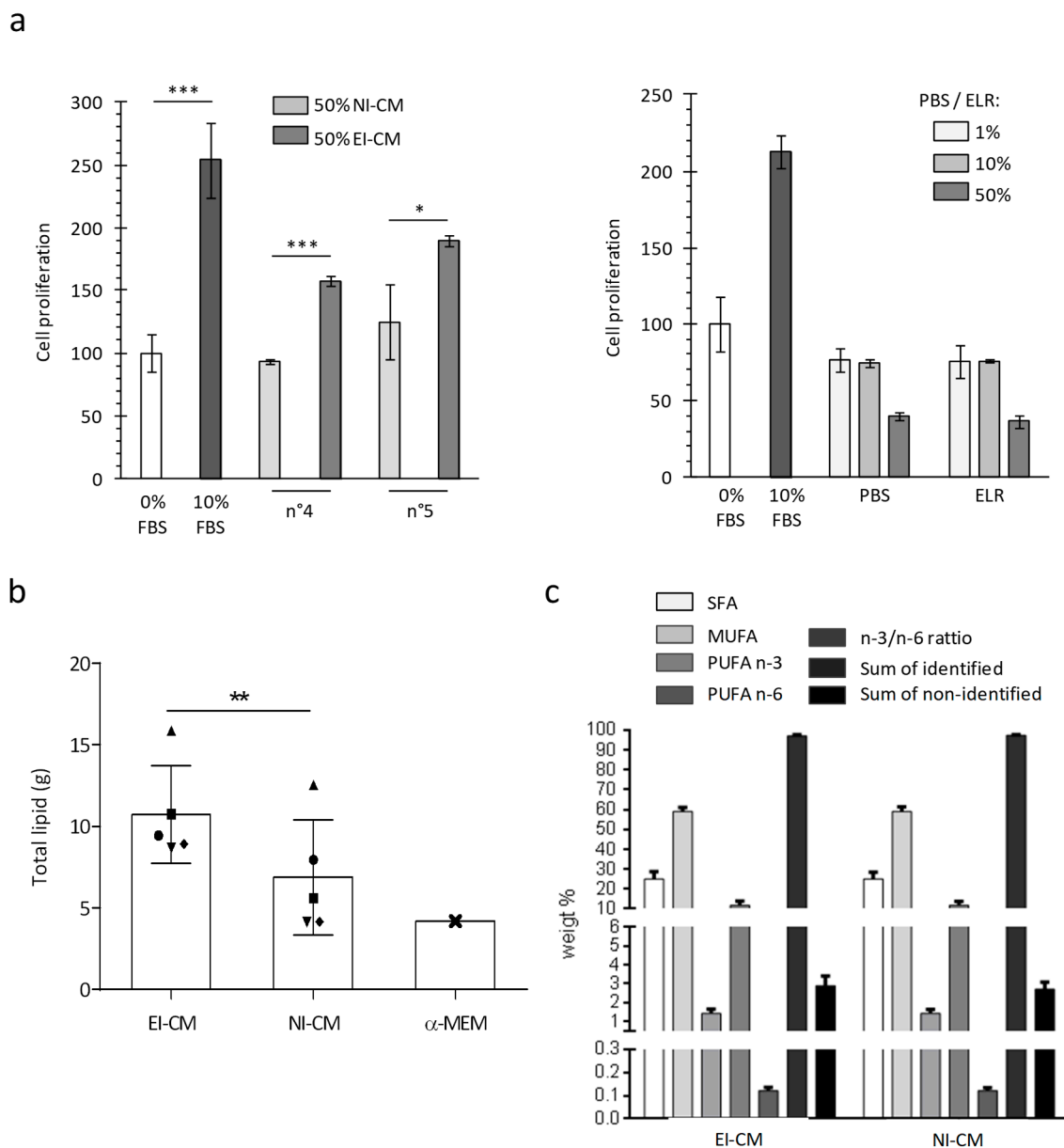


Figure 3. MCF7 cell growth and lipid composition depending on ELR solution infiltration of harvested adipose tissue. **(a)** Histogram shows the mitochondrial activity of MCF7 cells measured after 24 h. For the left panel, cells were cultured in medium without FBS (0% FBS) or supplemented with 10% FBS or with 50% EI-CM and 50% MEM α with 0%FBS. AT samples were obtained from 2 different donors (n⁴ and n⁵) and were initially not-infiltrated (NI) or infiltrated with ELR (EI). For right panel, cells were cultured in a medium without FBS (0% FBS) or supplemented with 10% FBS, PBS or ELR, representing 1 to 50% of the total volume. *: $p < 0.05$; ***: $p < 0.0001$. **(b)** Histogram shows the total lipid amount detected in conditioned medium from infiltrated with ELR (EI-CM) or not-infiltrated AT (NI-CM) for 5 patients (n⁶ to n¹⁰) who are represented by a distinct geometric forms. Lipid amount is indicated in standard culture medium without FBS (MEM α). **: $p = 0.0045$ paired t-test. **(c)** Histogram shows the weight % of fatty acids derived from 5 donors either infiltrated or non-infiltrated with ELR. Saturated, mono-unsaturated or polyunsaturated fatty acids (SFA, MUFA or PUFA) were measured in a conditioned medium of epinephrine lactated Ringer’s solution-infiltrated or non-infiltrated adipose tissue (EI-CM or NI-CM).

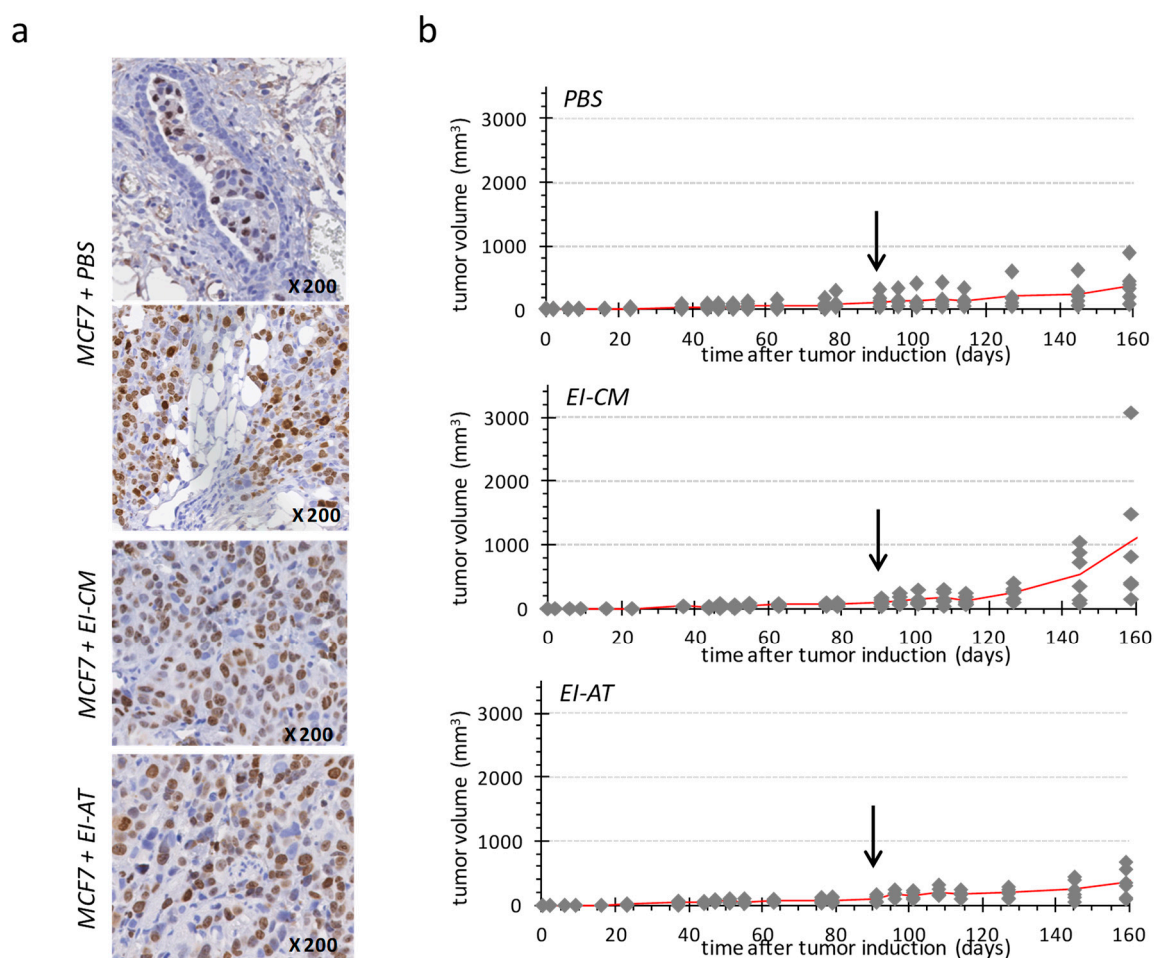


Figure 4. Single injection of either EI-AT or EI-CM in MCF7 tumor induced in athymic mouse. (a) Immunohistochemical staining of human Ki-67 protein in MCF7 tumors injected with PBS, EI-CM or EI-AT. Observation of mammary duct (top panel) and mammary fat pad (middle panel). (b) Evolution of tumor volume is reported for each group of mice ($n = 6$); the mean tumor volume is represented by a red line. The arrows indicate time of the intra-tumor injection of either PBS (top panel), or EI-CM (middle panel group) or EI-AT (low panel). At days 145 and 160, no significant difference between groups was detected by unpaired nonparametric method.

3. Discussion

AT transplantation has become an increasingly common technique in aesthetic breast augmentation, in non-oncological and in oncological breast reconstruction [25]. Low complication rates, readily available donor sites with low donor-site morbidity and an aesthetic benefit are some of the advantages of the AT transfer. Although AT transplantation has proven effective in breast reconstruction, safety concerns have been raised regarding its use in patients with a history of breast cancer [26–28]. At present, large cohort retrospective studies or systematic literature reviews and meta-analyses suggest that AT transplantation is safe with no increase of cancer recurrence risk for breast cancer patients after treatments [29–33]. However AT harvesting procedures have been poorly described in these clinical studies, whereas the lack of standardized protocols for harvesting may explain unpredictable clinical outcomes with AT engraftment [34–36].

Ephrinephrine-lactated Ringer's solution is often used to infiltrate AT before harvesting, in order to reduce bleeding, but it may modify the metabolite composition, especially cholesterol and fatty acids, of AT samples since catecholamines induce lipolysis in adipocytes [37–39]. Interestingly,

polyunsaturated n-3 fatty acids in peritumoral AT of breast cancer patients may have beneficial effects on the disease progression.

In this study, we sought to understand how soluble factors secreted by EI-AT may influence the proliferation and quiescent state of breast cancer cells. EI-AT secreted factors that were collected in the conditioned culture medium induced a significant increase in the proliferation rate (150% to 200%) of MCF7 breast cancer cells, while non-infiltrated AT soluble factors did not. EI-AT secreted factors increased MCF7 cell proliferation at least partially through the extracellular-regulated kinase (ERK) 1/2 signaling pathway. In a previous study using similar EI-CM samples, multi cytokine assay has identified interleukin 6 (IL-6) and leptin as molecular candidates to induce increase of osteosarcoma cell proliferation; however neither IL-6 nor leptin have been able to mimic the pro-proliferative effects of EI-CM. By in vitro and preclinical studies, Danilo C. et al. have shown that cholesteryl ester via its cellular receptor (scavenger receptor class B type I, SR-BI) increase breast cancer cell proliferation through the phosphatidylinositol 3-kinase (PI3K)/protein kinase B (AKT) pathway but not through the mitogen-activated protein kinase (MAPK)/ERK1/2 pathway [40]. Despite the important role of ERK1/2 in the proliferation of breast cancer cells in vitro, activation of ERK1/2 was not associated with enhanced proliferation and invasion of 148 clinical mammary carcinomas [41].

During clinical procedures, EI-AT transplantation is never performed in a tumor site with proliferative cancer cells. Plastic surgery is performed following a cancer-free period and at worst, the primary tumor site may contain quiescent/dormant cancer cells. The quiescent state of breast cancer cells in vitro was induced by culture under anchorage-independent conditions, using methylcellulose in the culture medium. We observed that EI-CM induced an output of the quiescent state of MCF7 cells when maintained in non-adherent spheres: 14% of cells in G₀ phase with EI-CM compared to 27% or 24% in 1% and 10% FBS supplementation, respectively. Such 3-D culture conditions induced a slight change from epithelial towards mesenchymal phenotypes of MCF7 cells, as suggested by *MYC*, *CD44*, *TWIST1/2* and *SNAIL* expression increase associated with a decrease of *CDH1* expression. We observed that EI-CM did not enhance such potential EMT in MCF7 cells. In this study, we did not test EI-CM effect on the migration of breast cancer cells and we did not use primary breast cancer stem cells which are of high interest in the progression, treatment resistance and recurrence. Originally, Charvet H.J. et al. have used one breast cancer cell line derived from one out of 10 patient specimens, and not a purchased banked cell line. Charvet H.J. et al. showed a 10-fold migration increase of primary breast cancer cells when cocultured with adipose-derived stem cells isolated from the same patient.

To conduct in vitro assays, an AT-conditioned medium (AT-CM) is usually used in the literature, instead of the whole AT sample itself which would be injected into a patient. AT-CM contains AT secreted and soluble factors including growth factors, cytokines and free fatty acids, but no adipocytes or adipose-derived stem cells. Dirat B. et al. have demonstrated that adipocytes obtained from breast AT during tumorectomy, exhibit a loss of lipid content, an expression increase of proinflammatory cytokines and the ability to increase invasive capacities of breast cancer cell lines.

Conditioned media derived from epinephrine-infiltrated AT showed a pro-proliferative effect on breast cancer cells and significantly higher lipid contents compared to non-infiltrated AT of corresponding patients. However, the percentages of saturated, mono-unsaturated or polyunsaturated fatty acids were similar in EI- or NI-CM. Recently, Wang Y.Y. et al. showed that free fatty acids released from adipocytes were incorporated into breast cancer cells as triglycerides in lipid droplets and that saturated fatty acids but not unsaturated ones were increased in cocultured cells [42]. Additionally, they demonstrated that lipolysis in adipocytes was induced by tumor cell secretions, but was not induced by catecholamines. In our study, only patients with a standard body mass index ranging from 20 to 22 were included. Because obesity is clearly related to a higher risk of cancer [43], including breast cancer risk, it would be of interest to compare the total lipid contents of EI-CM derived from obese and lean patients.

Epinephrine-infiltrated adipose tissue-conditioned medium (EI-CM) and whole epinephrine-infiltrated adipose tissue (EI-AT) of the same patient were compared following

a single injection within breast carcinomas induced in athymic mice by intraductal injection of MCF7 cells. Interestingly, carcinoma growth was slow in this preclinical model; tumors were visible only 90 days after MCF7 cell injection, despite implantation of pellet delivering 17β -estradiol, and tumor volumes were less than 400 mm^3 two weeks after EI-AT or EI-CM single injections. A single injection of EI-CM may have slightly but not significantly increased MCF7 tumor growth compared to a single PBS injection. The untranslation of the EI-CM cellular effects to in vivo effects may be due to reversed or transient effects that have not been tested in our in vitro study, or due to neutralization through molecular interactions with physiological liquids. In contrast, corresponding whole EI-AT injection did not modify breast tumor growth, in agreement with clinical studies which show that AT transfer did not increase tumor recurrence and then, may have no effect on quiescent tumor cells.

MCF-7 cell line which is a luminal A subtype of breast cancer expressing estrogen and progesterone receptors, is not the more aggressive and invasive model. It will be of high interest to test a model with a higher metastatic potential such as the MDA-MB-231 cell line, a basal subtype of triple negative breast cancer. We observed that EI-CM of patients n°1 to 3 induced 50% increase in the proliferation rate of MDA-MB-231 cells in culture (data not shown), but we did not investigate further this cell line as we were not able to establish an adequate in vivo model using it. A low tumor incidence (50%) with high variability of tumor size was obtained using MDA-MB-231 cell injection in nude mice.

In conclusion, epinephrine-infiltration of AT induces secretion of factors including lipids. This may contribute to the pro-proliferative effect and output of the quiescent state that were observed in vitro on MCF7 breast cancer cells. Moreover, such epinephrine-induced secreted factors seem to increase the in vivo growth of MCF7-induced tumor in mice. However, a single injection of whole epinephrine-infiltrated AT did not increase the slow progression of MCF7-induced tumor in mice, revealing a discrepancy between the effects of AT-secreted soluble factors in the conditioned medium and the whole AT sample which would be injected into a patient. The proportion of polyunsaturated fatty acids was not modified by the epinephrine infiltration, despite the significant increase in secreted lipids by EI-AT. The results of the EI-AT presented here do not call into question the safety of AT transplantation, however it would be of interest to compare cancer recurrences in breast cancer patients following the transplantation of AT harvested with or without epinephrine infiltration.

4. Materials and Methods

4.1. Adipose Tissue (AT)

AT samples: Human adipose tissue (AT) was obtained from abdominal liposuction during plastic surgery at the University Hospital of Nantes. Donors (patients n°1 to 10) with no significant medical history gave informed consent for the use of surplus AT sample for anonymized unlinked research, as validated by the “Comité de Protection des Personnes des Pays de la Loire” and by the “Ministère de la Recherche” (Art. L. 1245-2 of the French public health code, Law no. 2004-800 of 6 August 2004, Official Journal of 7 August 2004) with declaration to the “Commission Nationale de l’Informatique et des Libertés”. Ten AT samples were collected using a 12-gauge, 12-hole cannula (Khouri Harvester) connected to a 10 mL Luer-Lock syringe after infiltration with 0.1% epinephrine lactated Ringer’s solution as performed in our department to reduce bleeding. All patients had a body mass index ranging from 20 to 22. For five patients, we obtained both epinephrine infiltrated (EI) and non-infiltrated (NI) samples. Samples were centrifuged at 3000 rpm with a 9.5 cm radius fixed angle rotor for 1 min (Medilite™, Thermo Fisher Scientific, Illkirch, France) at room temperature. After centrifugation, the samples were separated into 3 layers: the upper one composed of oil, the middle one composed of the adipose tissue and the bottom one with blood and infiltration solution. Only middle layers corresponding to AT samples were collected.

AT-Conditioned Medium (AT-CM): AT samples were placed in cell culture inserts (pore size $3\text{ }\mu\text{m}$; Becton Dickinson, Le Pont de Claix, France) with Minimum Essential Medium alpha (Gibco® MEM α ; Life technologies, St Aubin, France) with nucleosides and 1 g/L D-Glucose (MEM) under serum-free

conditions. After 24 h, inserts with AT were removed and AT-CM was collected and frozen at minus 20 °C.

4.2. Culture Conditions

MCF7 cells were initially derived from a human breast adenocarcinoma ATCC number HTB-22, (ATCC, Manassas, VA, USA). They are a luminal subtype and express estrogen, progesterone and glucocorticoid receptors. MEM α medium was supplemented with 10% fetal bovine serum (FBS) and used to culture cells at 37 °C in a humidified atmosphere (5% CO₂/95% air). For culture under anchorage-independent conditions, 1 mL MEM α medium was supplemented with 1.05% of methylcellulose (R&D Systems, Lille, France) and 1% FBS, and was seeded with 1×10^5 cells into a well of 24-well plate for 3 days. Then 0.5 mL MEM α medium supplemented with 1% or 10% FBS or with 25% EI-CM were added for 2 days. Complete FBS starving (0%) was avoided in 3-D culture to maintain a low proportion (<5%) of cells in subG0 phase.

4.3. Cell Viability

Three thousand cells per well were cultured into 96-well plates with medium supplemented with FBS, CM or chemical inhibitor of ERK1/2 phosphorylation, UO126 (R&D Systems). After 24 h, WST-1 reagent (Roche Diagnostics, Meylan, France) was added to each well for 2 h at 37 °C. Then absorbance was read at 450 nm.

4.4. Cell Cycle Analysis

MCF7 cells were obtained and analyzed as previously described [44]. Briefly, DNA was stained in ethanol-fixed cells with propidium iodide (50 μ g/mL; Sigma-Aldrich, Lyon, France) and Ki-67 protein was eventually detected using a FITC-coupled mouse anti-human Ki-67 antibody (Becton-Dickinson, Le pont de Claix, France). Cell fluorescence was measured by flow cytometry (Cytomics FC500; Beckman Coulter, Villepinte, France). Cell-cycle distribution was analyzed for 20,000 events using MultiCycle AV Software, Windows version (Phoenix Flow System, San Diego, CA, USA) to obtain histograms of cell repartition in each cell-cycle phase and CXP Analysis software version 2.2 (Beckman Coulter, Villepinte, France) to obtain dot-plots of DNA/Ki-67 double-staining.

4.5. Reverse Transcription and Quantitative PCR

Gene expression was observed as previously described [45], after RNA extraction (NucleoSpin RNA II; Machery-Nagel, Düren, Germany), reverse transcription with ThermoScript RT (Invitrogen Life Technologies, Villebon sur Yvette, France) and cDNA amplification using the IQ SYBR Green Supermix (Bio-Rad, Marne la Coquette, France). For quantitative analysis, the iCycler iQ Real-time PCR Detection system (Bio-Rad), was used to calculate relative fold change of gene expression, following the delta delta Ct method [46]. The *HPRT1* reference gene was used for normalization. Primer sequences with corresponding gene symbol and name are indicated in Table 1.

4.6. Breast Carcinoma Model

Eight-week-old female athymic mice (NMRI nu/nu) were obtained from Elevages Janvier (Le Genest St Isle, France). They were housed under pathogen-free conditions at the Experimental Therapy Unit (Faculty of Medicine, Nantes, France). The experimental protocol was approved by the regional committee on animal ethics (CEEAPdL.06) and the Minister of Agriculture (Authorisation number: 9634) and was conducted following the guidelines “Charte nationale portant sur l'éthique de l'expérimentation animale” of the French ethical committee. The mice were anaesthetized by inhalation of an isoflurane-air mix (2% for induction and 0.5% for maintenance, 1 L/min) before injection with 2×10^6 MCF7 cells in 30 μ L of Matrigel (R&D Systems) diluted in phosphate buffered saline (PBS 50%) into the 4th left mammary duct. At the time of cell injection, a pellet delivering 17 β -estradiol

(Innovative Research of America, Sarasota, FL, USA) was subcutaneously implanted between the neck and the left shoulder. Formula $(l^2 \times L)/2$, where l and L represent the smallest and largest diameter respectively, was used to calculate the tumor volume [47].

4.7. Histology Analysis

Tumor samples were fixed in 4% buffered paraformaldehyde (PFA) for 48 h, while sphere samples were fixed in 4% PFA for 15. Three μm -thick sections of tumors or spheres embedded in paraffin were dewaxed, rehydrated and then treated with 3% H_2O_2 for 15 min at room temperature. Human Ki-67 immunohistochemistry detection was then performed with a mouse monoclonal anti-human Ki-67 (MIB-1 clone; Dako, Les Ulis, France) and revealed with a biotinylated goat anti-mouse Immunoglobulin G secondary antibody and Streptavidin-Horse Radish Peroxydase complexes (Dako) that were observed following an incubation with 3,3'-Diaminobenzidine (DAB, Dako). Nuclei were counterstained with a Gill-Haematoxylin solution. ImageJ software (NIH, Bethesda, MD, USA) was used to calculate the proportion of Ki-67-positive cells, from counting >15,000 nuclei in 6 sections of each tumor sample or >5000 nuclei in 6 sections of each sphere sample.

4.8. Lipid Analysis

Fatty acid composition analysis using gas chromatography: AT-CM were frozen in liquid nitrogen before total lipid extraction according to the FOLCH method with chloroform-methanol 2:1 (*v/v*). Extracts from AT-CM were washed with saline and separated into two phases. The chloroform phase transferred to a new tube was evaporated. Lipid extracts were resuspended with 200 μl of chloroform-methanol 2:1 (*v/v*). Triglycerids (TG) were separated on silica gel TLC plates (LK5, 20*20; Merck St Quentin, Yvelines, France) for thin layer chromatography. After spot scraping, TG were collected and treated as fatty acids methyl esters (FAME) for gas chromatography analysis.

Derivatization of fatty acids was performed with 14% boron trifluoride (in methanol), which resulted in the formation of methyl esters. The derivatization mixture was incubated and shaken for 30 min at 100 °C. Finally, FAME were extracted twice with hexane and then evaporated to dryness. Batch samples were analyzed with a gas chromatograph (GC-2010plus; Shimadzu Scientific instruments, Noisiel, France) through a capillary column (SGE BPX70 GC Capillary Columns; Chromoptic SAS, Courtaboeuf, France). A hydrogen carrier gas was maintained at 120 kPa. Oven temperature was set to 60 °C to 220 °C and flame ionization detector temperature at 280 °C for fatty acid detection. FAME identification was done by comparing relative retention times of samples to those obtained for pure standard mixtures (Supelco 37 fatty acid methyl Ester mix; Sigma Aldrich). The relative amount of each fatty acid (saturated, mono-unsaturated or polyunsaturated fatty acid) was quantified by integrating the baseline peak divided by the peak area corresponding to all fatty acids, using the GC solutions software (Shimadzu Scientific instruments, Noisiel, France).

4.9. Statistical Analysis

Microsoft Excel software (Redmond, WA, USA) was used. In vitro experiments results were analyzed following the analysis of variance t-test. In vivo experimentation results were analyzed with the unpaired nonparametric method and Dunn's multiple comparisons following the Kruskal-Wallis test.

Author Contributions: Conceptualization, S.B.-N., P.P. and V.T.; methodology, P.A. and M.P.; validation, L.-R.L.N., P.P. and V.T.; formal analysis, P.A. and V.T.; writing—original draft preparation, L.V., S.C. and V.T.; writing—review and editing, L.-R.L.N., V.T. and P.P.; project administration, V.T.; funding acquisition, F.R., P.L. and V.T.

Funding: This work was partly supported by INSERM, the University of Nantes and Cancéropole Grand Ouest (AOE2016).

Acknowledgments: The authors wish to thank Brennan M for the manuscript revision, Guiho R and Bitteau K for their help with in vivo experiments and Charrier C for the histology experiments.

Conflicts of Interest: The authors declare no conflicts of interest. The funders had no role in the design of the study; in the collection, analyses, or interpretation of data; in the writing of the manuscript, or in the decision to publish the results.

References

1. Wolfson, B.; Eades, G.; Zhou, Q. Adipocyte activation of cancer stem cell signaling in breast cancer. *World J. Biol. Chem.* **2015**, *6*, 39–47. [[CrossRef](#)]
2. D'Esposito, V.; Liguoro, D.; Ambrosio, M.R.; Collina, F.; Cantile, M.; Spinelli, R.; Raciti, G.A.; Miele, C.; Valentino, R.; Campiglia, P.; et al. Adipose microenvironment promotes triple negative breast cancer cell invasiveness and dissemination by producing CCL5. *Oncotarget* **2016**, *7*, 24495–24509.
3. Nieman, K.M.; Romero, I.L.; Van Houten, B.; Lengyel, E. Adipose tissue and adipocytes supports tumorigenesis and metastasis. *Biochim. Biophys. Acta* **2013**, *1831*, 1533–1541. [[CrossRef](#)]
4. Iyengar, P.; Combs, T.P.; Shah, S.J.; Gouon-Evans, V.; Pollard, J.W.; Albanese, C.; Flanagan, L.; Tenniswood, M.P.; Guha, C.; Lisanti, M.P.; et al. Adipocyte-secreted factors synergistically promote mammary tumorigenesis through induction of anti-apoptotic transcriptional programs and proto-oncogene stabilization. *Oncogene* **2003**, *22*, 6408–6423. [[CrossRef](#)]
5. Dirat, B.; Bochet, L.; Dabek, M.; Daviaud, D.; Dauvillier, S.; Majed, B.; Wang, Y.Y.; Meulle, B.; Salles, B.; Gonidec, S.L.; et al. Cancer-associated adipocytes exhibit an activated phenotype and contribute to breast cancer invasion. *Cancer Res.* **2011**, *71*, 2455–2465. [[CrossRef](#)] [[PubMed](#)]
6. Kornfeld, S.; Goupille, C.; Vibet, S.; Chevalier, S.; Pinet, A.; Lebeau, J.; Tranquart, F.; Bougnoux, P.; Martel, E.; Maurin, A.; et al. Reducing endothelial NOS activation and interstitial fluid pressure with n-3 PUFA offset tumor chemoresistance. *Carcinogenesis* **2012**, *33*, 260–267. [[CrossRef](#)]
7. Ouldamer, L.; Goupille, C.; Vildé, A.; Arbion, F.; Body, G.; Chevalier, S.; Cottier, J.P.; Bougnoux, P. N-3 Polyunsaturated Fatty Acids of Marine Origin and Multifocality in Human Breast Cancer. *PLoS ONE* **2016**, *11*, e0147148. [[CrossRef](#)]
8. Chauvin, L.; Goupille, C.; Blanc, C.; Pinault, M.; Domingo, I.; Guimaraes, C.; Bougnoux, P.; Chevalier, S.; Maheo, K. Long chain n-3 polyunsaturated fatty acids increase the efficacy of docetaxel in mammary cancer cells by downregulating Akt and PKC ϵ/δ -induced ERK pathways. *Biochim. Biophys. Acta* **2016**, *1861*, 380–390. [[CrossRef](#)] [[PubMed](#)]
9. Biondo, P.D.; Brindley, D.N.; Sawyer, M.B.; Field, C.J. The potential for treatment with dietary long-chain polyunsaturated n-3 fatty acids during chemotherapy. *J. Nutr. Biochem.* **2008**, *19*, 787–796. [[CrossRef](#)]
10. Calviello, G.; Serini, S.; Piccioni, E.; Pessina, G. Antineoplastic effects of n-3 polyunsaturated fatty acids in combination with drugs and radiotherapy: Preventive and therapeutic strategies. *Nutr. Cancer* **2009**, *61*, 287–301. [[CrossRef](#)]
11. Bougnoux, P.; Hajjaji, N.; Maheo, K.; Couet, C.; Chevalier, S. Fatty acids and breast cancer: Sensitization to treatments and prevention of metastatic re-growth. *Prog. Lipid. Res.* **2010**, *49*, 76–86. [[CrossRef](#)]
12. Kronowitz, S.J.; Mandujano, C.C.; Liu, J.; Kuerer, H.M.; Smith, B.; Garvey, P.; Jagsi, R.; Hsu, L.; Hanson, S.; Valero, V. Lipofilling of the breast does not increase the risk of recurrence of breast cancer: A matched controlled study. *Plast. Reconstr. Surg.* **2016**, *137*, 385–393. [[CrossRef](#)]
13. Charvet, H.J.; Orbay, H.; Wong, M.S.; Sahar, D.E. The oncologic safety of breast fat grafting and contradictions between basic science and clinical studies: A systematic review of the recent literature. *Ann. Plast. Surg.* **2015**, *75*, 471–479. [[CrossRef](#)]
14. Gentile, P.; Casella, D.; Palma, E.; Calabrese, C. Engineered fat graft enhanced with adipose-derived stromal vascular fraction cells for regenerative medicine: Clinical, histological and instrumental evaluation in breast reconstruction. *J. Clin. Med.* **2019**, *8*, 504. [[CrossRef](#)]
15. Petit, J.Y.; Rietjens, M.; Botteri, E.; Rotmensz, N.; Bertolini, F.; Curigliano, G.; Rey, P.; Garusi, F.; De Lorenzi, S.; Martella, S.; et al. Evaluation of fat grafting safety in patients with intraepithelial neoplasia: A matched-cohort study. *Ann. Oncol. Off. J. Eur. Soc. Med. Oncol.* **2013**, *24*, 1479–1484. [[CrossRef](#)]
16. Geissler, P.J.; Davis, K.; Roostaeian, J.; Unger, J.; Huang, J.; Rohrich, R.J. Improving fat transfer viability: The role of aging, body mass index, and harvest site. *Plast. Reconstr. Surg.* **2014**, *134*, 227–232. [[CrossRef](#)]

17. Gentile, P.; De Angelis, B.; Di Pietro, V.; Amorosi, V.; Scioli, M.G.; Orlandi, A.; Cervelli, V. Gentle Is Better: The original “Gentle Technique” for fat placement in breast lipofilling. *J. Cutan. Aesthet. Surg.* **2018**, *11*, 120–126. [[CrossRef](#)] [[PubMed](#)]
18. Gentile, P.; Orlandi, A.; Scioli, M.G.; Di Pasquali, C.; Bocchini, I.; Curcio, C.B.; Floris, M.; Fiaschetti, V.; Floris, R.; Cervell, V. A comparative translational study: The combined use of enhanced stromal vascular fraction and platelet-rich plasma improves fat grafting maintenance in breast reconstruction. *Stem Cells Transl. Med.* **2012**, *1*, 341–351. [[CrossRef](#)]
19. Gentile, P.; Scioli, M.G.; Orlandi, A.; Cervelli, V. Breast reconstruction with enhanced stromal vascular fraction fat grafting: What is the best method? *Plast. Reconstr. Surg. Glob. Open* **2015**, *3*, e406. [[CrossRef](#)]
20. Hamza, A.; Lohsiriwat, V.; Rietjens, M. Lipofilling in breast cancer surgery. *Gland Surg.* **2013**, *2*, 7–14. [[PubMed](#)]
21. Large, V.; Hellström, L.; Reynisdottir, S.; Lönnqvist, F.; Eriksson, P.; Lannfelt, L.; Arner, P. Human beta-2 adrenoceptor gene polymorphisms are highly frequent in obesity and associate with altered adipocyte beta-2 adrenoceptor function. *J. Clin. Investig.* **1997**, *100*, 3005–3013. [[CrossRef](#)] [[PubMed](#)]
22. Girard, Y.K.; Wang, C.; Ravi, S.; Howell, M.C.; Mallela, J.; Alibrahim, M.; Green, R.; Hellemann, G.; Mohapatra, S.S.; Mohapatra, S. A 3D fibrous scaffold inducing tumoroids: A platform for anticancer drug development. *PLoS ONE* **2013**, *8*, e75345. [[CrossRef](#)]
23. Al-Hajj, M.; Wicha, M.S.; Benito-Hernandez, A.; Morrison, S.J.; Clarke, M.F. Prospective identification of tumorigenic breast cancer cells. *Proc. Natl. Acad. Sci. USA* **2003**, *100*, 3983–3988. [[CrossRef](#)]
24. Cuylen, S.; Blaukopf, C.; Politi, A.Z.; Müller-Reichert, T.; Neumann, B.; Poser, I.; Ellenberg, J.; Hyman, A.A.; Gerlich, D.W. Ki-67 acts as a biological surfactant to disperse mitotic chromosomes. *Nature* **2016**, *535*, 308–312. [[CrossRef](#)]
25. Niddam, J.; Vidal, L.; Hersant, B.; Meningaud, J.P. Primary Fat Grafting to the Pectoralis Muscle during Latissimus Dorsi Breast Reconstruction. *Plast. Reconstr. Surg. Glob. Open* **2016**, *4*, 1059. [[CrossRef](#)]
26. Lohsiriwat, V.; Curigliano, G.; Rietjens, M.; Goldhirsch, A.; Petit, J.Y. Autologous fat transplantation in patients with breast cancer: «silencing» or “fueling” cancer recurrence? *Breast Edinb. Scotl.* **2011**, *20*, 351–357. [[CrossRef](#)] [[PubMed](#)]
27. Charvet, H.J.; Orbay, H.; Harrison, L.; Devi, K.; Sahar, D.E. In vitro effects of adipose-derived stem cells on breast cancer cells harvested from the same patient. *Ann. Plast. Surg.* **2016**, *76*, S241–S245. [[CrossRef](#)]
28. Fraser, J.K.; Hedrick, M.H.; Cohen, S.R. Oncologic risks of autologous fat grafting to the breast. *Aesthet. Surg. J.* **2011**, *31*, 68–75. [[CrossRef](#)]
29. Silva-Vergara, C.; Fontdevila, J.; Weshahy, O.; Yuste, M.; Descarrega, J.; Grande, L. Breast cancer recurrence is not increased with lipofilling reconstruction: A case-controlled study. *Ann. Plast. Surg.* **2017**, *79*, 243–248. [[CrossRef](#)] [[PubMed](#)]
30. Largo, R.D.; Tchang, L.A.H.; Mele, V.; Scherberich, A.; Harder, Y.; Wettstein, R.; Schaefer, D. Efficacy, safety and complications of autologous fat grafting to healthy breast tissue: A systematic review. *J. Plast. Reconstr. Aesthetic Surg.* **2014**, *67*, 437–448. [[CrossRef](#)]
31. Cohen, O.; Lam, G.; Karp, N.; Choi, M. Determining the oncologic safety of autologous fat grafting as a reconstructive modality: An institutional review of breast cancer recurrence rates and surgical outcomes. *Plast. Reconstr. Surg.* **2017**, *140*, 382e–392e. [[CrossRef](#)]
32. Wazir, U.; El Hage Chehade, H.; Headon, H.; Oteifa, M.; Kasem, A.; Mokbel, K. Oncological safety of lipofilling in patients with breast cancer: A meta-analysis and update on clinical practice. *Anticancer Res.* **2016**, *36*, 4521–4528. [[CrossRef](#)]
33. Gigli, S.; Amabile, M.I.; Pastena, F.D.; De Luca, A.; Gulia, C.; Manganaro, L.; Monti, M.; Ballesio, L. Lipofilling outcomes mimicking breast cancer recurrence: Case report and update of the literature. *Anticancer. Res.* **2017**, *37*, 5395–5398.
34. Suszynski, T.M.; Sieber, D.A.; Van Beek, A.L.; Cunningham, B.L. Characterization of adipose tissue for autologous fat grafting. *Aesthet. Surg. J.* **2015**, *35*, 194–203. [[CrossRef](#)]
35. Spear, S.L.; Coles, C.N.; Leung, B.K.; Gitlin, M.; Parekh, M.; Macarios, D. The safety, effectiveness, and efficiency of autologous fat grafting in breast surgery. *Plast. Reconstr. Surg. Glob. Open* **2016**, *4*, e827. [[CrossRef](#)]
36. Waked, K.; Colle, J.; Doornaert, M.; Cocquyt, V.; Blondeel, P. Systematic review: The oncological safety of adipose fat transfer after breast cancer surgery. *Breast Edinb. Scotl.* **2017**, *31*, 128–136. [[CrossRef](#)]

37. Lafontan, M.; Berlan, M. Fat cell adrenergic receptors and the control of white and brown fat cell function. *J. Lipid Res.* **1993**, *34*, 1057–1091.
38. Bougnères, P.; Stunff, C.L.; Pecqueur, C.; Pinglier, E.; Adnot, P.; Ricquier, D. In vivo resistance of lipolysis to epinephrine. A new feature of childhood onset obesity. *J. Clin. Investig.* **1997**, *99*, 2568–2573. [[CrossRef](#)]
39. Jocken, J.W.E.; Blaak, E.E. Catecholamine-induced lipolysis in adipose tissue and skeletal muscle in obesity. *Physiol. Behav.* **2008**, *94*, 219–230. [[CrossRef](#)]
40. Danilo, C.; Gutierrez-Pajares, J.L.; Mainieri, M.A.; Mercier, I.; Lisanti, M.P.; Frank, P.G. Scavenger receptor class B type I regulates cellular cholesterol metabolism and cell signaling associated with breast cancer development. *Breast Cancer Res.* **2013**, *15*, R87. [[CrossRef](#)]
41. Milde-Langosch, K.; Bamberger, A.M.; Rieck, G.; Grund, D.; Hemminger, G.; Müller, V.; Longing, T. Expression and prognostic relevance of activated extracellular-regulated kinases (ERK1/2) in breast cancer. *Br. J. Cancer* **2005**, *92*, 2206–2215. [[CrossRef](#)]
42. Wang, Y.Y.; Attané, C.; Milhas, D.; Dirat, B.; Dauvillier, S.; Guerard, A.; Gilhodes, G.; Lazar, I.; Alet, N.; Laurent, V.; et al. Mammary adipocytes stimulate breast cancer invasion through metabolic remodeling of tumor cells. *JCI. Insight.* **2017**, *2*, e87489. [[CrossRef](#)]
43. Basen-Engquist, K.; Chang, M. Obesity and cancer risk: Recent review and evidence. *Curr. Oncol. Rep.* **2011**, *13*, 71–76. [[CrossRef](#)]
44. Chipoy, C.; Brounais, B.; Trichet, V.; Battaglia, S.; Berreux, M.; Oliver, L.; Juin, P.; Redini, F.; Heymann, D.; Blanchard, F. Sensitization of osteosarcoma cells to apoptosis by oncostatin M depends on STAT5 and p53. *Oncogene* **2007**, *26*, 6653–6664. [[CrossRef](#)]
45. Avril, P.; Le Nail, L.R.; Brennan, M.Á.; Rosset, P.; De Pinieux, G.; Layrolle, P.; Heymann, D.; Trichet, V.; Perrot, P. Mesenchymal stem cells increase proliferation but do not change quiescent state of osteosarcoma cells: Potential implications according to the tumor resection status. *J. Bone Oncol.* **2015**, *5*, 5–14. [[CrossRef](#)]
46. Livak, K.J.; Schmittgen, T.D. Analysis of relative gene expression data using real-time quantitative PCR and the 2(-Delta Delta C(T)) Method. *Methods* **2001**, *25*, 402–408. [[CrossRef](#)]
47. Gernapudi, R.; Yao, Y.; Zhang, Y.; Wolfson, B.; Roy, S.; Duru, N.; Eades, G.; Yang, P.; Zhou, Q. Targeting exosomes from preadipocytes inhibits preadipocyte to cancer stem cell signaling in early-stage breast cancer. *Breast Cancer Res. Treat.* **2015**, *150*, 685–695. [[CrossRef](#)]



© 2019 by the authors. Licensee MDPI, Basel, Switzerland. This article is an open access article distributed under the terms and conditions of the Creative Commons Attribution (CC BY) license (<http://creativecommons.org/licenses/by/4.0/>).

Titre : Apport de l'impression 3D et de la vascularisation dans la régénération de grands défauts osseux

Mots clés : Chirurgie reconstructive - Ingénierie tissulaire - Impression 3D – Grands défauts osseux

Résumé : La reconstruction de grands défauts osseux d'origine traumatique ou tumorale constitue un défi pour les orthopédistes et les chirurgiens plasticiens. Cette thèse est divisée en trois chapitres.

Le premier chapitre décrit les différentes options chirurgicales actuelles et propose de nouvelles technologies telles que l'impression 3D dans la régénération de grands défauts osseux. La technique de référence en matière de reconstruction osseuse est la greffe autologue à lambeau libre qui contient les cellules du patient, ses facteurs de croissance et un apport vasculaire mais induit une morbidité importante au site de prélèvement.

Le deuxième chapitre évalue une approche expérimentale consistant à produire in situ un greffon osseux synthétique pré-vascularisé et à le greffer dans un second temps dans un défaut

osseux de taille critique chez le lapin. Cette étude animale démontre l'intérêt de la vascularisation dans la régénération osseuse mais nécessite deux chirurgies.

Le troisième chapitre vise à étudier la faisabilité de régénérer de grands défauts osseux en une seule étape chirurgicale en utilisant des biomatériaux en phosphate de calcium personnalisés et imprimés en 3D, avec ou sans vascularisation. Cette dernière étude démontre la faisabilité de la planification pré-chirurgicale et de la reconstruction de grands défauts osseux avec des biomatériaux anatomiques et l'apport d'une vascularisation axiale dans la régénération osseuse.

En conclusion, ce travail permet de proposer une nouvelle approche en médecine régénérative, personnalisée et vascularisée, pour la reconstruction de grands défauts osseux.

Title : Large bone defects reconstruction by using 3D printing and vascularization

Keywords : Reconstructive Surgery -Tissue Engineering - 3D Printing - Large Bone Defect

Abstract : Large bone defect reconstruction constitutes a challenge for orthopedists and plastic surgeons. This thesis is divided into three chapters. The first chapter gives a review of the current surgical options and future technologies such as 3D printing for regeneration of large bone defects. The gold standard technique for bone reconstruction is autologous free flap transplantation that contains patient's own cells, growth factors and a vascularization bed but induces morbidity. The second chapter evaluates an experimental approach consisting of the in situ production of a pre-vascularized synthetic bone graft and its subsequent transplantation to a critical-sized bone defect in rabbits. This animal study demonstrated the benefit of pre-

vascularization of synthetic bone grafts for regenerating large bone defects but still required two surgeries.

The third chapter aimed to investigate the feasibility of regenerating large bone defects in one surgical step by using 3D-printed customized calcium phosphate scaffolds with or without vascularization. This pre-clinical study demonstrated the benefits of pre-surgical planning for reconstruction of large bone defects with 3D-printed personalized scaffolds and axial vascularization.

In conclusion, this work enables to propose a new approach in regenerative medicine with customized and vascularized for large bone defect reconstruction.